

SYNTHESIS AND BIOEVALUATION OF LACCASE SUBSTRATES AND SUBSTITUTED
QUINOLINES

by

KESHAR PRASAIN

M.Sc., Tribhuvan University, Nepal, 2001

AN ABSTRACT OF A DISSERTATION

submitted in partial fulfillment of the requirements for the degree

DOCTOR OF PHILOSOPHY

Department of Chemistry

College of Arts and Sciences

KANSAS STATE UNIVERSITY

Manhattan, Kansas

2013

Abstract

Our research work is divided into three chapters. In the first chapter, synthesis of substituted phenolic compounds including halogenated di- and trihydroxybenzenes, aminophenols, and substituted di-*tert*-butylphenols, their redox potential, laccase oxidation, and mosquito anti-larval activities are discussed. The synthesized substituted phenols were found to be the substrates but not the inhibitors of laccase. An inverse correlation between the oxidation potential and the laccase oxidation efficiency of halogenated hydroxybenzenes and aminophenols was established. However, substituted di-*tert*-butylphenols were found to have anti-larval activities in mosquitoes resulting in the death of the larvae just before reaching pupation. Among the di-*tert*-butyl phenols studied, water insoluble, 2,4-di-*tert*-butyl-6-(3-methyl-2-butenyl)phenol (**16**), 2-(3,5-di-*tert*-butyl-4-hydroxyphenyl)-2-methylpropanal oxime (**14**), and 6,8-di-*tert*-butyl-2,2-dimethyl-3,4-dihydro-2*H*-chromene (**17**) caused the mortality of 98%, 93%, and 92% of *Anopheles gambiae* larvae in the concentration of 182 nM, 3.4 μ M, and 3.7 μ M, respectively. In particular, compound **16** had similar anti-larval activities as compared to MON-0585, an anti-larval agent reported by Monsanto in the 70's.

In the second chapter, inhibition of protein kinase C (PKC) phosphorylation by substituted quinolines (PQs) is investigated. PQ compounds such as *N*-(3-aminopropyl)-6-methoxy-4-methyl-5-(3-(trifluoromethyl)phenoxy)quinolin-8-amine (PQ1), *N*-(furan-2-ylmethyl)-6-methoxy-4-methyl-5-(3-(trifluoromethyl)phenoxy)quinolin-8-amine (PQ11), and 6-methoxy-4-methyl-*N*-(quinolin-4-ylmethyl)-5-(3-(trifluoromethyl)phenoxy)quinolin-8-amine (PQ15) were found to inhibit PKC phosphorylation with IC_{50} values of 35 nM, 42.3 nM, and 216.3 nM respectively, among which PQ1 and PQ11 were found to be potent PKC inhibitors as comparable to that of staurosporine ($IC_{50} = 33$ nM).

In chapter three, the tissue distribution of PQ1 and PQ11 in normal C57BL/6J mice and the effect of PQ1 on the normal tissues of mice were investigated. Substituted quinolines, PQ1 and PQ11 were distributed in the tissues in concentrations that were more than 40 folds of their effective dose. PQ1 and PQ11 were also found to penetrate the blood brain barrier and collect in the tissue in significant amounts. The administration of PQ1 and PQ11 had no effect in the normal behavior of the animals indicating no short term adverse effects. PQ1 was found to increase the expression of survivin, an anti-apoptotic factor and decrease the expression of cleaved caspase-3 and caspase-8, pro-apoptotic proteins. These studies suggests that PQ1 might have anti-apoptotic activities in normal cells, in contrast to the role of PQ1 in cancer cells where it has demonstrated to induce apoptosis. The study also indicated that PQ11 was better metabolized from the tissues over time as compared to PQ1.

SYNTHESIS AND BIOEVALUATION OF LACCASE SUBSTRATES AND SUBSTITUTED
QUINOLINES

by

KESHAR PRASAIN

M.Sc., Tribhuvan University, Nepal, 2001

A DISSERTATION

submitted in partial fulfillment of the requirements for the degree

DOCTOR OF PHILOSOPHY

Department of Chemistry

College of Arts and Sciences

KANSAS STATE UNIVERSITY

Manhattan, Kansas

2013

Approved by:

Major Professor
Duy H. Hua

Abstract

Our research work is divided into three chapters. In the first chapter, synthesis of substituted phenolic compounds including halogenated di- and trihydroxybenzenes, aminophenols, and substituted di-*tert*-butylphenols, their redox potential, laccase oxidation, and mosquito anti-larval activities are discussed. The synthesized substituted phenols were found to be the substrates but not the inhibitors of laccase. An inverse correlation between the oxidation potential and the laccase oxidation efficiency of halogenated hydroxybenzenes and aminophenols was established. However, substituted di-*tert*-butylphenols were found to have anti-larval activities in mosquitoes resulting in the death of the larvae just before reaching pupation. Among the di-*tert*-butyl phenols studied, water insoluble, 2,4-di-*tert*-butyl-6-(3-methyl-2-butenyl)phenol (**16**), 2-(3,5-di-*tert*-butyl-4-hydroxyphenyl)-2-methylpropanal oxime (**14**), and 6,8-di-*tert*-butyl-2,2-dimethyl-3,4-dihydro-2*H*-chromene (**17**) caused the mortality of 98%, 93%, and 92% of *Anopheles gambiae* larvae in the concentration of 182 nM, 3.4 μ M, and 3.7 μ M, respectively. In particular, compound **16** had similar anti-larval activities as compared to MON-0585, an anti-larval agent reported by Monsanto in the 70's.

In the second chapter, inhibition of protein kinase C (PKC) phosphorylation by substituted quinolines (PQs) is investigated. PQ compounds such as *N*-(3-aminopropyl)-6-methoxy-4-methyl-5-(3-(trifluoromethyl)phenoxy)quinolin-8-amine (PQ1), *N*-(furan-2-ylmethyl)-6-methoxy-4-methyl-5-(3-(trifluoromethyl)phenoxy)quinolin-8-amine (PQ11), and 6-methoxy-4-methyl-*N*-(quinolin-4-ylmethyl)-5-(3-(trifluoromethyl)phenoxy)quinolin-8-amine (PQ15) were found to inhibit PKC phosphorylation with IC₅₀ values of 35 nM, 42.3 nM, and 216.3 nM

respectively, among which PQ1 and PQ11 were found to be potent PKC inhibitors as comparable to that of staurosporine ($IC_{50} = 33$ nM).

In chapter three, the tissue distribution of PQ1 and PQ11 in normal C57BL/6J mice and the effect of PQ1 on the normal tissues of mice were investigated. Substituted quinolines, PQ1 and PQ11 were distributed in the tissues in concentrations that were more than 40 folds of their effective dose. PQ1 and PQ11 were also found to penetrate the blood brain barrier and collect in the tissue in significant amounts. The administration of PQ1 and PQ11 had no effect in the normal behavior of the animals indicating no short term adverse effects. PQ1 was found to increase the expression of survivin, an anti-apoptotic factor and decrease the expression of cleaved caspase-3 and caspase-8, pro-apoptotic proteins. These studies suggests that PQ1 might have anti-apoptotic activities in normal cells, in contrast to the role of PQ1 in cancer cells where it has demonstrated to induce apoptosis. The study also indicated that PQ11 was better metabolized from the tissues over time as compared to PQ1.

Table of Contents

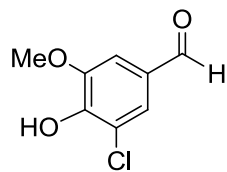
Structure Number Correlation List	xi
List of Figures	xvi
List of Schemes	xix
List of Tables	xx
Abbreviations	xxi
Acknowledgements	xxiii
Dedication	xxv
Chapter 1. Synthesis, redox potential, laccase substrate activity, and antilarval activity of substituted phenols.....	1
1.1 Introduction.....	1
1.2 Background.....	3
1.2.1 Molecular structure of laccase	3
1.2.2 Insect laccase in cuticle sclerotization	5
1.2.3 Laccase inhibitors	7
1.3 Synthesis	7
1.3.1 Synthesis of halogen substituted phenols and polyphenols	12
1.3.1.1 Synthesis of compound 2	12
1.3.1.2 Synthesis of compound 3 and 4	14
1.3.1.3 Synthesis of compound 5	16
1.3.1.4 Synthesis of compound 6	18
1.3.2 Synthesis of aminophenols 7 and 8	19
1.3.3 Synthesis of di- <i>tert</i> -butyl phenols	20

1.3.3.1 Synthesis of compounds 9 - 15	20
1.3.3.2 Synthesis of compound 16, 17 and MON-0585 (18)	23
1.4 Results and discussions.....	25
1.4.1 Redox potentials and laccase substrate oxidation studies	26
1.4.2 Anti-mosquito larval activities.....	30
1.5 Conclusions.....	32
1.6 Experimental Section.....	33
1.7 References.....	56
Chapter 2. Inhibition of PKC phosphorylation by substituted quinolines (PQs).....	62
2.1 Introduction.....	62
2.2 Background.....	64
2.2.1 PKC as a target in cancer therapy	66
2.2.2 PKC and breast cancer	68
2.2.3 Gap junction and cancer.....	69
2.2.4 Inhibition of gap junction intercellular communication by PKC.....	69
2.2.5 PKC inhibitors and cancer	70
2.3 PKC inhibition by substituted quinolines (PQs).....	75
2.3.1 Methods and materials	75
2.3.2 Experimental	79
2.3.2.1 PKC inhibition studies	79
2.3.2.2 Preparation of agarose gel.....	79
2.3.2.3 Preparation of reaction solutions	80

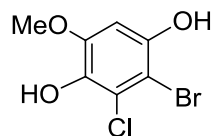
2.3.2.4 Separation of phosphorylated and nonphosphorylated peptides by electrophoresis	81
2.3.2.5 Quantification of phosphorylated and nonphosphorylated bands.....	81
2.4 Results and discussions.....	83
2.4.1 Studies of the correlation between peptide phosphorylation verse (1) concentrations of PKC, and (2) time	83
2.4.1.1 Correlation between peptide phosphorylation verses concentrations of PKC.....	83
2.4.1.2 Correlation between the changes in peptide phosphorylation over time (15 - 60 min).....	85
2.4.2 Inhibition of PKC phosphorylation by staurosporine	87
2.4.3 Inhibition of PKC phosphorylation by PQs (PQ1, PQ10, PQ11, and PQ15)	88
2.5 Conclusions.....	95
2.6 References.....	97
Chapter 3. Distribution of PQ1 and PQ11 in tissues of mice and effect of PQ1 in normal tissues	110
3.1 Introduction.....	110
3.2 Background.....	112
3.3 Experimental.....	114
3.3.1 PQ1 and PQ11 administration and tissue collection.....	115
3.3.2 Extraction of PQ1 and PQ11 from organs and plasma	116
3.3.3 Quantification of PQ1 and PQ11 using HPLC	116
3.4 Results and discussions.....	118
3.4.1 Tissue distribution of PQ1	119

3.4.2 Effect of PQ1 in normal tissues	125
3.4.2.1 Effect of PQ1 on apoptosis in normal tissues	125
3.4.2.2 Effect of PQ1 on connexin in normal tissues.....	127
3.4.2.3 Histological analysis of normal tissues.....	127
3.4.3. Tissue distribution of PQ11	128
3.5 Conclusions.....	137
3.6 References.....	138
Appendix A: ^1H NMR, ^{13}C NMR, and IR spectra.....	141
Appendix B: Permission for figures	213

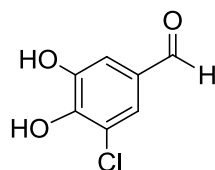
Structure Number Correlation List



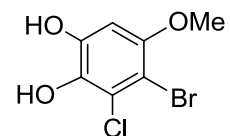
1



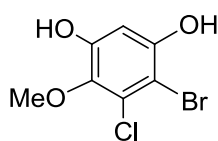
2



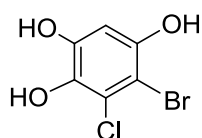
3



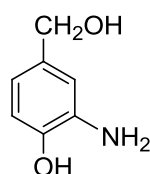
4



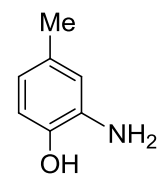
5



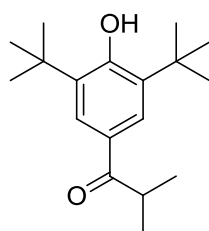
6



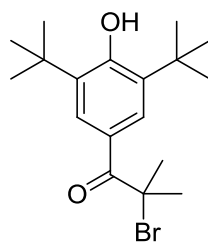
7



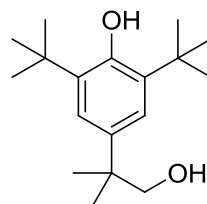
8



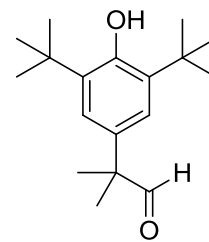
9



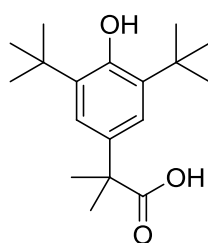
10



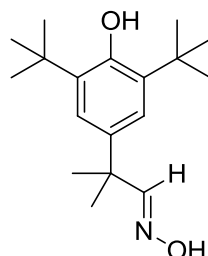
11



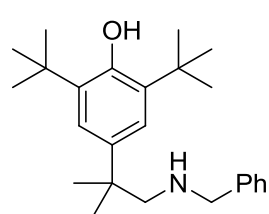
12



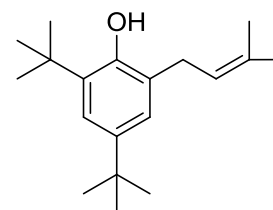
13



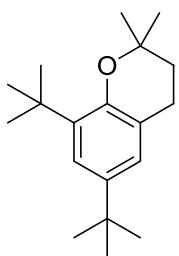
14



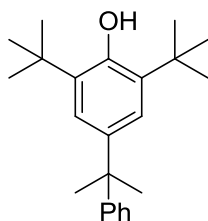
15



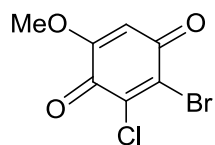
16



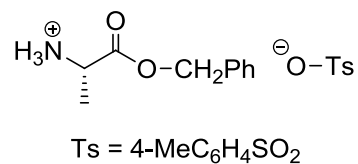
17



18
MON-0585

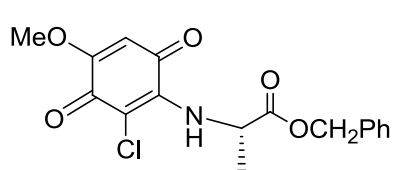


19

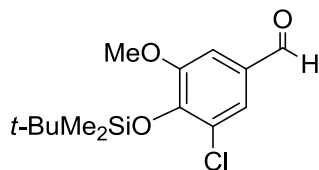


Ts = 4-MeC₆H₄SO₂

20



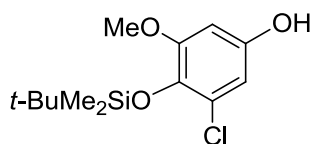
21



22



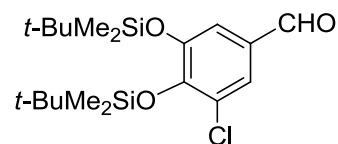
23



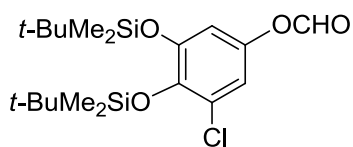
24



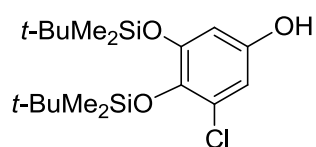
25



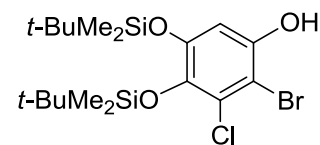
26



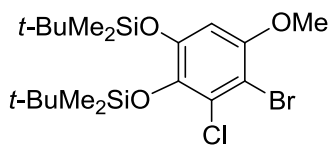
27



28



29



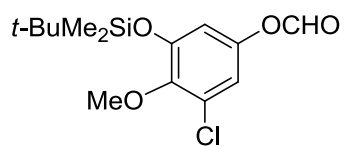
30



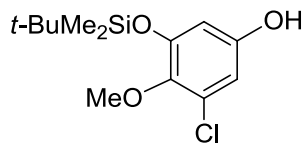
31



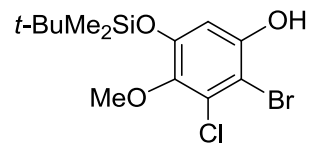
32



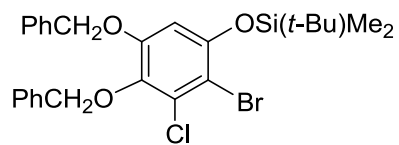
33



34



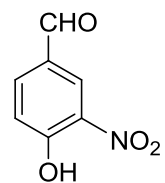
35



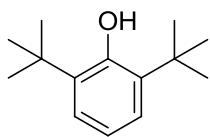
36



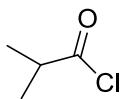
37



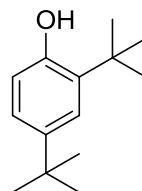
38



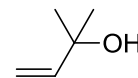
39



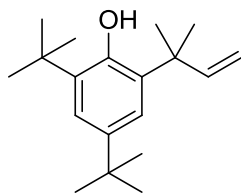
40



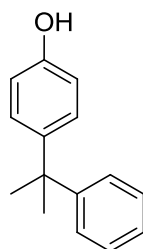
41



42



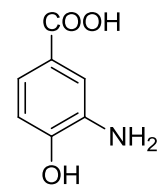
43



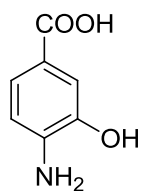
44



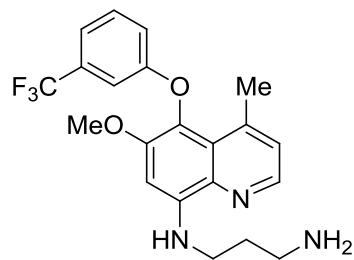
45



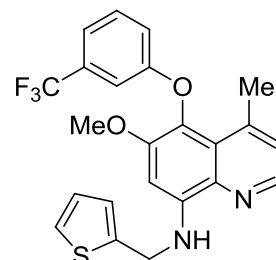
46



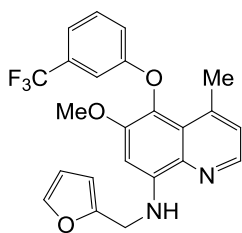
47



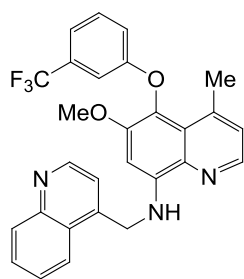
48



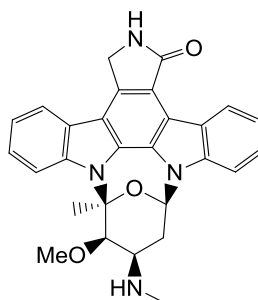
49



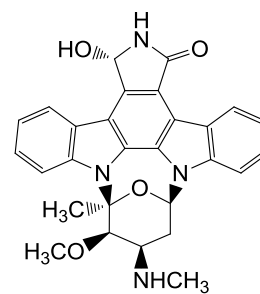
50



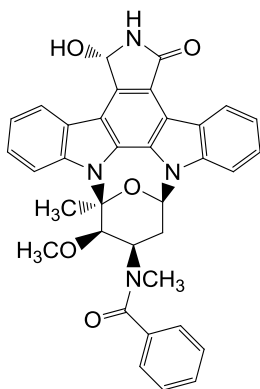
51



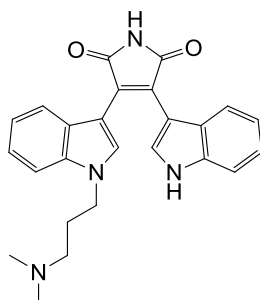
52



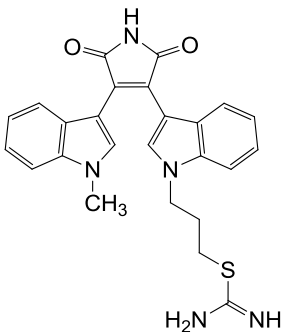
53



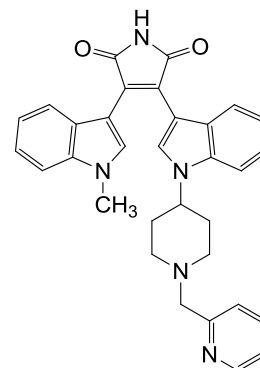
54



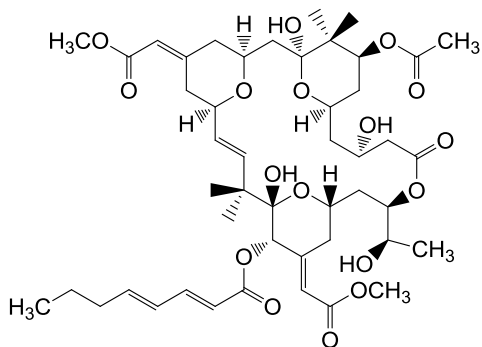
55



56



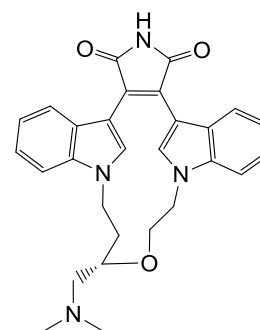
57



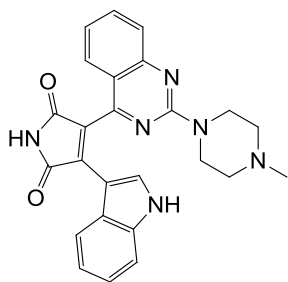
58



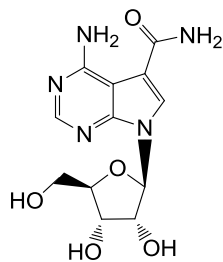
59



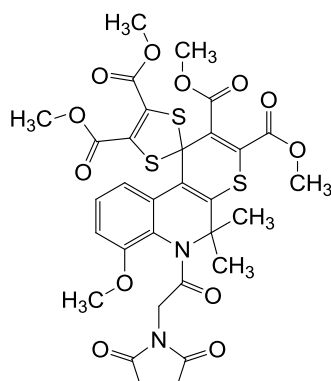
60



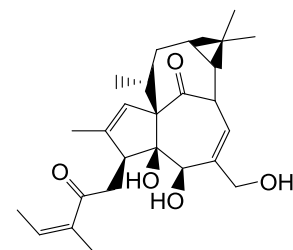
61



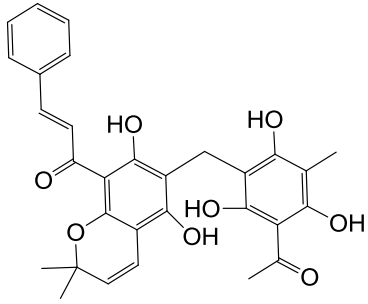
62



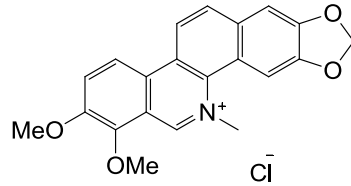
63



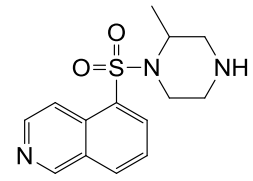
64



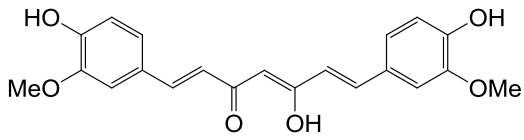
65



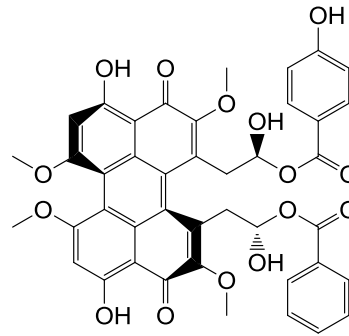
66



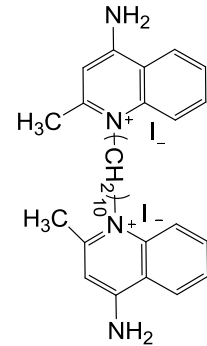
67



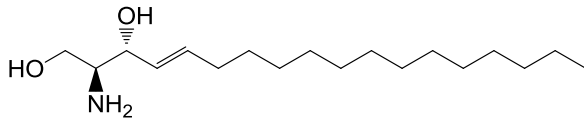
68



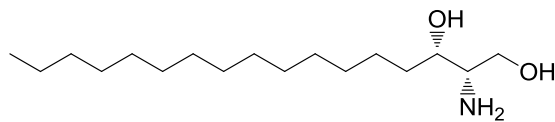
69



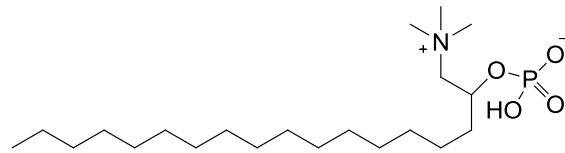
70



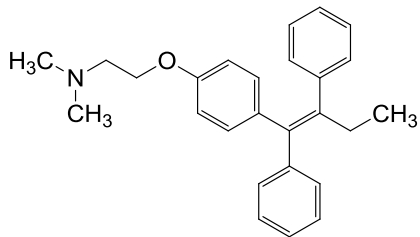
71



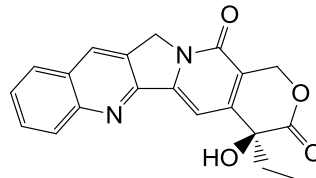
72



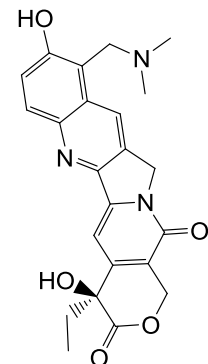
73



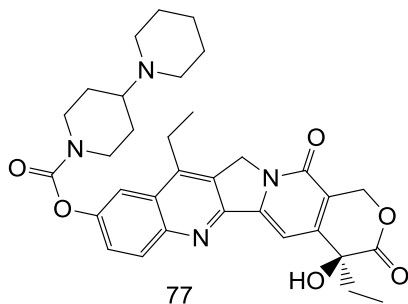
74



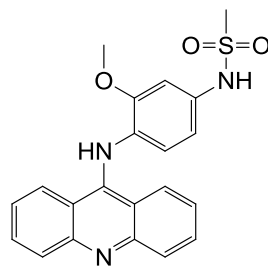
75



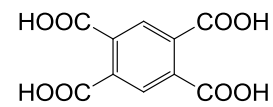
76



77



78



79

List of Figures

Figure 1: Crystal structure of laccase from <i>Trametes versicolor</i> , elaborated with PyMol from crystallographic structure, PDB code 1GYC.	3
Figure 2: Schematic representation of oxidation of phenolic substrates and reduction of molecular oxygen to water by laccase..	5
Figure 3: Proposed protein cross-linking during cuticle sclerotization in pupa of <i>Manduca sexta</i>	6
Figure 4: Synthesized halogen substituted phenols and polyphenols, aminophenols, and di- <i>tert</i> -butyl substituted phenols.....	11
Figure 5: Crystal structure of compound 31	18
Figure 6: Inverse correlation between the laccase oxidation efficiency and oxidation potential of Compounds 1 – 8, 46, 47 , ABTS, 2-aminophenol, catechol, hydroquinone, and 1,2-phenylenediamine..	29
Figure 7: Microscopic slides of larvae of <i>Anopheles gambiae</i> both treated and untreated with compound 16	32
Figure 8: Structure of PQ1, PQ10, PQ11, PQ15, and staurosporine.	64
Figure 9: Schematic representation showing the conserved regions (C1 - C4) and variable regions (V1 - V5) in all three classes of PKC ioszymes.	66
Figure 10: Structures of known PKC inhibitors.	72
Figure 11: Amino acid sequence of C1 peptide and the change in net charge (+1) of nonphosphorylated peptide to the net charge of (-1) of phosphorylated peptide at pH = 7.4.	76

Figure 12: Schematic diagram showing the phosphorylation of C1 peptide by PKC and the separation of phosphorylated and nonphosphorylated C1 peptide by agarose gel electrophoresis..	78
Figure 13: Gel image and graphs of C1 peptide phosphorylation with the amount of PKC.....	85
Figure 14: Gel image and linear correlation between percentage phosphorylation of C1 peptide catalyzed by PKC (15 ng) over time (15 - 60 min).....	86
Figure 15: Gel image, percentage of C1 peptide phosphorylation catalyzed by PKC, and percentage inhibition of PKC phosphorylation in the presence and absence of staurosporine.	88
Figure 16: Gel image, percentage of C1 peptide phosphorylation catalyzed by PKC, and percentage inhibition of PKC phosphorylation in the absence and presence of PQ1.....	90
Figure 17: Gel image, percentage of C1 peptide phosphorylation catalyzed by PKC, and inhibition of PKC phosphorylation in the presence and absence of PQ11.....	92
Figure 18: Gel image, percentage of C1 peptide phosphorylation catalyzed by PKC, and percentage inhibition of PKC in the absence and presence of PQ15.....	93
Figure 19: Gel image and percentage of C1 peptide phosphorylation by PKC in the absence and presence of PQ10. All the reactions have 0.8 μ g of C1 peptide and 15 ng of PKC.	94
Figure 20: IC ₅₀ values of staurosporine (ST), PQ1, PQ11, and PQ15.....	95
Figure 21: Structures of quinoline motif bearing anticancer drugs: camptothecin, topotecan, irinotecan, and amsacrine.....	111
Figure 22: Schematic representation of blood circulation in mammals.	114
Figure 23: Correlation of ratios of peak areas of authentic BTA and PQ1 from HPLC chromatogram and molar ratios of PQ1 and BTA injected..	120

Figure 24: Representative HPLC chromatograms of PQ1 and BTA.....	121
Figure 25: Percentage distribution of PQ1 in various tissues in female C57BL/6J mice in 1, 12, and 24 hours of PQ1 exposure.	122
Figure 26: Concentration of PQ1 (μM) in various tissues in 1, 12, and 24 hours of the drug exposure..	124
Figure 27: Correlation of ratios of peak areas of authentic BTA and PQ11 from HPLC chromatogram and molar ratios of PQ11 and BTA injected.	129
Figure 28: Representative HPLC chromatograms of PQ11 and BTA.....	130
Figure 29: Percentage distribution of PQ11 in various tissues in female C57BL/6J mice in 6, 12, 24, and 36 hours of PQ11 exposure.	132
Figure 30: Concentration of PQ11 (μM) in various tissues in 6, 12, 24, and 36 hours of the drug exposure..	134
Figure 31: Mass spectrum of the eluant corresponding to the peak at 28.8 minutes (Figure 24C) which is identical to the authentic PQ1.....	135
Figure 32: Mass spectrum of the eluant corresponding to the peak at 9.5 minutes (Figure 28C) which is identical to the authentic PQ11.....	136

List of Schemes

Scheme 1: a) Proposed laccase oxidation of <i>p</i> -dihydroquinone 2 to <i>p</i> -quinone 19 and b) Reaction of <i>p</i> -quinone 19 with L-alanine benzyl ester 20 to form a covalently linked adduct 21	8
Scheme 2: Synthesis of compound 2	12
Scheme 3: Synthesis of compound 3 and 4	14
Scheme 4: Synthesis of compound 5	17
Scheme 5: Synthesis of compound 6	18
Scheme 6: Synthesis of compound 7 and 8	20
Scheme 7: Synthesis of compound 9 - 15	21
Scheme 8: a) Synthesis of compound 16 and 17 and b) proposed mechanism for the formation of 16 and 17	24
Scheme 9: Synthesis of MON-0585.....	25
Scheme 10: Schematic representation of the regeneration of BTA from the salt of BTA with PQ compounds	117

List of Tables

Table 1: Percentage phosphorylation of C1 peptide with varying amounts of PKC (0, 5, 15, 20, 30, and 40 ng) as determined by spectrofluorometric analysis.....	84
Table 2: Percentage phosphorylation of C1 peptide with varying amounts of PKC (0, 5, 15, 20, 30, and 40 ng) as determined by photoimaging analysis	84
Table 3: Percentage phosphorylation of C1 peptide with varying time (15 - 60 minutes)	86

Abbreviations

ABTS	2,2'-azino-bis(3-ethylbenzothiazoline-6-sulphonic acid)
aPKC	atypical protein kinase C
ATP	adenosine triphosphate
BTA	1,2,4,5-benzenetetracarboxylic acid
cAMP	cyclic adenosine monophosphate
CK1	casein kinase 1
cPKC	classical protein kinase C
CV	cyclic voltametry
DTT	dithiothreitol
DAG	diacylglycerol
DMAP	4-dimethylaminopyridine
DMF	dimethyl formamide
DMSO	dimethyl sulfoxide
EDTA	ethylenediaminetetraacetic acid
EPR	electronic paramagnetic resonance
ER	estrogen receptor
GI	gastro intestinal tract
GJIC	gap junctional intercellular communication
GPCR	G-protein coupled receptor
HMEC	normal human mammary epithelial cells
HPLC	high performance liquid chromatography
IBX	<i>o</i> -iodoxybenzoic acid

IP	intraperitoneal
IP ₃	inositol triphosphate
IV	intravenous
MAPK	mitogen activated protein kinase
MCPBA	<i>m</i> -chloroperbenzoic acid
MsCP36	<i>Manduca sexta</i> cuticular protein 36
NABD	<i>N</i> -β-alanyldopamine
NADA	<i>N</i> -acetyldopamine
NBS	<i>N</i> -bromosuccinimide
nPKC	novel protein kinase C
PBS	phosphate buffered saline
PDK-1	phosphoinositide dependent kinase 1
PIP ₂	phosphoinositide 4,5-biphosphate
PIP ₃	3-phosphoinositides
PKA	protein kinase A
PKC	protein kinase C
PLC	phospholipase C
PMA	phorbol 12-myrsitate 13-acetate
PQ	polysubstituted quinolines
PS	phosphatidylserine
RTK	receptor tyrosine kinase
TBAF	tetra- <i>n</i> -butylammonium fluoride
THF	tetrahydrofuran

Acknowledgements

I am sincerely thankful to my research advisor, Dr. Duy H. Hua, for his continuous guidance, instructions, and support during my graduate study at Kansas State University. I have always been motivated by his patience, enthusiasm, hard work, immense knowledge, and positive attitude towards research. He has been a role model in my life.

I would like to thank Dr. Michael R. Kanost, Dr. Christer B. Aakeröy, and Dr. Takashi Ito for serving on my PhD committee and helping me with their valuable suggestions. I am thankful to have Dr. R. Scott Beyer as my outside chairperson for the committee.

I would like to thank our collaborators Dr. Michael R. Kanost, Dr. Maureen J. Gorman, and Zeyu Peng for studying the laccase oxidation activities of the synthesized substituted phenols and providing us valuable suggestions for the progress of laccase project. I am thankful to Dr. Kun Yan Zhu for studying mosquito anti-larval activities of the synthesized substituted phenols which highlighted our compounds to have potent anti-larval activities. I am grateful to Dr. Thu Annelise Nguyen for mentoring me in performing cell culture, trypan blue assay, MTT assay, PKC assay, gel electrophoresis, and oral gavage in mice. I also want to thank our collaborators Dr. Thu Annelise Nguyen, Ying Ding, and Stephanie N. Shishido for studying the effect of PQ1 and PQ11 on the tissues of normal mice. I would like to thank Dr. Mafuz Elmastas for mentoring me in performing gel electrophoresis and PKC assay. I am thankful to Dr. Govindsamy VEDIYAPPAN for teaching and allowing me to use his facility for obtaining gel picture and gel quantification and Dr. John Desper for the crystal structure determination.

My PhD would not be possible without the cooperation and help of Ron Jackson and Tobe Eggers for the maintenance of the lab instruments and electronics; Leila Maurmann for the maintenance of NMR instruments; Jim Hodgson for designing and making glass apparatus for

research; and Arlon Meek, Mary Dooley, Kimberly Ross, Lisa Percival, and Ralph Hudson for their continuous support.

I like to thank Thi Nguyen for working with me in the laccase and bioavailability projects and Jianyu Lu for providing PQ compounds for the PKC inhibition and bioavailability studies. I would like to thank my past labmates: Dr. Angelo Aguilar, Dr. Bernard Wiredu, Dr. Sandeep Rana, and Dr. Aibin Shi for their guidance in my research. I am very thankful to my current labmates: Dr. Mahendra Thapa, Laxman Pokhrel, Allan Prior, Duy Le, and Sahani Weerasekara for their love, care, support, and motivation in both of my good and bad times. I can't stop thanking Nepalese Student Association, KSU, Manhattan, Kansas for providing me homely environment during my PhD studies and stay at Manhattan. Thanks to all wonderful people in the department of chemistry.

I like to thank my family and my wife for providing me with care, enough strength, and endless support. Thank to my newly born son for giving me new hope and strength for the future.

My special thanks goes to Kansas State University for providing me this wonderful opportunity to pursue my PhD degree. Above all, I thank almighty god for giving me this wonderful life.

Dedication

I like to dedicate this dissertation to my late sister, Rekha Prasain, who shall always remain in my heart for ever.

Chapter 1. Synthesis, redox potential, laccase substrate activity, and antilarval activity of substituted phenols

1.1 Introduction

Laccases (E.C 1.10.3.2) belong to the family of multi copper oxidases along with ceruloplasmin (E.C 1.16.3.1) and ascorbate oxidase (E.C 1.10.3.3).¹ Laccase was first reported from the sap of *Rhus vernicifera*, a Japanese lacquer tree by Yoshida in 1883.² Laccases are widely distributed among fungi, higher plants, insects, and bacteria and are known to catalyze one electron oxidation of four substrate molecules including substituted *o*-, *m*-, and *p*-phenols, polyphenols, methoxy-phenols, and aromatic amines with subsequent four-electron reduction of molecular oxygen to water.³⁻⁷

Laccases are known to have diverse physiological functions depending on the organism where they are found. Fungi are the largest source of laccases. In fungi, laccases are found to play important roles in activities including lignin biodegradation of wood, pigmentation, morphogenesis, and plant pathogenesis.^{1,8} In plants, laccases are involved in the synthesis of lignin, a component of the plant cell wall and in wound healing.^{4,9} Laccases in bacteria and insects are less studied. In bacteria, laccases are believed to participate in the endospore coat formation, melanin production, morphogenesis, and detoxification.¹⁰ In insects, laccases are believed to participate in sclerotization and tanning of the new exoskeleton.¹¹⁻¹³ These diverse activities of laccases have attracted attention of a large number of researchers. Since only molecular oxygen is required for the catalysis, laccases are useful in many biotechnological applications. Presently, laccases find wide range of applications such as wood pulp bleaching and delignification in paper industries; detoxification and decontamination of industrial wastes,

pesticides, and herbicides; decolorization of dyes in textile industries; color alternation in food and wine industries; medicinal application; and biosensors for phenol or oxygen.^{3,14}

Mosquitoes are the most important vector of human diseases like malaria, dengue, encephalitis, etc.¹⁵ In 2010, about 216 million cases of malaria were estimated with an expected deaths of 655,000 worldwide (World Malarial Report, 2011, WHO). Since laccases have not been reported in vertebrates but are predicted to play important role in insects' cuticle sclerotization,¹¹⁻¹³ a vital process in the growth and survival of the insects including mosquitoes, insecticides selectively inhibiting laccase would have no adverse effect on vertebrates including humans. If laccase substrates upon laccase oxidation produced compound toxic to the mosquito larvae either by covalently bonding to the laccase or by targeting other molecular target within the insect, they could be developed as a potent pro-insecticides to kill mosquito larvae and help in the prevention of mosquito borne diseases like malaria, dengue, etc. Therefore, it is noteworthy to synthesize compounds that disrupt cuticle development in insects by selectively targeting laccase.

Since phenolic compounds like catechols are oxidized by laccase during cuticle sclerotization or tanning in insects,^{16,17} several halogen substituted phenols and polyphenols, amino phenols, and substituted di-*tert*-butyl phenols were synthesized and their redox potential, laccase oxidation activity, and mosquito anti-larval activities were investigated. The synthesized substituted phenols are highlighted in Figure 4.

The redox potentials of these compounds were measured by Thi Nguyen, a graduate student in Dr. Hua's group using the facilities in Dr. Jun Li's laboratory. The laccase substrate activities were measured by Dr. Maureen Gorman and Zeyu Peng in Dr. Michael Kanost

laboratory and the anti-mosquito larval activities were studied in Dr. Kun Yan Zhu's laboratory. All of the above mentioned laboratories are located at Kansas State University.

1.2 Background

1.2.1 Molecular structure of laccase

Laccases, blue multi-copper oxidases, in general are extracellular globular glycoproteins with molar mass of 60-80 kD and isoelectric point ranging from pH 3.0 to 9.0.^{1,18} In laccase, the extent of glycosylation usually ranges between 15 - 20% of the total weight of the protein and is related to secretion, activity, copper retention, and thermal stability of the enzyme.^{1,19} The protein mainly consists of three domains (D1, D2, and D3) with similar β -barrel type architecture as shown in Figure 1.^{20,21}

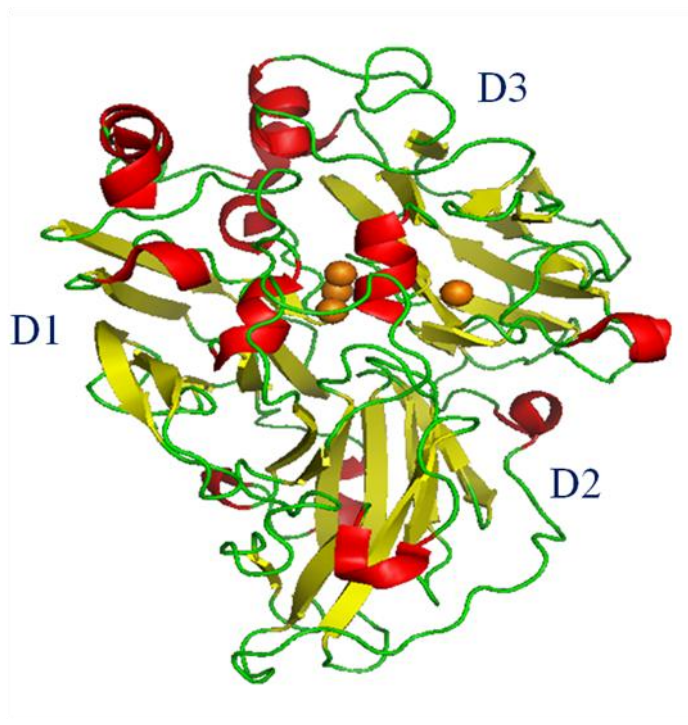


Figure 1: Crystal structure of laccase from *Trametes versicolor*, elaborated with PyMol from crystallographic structure, PDB code 1GYC.

Laccases are commonly found to contain four copper atoms per monomer that include one type I, one type II, and two type III coppers bonded to three redox sites designated as T1, T2 and T3 respectively.¹ These coppers can be differentiated by UV/Vis and electronic paramagnetic resonance (EPR) spectroscopy. In fungal laccase, T1 copper exhibits a planar trigonal geometry by coordinating with one cysteine and two histidines residues through sulfur and nitrogen atoms respectively.⁴ T1 copper is EPR active and the charge transfer transition from the sulfur of cysteine to the T1 copper results in an intense absorbance at around 600 nm giving characteristic deep blue color to the enzyme.⁴ T2 copper is also EPR active but does not show absorbance in the UV/Vis region, whereas two T3 coppers absorb weakly at 330 nm but are EPR silent due to strong antiferromagnetic coupling by a bridging ligand.⁴ One T2 and two T3 copper atoms are arranged in a trinuclear cluster and coordinated to two and six histidines residues, respectively (Figure 2).²² The T1 copper is the primary electron acceptor site in laccase catalyzed reaction, where a single-electron oxidation of a substrate occurs.^{22,23} The electrons from the T1 copper site are transferred through the highly conserved His-Cys-His tripeptide to the T2/T3 copper trinuclear cluster, where four-electron reduction of molecular oxygen to water takes place.^{22,23} The schematic representation of the oxidation of phenolic substrates and the reduction of molecular oxygen to water is highlighted in Figure 2.⁶

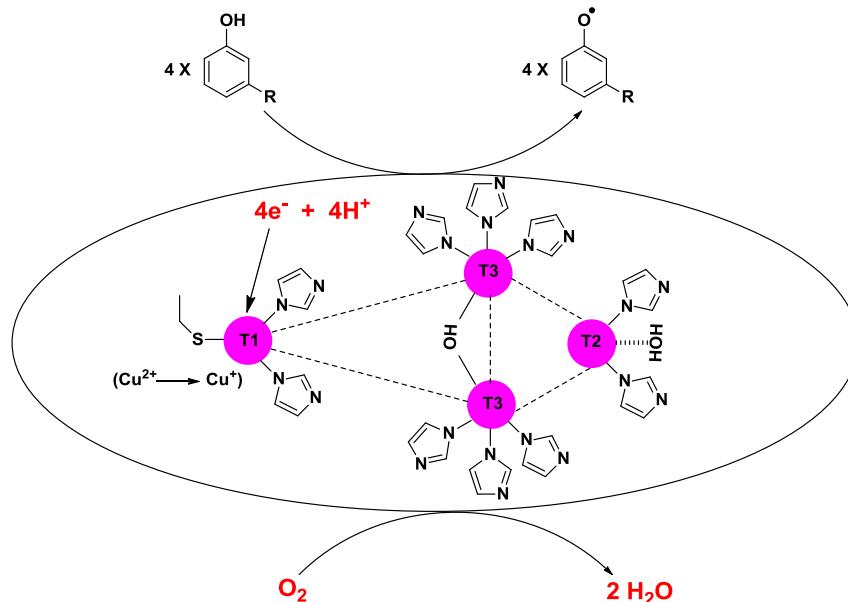


Figure 2: Schematic representation of oxidation of phenolic substrates and reduction of molecular oxygen to water by laccase.⁶ Figure adapted from P. Baldrian, *FEMS Microbiol. Rev.* **2006**, 30, 215-242 with permission from John Wiley and Sons (copyright © 2005).

1.2.2 Insect laccase in cuticle sclerotization

Insect cuticles or exoskeleton are extremely diverse materials differing in both physical and chemical properties, and play important roles in several activities including protection against the environment, excretion, locomotion, and respiration.²⁴ In cuticular sclerotization, *N*-acylcatecholamines in the procuticle are oxidized to *o*-quinones or *p*-quinone methides by laccase and/or tyrosinase followed by the Michael addition of nucleophilic side chain function of histidines and other amino acids of cuticular proteins to form covalently bonded cross-linked adduct as shown in Figure 3.¹²

dsRNAs for tyrosinase gene had no effect on cuticle tanning.¹³ The leading role of laccase in cuticle sclerotization as compared to tyrosinase was further supported by the design of an *in vitro* sclerotization reaction, in which *N*-acylcatecholamines, compounds known to take part in cuticle sclerotization, were incubated with recombinant cuticular proteins MsCP36 derived from the tobacco hornworm, *Manduca sexta* in the presence of laccase and tyrosinase separately.²⁶ Reaction of MsCP36 with *N*- β -alanyldopamine (NABD) and laccase produced cross-linked oligomers and polymers immediately, whereas such cross-linking was not observed in the absence of either NABD or laccase. Substituting laccase with tyrosinase and performing reaction under similar conditions also gave cross-linked products but in lesser extent and the cross-linked product consisted largely of oligomers; no polymers formation was detected.²⁶

1.2.3 Laccase inhibitors

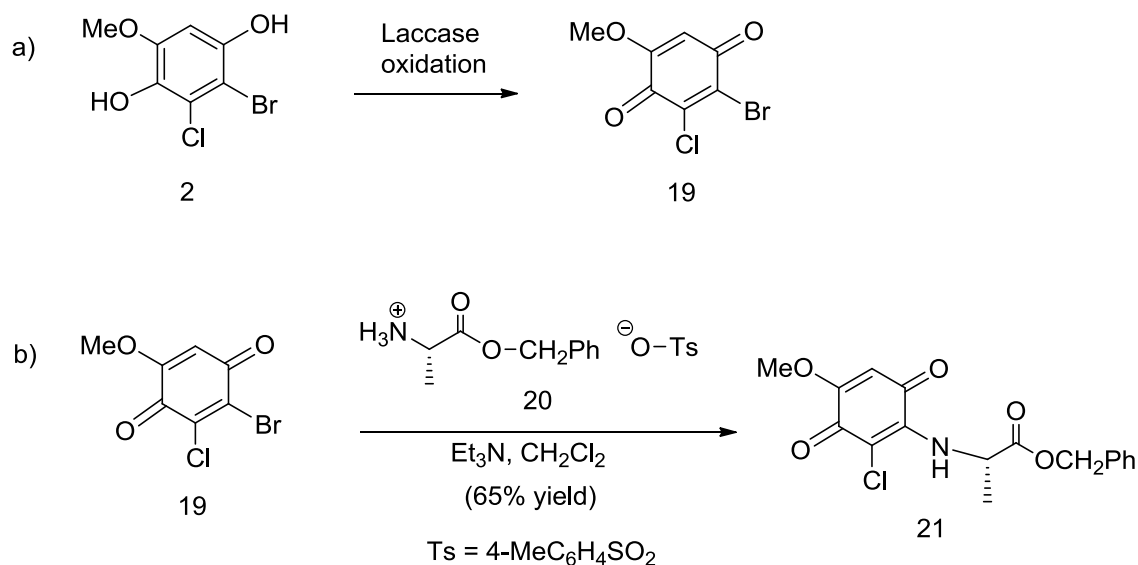
Laccase inhibitors are rare and limited to few inorganic and organic compounds.^{27,28} Small inorganic anions such as the azide, halides, cyanide, and hydroxide have shown to inhibit laccase activity by binding to the T2 and T3 copper atoms disrupting the electron transfer process.^{29,30} Some other laccase inhibitors include sulfhydryl compounds, hydroxyglycine, kojic acid, and cationic quaternary ammonium detergents.^{18,27,31}

1.3 Synthesis

With an objective to synthesize laccase inhibitors several halogen substituted phenols and polyphenols, methoxy-phenols, amino phenols, and substituted di-*tert*-butyl phenols were synthesized (Figure 4).

The synthesis of halogenated phenols (compound **1** – **6**) was based on the idea that: upon laccase oxidation the halogenated phenol would produce reactive cyclic haloenone, which might undergo substitution of halogen moiety by the nucleophilic function such as amino group of lysine or hydroxyl group of serine or tyrosine of laccase resulting in the formation of covalently linked adduct. This covalent linkage might lead to the irreversible inhibition of laccase and disrupt the cuticle sclerotization process in mosquitoes causing their death.

Scheme 1: a) Proposed laccase oxidation of *p*-dihydroquinone **2** to *p*-quinone **19** and b) Reaction of *p*-quinone **19** with L-alanine benzyl ester **20** to form a covalently linked adduct **21**



As expected, *p*-quinone **19**, compound that would form by the laccase oxidation of *p*-hydroquinone **2**, was found to undergo nucleophilic addition-elimination reaction to produce substituted product **21** on treatment with L-alanine benzyl ester *p*-toluenesulfonic acid salt **20** and two equivalents of triethylamine in dichloromethane at 25°C (Scheme 1). The amino function of L-alanine benzyl ester **20** mimics the amino function of lysine residue of laccase.

Synthesized diphenols: **2**, **4**, and **5** are positional isomers having the hydroxyl groups oriented towards para, ortho, and meta positions, respectively. Since the ease of oxidation of diphenols is para (dihydroquinone) > ortho (catechol) > meta (resorcinol),^{32,33} compound **4** (*o*-diol) would show lesser activity than compound **2** (*p*-diol) towards laccase oxidation and produce *o*-quinone. Compound **3** (*o*-diol) also would produce *o*-quinone upon laccase oxidation and is expected to have similar laccase activity as compared to compound **4**. Among the diphenols, compound **5** (*m*-diol) would show lower laccase oxidation activity as compared to its ortho and meta isomers. Compound **1**, on laccase oxidation would produce hydroxymethine quinone and should possess similar laccase oxidation activity as compared to compound **2**. Compound **6** (triol) having both ortho and para oriented hydroxyl groups would have the highest laccase activity among the synthesized halogen substituted phenols. The introduction of methoxy group in phenolic compounds has been found to increase their laccase oxidation activity;³⁴ therefore, the presence of methoxy group in compounds **1**, **2**, **4**, and **5** should enhance their laccase oxidation activity.

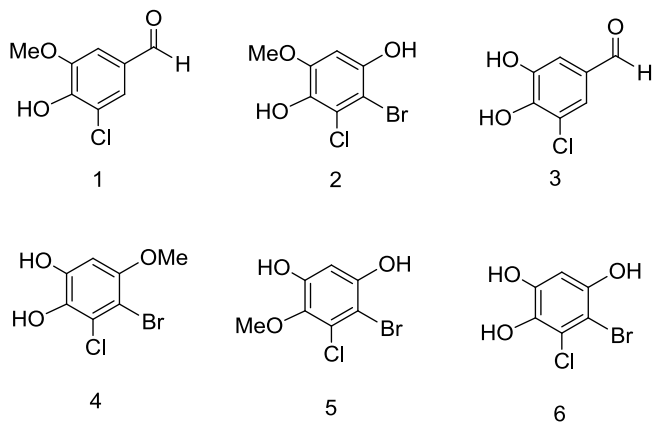
Moreover, the amino function of synthesized *o*-aminophenols **7**³⁵ and **8**³⁶ might strongly bind to the T1 copper of laccase and upon laccase oxidation would produce more reactive iminoquinone. The nucleophilic moieties like amino or hydroxyl function present in the laccase protein close to the T1 copper site might add irreversibly to the iminoquinone producing a covalently linked adduct and inhibit laccase activity.^{37,38}

MON-0585, 2,6-di-*tert*-butyl-4-(α,α -dimethylbenzyl)phenol, developed by Monsanto Co. in the 70's, is a juvenile hormone mimic and found to inhibit cuticle sclerotization in mosquitoes.³⁹ Moreover, 2,6-di-*tert*-butyl phenols are oxidized by Co(II)-Schiff base complex and oxygen to give 4-substituted 2,6-di-*tert*-butyl-6-hydroperoxy-2,4-cyclohexadienones.^{40,41} Therefore, various substituted di-*tert*-butyl phenols **10** – **16** were synthesized as shown in Figure

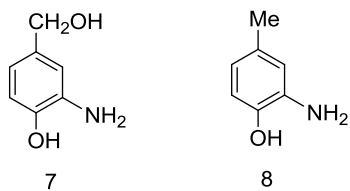
4. Compound **17** was derived as a byproduct during the synthesis of compound **16**. These 4-substituted di-*tert*-butyl phenols may undergo oxidation in the presence of copper and oxygen in the active site of laccase resulting in the formation of phenoxy radicals or corresponding cyclohexadienone disrupting cuticle sclerotization in mosquitoes. As compared to MON-0585, 2,6-di-*tert*-butyl-4-(1-hydroxy-2-methylpropan-2-yl)phenol **11** has an additional primary alcohol group which might lead to its binding with laccase. Furthermore, the alcohol function in compound **11** could be transformed to various functional groups such as aldehyde in compound **12**, carboxylic acid in compound **13**, oxime in compound **14**, and amine in compound **15**. The presence of additional functional group such as -OH, -CHO, -COOH, -N=OH, and -NHR in compounds **11** - **15** as compared to MON-0585 might increase their binding with laccase resulting in the effective disruption of cuticle sclerotization in mosquitoes.

Hence, in this chapter, various halogen substituted phenols and polyphenols, aminophenols, and di-*tert*-butyl phenols were synthesized and their redox potentials, laccase substrate activities, and mosquito anti-larval activities were studied. Synthesis of compound **1** has been previously reported by Dr. Hua's laboratory,⁴² and Compound **13** and **21** were synthesized by Thi Nguyen, a graduate student in Dr. Hua's laboratory.⁴³

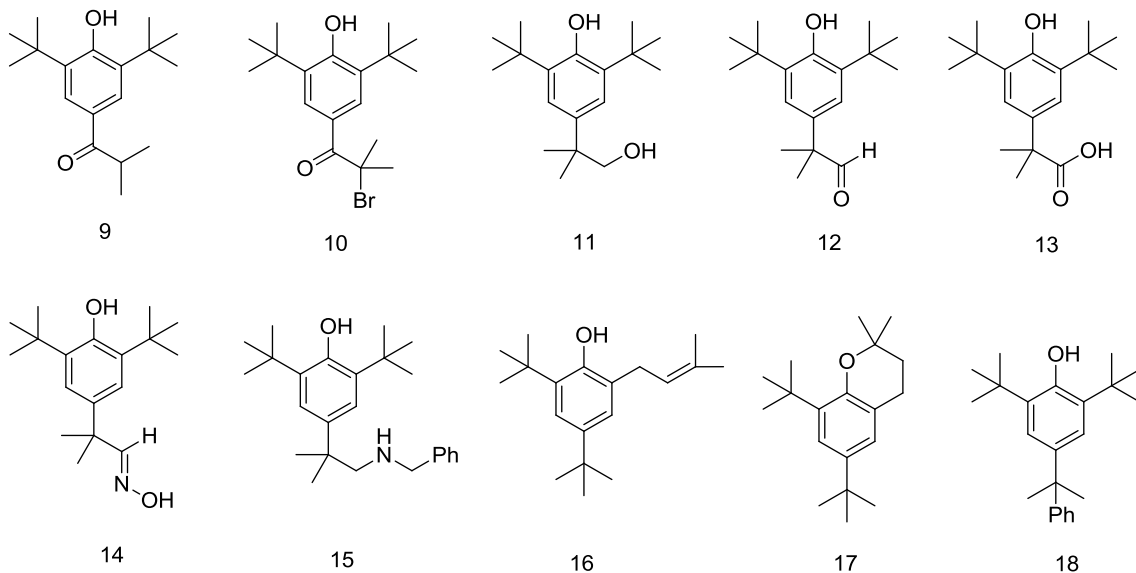
Halogen substituted phenols and polyphenols



Aminophenols



Di-*tert*-butyl substituted phenols



MON-0585

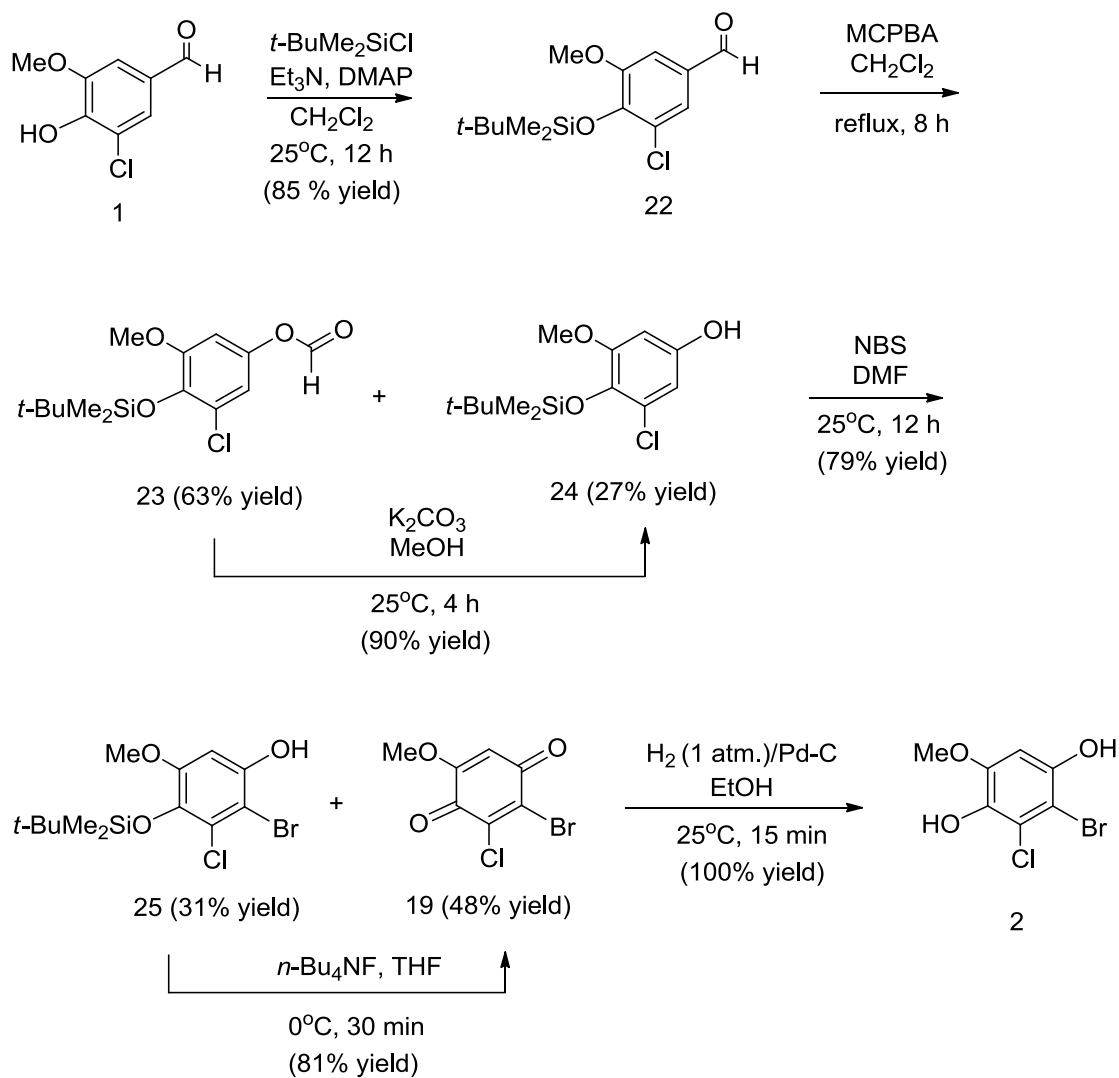
Figure 4: Synthesized halogen substituted phenols and polyphenols, aminophenols, and di-*tert*-butyl substituted phenols.

1.3.1 Synthesis of halogen substituted phenols and polyphenols

1.3.1.1 Synthesis of compound 2

2-Bromo-3-chloro-5-methoxy-1,4-dihydroxybenzene (compound **2**) was synthesized from its precursor 3-chloro-4-hydroxy-5-methoxybenzaldehyde (**1**), an intermediate previously reported by Hua's lab in the synthesis of (+)-chloropuuphenone,⁴² following a sequence of reactions as outlined in Scheme 2.

Scheme 2: Synthesis of compound **2**



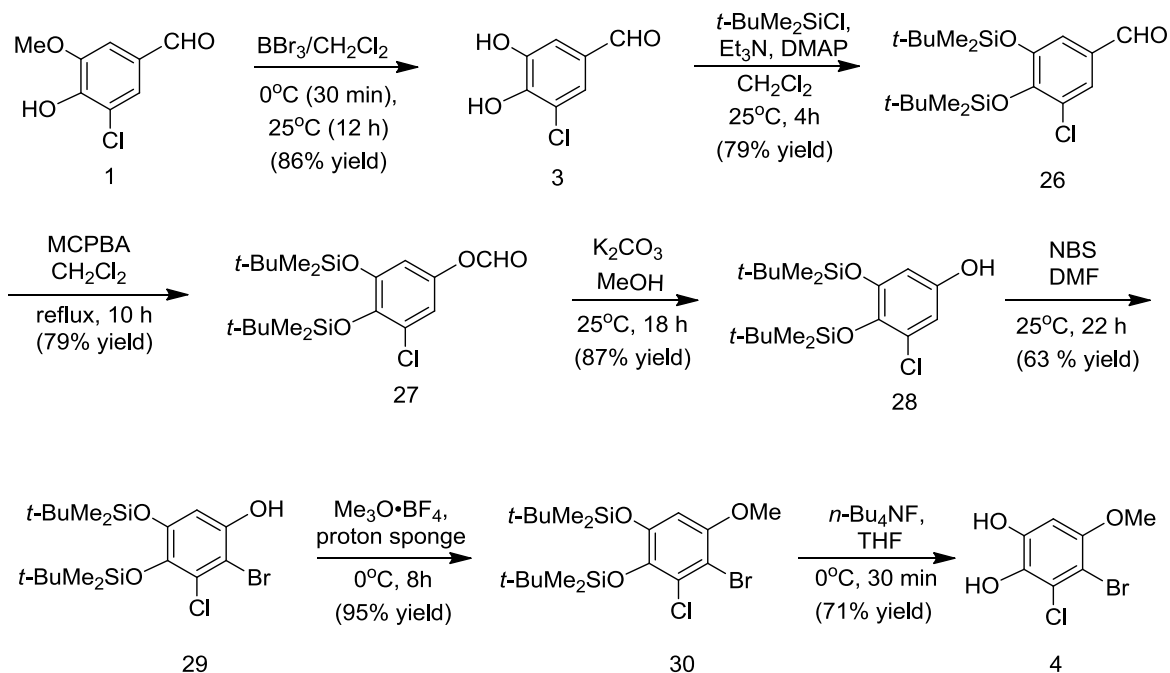
The free hydroxyl function of 3-chloro-4-hydroxy-5-methoxybenzaldehyde (**1**) was protected as silyl ether by the use of *tert*-butyldimethylsilyl chloride in the presence of triethylamine and 4-dimethylaminopyridine (DMAP) in dichloromethane at 25°C for 12 hours to give 4-(*tert*-butyldimethylsilyloxy)-3-chloro-5-methoxybenzaldehyde (**22**) in 85% yield. Baeyer-Villiger oxidation of compound **22** with the use of *m*-chloroperbenzoic acid (MCPBA) in dichloromethane under reflux for 8 hours gave 4-(*tert*-butyldimethylsilyloxy)-3-chloro-5-methoxyphenyl formate (**23**) along with the hydrolyzed product 4-(*tert*-butyldimethylsilyloxy)-3-chloro-5-methoxyphenol (**24**) in the yield of 63% and 27%, respectively. The formate function of compound **23** was hydrolyzed to the phenolic function by basic methanolysis using potassium carbonate (K₂CO₃) in methanol at 25°C for 4 hours to give phenol **24** in 90% yield. The less hindered C-2 position in compound **24** was regioselectively brominated by the use of *N*-bromosuccinimide (NBS) in dimethylformamide (DMF) at room temperature for 12 hours following the literature published by Hua's group in the total synthesis of (+)-chloropuupehenone.⁴² However, bromination of compound **24** under NBS condition gave 2-bromo-3-chloro-5-methoxy-1,4-benzoquinone (**19**) along with the desilylated product 2-bromo-4-(*tert*-butyldimethylsilyloxy)-3-chloro-5-methoxyphenol (**25**) in 48% and 31% yield, respectively. Compound **19** might have formed by the hydrolytic cleavage of silyl ether **25** by the HBr generated from the action of NBS and trace amount of water in the reaction mixture followed by the oxidation to the quinone. NBS oxidation of dihydroquinone to benzoquinone has been previously reported by Barakat et al.⁴⁴ Interestingly, desilylation of compound **25** by the use of tetra-*n*-butylammonium fluoride (TBAF) in THF at 0°C for 30 minutes gave quinone **19** in 81% yield. Reduction of compound **19** in presence of 10% palladium/carbon in ethanol under hydrogen (1 atm.) at 25°C for 15 minutes afforded the desired compound 2-bromo-3-chloro-5-

methoxy-1,4-dihydroxybenzene (**2**) in 100% yield. Infrared spectra of compound **19** does not show a characteristic hydroxyl stretch but shows a quinone stretch at 1683 cm^{-1} , whereas compound **2** shows hydroxyl absorption at 3303 cm^{-1} implying compounds **19** and **2** are quinone and dihydroquinone, respectively.

1.3.1.2 Synthesis of compound 3 and 4

The synthetic route of 3-chloro-4,5-dihydroxybenzaldehyde (**3**) and 4-bromo-3-chloro-5-methoxybenzene-1,2-diol (**4**) is outlined in Scheme 3. Compound **3**, and **26** – **29** were synthesized from 3-chlorovanillin (**1**) following the literature previously reported by Hua's lab.⁴²

Scheme 3: Synthesis of compound **3** and **4**



Compound **3** was obtained in 86% yield by demethylation of 3-chlorovanillin (**1**) with boron tribromide (BBr₃) in CH₂Cl₂ at 0°C for 30 minutes and 25°C for 12 hours. The two hydroxyl functions on C-4 and C-5 position of compound **3** were then protected by the use of *tert*-butyldimethylsilyl chloride, triethylamine, and 4-dimethylaminopyridine (DMAP) in CH₂Cl₂ at 0°C for 1 hour and 25°C for 3 hours to give 3,4-bis(*tert*-butyldimethylsilyloxy)-5-chlorobenzaldehyde (**26**) in 79% yield. Compound **26** on Baeyer-Villiger oxidation using MCPBA (70% pure) in CH₂Cl₂ under reflux for 10 hours afforded 3,4-bis(*tert*-butyldimethylsilyloxy)-5-chlorophenyl formate (**27**) in 79% yield. Basic methanolysis of formate **27** was carried out with K₂CO₃ in methanol at 25°C for 12 hours to give 3,4-bis(*tert*-butyldimethylsilyloxy)-5-chlorophenol (**28**) in 87% yield. The less hindered C-2 position of compound **28** was regioselectively brominated by the use of NBS in DMF for 22 hours to give 2-bromo-4,5-bis(*tert*-butyldimethylsilyloxy)-3-chlorophenol (**29**) in 63% yield; based on the recovery of the starting material. Methylation of the phenolic hydroxyl moiety in compound **29** was achieved by the use of trimethyloxonium tetrafluoroborate (Me₃O⁺•BF₄⁻) in the presence of proton sponge in CH₂Cl₂ at 0°C for 8 hours to give 2-bromo-4,5-bis(*tert*-butyldimethylsilyloxy)-3-chloro-1-methoxybenzene (**30**) in 95% yield. Finally, the desired compound, 4-bromo-3-chloro-5-methoxybenzene-1,2-diol (**4**) was obtained by the desilylation of compound **30** with TBAF in THF at 0°C for 30 minutes in 71% yield.

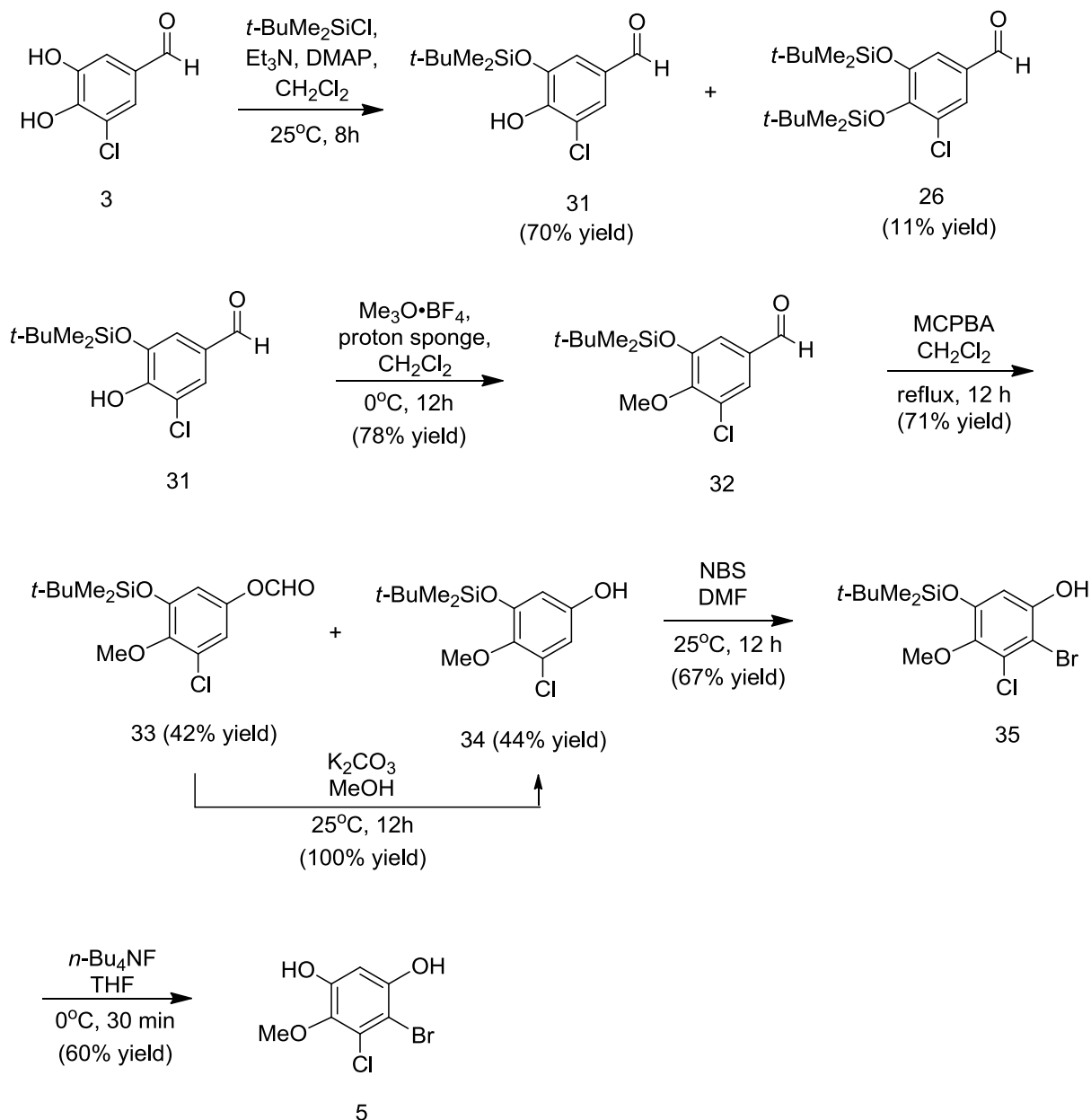
Under TBAF reaction conditions compound **4** does not undergo oxidation to give the corresponding *o*-quinone as that of *p*-dihydroxybenzene **2** which is evident from IR spectrum showing strong hydroxyl absorptions at 3436 cm⁻¹ and 3219 cm⁻¹.

1.3.1.3 Synthesis of compound 5

The synthesis of 4-bromo-5-chloro-6-methoxybenzene-1,3-diol (**5**) is outlined in Scheme 4. Selective protection of hydroxyl moiety on C-5 position of compound **3** was achieved by the use of equivalent amount of *tert*-butyldimethylsilyl chloride in the presence of triethylamine and 4-dimethylaminopyridine (DMAP) in dichloromethane at 25°C for 8 h to give 3-(*tert*-butyldimethylsilyloxy)-5-chloro-4-hydroxybenzaldehyde (**31**) and compound **26** (with both protected hydroxyl groups) in 70% and 11% yield, respectively. The structure of compound **31** was confirmed by single-crystal X-ray analysis as shown in Figure 5. The less hindered C-5 hydroxyl moiety in compound **3** is likely to react faster with *tert*-butyldimethylsilyl chloride than the more hindered C-4 hydroxyl moiety giving compound **31** predominantly. Methylation of the phenolic hydroxyl moiety in compound **31** was achieved by the treatment with trimethyloxonium tetrafluoroborate and proton sponge in dichloromethane at 0°C for 8 hours to give 3-(*tert*-butyldimethylsilyloxy)-5-chloro-4-methoxybenzaldehyde (**32**) in 78% yield; based on the recovery of starting material **31**. Compound **32** on Baeyer-Villiger oxidation by the use of MCPBA (70% pure) in CH₂Cl₂ under reflux for 12 hours afforded 3,4-bis(*tert*-butyldimethylsilyloxy)-5-chloro-4-methoxyphenyl formate (**33**) along with the hydrolyzed product 3-(*tert*-butyldimethylsilyloxy)-5-chloro-4-methoxyphenol (**34**) in 42% and 44% yield, respectively. Basic methanolysis of the formate function in compound **33** with potassium carbonate (K₂CO₃) in methanol at 25°C for 12 hours afforded phenol **34** in quantitative yield. Regioselective bromination on the less hindered C-2 position of compound **34** was achieved by the use of NBS in DMF for 12 hours giving 2-bromo-5-(*tert*-butyldimethylsilyloxy)-3-chloro-4-methoxyphenol (**35**) in 67% yield. Finally, desilylation of compound **35** by treating with TBAF

in THF at 0°C for 30 minutes led to the formation of desired product 4-bromo-5-chloro-6-methoxybenzene-1,3-diol (**5**) in 60% yield.

Scheme 4: Synthesis of compound 5



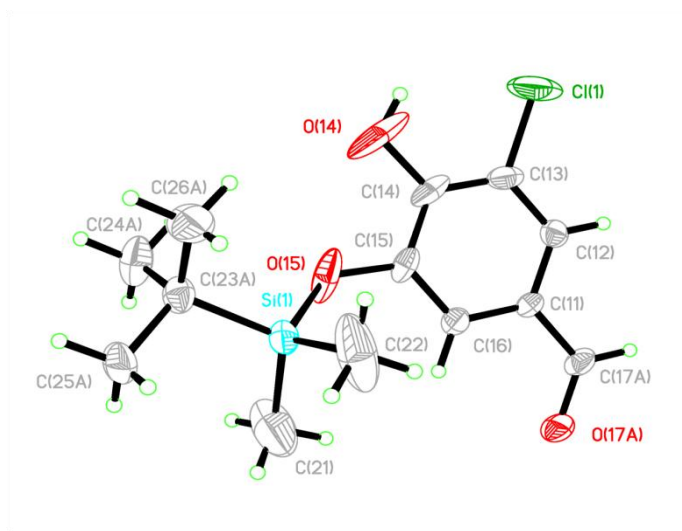
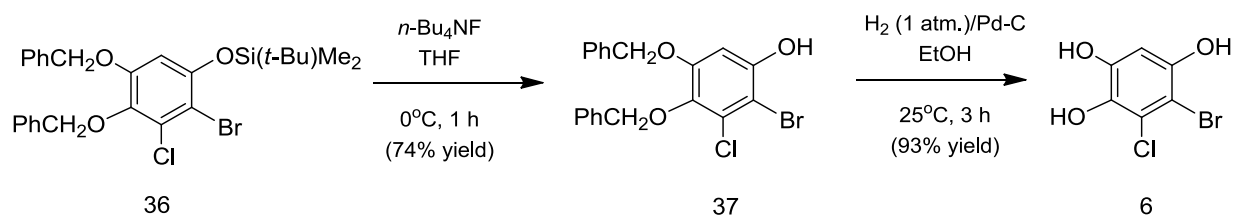


Figure 5: Crystal structure of compound **31**.

1.3.1.4 Synthesis of compound **6**

5-Bromo-6-chlorobenzene-1,2,4-triol (**6**) was synthesized from 4-bromo-3-chloro-1,2-dibenzoyloxy-5-(*tert*-butyldimethylsiloxy)benzene (**36**), an intermediate previously reported by Hua's lab in the synthesis of (+)-chloropuupehenone,⁴² in two steps as outlined in Scheme 5.

Scheme 5: Synthesis of compound **6**



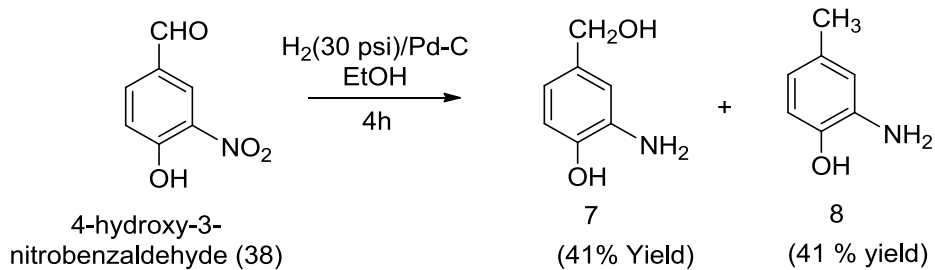
Desilylation of 4-bromo-3-chloro-1,2-dibenzoyloxy-5-(*tert*-butyldimethylsiloxy) benzene (**36**) by the use of TBAF in THF at 0°C for 1 hour afforded 2-bromo-3-chloro-4,5-dibenzoyloxyphenol (**37**) in 74% yield. Finally, removal of two benzyl groups in compound **37** by

catalytic hydrogenation (H_2 , 1 atm.) in the presence of 10% palladium/carbon in ethanol at 25°C for 3 hours gave 5-bromo-6-chlorobenzene-1,2,4-triol (**6**) as the desired product in 93 % yield. The infrared spectrum of triol **6** shows strong hydroxyl absorption at 3382 cm^{-1} . Triol **6** on standing in air produced a black solid which might have resulted from its air oxidation to quinone followed by decomposition. Hence, triol **6** was immediately stored in a dry box under nitrogen atmosphere.

1.3.2 Synthesis of aminophenols 7 and 8

A reaction for the selective reduction of the nitro function in 4-hydroxy-3-nitrobenzaldehyde (**38**) by the use of iron in the presence of acetic acid led to the formation of mixture of several compounds, as indicated by TLC analysis, which could not be separated and analyzed. However, catalytic hydrogenation of 4-hydroxy-3-nitrobenzaldehyde by the use of catalytic amount of palladium/carbon under 30 psi of hydrogen in ethanol for 4 hours gave 2-amino-4-(hydroxymethyl)phenol (**7**)³⁵ and 2-amino-4-methylphenol (**8**)³⁶ each with 41% yield as shown in Scheme 6. The products were formed by the reduction of both nitro and aldehyde functions of 4-hydroxy-3-nitrobenzaldehyde. Compound **8** is formed by the further reduction of benzylic hydroxyl function in compound **7** under hydrogenation condition. No reaction was observed when the catalytic hydrogenation was carried out in the presence of Raney Nickel under similar reaction conditions. On reducing the pressure of hydrogen to 1 atmosphere and time to one hour, compound **7** and **8** were obtained in 24% and 61% yield, respectively.

Scheme 6: Synthesis of compound **7** and **8**

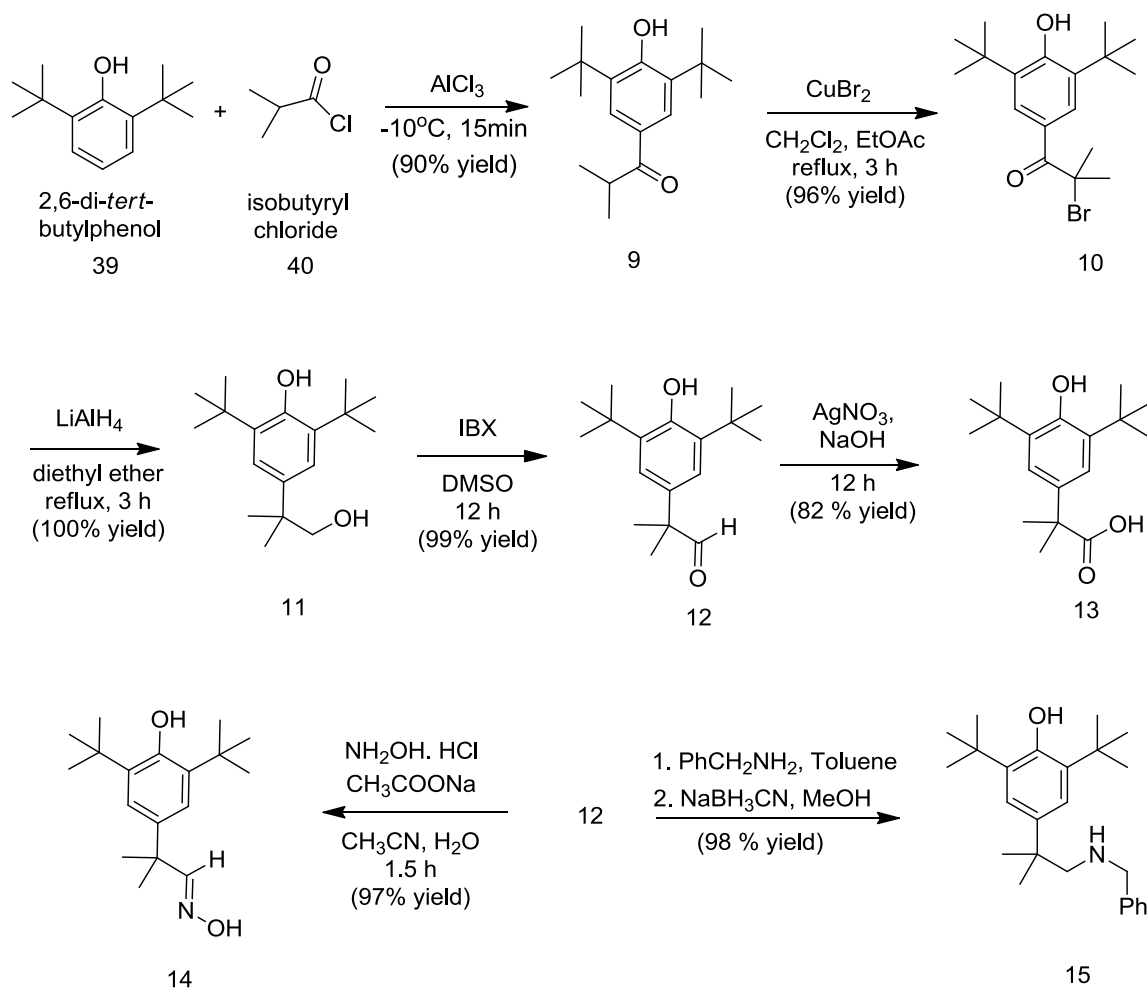


1.3.3 Synthesis of di-*tert*-butyl phenols

1.3.3.1 Synthesis of compounds 9 - 15

MON-0585 (**18**) is a juvenile hormone mimic and implicated as insect growth regulators.⁴⁵ MON-0585 is also known to affect cuticle sclerotization in mosquitoes.³⁹ In search of new anti-larval agents, several 2,6-di-*tert*-butyl phenols **9** – **15** were synthesized mimicking the structure of MON-0585 as outlined in Scheme 7.

Scheme 7: Synthesis of compound 9 - 15



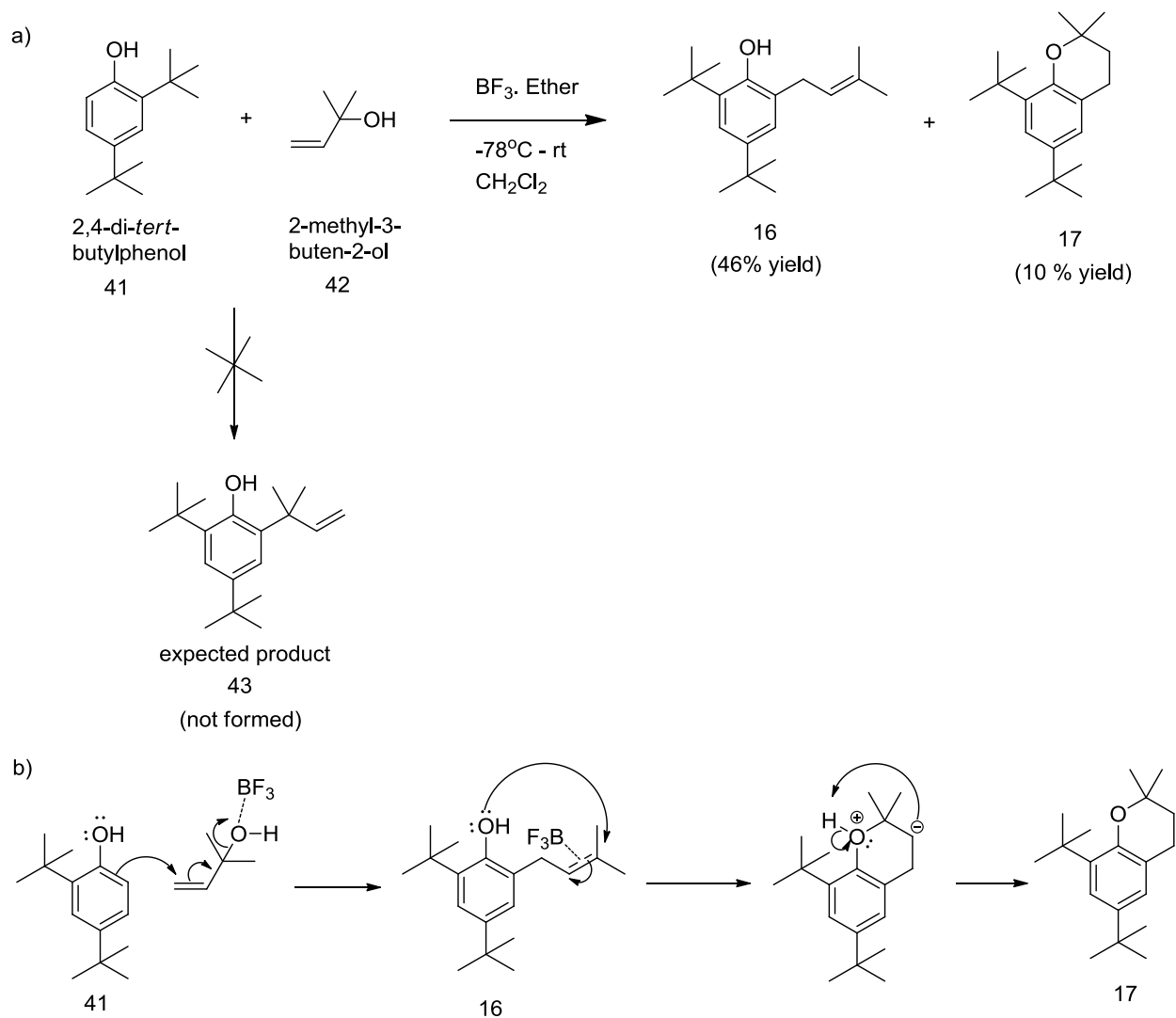
Following the reported procedure,⁴⁶ Friedel-Craft acylation of 2,6-di-*tert*-butylphenol (39) with isobutyryl chloride (40) in the presence anhydrous aluminum chloride (AlCl₃) at -10°C for 15 minutes gave compound 1-(3,5-di-*tert*-butyl-4-hydroxyphenyl)-2-methylpropan-1-one (9) in 90% yield. Bromination of compound 9 with cupric bromide in a solvent mixture of dichloromethane and ethyl acetate for 3 h afforded 2-bromo-1-(3,5-di-*tert*-butyl-4-hydroxyphenyl)-2-methylpropan-1-one (10) in 96% yield which on further treatment with excess of lithium aluminum hydride (LiAlH₄) in dry diethyl ether under reflux for 3 h gave 2,6-di-*tert*-

butyl-4-(1-hydroxy-2-methylpropan-2-yl)phenol (**11**)⁴⁷ in 100% yield.⁴⁷ Compound **11** is likely formed by the hydride attack on the carbonyl carbon followed by aryl group rearrangement.⁴⁷ Compound **11** on oxidation with *o*-iodoxybenzoic acid (IBX) in dimethyl sulfoxide (DMSO) for 12 hours furnished 2-(3,5-di-*tert*-butyl-4-hydroxyphenyl)-2-methylpropanal (**12**) in 99% yield. Aldehyde **12** was further oxidized to 2-(3,5-di-*tert*-butyl-4-hydroxyphenyl)-2-methylpropanoic acid (**13**)⁴¹ in 82% yield by treating with silver oxide, prepared in situ by reacting silver nitrate (AgNO₃) and sodium hydroxide (NaOH) in the solvent mixture of water and 1,4-dioxane at 25°C for 12 hours. Treatment of aldehyde **12** with hydroxylamine hydrochloride and sodium acetate in a solvent mixture of acetonitrile and water (2:1) for 1.5 hour gave (*E*)-2-(3,5-di-*tert*-butyl-4-hydroxyphenyl)-2-methylpropanal oxime (**14**) in 97% yield. The oxime **14** could not be reduced to its corresponding amine on catalytic hydrogenation by the use of 10 % palladium/carbon in ethanol under 30 psi of hydrogen for 16 hours. Reductive amination of aldehyde **12** by the use of benzylamine in toluene under reflux condition for 12 hours followed by the removal of toluene under rotovapor and addition of methanol and sodium cyanoborohydride (NaBH₃CN) gave 4-(1-(benzylamino)-2-methylpropan-2-yl)-2,6-di-*tert*-butylphenol (**15**) in 97% yield. The removal of benzyl group in compound **15** to give its corresponding amine was not achieved under catalytic hydrogenation condition by the use of hydrogen (30 psi) in the presence of 10% palladium/carbon in ethanol for 12 hours. Moreover, increasing the temperature to 50°C had no effect on the reaction and resulted in the recovery of the starting material. Changing the catalyst to platinum oxide (PtO₂) also failed in the removal of benzyl group. The reaction might have failed due to the poisoning of the catalyst by the trace amount of the product formed.

1.3.3.2 Synthesis of compound 16, 17 and MON-0585 (18)

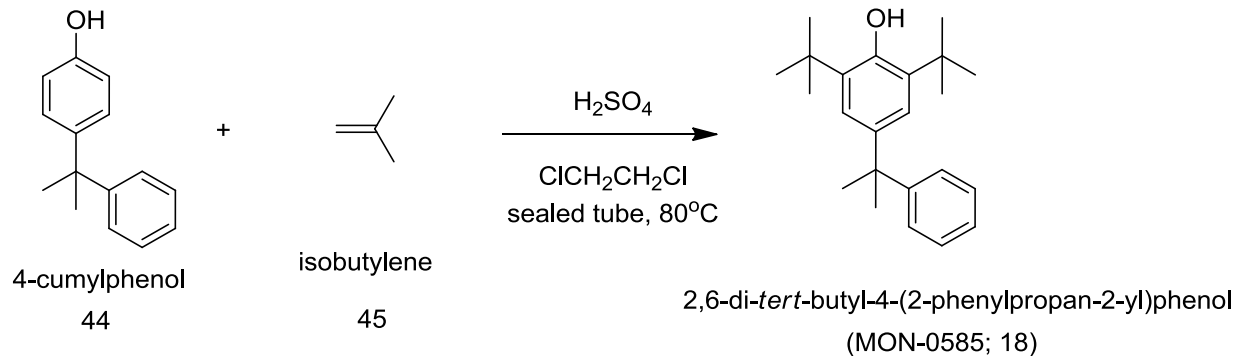
In addition to the 2,6-di-*tert*-butyl phenolic compounds as highlighted in Scheme 7, synthesis of 2,4-di-*tert*-butyl-6-(2-methylbut-3-en-2-yl)phenol (**43**) was envisioned by following Friedel-Crafts alkylation of 2,4-di-*tert*-butyl phenol (**41**) and 2-methyl-3-buten-2-ol (**42**) as highlighted in Scheme 8. Compound **43** would have all the major structural features of MON-0585; moreover, would have an additional side chain with a terminal double bond that could be manipulated into different functional groups as required. However, instead of giving compound **43**, treatment of 2,4-di-*tert*-butyl phenol with 2-methyl-3-buten-2-ol in the presence of borontrifluoro etherate ($\text{BF}_3 \cdot \text{O}(\text{Et})_2$) in dichloromethane at 25°C for 1 hour afforded 2,4-di-*tert*-butyl-6-(3-methyl-2-butenyl)phenol (**16**) and 6,8-di-*tert*-butyl-2,2-dimethyl-3,4-dihydro-2*H*-chromene (**17**) in 46% and 10% yield respectively (Scheme 8a). Benzopyran **17** appears to be derived from an acid-catalyzed ring closing reaction of compound **16** as highlighted in Scheme 8b.

Scheme 8: a) Synthesis of compound **16** and **17** and b) proposed mechanism for the formation of **16** and **17**



Similarly, 2,6-di-*tert*-butyl-4-cumylphenol (**18**) was prepared by a Friedel-Crafts alkylation reaction of 4-cumylphenol (**44**) and isobutylene (**45**) in the presence of catalytic amount of sulfuric acid in dichloroethane in a sealed tube at 80°C for 6 h as shown in Scheme 9.

Scheme 9: Synthesis of MON-0585



1.4 Results and discussions

Laccases are predicted to be vital in the cuticle tanning or sclerotization in insects.¹³ The redox potential of the T1 copper is found to vary from 430 mV to 780 mV depending on the type of laccases.⁴⁸ Moreover, the oxidation of phenols by laccases depends on the redox potential difference between the phenolic compound and the T1 copper, and in many cases the higher the redox potential of T1 copper (or lower the redox potential of the substrates) the higher is the catalytic efficiency of laccases towards the substrates.³⁰ In other words, the laccase catalytic efficiency is inversely correlated with the oxidation potential of substrates.¹⁸ To determine the activity of the synthesized compounds towards laccase, redox potential and laccase substrate activities of these compounds were determined. Inverse correlations between the oxidation potentials and the laccase oxidation efficiency of these compounds was also established.⁴³

The redox potentials of these compounds were measured by Thi Nguyen, a graduate student in Dr. Hua's group using the facilities in Dr. Jun Li's laboratory. The laccase activities were measured by Dr. Maureen Gorman and Zeyu Peng in Dr. Michael Kanost laboratory and the mosquito anti-larval activities were studied in Dr. Kun Yan Zhu's laboratory.

Synthesized compounds **1 – 8** along with two commercially available compounds 3-amino-4-hydroxybenzoic acid (**46**) and 4-amino-3-hydroxybenzoic acid (**47**) were tested for irreversible inhibition of fungal laccase in Dr. Michael Kanost laboratory by Dr. Maureen Gorman and were found to be the substrates but not the inhibitors of laccase.

1.4.1 Redox potentials and laccase substrate oxidation studies

Cyclic voltammetry (CV) experiments were carried out to study the redox properties of compounds **1 - 8, 10 - 17, MON-0585 (18), 46, 47** including other known laccase substrates like hydroquinone, catechol, 2-aminophenol, 1,2-phenylenediamine, and 2,2'-azino-bis-(3-ethylbenzothiazoline-6-sulfonic acid) (ABTS). The known laccase substrates were used as positive control in the experiment. The CV measurements were obtained by Thi Nguyen, a graduate student in Dr. Hua's lab and has been published,⁴³ therefore, only the summary of the result will be highlighted here.

Most of the compounds with the exception to compounds **11 - 13, 16, 17** and **21** showed redox properties (redox potential values) as indicated by the presence of both oxidation and reduction peaks in their cyclic voltammogram. Interestingly, the redox potentials for the synthesized compounds were found in the range of 10 mV to 340 mV; generally lower than the redox potential of T1 copper site in laccases.⁴⁸ Under identical condition, the redox potential of the known laccase substrates like hydroquinone, catechol, 2-aminophenol, 1,2-phenylenediamine, and ABTS were measured as 198 mV, 310 mV, 245 mV, 225mV, and 570 mV, respectively. Therefore, the synthesized compounds having lower or similar redox potentials as that of the known laccase substrates could be easily oxidized by laccase. As expected, *p*-diphenols **2** and **6** (triol) had lower redox potential of 95 mV and 45 mV respectively

as compared to the *o*-diphenols **3** and **4** with 265 mV and 185 mV respectively. Furthermore, the *m*-diphenol **5** was found to have the highest redox potential of 340 mV among the polyphenols. These results are in agreement with the oxidation order of *p*-diphenols > *o*-diphenols > *m*-diphenols.³² Comparing the redox potentials of hydroquinone (198 mV) to compound **1** (95 mV) and catechol (310 mV) to compound **4** (185 mV), it is found that the introduction of electron donating methoxy group in phenolic compound increase their oxidation tendency; which is consistent to previous study.³⁴ Aminophenols **7** and **8** were found to have redox potential of 165 mV and 210 mV respectively and also would be easily oxidized by laccase. However, substituted di-*tert*-butyl phenolic compound **10 - 16**, benzopyran **17**, and MON-0585 (**18**) caused unreliable CV measurements due to their lower solubility in the aqueous PBS buffer solution containing 20% of ethanol. These compounds either showed higher redox potentials (> 530 mV) or failed to show oxidation or reduction wave within the experimental range of + 0.8 to 1.2 V.

Since the redox potential values of water soluble compounds **1 - 8** indicated that they could be easily oxidized by laccase, the laccase oxidation activity of these compounds along with known laccase substrates such as hydroquinone, catechol, 2-aminophenol, 1,2-diphenyleneaminem and ABTS were studied with fungal laccase *Trametes versicolor*.⁴⁹ The known laccase substrates were used as positive control and for comparison. Due to the water insolubility of substituted di-*tert*-butyl phenolic compounds **10 - 16**, benzopyran **17**, and MON-0585 (**18**), they were not oxidized by laccase. Laccase oxidation studies of these compounds were carried by Dr. Maureen Gorman and Zeyu Peng in Dr. Michael Kanost laboratory and the result has been published;⁴³ therefore, only the summary of the result is highlighted here.

The laccase oxidation efficiency (k_{cat}/K_m) for the known laccase substrates: hydroquinone, catechol, 2-aminophenol, 1-2-phenylenediamine, and ABTS against fungal

laccase, *Trametes versicolor* were measured as 35650, 3350, 11840, 2420, and 92890 $\text{min}^{-1}\text{mM}^{-1}$ respectively. Compound **6**, a triol having both ortho- and para-substituted phenolic moieties had the highest laccase oxidation efficiency of 173600 $\text{min}^{-1}\text{mM}^{-1}$. Though, compound **1**, a *p*-diphenol had lower laccase oxidation efficiency (15710 $\text{min}^{-1}\text{mM}^{-1}$) than *p*-hydroquinone, but still was a better laccase substrate as compared to catechol (*o*-diphenol) and 2-aminophenol. Moreover, the *o*-diphenol **4** was found to be better laccase substrate than *m*-diphenol **5** as indicated by their k_{cat}/K_m values of 134500 and 82290 $\text{min}^{-1}\text{mM}^{-1}$, respectively. Comparing the laccase oxidation efficiency of compound **1** (2-methoxy substituted phenol; $k_{cat}/K_m = 2870 \text{ min}^{-1}\text{mM}^{-1}$) with compound **3** (1,2-diol; $k_{cat}/K_m = 47500 \text{ min}^{-1}\text{mM}^{-1}$) and compound **4** (4-methoxy substituted 1,2-diol; $k_{cat}/K_m = 134500 \text{ min}^{-1}\text{mM}^{-1}$) with compound **6** (1,2,4-triol; $k_{cat}/K_m = 173600 \text{ min}^{-1}\text{mM}^{-1}$), indicated that the substitution of methoxy group by hydroxyl group in the phenolic compound increases the laccase oxidation efficiency of the compound. The result also indicated that; higher the number of hydroxyl group in the substrate, greater is the laccase oxidation efficiency of the compound. Moreover, the laccase oxidation efficiency of compound **4** was greater than that of compound **5** indicating that *o*-diphenols are better laccase substrates than *m*-diphenols. Aminophenols **7** and **8** had k_{cat}/K_m values of 71550 and 47250 $\text{min}^{-1}\text{mM}^{-1}$ respectively indicating that they are better oxidized by laccase than 2-aminophenol, a known laccase substrate. However, among the known laccase substrates studied, ABTS was only found to have comparable laccase oxidation efficiency as that of the synthesized polyphenols and aminophenols. In summary, the laccase oxidation efficiency of most of the synthesized polyphenols and aminophenols were found to be higher than that of the known laccase substrates including hydroquinone, catechol, 2-aminophenol, and 1,2-phenylenediamine indicating their role as better laccase substrates.

The redox potential and laccase oxidation efficiency of the compound studied could not be correlated; however, the inverse correlation between the oxidation potential and the laccase oxidation efficiency of the studied compounds including hydroquinone, catechol, 2-aminophenols, 1,2-phenylenediamine, ABTS, compounds **1** - **8**, **34**, and **35** was established and is highlighted in Figure 6. For example, compound **6** with the lowest oxidation potential (80 mV) was found to have the highest laccase oxidation efficiency. On other hand, compound **1** with the highest oxidation potential (670 mV) was found to have the lowest laccase oxidation efficiency.

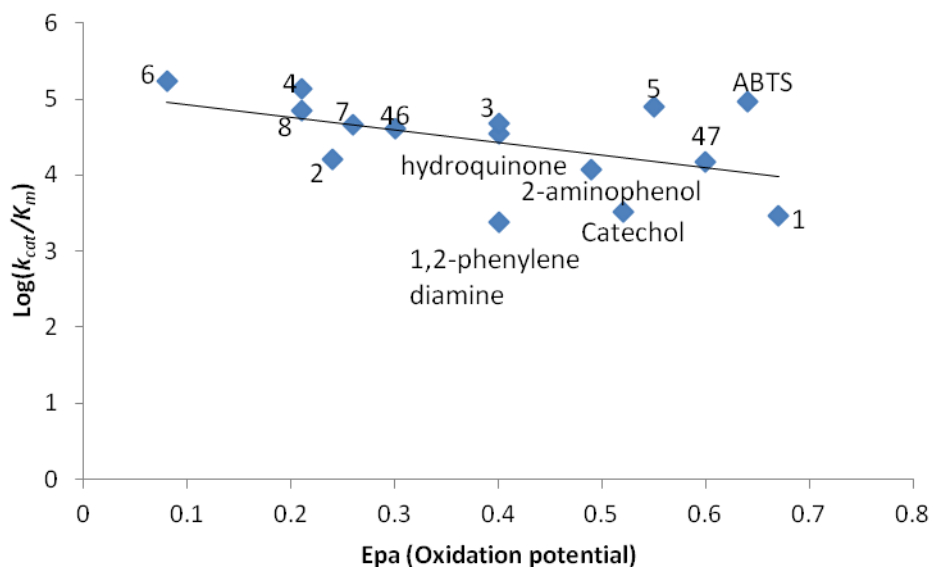


Figure 6: Inverse correlation between the laccase oxidation efficiency and oxidation potential of Compounds **1** – **8**, **46**, **47**, ABTS, 2-aminophenol, catechol, hydroquinone, and 1,2-phenylenediamine.⁴³ Figure adapted from Prasain et al. *Bioorganic & Medicinal Chemistry* **2012**, 20, 1679-1689 with permission from Elsevier (copyright © 2012).

1.4.2 Anti-mosquito larval activities

The phenolic substrates oxidized by laccase are used as the building blocks in the insect cuticle sclerotization,^{16,17} and MON0585, a substituted di-*tert*-butyl phenolic compound is known to disrupt the cuticle sclerotization in insects.³⁹ Therefore, mosquito anti-larval activities of laccase substrates such as triol **6** and dihydroquinone, and various di-*tert*-butyl phenolic compounds including compound **10 - 16**, MON-0585 (**18**), and di-*tert*-butyl substituted benzopyran **17** were investigated in the third-instar larvae of *Anopheles gambiae* in a three-day bioassay. MON-0585 was used as control and for comparison. This study was performed in Dr. Kun Yan Zhu laboratory and the result has been published;⁴³ therefore, only the results are summarized here.

For the anti-larval assay, water soluble compounds like hydroquinone and triol **6** were dissolved in water and used; whereas di-*tert*-butyl phenol derivatives **10 - 16** and benzopyran **17** were first dissolved in acetone and used for the assay in aqueous solution. The toxicity studies were investigated for two concentrations for each compound; 50 and 1000 µg/mL.

Compound **6** and dihydroquinone, water soluble laccase substrates, were not toxic to the larvae at the studied concentrations. Moreover, compound **13** and **15** (used as a sodium salt and trifluoroacetic acid salt, respectively), were also water soluble and also did not produce any toxicity at the studied concentrations. On the other hand, all the water insoluble di-*tert*-butyl phenolic compounds (**10 - 12**, **14**, and **16**) and benzopyran **17** showed more than 46% mortality of larvae at 1000 µg/mL concentration. Interestingly, 2,4-di-*tert*-butyl-6-(3-methylbut-2-en-1-yl)phenol **16** was found to have similar toxicity towards the larvae as compared to MON-0585 at both studied concentrations. Compound **14** and benzopyran **17** also produced significant toxicity to the mosquito larvae with mortality of 93% and 91% at the concentration of 1000 µg/mL. In a

similar study by Spafford et al., it was found that methoprene, an insect growth regulator and commonly used insecticides caused about 60% mortality at 100 µg/L in 3 days bioassay against the third-instar larvae of *Culex molestus*.³⁰ Therefore, compound **16** appears to have higher toxicity than methoprene towards mosquito larvae. In comparison to the water soluble di-*tert*-butyl phenolic compounds (sodium salt of **13** and trifluoroacetic acid salt of amine **15**), dihydroquinone, and compound **4**; water insoluble di-*tert*-butyl phenolic compounds including **10 – 12, 14, 16**, and benzopyran **17** were found to be toxic to the larvae. This suggests that the water insoluble compounds, but not the water soluble compounds, may be absorbed through the body of the larvae resulting in its death.

The larvae treated with di-*tert*-butyl phenolic compounds died over the course of 3 days indicating a target different from the neurological system, a common target in case of most insecticides. The treated larvae died before pupation.

To better understand the effect of compound **16** on the larvae, the microscopic sections of the larvae killed by compound **16** were compared with that of untreated larvae as shown Figure 7. The larvae treated with compound **16** had thin cuticle and appeared to start molting; however, failed to remove the old cuticle. Moreover, the larvae treated with compound **16** showed very little synthesis of new pupal cuticle as compared to the untreated larvae. This phenomenon was observed in all the three parts of the insect studied that is head, thorax, and abdomen. This indicated that the compound **16**, other toxic di-*tert*-butyl phenolic derivative and compound **17** might attack the target related to the insect cuticle formation. However, the target and mechanism of action of these water insoluble di-*tert*-butyl phenolic compounds and benzopyran **17** needs to be investigated.

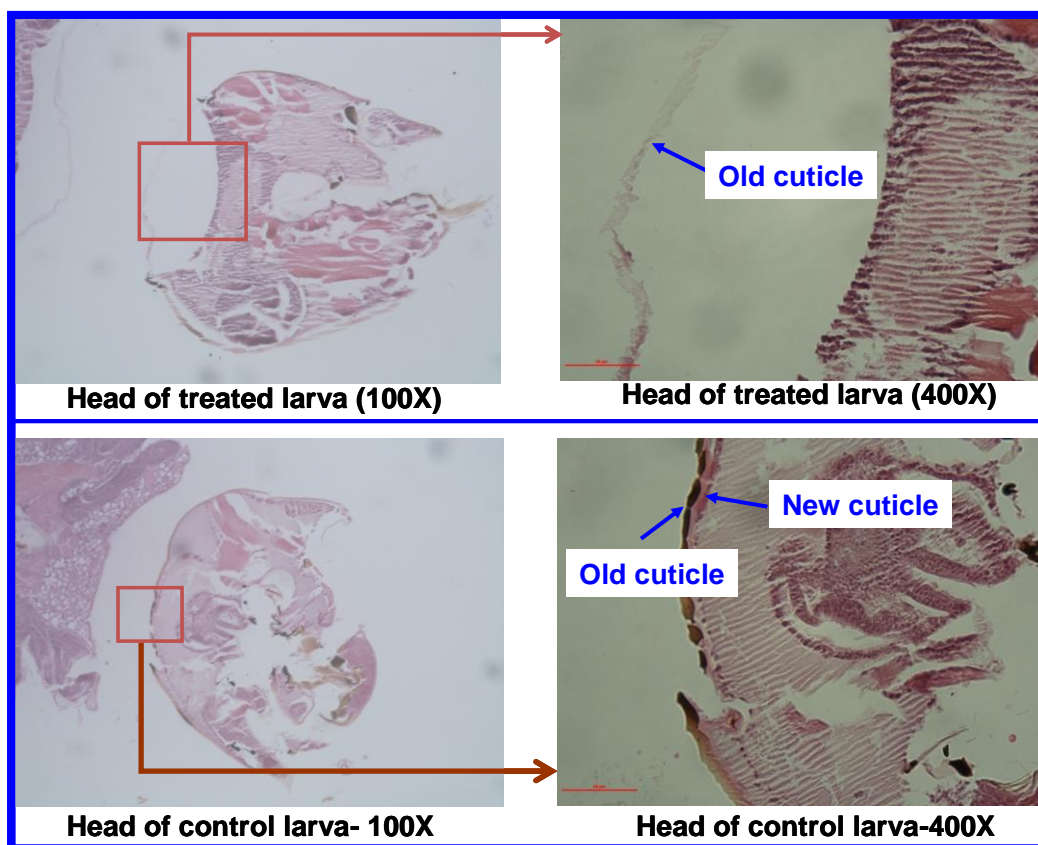


Figure 7: Microscopic slides of larvae of *Anopheles gambiae* both treated and untreated with compound **16**.⁴³ Figure reprinted from Prasain et al. *Bioorganic & Medicinal Chemistry*. **2012**, 20, 1679-1689 with permission from Elsevier (copyright © 2012).

1.5 Conclusions

Since laccase are known to oxidize phenolic compounds during cuticle sclerotization or tanning, various phenolic compounds containing halide, hydroxyl, aldehyde, methoxy, amino, and di-*tert*-butyl functions were synthesized and their redox potential, laccase oxidation, and mosquito anti-larval activities were examined. Synthesized phenolic compounds **1 - 8** were found to be laccase substrates but not the inhibitors of laccase. An inverse correlation between the oxidation potentials and the laccase oxidation activities of these compounds including some known laccase substrates such as dihydroquinone, catechol, 2-aminophenol, 1-2-

phenylenediamine, and ABTS was established indicating that the compounds with lower oxidation potential had higher laccase activities.

Mosquito anti-larval activity studies showed that water insoluble di-*tert*-butyl substituted compound **14**, **16**, and **17** were found to have potent anti-larval activity. Moreover, compound **16** had similar anti-larval activity as compared to that of MON-0585. The mode of action of compound **16** and its target in the disruption of the cuticle formation in mosquito larvae needs further investigation.

1.6 Experimental Section

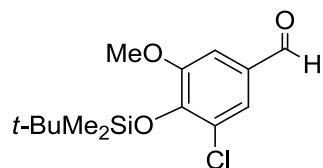
General Methods

Nuclear magnetic resonance (NMR) spectra were recorded on a Varian Unity plus 400 MHz or 200 MHz spectrometer for ^1H and ^{13}C in deuteriochloroform (CDCl_3), unless otherwise indicated. Tetramethylsilane was used as the internal reference and the data reported in ppm. Infrared (IR) spectra were recorded on a Nicolet 380 FT-IR and are reported in wavenumbers (cm^{-1}). High-resolution Mass spectra were recorded on LCT Premier (Waters corp., Milford MA), a time of flight mass analyzer with an electrospray ion source. Column chromatography was carried out on silica gel (200 – 400 mesh) from Natland International Corporation. Tetrahydrofuran (THF) and diethyl ether were dried and distilled over sodium and benzophenone, methylene chloride was dried and distilled over calcium hydride (CaH_2), and toluene was dried and distilled over LiAlH_4 . The purity of compounds, **1** - **17** and MON 0585 were found to be ~ 98% as indicated by HPLC analysis carried on Varian Prostar 210 with a UV-

Vis detector and a reverse phase column from Phenomenex (250 x 21.20 mm, 10 micron, S. No: 552581-1).

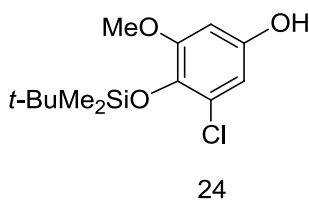
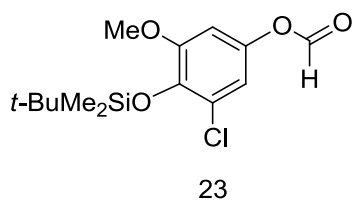
Experimental section for synthesis

4-(*tert*-Butyldimethylsilyloxy)-3-chloro-5-methoxybenzaldehyde (**22**)



To a solution of 400 mg (2.15 mmol) of 3-chloro-4-hydroxy-5-methoxybenzaldehyde (**1**)⁴² in 5 mL of dichloromethane at 0°C under argon, were added 0.6 mL (4.3 mmol) of triethylamine, 40 mg (0.33 mmol) of 4-dimethylaminopyridine (DMAP), and 648 mg (4.3 mmol) of *tert*-butyldimethylsilyl chloride and the solution was stirred at 25°C for 12 hours. The reaction was diluted with 100 mL of diethyl ether and washed with 20 mL of saturated aqueous NH₄Cl solution, 20 mL of water, and 20 mL of brine. The organic layer was dried over anhydrous MgSO₄, solvent evaporated, and the crude was column chromatographed on silica gel using a mixture of hexane and diethyl ether (4:1) as eluent to give 550 mg of 4-(*tert*-butyldimethylsilyloxy)-3-chloro-5-methoxybenzaldehyde (**22**) in 85% yield. ¹H NMR δ 9.76 (s, 1 H), 7.45 (d, *J* = 2.0 Hz, 1 H), 7.27 (d, *J* = 2.0 Hz, 1 H), 3.85 (s, 3 H), 1.01 (s, 9 H), 0.21 (s, 6 H); ¹³C NMR δ 190.0, 151.9, 147.7, 130.0, 126.6, 126.3, 108.4, 55.6, 25.8 (3 C), 19.0, -3.8 (2 C); HRMS calcd for C₁₄H₂₂ClO₃Si (M+H⁺) 301.1021, found 301.1028.

4-(*tert*-Butyldimethylsilyloxy)-3-chloro-5-methoxyphenyl formate (23) & 4-(*tert*-butyldimethylsilyloxy)-3-chloro-5-methoxyphenol (24)

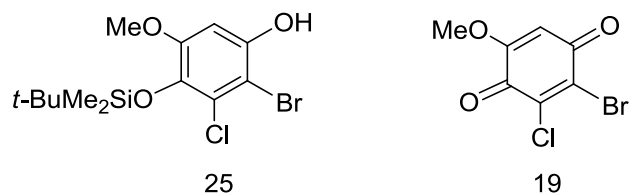


To a solution of 600 mg (2 mmol) of 4-(*tert*-butyldimethylsilyloxy)-3-chloro-5-methoxybenzaldehyde (**22**) in 5 mL of dichloromethane at 0°C under argon, was added 750 mg (3 mmol) of *m*-chloroperbenzoic acid (70% pure) and heated to reflux for 8 hours. The reaction was cooled to room temperature and 5 mL of aqueous sodium thiosulfate and 200 mL of diethyl ether were added to it. The solution was washed with 20 mL of saturated aqueous NaHCO₃, 20 mL of water, and 20 mL of brine. The organic layer was dried over anhydrous MgSO₄, solvent evaporated, and the crude was column chromatographed on silica gel using a mixture of hexane and diethyl ether (5:1) as eluent to give 400 mg of 4-(*tert*-butyldimethylsilyloxy)-3-chloro-5-methoxyphenyl formate (**23**) and 150 mg of 4-(*tert*-butyldimethylsilyloxy)-3-chloro-5-methoxyphenol (**24**) in 63% and 27% yield, respectively. **Formate 23:** ¹H NMR δ 8.26 (s, 1H, OCHO), 6.78 (d, *J* = 2.9 Hz, 1 H), 6.58 (d, *J* = 2.9 Hz, 1 H), 3.80 (s, 3 H), 1.03 (s, 9 H), 0.20 (s, 6 H); ¹³C NMR δ 159.3, 151.8, 143.2, 140.4, 125.9, 114.4, 104.1, 55.7, 26.0, 19.0, -3.9; HRMS calcd for C₁₄H₂₂ClO₄Si (M+H⁺) 317.0976, found 317.0968. **Phenol 24:** ¹H NMR δ 6.43 (d, *J* = 2.9 Hz, 1 H), 6.32 (d, *J* = 2.9 Hz, 1 H), 3.78 (s, 3 H), 1.02 (s, 9 H), 0.17 (s, 6 H); ¹³C NMR δ 152.2, 149.8, 135.8, 125.7, 108.2, 99.2, 55.5, 26.1 (3 C), 19.0, -4.0 (2 C); HRMS calcd for C₁₃H₂₂ClO₃Si (M+H⁺) 289.1027, found 289.1000.

Conversion of formate **23** to phenol **24**

To a solution of 45 mg (0.142 mmol) of 4-(*tert*-butyldimethylsilyloxy)-3-chloro-5-methoxyphenyl formate (**23**) in 2 mL of methanol, was added 98 mg (0.71 mmol) of K₂CO₃ and stirred at 25°C for 4 hours. The reaction was diluted with 100 mL of diethyl ether and washed with 10 mL of aqueous NH₄Cl, 10 mL of water, and 10 mL of brine. The organic layer was dried over anhydrous MgSO₄, solvent evaporated, and the crude was column chromatographed on silica gel using a mixture of hexane and diethyl ether (2:1) as eluent to give 37 mg of phenol **24** in 90% yield, which ¹H NMR spectrum is identical to that described above.

2-Bromo-4-(*tert*-butyldimethylsilyloxy)-3-chloro-5-methoxyphenol (**25**) & 2-bromo-3-chloro-5-methoxy-1,4-benzoquinone (**19**)



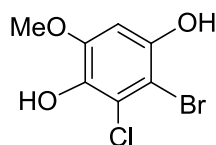
To a solution of 84 mg (0.29 mmol) of 4-(*tert*-butyldimethylsilyloxy)-3-chloro-5-methoxyphenol (**24**) in 2 mL of DMF under argon, was added 57 mg (0.32 mmol) of NBS and was stirred at 25°C for 12 h. The reaction solution was diluted with 100 mL of diethyl ether and washed with 10 mL of water followed by 10 mL of brine. The organic layer was dried over anhydrous MgSO₄, solvent evaporated, and the crude was column chromatographed on silica gel using a gradient mixture of hexane and diethyl ether as eluent to give 27 mg of 2-bromo-4-(*tert*-butyldimethylsilyloxy)-3-chloro-5-methoxyphenol (**25**) and 35 mg of 2-bromo-3-chloro-5-methoxy-1,4-benzoquinone (**19**) in 31% and 48% yield, respectively. **Bromophenol 25**: ¹H NMR δ 6.56 (s, 1 H), 5.33 (s, 1 H, OH), 3.78 (s, 3 H), 1.03 (s, 9 H), 0.18 (s, 6 H); ¹³CNMR δ

151.5, 147.4, 136.8, 125.8, 101.5, 98.4, 55.6, 26.1, 19.0, -3.9; HRMS calcd for C₁₃H₁₉BrClO₃Si (M-H) 364.9975, found 365.0076; C₁₃H₂₀BrClO₃SiNa (M+Na⁺) 388.9951, found 388.9934. *p*-**Benzoquinone 16** (light yellow solid): Mp. 167 – 170°C; IR (neat) ν 2953, 2913, 2839, 1683, 1638, 1613, 1556, 1454, 1229, 1168 cm⁻¹; ¹H NMR δ 6.16 (s, 1 H), 3.89 (s, 3 H); ¹³C NMR δ 177.5, 172.4, 158.9, 137.4, 107.9, 107.2, 57.3; HRMS calcd for C₇H₅BrClO₃ (M+1⁺) 250.9105, found 251.0593.

Conversion of silyl ether **25** to *p*-benzoquinone **19**

To a solution of 25 mg (0.068 mmol) of silyl ether **25** in 2 mL of THF was added 68 μ L (0.068 mmol) of *n*-Bu₄NF (1 M in THF) and stirred under argon from 0°C for 30 minutes. The reaction was diluted with 50 mL of diethyl ether and washed with 10 mL of aqueous NH₄Cl, 10 mL of water, and 10 mL of brine. The organic layer was dried over anhydrous MgSO₄, solvent evaporated, and the crude was column chromatographed on silica gel using a mixture of hexane and diethyl ether (1:1) as eluent to give 14 mg of *p*-benzoquinone **19** in 81% yield, which ¹H NMR spectrum is identical to that described above.

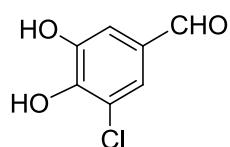
2-Bromo-3-chloro-5-methoxy-1,4-dihydroxybenzene (**2**)



A mixture of 10 mg (0.040 mmol) of 2-bromo-3-chloro-5-methoxy-1,4-benzoquinone (**19**) and 2 mg of 10% palladium over carbon in 1 mL of ethanol under 1 atm. of hydrogen (a balloon filled with hydrogen connected to the round bottom flask) was stirred at 25°C for 15 minutes, filtered through Celite, and rinsed with 10 mL of ethanol. The filtrate was concentrated

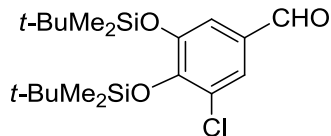
to give 10 mg of 2-bromo-3-chloro-5-methoxy-1,4-dihydroxybenzene (**2**) in quantitative yield: IR (neat) ν 3303, (s), 2935, 2851, 1601, 1497, 1441, 1210, 1071, 1046, 994, 864, 842, 825 cm^{-1} ; ^1H NMR δ 6.60 (s, 1 H), 5.50 (bs, 1 H, OH), 5.30 (bs, 1 H, OH), 3.89 (s, 3 H, OMe); ^{13}C NMR δ 148.2, 147.7, 136.7, 121.1, 100.2, 99.4, 56.0; HRMS calcd for $\text{C}_7\text{H}_6\text{BrClO}_3$ (M^+) 251.9189, found 252.0427.

3-Chloro-4,5-dihydroxybenzaldehyde (**3**)⁴²



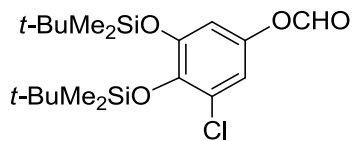
To a solution of 10.14 g (5.43 mmol) of 3-chloro-4-hydroxy-5-methoxybenzaldehyde (**1**)⁴² in 40 mL of dry CH_2Cl_2 at 0°C , was added 564 μL (6 mmol) of boron tribromide (BBr_3) drop wise and the mixture was stirred under argon at 0°C for 30 minutes and then at 25°C for 12 hours. The reaction was quenched with the slow addition of 50 mL of methanol followed by the solvent evaporation under rotavap. The addition and evaporation of methanol were repeated 3 times (50 mL each time) to remove excess BBr_3 . The crude was then treated with 30 mL of 1:1 hexane and diethyl ether solution, filtered and washed with small amount of 1:1 hexane and diethyl ether solution to get 8.8 g (93.9%) of 3-chloro-4,5-dihydroxybenzaldehyde (**3**)⁴² as pure green solid. ^1H NMR (Acetone-*d*6) δ 9.78 (s, 1H), 7.47 (d, $J = 2.0$ Hz), 7.34 (d, $J = 2.0$ Hz); ^{13}C NMR (Acetone-*d*6) δ 190.6, 148.8, 147.4, 130.8, 125.2, 121.5, 113.8.

3,4-Bis(*tert*-butyldimethylsilyoxy)-5-chlorobenzaldehyde (**26**)⁴²



To a solution of 800 mg (4.64 mmol) of 3-chloro-4,5-dihydroxybenzaldehyde (**3**)⁴² and 170 mg (1.39 mmol) of 4-dimethylaminopyridine (DMAP) in 10 mL of dry CH₂Cl₂ at 0°C under argon, were added 2.6 mL (18.56 mmol) of triethyl amine and 2.8 g (18.56 mmol) of *tert*-butyldimethylsilyl chloride and stirred at 0°C for 1 hour and then at 25°C for 3 hours. The reaction was diluted with 100 mL of diethyl ether, washed with 20 mL of NH₄Cl (aq.) followed by 20 mL of brine, dried over anhydrous MgSO₄, and the solvent evaporated. The crude was column chromatographed on silica gel using a 10:1 mixture of hexane and diethyl ether as eluent to give 1.46 g of desired 3,4-bis(*tert*-butyldimethylsilyoxy)-5-chlorobenzaldehyde (**26**)⁴² in 79% yield. ¹H NMR δ 9.78 (s, 1 H), 7.50 (d, *J* = 2 Hz, 1 H), 7.29 (d, *J* = 2 Hz, 1 H), 1.05 (s, 9 H), 0.99 (s, 9 H), 0.27 (s, 6 H), 0.24 (s, 6 H); ¹³C NMR δ 190.1, 149.9, 149.4, 130.3, 128.0, 126.0, 119.0, 26.3 (3 C), 26.2 (3 C), 19.0, -3.2, -3.4; HRMS calcd for C₁₉H₃₄ClO₃Si₂ (M+H⁺) 401.1735, found 401.1747.

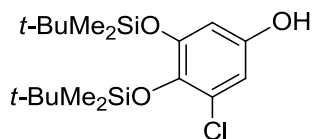
3,4-Bis(*tert*-butyldimethylsilyoxy)-5-chlorophenyl formate (**27**)⁴²



To a solution of 1.014 g (5.43 mmol) of the 3,4-bis(*tert*-butyldimethylsilyoxy)-5-chlorobenzaldehyde (**26**) in 20 mL of dry CH₂Cl₂ was added 1.6 g (6.45 mmol) of *m*-chloroperoxybenzoic acid (70% pure) and refluxed at 50°C for 10 hours. The reaction was

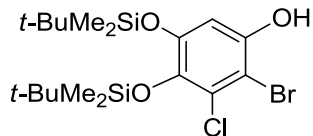
diluted with 500 mL of diethyl ether, washed with 100 mL of NaHCO₃ (aq.), 100 mL of water and 100 mL of brine. The organic layer was dried over anhydrous MgSO₄, solvent evaporated, and the crude was column chromatographed on silica gel using a mixture of diethyl ether and hexane (10:1) as eluent to give 1.42 g of 3,4-bis(*tert*-butyldimethylsilyloxy)-5-chlorophenyl formate (**27**)⁴² in 79% yield. ¹H NMR δ 8.22 (s, 1 H, OCHO), 6.79 (d, *J* = 3.2 Hz, 1 H), 6.58 (d, *J* = 3.2 Hz, 1 H), 1.03 (s, 9 H, *t*-Bu), 0.96 (s, 9 H, *t*-Bu), 0.22 (s, 6 H, Me), 0.19 (s, 6 H, Me); ¹³C NMR δ 159.0 (CHO), 148.8, 143.0, 142.4, 127.1, 115.5, 113.1, 26.2 (6 C, *t*-Bu), 18.8 (2 C, *t*-Bu), -3.3 (2 C, Me), -3.6 (2 C, Me).

3,4-Bis(*tert*-butyldimethylsilyloxy)-5-chlorophenol (**28**)⁴²



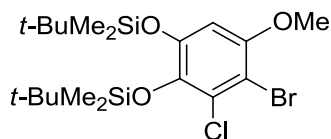
To a solution of 1.24 g (3 mmol) of 3,4-bis(*tert*-butyldimethylsilyloxy)-5-chlorophenyl formate (**27**) in 30 mL of methanol, was added 2.21 g (15 mmol) of K₂CO₃ and stirred at room temperature for overnight. The reaction was diluted with 70 mL ethyl acetate and washed with 20 mL of NH₄Cl (aq.) followed by 20 mL of brine. The organic layer was dried over anhydrous MgSO₄ and solvent evaporated to give 0.6 g of 3,4-bis(*tert*-butyldimethylsilyloxy)-5-chlorophenol (**28**)⁴² which was used in the next step without further purification. ¹H NMR δ 6.47 (d, *J* = 2.9 Hz, 1 H), 6.30 (d, *J* = 2.9 Hz, 1 H), 1.02 (s, 9 H, *t*-Bu), 0.97 (s, 9 H, *t*-Bu), 0.22 (s, 6 H, Me), 0.17 (s, 6 H, Me); ¹³C NMR δ 149.7, 148.9, 137.7, 126.9, 109.8, 107.8, 26.3 (3 C), 26.2 (3 C), -3.6 (2C, Me), -3.4 (2 C, Me).

2-Bromo-4,5-bis(*tert*-butyldimethylsilyloxy)-3-chlorophenol (**29**)⁴²



To a solution of 420 mg (1.08 mmol) of 3,4-bis(*tert*-butyldimethylsilyloxy)-5-chlorophenol (**28**) in 8 mL of dry DMF under argon at 25°C, was added 191.2 mg (1.08 mmol) of *N*-bromosuccinimide and stirred for 22 hours. The reaction was diluted with 50 mL of ethyl acetate and washed twice with 15 mL of water followed by 15 mL of brine. The organic layer was dried over anhydrous MgSO₄, solvent evaporated, and the crude was column chromatographed using a gradient mixture of hexane and diethyl ether as eluent to give 182 mg of 2-bromo-4,5-bis(*tert*-butyldimethylsilyloxy)-3-chlorophenol (**29**)⁴² in 63% yield; based on the recovery of 178 mg of starting material **28**. ¹H NMR δ 6.65 (s, Ar, 1 H), 5.27 (s, OH), 1.03 (s, *t*-Bu, 9 H), 0.97 (s, *t*-Bu, 9 H), 0.23 (s, CH₃, 6 H), 0.17 (s, CH₃, 6 H); ¹³C NMR δ 148.3, 147.4, 138.8, 127.0, 106.9, 102.9, 26.2 (*t*-Bu), 18.8, -3.3 (Me), -3.5 (Me).

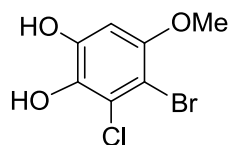
2-Bromo-4,5-bis(*tert*-butyldimethylsilyloxy)-3-chloro-1-methoxybenzene (**30**)



To a solution of 100 mg (0.21 mmol) of 2-bromo-4,5-bis(*tert*-butyldimethylsilyloxy)-3-chlorophenol (**29**) in 2 mL of dichloromethane at 0°C and under argon, were added 55 mg (0.26 mmol) of proton sponge and 38 mg (0.26 mmol) of trimethyloxonium tetrafluoroborate, and the mixture was stirred at 0°C for 8 h. The reaction was diluted with 15 mL of water and extracted twice with 50 mL of diethyl ether. The organic layer was washed with 10 mL of water followed

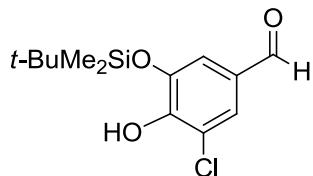
by 10 mL of brine, dried over anhydrous MgSO_4 , solvent evaporated, and the crude was column chromatographed on silica gel using a mixture of hexane and diethyl ether (10:1) as eluent to give 67 mg of 2-bromo-4,5-bis-(*tert*-butyldimethylsilyloxy)-3-chloro-1-methoxybenzene (**30**) in 95% yield; based on the recovery of 31 mg of compound **29**. ^1H NMR δ 6.43 (s, 1 H), 3.80 (s, 3 H), 1.03 (s, 9 H), 0.98 (s, 9 H), 0.23 (s, 6 H), 0.17 (s, 6 H); ^{13}C NMR δ 151.0, 147.5, 138.9, 128.9, 104.7, 104.5, 56.9, 26.3 (6 C), 18.9, 18.8, -3.3 (2 C), -3.5 (2 C); HRMS calcd for $\text{C}_{19}\text{H}_{35}\text{BrClO}_3\text{Si}_2$ ($\text{M}+\text{H}^+$) 481.0996, found 481.0951.

4-Bromo-3-chloro-5-methoxybenzene-1,2-diol (**4**)



To a solution of 51 mg (0.10 mmol) of 2-bromo-4,5-bis-(*tert*-butyldimethylsilyloxy)-3-chloro-1-methoxybenzene (**30**) in 2 mL of THF at 0°C under argon, was added 0.20 mL (0.20 mmol) of *n*- Bu_4NF , and the solution was stirred for 30 min. The reaction was diluted with 100 mL of diethyl ether, washed with 10 mL of water followed by 10 mL of brine, dried over anhydrous MgSO_4 , solvent evaporated, and the crude column chromatographed on silica gel using a gradient mixture of dichloromethane and methanol as eluent to give 19 mg of 4-bromo-3-chloro-5-methoxybenzene-1,2-diol (**4**) in 71% yield. IR (neat) ν 3436, 3219 (broad & s), 2917, 2851, 1580, 1462, 1417, 1315, 1188, 1070, 984, 820 cm^{-1} ; ^1H NMR δ 6.59 (s, 1 H), 5.60 (bs, 1 H, OH), 5.24 (bs, 1 H, OH), 3.83 (s, 3 H); ^{13}C NMR δ 151.4, 144.4, 134.2, 121.8, 101.7, 99.7, 57.1; HRMS calcd. for $\text{C}_7\text{H}_7\text{BrClO}_3$ ($\text{M}+\text{H}^+$) 252.9267, found 252.9254.

3-(*tert*-Butyldimethylsilyloxy)-5-chloro-4-hydroxybenzaldehyde (**31**)



To a solution of 3.2 g (19 mmol) of 3-chloro-4,5-dihydroxybenzaldehyde (**3**) in 60 mL of CH_2Cl_2 at 0°C under argon, were added 2.9 mL (22 mmol) of triethylamine, 0.45 g (3.7 mmol) of 4-dimethylaminopyridine, and 3.4 g (22 mmol) of *tert*-butyldimethylsilyl chloride and the solution was stirred at 25°C for 8 h. The reaction was diluted with 500 mL of diethyl ether and washed with 50 mL water and 50 mL of brine. The organic layer was dried over anhydrous MgSO_4 , solvent evaporated, and the crude was column chromatographed on silica gel using hexane and dichloromethane (1:1) as eluent to give 3.7 g of 3-(*tert*-butyldimethylsilyloxy)-5-chloro-4-hydroxybenzaldehyde (**31**) and 0.84 g of 5-chloro-3,4-bis-(*tert*-butyldimethylsilyloxy)benzaldehyde (**26**) in 70% and 11% yield, respectively. Compound **31** was crystallized from diethyl ether to provide single crystals and its structure was unequivocally identified by a single-crystal X-ray analysis (Figure 5). **Compound 31:** $^1\text{H NMR}$ δ 9.76 (s, 1H, CHO), 7.51 (d, $J = 2.8$ Hz, 1 H), 7.27 (d, $J = 2.8$ Hz, 1 H), 6.24 (s, 1 H, OH), 1.03 (s, 9 H), 0.32 (s, 6 H); $^{13}\text{C NMR}$ δ 189.9, 149.9, 144.2, 129.4, 126.8, 120.7, 115.9, 25.8, 18.4, -4.2; HRMS calcd for $\text{C}_{13}\text{H}_{20}\text{ClO}_3\text{Si}$ ($\text{M}+\text{H}^+$) 287.0870, found 287.0858. **Compound 26:** $^1\text{H NMR}$ δ 9.78 (s, 1 H), 7.50 (d, $J = 2$ Hz, 1 H), 7.29 (d, $J = 2$ Hz, 1 H), 1.05 (s, 9 H), 0.99 (s, 9 H), 0.27 (s, 6 H), 0.24 (s, 6 H); $^{13}\text{C NMR}$ δ 190.1, 149.9, 149.4, 130.3, 128.0, 126.0, 119.0, 26.3 (3 C), 26.2 (3 C), 19.0, -3.2, -3.4; HRMS calcd for $\text{C}_{19}\text{H}_{34}\text{ClO}_3\text{Si}_2$ ($\text{M}+\text{H}^+$) 401.1735, found 401.1747.

3-(*tert*-Butyldimethylsilyloxy)-5-chloro-4-methoxybenzaldehyde (32)

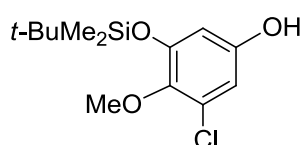


To a solution of 450 mg (1.57 mmol) of 3-(*tert*-butyldimethylsilyloxy)-5-chloro-4-hydroxybenzaldehyde (**31**) in 10 mL of dichloromethane at 0°C under argon, were added 673 mg (3.14 mmol) of proton sponge and 465 mg (3.14 mmol) of trimethyloxonium tetrafluoroborate, and stirred at 0°C for 12 hours. The reaction mixture was diluted with 200 mL of diethyl ether and washed with 30 mL of aqueous NH₄Cl solution, 30 mL of water, and 30 mL of brine. The organic layer was dried over anhydrous MgSO₄, solvent evaporated, and the crude was column chromatographed on silica gel using a mixture of hexane and diethyl ether (10:1) as eluent to give 200 mg of 3-(*tert*-butyldimethylsilyloxy)-5-chloro-4-methoxybenzaldehyde (**32**) in 78% yield; based on the recovery of 206 mg of **31**: ¹H NMR δ 9.83 (s, 1H, CHO), 7.54 (d, *J* = 1.8 Hz, 1 H), 7.28 (d, *J* = 1.8 Hz, 1 H), 3.91 (s, 3 H), 1.03 (s, 9 H), 0.23 (s, 6 H); ¹³C NMR δ 190.1, 153.4, 150.9, 132.8, 129.8, 125.5, 119.9, 60.7, 25.8, 18.4, -4.4; HRMS calcd for C₁₄H₂₂ClO₃Si (M+H⁺) 301.1027, found 301.1421; negative ion detection mode: C₁₄H₂₀ClO₃Si (M-H) 299.0870, found 298.9978.

3-(*tert*-Butyldimethylsilyloxy)-5-chloro-4-methoxyphenyl formate (33) & 3-(*tert*-butyldimethylsilyloxy)-5-chloro-4-methoxyphenol (34)



33



34

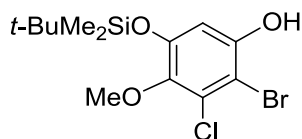
To a solution of 130 mg (0.432 mmol) of 3-(*tert*-butyldimethylsilyloxy)-5-chloro-4-methoxybenzaldehyde (**32**) in 2 mL of dichloromethane at 0°C and under argon, was added 160 mg (70% pure; 0.648 mmol) of *m*-chloroperbenzoic acid, and the solution was refluxed for 12 hours. The reaction solution was diluted with 5 mL of aqueous sodium thiosulfate and 200 mL of diethyl ether. The solution was washed with 20 mL water followed by 20 mL of brine. The organic layer was dried over anhydrous MgSO₄, solvent evaporated, and the crude was column chromatographed on silica gel using a mixture of hexane and diethyl ether (10:1) as eluent to give 58 mg of 3-(*tert*-butyldimethylsilyloxy)-5-chloro-4-methoxyphenyl formate (**33**) and 55 mg of hydrolyzed product, 3-(*tert*-butyldimethylsilyloxy)-5-chloro-4-methoxyphenol (**34**) in 42% and 44% yield, respectively. **Compound 33**: ¹H NMR δ 8.23 (s, 1 H, OCHO), 6.83 (d, *J* = 2.6 Hz, 1 H), 6.59 (d, *J* = 2.6 Hz, 1 H), 3.81 (s, 3 H), 1.01 (s, 9 H), 0.21 (s, 6 H); ¹³C NMR δ 158.9, 150.7, 146.6, 145.4, 129.1, 115.8, 113.6, 60.7, 25.8 (3 C), 18.4, -4.5; HRMS calcd for C₁₄H₂₂ClO₄Si (M+H⁺) 317.0976, found 317.1355. **Compound 34**: ¹H NMR δ 6.48 (d, *J* = 2.6 Hz, 1 H), 6.29 (d, *J* = 2.6 Hz, 1 H), 3.75 (s, 3 H), 1.01 (s, 9 H), 0.20 (s, 6 H); ¹³C NMR δ 152.0, 150.7, 142.6, 128.1, 110.8, 108.6, 60.7, 25.8 (3 C), 18.4, -4.5; HRMS calcd for C₁₃H₂₂ClO₃Si (M+H⁺) 289.1027, found 289.1041.

Conversion of formate **33** to phenol **34**

A solution of 55 mg (0.182 mmol) of compound **33** and 126 mg (0.914 mmol) of K₂CO₃ in 1 mL of methanol was stirred at 25°C for 12 h. The reaction was diluted with 10 mL of water and 30 mL of ethyl acetate and the solution washed with 5 mL of aqueous NH₄Cl solution, 5 mL of water, and 5 mL of brine. The organic layer was dried over anhydrous MgSO₄, solvent evaporated, and the crude was column chromatographed on silica gel using a mixture of hexane

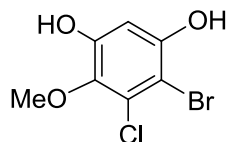
and diethyl ether (10: 1) as eluent to give 50 mg of compound **34** in quantitative yield, which ^1H NMR spectrum is identical to that described above.

2-Bromo-5-(*tert*-butyldimethylsilyloxy)-3-chloro-4-methoxyphenol (**35**)



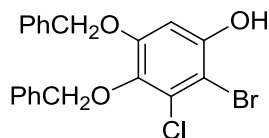
To a solution of 75 mg (0.26 mmol) of 3-(*tert*-butyldimethylsilyloxy)-5-chloro-4-methoxyphenol (**34**) in 2 mL of dimethylformamide (DMF) under argon, was added 51 mg (0.28 mmol) of *N*-bromosuccinimide and the solution was stirred at 25°C for 12 h. The reaction was diluted with 100 mL of diethyl ether, washed with 10 mL of water followed by 10 mL of brine, and the organic layer was dried over anhydrous MgSO_4 . The solvent was evaporated and the crude was column chromatographed on silica gel using a mixture of hexane and diethyl ether (10:1) as eluent to give 64 mg of 2-bromo-5-(*tert*-butyldimethylsilyloxy)-3-chloro-4-methoxyphenol (**35**) in 67% yield: Mp. 44 – 45°C; ^1H NMR δ 6.55 (s, 1 H), 5.42 (s, 1 H, OH), 3.77 (s, 3 H), 1.01 (s, 9 H), 0.20 (s, 6 H); ^{13}C NMR δ 150.2, 149.6, 143.1, 124.2, 107.2, 103.0, 60.8, 25.8 (3 C), 18.5, -4.5; HRMS calcd for $\text{C}_{13}\text{H}_{21}\text{BrClO}_3\text{Si}$ ($\text{M}+\text{H}^+$) 367.0132, found 367.0142.

4-Bromo-5-chloro-6-methoxybenzene-1,3-diol (**5**)



To a solution of 40 mg (0.108 mmol) of 2-bromo-5-(*tert*-butyldimethylsilyloxy)-3-chloro-4-methoxyphenol (**35**) in 2 mL of dry THF under argon at 0°C, was added 120 μL (0.12 mmol) of *n*-Bu₄NF (1 M solution in THF) and the solution was stirred at 0°C for 30 min. The reaction was diluted with 70 mL of diethyl ether, washed with 10 mL of water followed by 10 mL of brine, and the organic layer was dried over anhydrous MgSO₄. The solvent was evaporated and the crude was column chromatographed on silica gel using a mixture of ethyl acetate and hexane (2:1) as eluent to give 15 mg of 4-bromo-5-chloro-6-methoxybenzene-1,3-diol (**5**) in 60% yield. IR (neat) ν 3321 (bs), 3260, 2917, 1589, 1421, 1241, 984, 800; ¹H NMR δ 6.65 (s, 1 H), 3.87 (s, 3 H); ¹³C NMR δ 150.5, 150.0, 138.7, 127.5, 101.8, 101.7, 61.5; HRMS calcd for C₇H₇BrClO₃ (M+H⁺) 252.9267, found 252.9279.

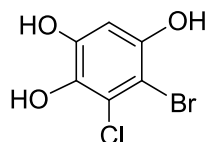
2-Bromo-3-chloro-4,5-dibenzyloxyphenol (**37**)



To a solution of 100 mg (0.188 mmol) of (4,5-bis(benzyloxy)-2-bromo-3-chlorophenoxy)(*tert*-butyl)dimethylsilane (**36**)⁴² in 3 mL of tetrahydrofuran (THF) at 0°C, was added 210 μL of *n*-Bu₄NF (1 M in THF) and stirred under argon at 0°C for 30 minutes. The solution was diluted with 100 mL of diethyl ether, washed with 10 mL of water followed by 10 mL of brine, and the organic layer was dried over anhydrous MgSO₄. The dry organic layer was concentrated and the crude was column chromatographed on silica gel using a mixture of hexane and diethyl ether (10:1) as eluent to give 56 mg of 2-bromo-3-chloro-4,5-dibenzyloxyphenol (**37**) as white solids in 74% yield. Mp.= 108 – 110°C; ¹H NMR δ 7.40 - 7.20 (m, 10 H), 6.66 (s, 1 H),

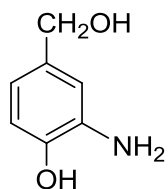
5.07 (s, 2 H), 4.96 (s, 2 H); ^{13}C NMR δ 153.1, 149.9, 139.8, 137.0, 136.1, 129.2, 128.8, 128.5, 128.44, 128.40, 127.6, 102, 100.6, 75.4, 71.3; HRMS calcd for $\text{C}_{20}\text{H}_{17}\text{BrClO}_3$ ($\text{M}+\text{H}^+$) 419.0044, found 419.0051.

5-Bromo-6-chlorobenzene-1,2,4-triol (**6**)

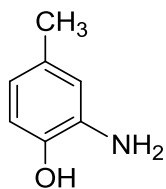


To a solution of 25 mg (0.06 mmol) of 2-bromo-3-chloro-4,5-dibenzyloxyphenol (**37**) in 1 mL of ethanol, was added 2.5 mg of 10% palladium/carbon and was stirred under 1 atmosphere of hydrogen (a balloon filled with hydrogen was connected to the round bottom flask) at 25°C for 3 h. The reaction mixture was filtered through Celite and concentrated to dryness to give 13 mg of 5-bromo-6-chlorobenzene-1,2,4-triol (**6**) in 93% yield. The triol **6** was stored in a dry box under nitrogen atmosphere: Mp. >350°C; IR (neat) ν 3382 (bs, OH stretch), 2932, 2843, 1614, 1437, 1285, 1170, 1070 cm^{-1} ; UV (in methanol) λ 209.6 ($\epsilon_{\text{max}} = 30300$), 291.8 (1250; likely derived from a partial oxidation of the polyphenol functions), 332.5 (4640), 397.1 (1785) nm; ^1H NMR (CD_3OD) δ 6.66 (s, 1 H, Ar), 5.58 (bs, 1 H, OH), 5.27 (bs, 1 H, OH), 5.21 (bs, 1 H, OH); ^{13}C NMR (CD_3OD) δ 149.4, 147.6, 137.4, 123.1, 103.2, 100.6; HRMS calcd for $\text{C}_6\text{H}_5\text{BrClO}_3$ ($\text{M}+\text{H}^+$) 238.9105, found 238.9111.

2-Amino-4-(hydroxymethyl)phenol (7)³⁵ & 2-amino-4-methylphenol (8)³⁶



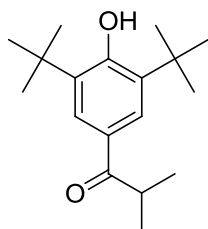
7



8

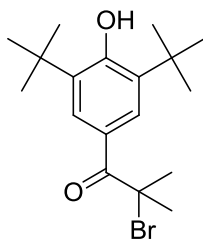
To a solution of 300 mg (1.8 mmol) of 4-hydroxy-3-nitrobenzaldehyde (**38**) in 30 mL of ethanol was added 150 mg of 10% palladium over carbon and shaken on a hydrogenator under 30 psi atmosphere of hydrogen for 4 h. The reaction was filtered through Celite, and the Celite was carefully rinsed with 30 mL ethyl acetate. The filtrate was concentrated and the crude was column chromatographed on silica gel using a mixture of dichloromethane and methanol (9:1) as eluent to give 104 mg of 2-amino-4-(hydroxymethyl)phenol (**7**)³⁵ and 91 mg of 2-amino-4-methylphenol (**8**)³⁶, both in 41% yield. **Compound 7**: IR (neat) ν 3387 (sharp, m), 3313 (sharp, m), 3047 (broad), 2802, 1605, 1515, 1454, 1364, 1286, 1221, 1155, 1008, 816 cm^{-1} ; ^1H NMR (D_2O) δ 6.88 (d, $J = 1.2$ Hz, 1 H), 6.85 (d, $J = 8$ Hz, 1 H), 6.77 (dd, $J = 8, 1.2$ Hz, 1 H), 4.49 (s, 2 H); ^{13}C NMR (DMSO-d_6) δ 144.9, 136.1, 133.4, 114.9, 113.8, 113.4, 63.3. **Compound 8**: IR (neat) ν 3370 (sharp, m), 3301 (sharp, m), 2921, 1601, 1519, 1458, 1388, 1286, 878, 800 cm^{-1} ; ^1H NMR δ 6.62 (d, $J = 7.6$ Hz, 1 H), 6.58 (d, $J = 1.6$ Hz, 1 H), 6.48 (dd, $J = 7.6, 1.6$ Hz, 1 H), 2.21 (s, 3 H); ^{13}C NMR δ 141.9, 134.4, 131.2, 120.0, 118.1, 115.4, 20.9.

1-(3,5-Di-*tert*-butyl-4-hydroxyphenyl)-2-methylpropan-1-one (**9**)⁴⁶



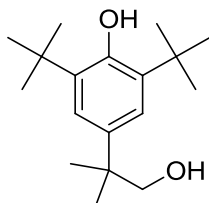
To 1 g (7.5 mmol) of anhydrous AlCl₃ under argon was added 1 mL (9.5 mmol) of isobutyryl chloride (**40**) at -10°C followed by 1.2 g (5.8 mmol) of 2,6-di-*tert*-butylphenol (**39**). To the reaction mixture, 1 mL (9.5 mmol) of isobutyryl chloride was again added and shaken vigorously for 15 minutes till light pink paste was formed. The reaction was quenched with 50 mL of ice cold water and extracted thrice with 50 mL of ethyl ether. The combined organic layers were washed with 20 mL brine, dried over anhydrous MgSO₄ and solvent evaporated to give 1.4208 g of 1-(3,5-di-*tert*-butyl-4-hydroxyphenyl)-2-methylpropan-1-one (**9**)⁴⁶ in 90% yield. Thin layer chromatography (TLC) and NMR analysis indicated that the compound was pure and was used in the next step without further purification. ¹H NMR δ 7.89 (s, Ar, 2 H), 5.71 (s, OH, 1 H), 3.55 (m, 1 H), 1.48 (s, *t*-Bu, 18 H), 1.25 (d, *J* = 6.6 Hz, CH₃, 6 H); ¹³C NMR δ 204.1, 158.4, 135.9, 127.9, 126.2, 34.91, 34.6, 30.3, 19.7.

2-Bromo-1-(3,5-di-*tert*-butyl-4-hydroxyphenyl)-2-methylpropan-1-one (**10**)⁴⁷



To a solution of 190 mg (0.69 mmol) of 1-(3,5-di-*tert*-butyl-4-hydroxyphenyl)-2-methylpropan-1-one (**9**) in a mixture of 0.5 mL of dry CH₂Cl₂ and 1 mL of dry ethyl acetate under argon, was added 375 mg (1.68 mmol) of cupric bromide and heated to reflux for 3 hours at 70°C. The reaction was filtered and solvent evaporated to give 234 mg of 2-bromo-1-(3,5-di-*tert*-butyl-4-hydroxyphenyl)-2-methylpropan-1-one (**10**)⁴⁷ as yellow colored solid in 96% yield. Thin layer chromatography (TLC) and NMR analysis indicated that the compound was pure and was used in the next step without further purification. ¹H NMR δ 8.17 (s, Ar, 2 H), 5.75 (s, OH, 1 H), 2.06 (s, CH₃, 6 H), 1.48 (s, *t*-Bu, 18 H); ¹³C NMR δ 195.7 (C=O), 158.2, 135.6, 128.8, 125.6, 60.6, 34.7, 32.4, 30.4.

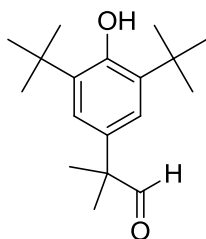
2,6-Di-*tert*-butyl-4-(1-hydroxy-2-methylpropan-2-yl)phenol (11**)⁴⁷**



To a solution of 230 mg (0.65 mmol) of 2-bromo-1-(3,5-di-*tert*-butyl-4-hydroxyphenyl)-2-methylpropan-1-one (**10**) in 3 mL of dry ethyl ether at 0°C under argon, was added 55 mg (1.46 mmol) of LiAlH₄ on vigorous stirring and refluxed at 55°C for 3 hours. The reaction was carefully quenched by the addition of 20 mL of water followed by the addition of 2 mL of 1M H₂SO₄. The reaction was then extracted with 100 mL of diethyl ether. The organic layer was washed with 20 mL of brine, dried over anhydrous MgSO₄, and solvent evaporated to give 180 mg of 2,6-di-*tert*-butyl-4-(1-hydroxy-2-methylpropan-2-yl)phenol (**11**)⁴⁷ as white solid in quantitative yield. Thin layer chromatography (TLC) and NMR analysis indicated that the

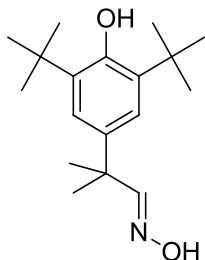
compound was pure and was used in the next step without further purification. ^1H NMR δ 7.19 (s, Ar, 2 H), 5.13 (s, Ar-OH, 1 H), 3.57 (d, $J = 6.6$ Hz, 2 H), 1.45 (s, *t*-Bu, 18 H), 1.33 (s, CH_3 , 6H); ^{13}C NMR δ 152.2, 136.4, 135.6, 123.0, 73.6, 40.1, 34.8, 30.5, 25.7.

2-(3,5-Di-*tert*-butyl-4-hydroxyphenyl)-2-methylpropanal (**12**)



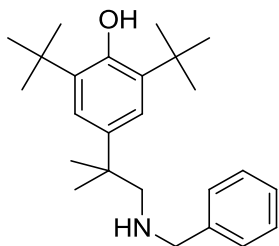
To a solution of 170 mg (0.61 mmol) of 2,6-di-*tert*-butyl-4-(1-hydroxy-2-methylpropan-2-yl)phenol (**11**) in 3 mL of dimethyl sulfoxide (DMSO), was added 0.21 g (0.73 mmol) of *o*-iodoxybenzoic acid (IBX) and stirred under argon at 25°C for 12 h. The reaction was diluted with 200 mL of CH_2Cl_2 , washed with 30 mL of water followed by 30 mL of brine, dried over anhydrous MgSO_4 , and the solvent evaporated to give 170 mg of 2-(3,5-di-*tert*-butyl-4-hydroxyphenyl)-2-methylpropanal (**12**) in quantitative yield. Thin layer chromatography (TLC) and NMR analysis indicated that the compound was pure and was used in the next step without further purification. IR (neat) ν 3603 (OH), 2952, 2900, 2700 (C-H aldehyde), 1714 (C=O aldehyde), 1435, 1360, 1230, 1141, 1120, 903, 826, 744; ^1H NMR δ 9.45 (s, 1 H, CHO), 7.06 (s, 2 H, Ar), 5.22 (s, 1 H, OH), 1.44 (s, 24 H, Me); ^{13}C NMR δ 202.8 (C=O), 153.1, 136.2 (2 C), 131.4, 123.6 (2 C), 50.4, 34.8, 30.4 (*t*-Bu), 22.7; MS negative mode: m/z 275.6 (M-1); positive mode: m/z 299.4 (M+Na⁺).

2-(3,5-Di-*tert*-butyl-4-hydroxyphenyl)-2-methylpropanal oxime (14)



To a solution of 40 mg (0.14 mmol) of 2-(3,5-di-*tert*-butyl-4-hydroxyphenyl)-2-methylpropanal (**12**) in 3 mL of acetonitrile and water (2:1), were added 25 mg (0.35 mmol) of $\text{NH}_2\text{OH}\cdot\text{HCl}$ and 60 mg (0.43 mmol) of sodium acetate, and the solution was stirred at 25°C for 1.5 h. The reaction was rotovaporated to remove acetonitrile, diluted with 20 mL of water, and extracted three times with diethyl ether (60 mL total). The combined extract was concentrated to give 41 mg of 2-(3,5-di-*tert*-butyl-4-hydroxyphenyl)-2-methylpropanal oxime (**14**) in 97% yield. Thin layer chromatography (TLC) and NMR analysis indicated that the compound was pure. ^1H NMR δ 7.49 (s, 1 H, CH=N), 7.12 (s, 2 H, Ar), 1.47 (s, 6 H, Me), 1.44 (s, 18 H, *t*-Bu); ^{13}C NMR δ 158.7 (C=N), 152.5, 135.9, 135.7, 122.9 (2 C), 41.0, 34.7, 30.5 (6 C), 26.9; MS m/z 314 ($\text{M}+\text{Na}^+$).

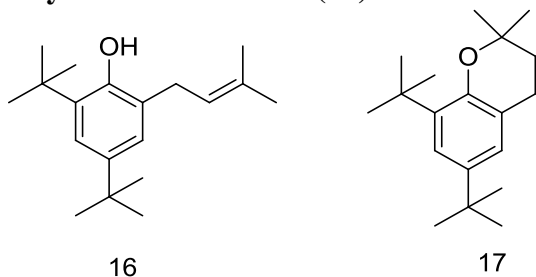
4-[(2-Benzylamino)-1,1-dimethylethyl]-2,6-di-*tert*-butylphenol (15)



To a solution of 50 mg (0.18 mmol) of 2-(3,5-di-*tert*-butyl-4-hydroxyphenyl)-2-methylpropanal (**12**) in 3 mL of toluene was added 19 μL (0.18 mmol) of benzylamine and

heated to reflux using a Diel's Stark apparatus for 12 h. Toluene was evaporated under rotovapor, the crude was dissolved in 2 mL of methanol, and 18 mg (0.29 mmol) of NaCNBH₃ was added. The resulting solution was stirred for 2 h, diluted with 20 mL of water, and extracted twice with ethyl acetate (100 mL total). The combined extract was washed with 10 mL of water and 10 mL of brine, dried over anhydrous MgSO₄, and solvent evaporated to give 68 mg of 4-((2-benzylamino)-1,1-dimethylethyl)-2,6-di-*tert*-butylphenol (**15**) in 98% yield. Thin layer chromatography (TLC) and NMR analysis indicated that the compound was pure. ¹H NMR δ 7.35 – 7.18 (m, 5 H, Ph), 7.13 (s, 2 H, Ar), 5.08 (broad s, 1 H), 3.72 (s, 2 H, CH₂N), 2.68 (s, 2 H, CH₂N), 1.43 (s, 18 H, *t*-Bu), 1.33 (s, 6 H, Me); ¹³C NMR δ 151.92, 140.4, 137.8, 135.4, 128.5, 128.1, 127.0, 122.7, 61.5, 54.2, 38.6, 34.7, 30.6, 27.9; MS m/z 368.5 (M+1).

2,4-Di-*tert*-butyl-6-(3-methyl-2-butenyl)phenol (16) and 6,8-di-*tert*-butyl-2,2-dimethyl-3,4-dihydro-2H-chromene (17)



To a solution of 200 mg (1.44 mmol) of 2-methyl-3-buten-2-ol (**42**) in 3 mL of dichloromethane at -78°C under argon, were added 180 μL (1.44 mmol) of BF₃•ether followed by 205 mg (0.96 mmol) of 2,4-di-*tert*-butylphenol (**41**). The solution was warmed to 25°C and stirred for 1 h. The reaction was diluted with 200 mL of diethyl ether, washed with 20 mL of aqueous NaHCO₃ followed by 20 mL of brine, the organic layer was dried over anhydrous Na₂SO₄, solvent evaporated, and the crude was column chromatographed on silica gel using 1%

diethyl ether in hexane as eluent to give 120 mg of 2,4-di-*tert*-butyl-6-(3-methyl-2-butenyl)phenol (**16**) and 26 mg of 6,8-di-*tert*-butyl-2,2-dimethyl-3,4-dihydro-2*H*-chromene (**17**) in 46% and 10% yield, respectively. **Compound 16:** $^1\text{H NMR } \delta$ 7.22 (d, $J = 3$ Hz, 1 H, Ar), 6.99 (d, $J = 3$ Hz, 1 H, Ar), 5.34 (t,hept, $J = 7$, 1 Hz, 1 H, =CH), 3.37 (d, $J = 7$ Hz, 2 H, CH₂), 1.85 (s, 3 H, Me), 1.80 (s, 3 H, Me), 1.43 (s, 9 H, *t*-Bu), 1.31 (s, 9 H, *t*-Bu); $^{13}\text{C NMR } \delta$ 151.5, 142.3, 135.9, 135.7, 126.0, 125.0, 122.6, 122.3, 35.1, 34.4, 31.9 (3 C), 31.7, 30.0 (3C), 26.0, 18.2; MS negative mode: m/z 273.8 (M-1). **Compound 17:** $^1\text{H NMR } \delta$ 7.14 (d, $J = 3$ Hz, 1 H, Ar), 6.93 (d, $J = 3$ Hz, 1 H, Ar), 2.79 (t, $J = 7$ Hz, 2 H, CH₂), 1.79 (t, $J = 7$ Hz, 2 H, CH₂), 1.39 (s, 9 H, *t*-Bu), 1.36 (s, 6 H, Me), 1.30 (s, 9 H, *t*-Bu); $^{13}\text{C NMR } \delta$ 150.3, 141.0, 136.9, 124.2, 121.8, 119.9, 73.9, 35.2, 34.3, 33.0, 31.9, 30.0, 27.3, 23.5; MS positive mode: m/z 275.2 (M+1).

1.7 References

- (1) Thurston, C. F. The structure and function of fungal laccases. *Microbiology (Reading, U. K.)* **1994**, *140*, 19-26.
- (2) Yoshida, H. Yoshida: Chemistry of lacquer (Urushi). Part I. *J. Chem. Soc., Trans.* **1883**, *43*, 472-486.
- (3) Kunamneni, A.; Plou, F. J.; Ballesteros, A.; Alcalde, M. Laccases and their applications: a patent review. *Recent Pat. Biotechnol.* **2008**, *2*, 10-24.
- (4) Piontek, K.; Antorini, M.; Choinowski, T. Crystal structure of a laccase from the fungus *Trametes versicolor* at 1.90 Å resolution containing a full complement of coppers. *Journal of Biological Chemistry* **2002**, *277*, 37663-37669.
- (5) Xu, F.; Deussen, H.-J. W.; Lopez, B.; Lam, L.; Li, K. Enzymatic and electrochemical oxidation of *N*-hydroxy compounds. Redox potential, electron-transfer kinetics, and radical stability. *Eur. J. Biochem.* **2001**, *268*, 4169-4176.
- (6) Baldrian, P. Fungal laccases - occurrence and properties. *FEMS Microbiol. Rev.* **2006**, *30*, 215-242.
- (7) Garzillo, A. M. V.; Colao, M. C.; Caruso, C.; Caporale, C.; Celletti, D.; Buonocore, V. Laccase from the white-rot fungus *Trametes trogii*. *Appl. Microbiol. Biotechnol.* **1998**, *49*, 545-551.
- (8) Geiger, J. P.; Nicole, M.; Nandris, D.; Rio, B. Root-rot diseases of *Havea brasiliensis*. I. Physiological and biochemical aspects of host aggression. *Eur. J. Forest Pathol.* **1986**, *16*, 22-37.
- (9) Mayer, A. M.; Staples, R. C. Laccase: new functions for an old enzyme. *Phytochemistry* **2002**, *60*, 551-565.

- (10) Sharma, P.; Goel, R.; Capalash, N. Bacterial laccases. *World J. Microbiol. Biotechnol.* **2007**, *23*, 823-832.
- (11) Dittmer, N. T.; Suderman, R. J.; Jiang, H.; Zhu, Y.-C.; Gorman, M. J.; Kramer, K. J.; Kanost, M. R. Characterization of cDNAs encoding putative laccase-like multicopper oxidases and developmental expression in the tobacco hornworm, *Manduca sexta*, and the malaria mosquito, *Anopheles gambiae*. *Insect Biochem. Mol. Biol.* **2004**, *34*, 29-41.
- (12) Kramer, K. J.; Kanost, M. R.; Hopkins, T. L.; Jiang, H.; Zhu, Y. C.; Xu, R.; Kerwin, J. L.; Turecek, F. Oxidative conjugation of catechols with proteins in insect skeletal systems. *Tetrahedron* **2001**, *57*, 385-392.
- (13) Arakane, Y.; Muthukrishnan, S.; Beeman, R. W.; Kanost, M. R.; Kramer, K. J. Laccase 2 is the phenoloxidase gene required for beetle cuticle tanning. *Proc. Natl. Acad. Sci. U. S. A.* **2005**, *102*, 11337-11342.
- (14) Desai, S. S.; Nityanand, C. Microbial laccases and their applications: a review. *Asian J. Biotechnol.* **2011**, *3*, 98-124.
- (15) Becker, N.; Petric, D.; Zgomba, M.; Boase, C.; Madon, M.; Dahl, C.; Kaiser, A. In *Mosquitoes and their control*; Second ed.; Springer: **2010**, p v.
- (16) Kramer, K. J.; Nuntnarumit, C.; Aso, Y.; Hawley, M. D.; Hopkins, T. L. Electrochemical and enzymic oxidation of catecholamines involved in sclerotization and melanization of insect cuticle. *Insect Biochem.* **1983**, *13*, 475-479.
- (17) Brunet, P. C. J. The metabolism of the aromatic amino acids concerned in the crosslinking of insect cuticle. *Insect Biochem.* **1980**, *10*, 467-500.
- (18) Madhavi, V.; Lele, S. S. Laccase: properties and applications. *BioResources* **2009**, *4*, 1694-1717.

- (19) Li, K.; Xu, F.; Eriksson, K.-E. L. Comparison of fungal laccases and redox mediators in oxidation of a nonphenolic lignin model compound. *Applied and Environmental Microbiology* **1999**, *65*, 2654-2660.
- (20) Ducros, V.; Brzozowski, A. M.; Wilson, K. S.; Brown, S. H.; Ostergaard, P.; Schneider, P.; Yaver, D. S.; Pedersen, A. H.; Davies, G. J.; Crystal structure of the type-2 Cu depleted laccase from *Coprinus cinereus* at 2.2 Å resolution. *Nature Structural Biology* **1998**, *5*, 310-316.
- (21) Bertrand, T.; Jolival, C.; Briozzo, P.; Caminade, E.; Joly, N.; Madzak, C.; Mougín, C. Crystal structure of a four-copper laccase complexed with an arylamine: insights into substrate recognition and correlation with kinetics. *Biochemistry* **2002**, *41*, 7325-7333.
- (22) Messerschmidt, A. In *Multi-Copper Oxidases*; Messerschmidt, A., Ed.; World Scientific: Singapore, **1997**, p 23-80.
- (23) Solomon, E. I.; Augustine, A. J.; Yoon, J. O₂ reduction to H₂O by the multicopper oxidases. *Dalton Trans.* **2008**, *30*, 3921-3932.
- (24) Nation, J. L. In *Encyclopedia of Entomology*; Second ed.; Capinera, J. L., Ed.; Springer: **2008**, p 2015.
- (25) Andersen, S. O. Insect cuticular sclerotization: a review. *Insect Biochem. Mol. Biol.* **2010**, *40*, 166-178.
- (26) Suderman, R. J.; Dittmer, N. T.; Kanost, M. R.; Kramer, K. J. Model reactions for insect cuticle sclerotization: Cross-linking of recombinant cuticular proteins upon their laccase-catalyzed oxidative conjugation with catechols. *Insect Biochem. Mol. Biol.* **2006**, *36*, 353-365.

- (27) Johannes, C.; Majcherczyk, A. Laccase activity tests and laccase inhibitors. *J. Biotechnol.* **2000**, *78*, 193-199.
- (28) Ferrar, P. H.; Walker, J. R. L. Inhibition of diphenol oxidases: a comparative study. *Journal of Food Biochemistry* **1996**, *20*, 15-30.
- (29) Xu, F. Effect of redox potential and hydroxide inhibition on the pH activity profile of fungal laccases. *The Journal of Biological Chemistry* **1997**, *272*, 924-928.
- (30) Xu, F. Oxidation of phenols, anilines, and benzenethiols by fungal laccases: correlation between activity and redox potentials as well as halide inhibition. *Biochemistry* **1996**, *35*, 7608-7614.
- (31) Murao, S.; Hinode, Y.; Matsumura, E.; Numata, A.; Kawai, K.; Jin, H.; Oyama, H.; Shin, T. A novel laccase inhibitor, *N*-hydroxyglycine, produced by *Penicillium citrinum* YH-31. *Biosci. Biotech. Biochem* **1992**, *56*, 987-988.
- (32) D'annibale, A.; Celletti, D.; Felici, M.; DiMattia, E.; Giovannozzi-Sermanni, G. Substrate specificity of laccase from *Lentinus edodes*. *Acta Biotechnol.* **1996**, *16*, 257-270.
- (33) Skvortsova, L. I.; Kiryushov, V. N.; Aleksandrova, T. P.; Karunina, O. V. Voltammetry determination of dihydroxybenzenes at a mechanically renewed electrode made from a graphite-epoxy composite. *Journal of Analytical Chemistry* **2007**, *63*, 284-290.
- (34) Quaratino, D.; Federici, F.; Petruccioli, M.; Fenice, M.; Fenice, A. D. A.; D'Annibale, A. Production, purification and partial characterisation of a novel laccase from the white-rot fungus *Panus tigrinus* CBS 577.79. *Antonie van Leeuwenhoek* **2007**, *91*, 57-69.
- (35) Touzeau, F.; Arrault, A.; Guillaumet, G.; Scalbert, E.; Pfeiffer, B.; Rettori, M.-C.; Renard, P.; Merour, J.-Y. Synthesis and biological evaluation of new 2-(4,5-dihydro-1*H*-imidazol-2-yl)-3,4-dihydro-2*H*-1,4-benzoxazine derivatives. *J. Med. Chem.* **2003**, *46*, 1962-1979.

- (36) Kikugawa, Y.; Tsuji, C.; Miyazawa, E.; Sakamoto, T. A new intramolecular migration of the imino group of *O*-aryl ketoximes to the aryl group under the Beckmann condition. *Tetrahedron Lett.* **2001**, *42*, 2337-2339.
- (37) Lyashenko, A. V.; Bento, I.; Zaitsev, V. N.; Zhukhlistova, N. E.; Zhukova, Y. N.; Gabdoulkhakov, A. G.; Morgunova, E. Y.; Voelter, W.; Kachalova, G. S.; Stepanova, E. V.; Koroleva, O. V.; Lamzin, V. S.; Tishkov, V. I.; Betzel, C.; Lindley, P. F.; Mikhailov, A. M. X-ray structural studies of the fungal laccase from *Cerrena maxima*. *J. Biol. Inorg. Chem.* **2006**, *11*, 963-973.
- (38) Giardina, P.; Faraco, V.; Pezzella, C.; Piscitelli, A.; Vanhulle, S.; Sannia, G. Laccases: a never-ending story. *Cell. Mol. Life Sci.* **2010**, *67*, 369-385.
- (39) Semensi, V.; Sugumaran, M. Effect of MON-0585 on sclerotization of *Aedes aegypti* cuticle. *Pestic. Biochem. Physiol.* **1986**, *26*, 220-230.
- (40) Nishinaga, A.; Shimizu, T.; Matsuura, T. Oxygenation of 2,6-di-*tert*-butylphenols bearing electron-withdrawing group at 4-position mediated by cobalt(II)-Schiff base complex. *Tetrahedron Lett.* **1981**, *22*, 5293-5296.
- (41) Lai, J. T. Totally hindered phenols. 2,6-di-*tert*-butyl-4-(1,1-dialkyl-1-acetamide)phenols and their persistent phenoxy radicals. *Tetrahedron Lett.* **2001**, *42*, 557-560.
- (42) Hua, D. H.; Huang, X.; Chen, Y.; Battina, S. K.; Tamura, M.; Noh, S. K.; Koo, S. I.; Namatame, I.; Tomoda, H.; Perchellet, E. M.; Perchellet, J.-P. Total syntheses of (+)-chloropuupehenone and (+)-chloropuupehenol and their analogues and evaluation of their bioactivities. *J. Org. Chem.* **2004**, *69*, 6065-6078.
- (43) Prasain, K.; Nguyen, T. D. T.; Gorman, M. J.; Barrigan, L. M.; Peng, Z.; Kanost, M. R.; Syed, L. U.; Li, J.; Zhu, K. Y.; Hua, D. H. Redox potentials, laccase oxidation, and

- antilarval activities of substituted phenols. *Bioorganic & Medicinal Chemistry* **2012**, *20*, 1679-1689.
- (44) Barakat, M. Z.; El-Wahab, M. F. A.; El-Sadr, M. M. Some reactions with *N*-bromosuccinimide. *J. Am. Chem. Soc.* **1955**, *77*, 1670-1672.
- (45) Biggers, W. J.; Laufer, H. Identification of juvenile hormone-active alkylphenols in the lobster *Homarus americanus* and in marine sediments. *Biol. Bull. (Woods Hole, MA, U. S.)* **2004**, *206*, 13-24.
- (46) Suda, H.; Kanoh, S.; Hasegawa, H.; Motoi, M. Acylation of sterically hindered phenols in the presence of anhydrous aluminum chloride. *Kanazawa Daigaku Kogakubu Kiyō* **1982**, *15*, 71-74.
- (47) Schwartz, L. H.; Flor, R. V. Lithium aluminum hydride reduction of phenacyl halides. Aryl rearrangement pathway. *J. Org. Chem.* **1969**, *34*, 1499-1500.
- (48) Xu, F.; Shin, W.; Brown, S. H.; Wahleithner, J. A.; Sundaram, U. M.; Solomon, E. I. A study of a series of recombinant fungal laccases and bilirubin oxidase that exhibit significant differences in redox potential, substrate specificity, and stability. *Biochim. Biophys. Acta, Protein Struct. Mol. Enzymol.* **1996**, *1292*, 303-311.
- (49) Osman, A. M.; Wong, K. K. Y.; Fernyhough, A. ABTS radical-driven oxidation of polyphenols: Isolation and structural elucidation of covalent adducts. *Biochem. Biophys. Res. Commun.* **2006**, *346*, 321-329.

Chapter 2. Inhibition of PKC phosphorylation by substituted quinolines (PQs)

2.1 Introduction

Protein kinases are enzymes that catalyze the transfer of a γ -phosphate group from adenosine triphosphate (ATP) to serine, threonine, or tyrosine residue of other proteins resulting in their phosphorylation and affecting their activities, cellular location, and protein-protein interaction.^{1,2} Protein kinase C (PKC) belongs to the family of serine/threonine protein kinases and was first reported by Yasutomi Nishizuka and his coworkers in several mammalian tissues in 1977.^{3,4} Few years later, PKC was found to be activated by diacylglycerol (DAG) in cyclic adenosine monophosphate (cAMP) independent but calcium and phospholipids dependent pathways and plays crucial role in signal transduction in several processes including cell proliferation, differentiation, migration, and apoptosis.^{2,5,6}

Activation of PKC by phorbol esters such as 12-*O*-tetradecanoylphorbol-13-acetate (TPA), a well known tumor-promoting agent, has established the potential role of PKC in tumor promotion and progression and heightened PKC as potential target in anticancer therapy.⁷ Phorbol esters are known to substitute diacylglycerol (DAG) with higher binding affinity towards PKC.⁷ Recognition of several isozymes of PKC with different mode of activation and tissue distribution has opened a door towards the development and use of isozymes-specific inhibitors targeting specific intracellular pathways and leading to the possible cure of cancer. Several broad spectrum and isozymes specific PKC inhibitors including staurosporine and its derivatives like 7-hydroxystaurosporine (UCN01) and *N*-benzoyl staurosporine (PKC412), tamoxifen, and ISIS3521 (an antisense phosphorothionate oligonucleotide) are known and found to

have anticancer properties but with low clinical efficiency that could be due to their poor specificity/selectivity towards PKC and its specific isozymes or poor bioavailability.^{8,9}

Previously, polysubstituted quinolines (abbreviated as PQs) were synthesized in Hua's laboratory by derivatizing the C-8 amino function of 6-methoxy-4-methyl-5-(3-(trifluoromethyl)phenoxy)quinolin-8-amine,¹⁰ to study their anticancer activities.¹¹ Among the synthesized PQs: *N*-(3-aminopropyl)-6-methoxy-4-methyl-5-(3-(trifluoromethyl)phenoxy)quinolin-8-amine (PQ1), *N*-(furan-2-ylmethyl)-6-methoxy-4-methyl-5-(3-(trifluoromethyl)phenoxy)quinolin-8-amine (PQ11), and 6-methoxy-4-methyl-*N*-(quinolin-4-ylmethyl)-5-(3-(trifluoromethyl)phenoxy)quinolin-8-amine (PQ15) were found to have anti-breast cancer activities.^{11,12} For example, PQ1 and PQ11 were found to attenuate xenograft breast cancer tumor growth.^{13,14} Combinational treatment of PQ1 and tamoxifen, an antiestrogen compound used for the prevention of some types of breast cancer in humans, was found to lower the effective dose of tamoxifen in T47D cells.¹³ Moreover, PQ11, an analog of PQ1, was found to have improved anti-breast cancer activity as compared to PQ1.¹⁴ The anti-cancer activities of PQs have been related to the enhancement of gap junction intercellular communication (GJIC) by restoring gap junctions and inducing apoptosis.¹²⁻¹⁵

With known anticancer activities and structures closely resembling to that of several known PKC inhibitors including MT477, dequalinium, and chelerythrine chloride; PQs could also function as PKC inhibitors. Therefore, in this chapter the inhibition of PKC phosphorylation by PQ1, PQ11, and PQ15 was evaluated. In this study, staurosporine,¹⁶ a known potent PKC inhibitor and 6-methoxy-4-methyl-*N*-(thiophen-2-ylmethyl)-5-(3-(trifluoromethyl)phenoxy)quinolin-8-amine (PQ10) were used as positive and negative

compound, respectively. The structures of PQ1, PQ10, PQ11, PQ15, and staurosporine are highlighted in Figure 8.

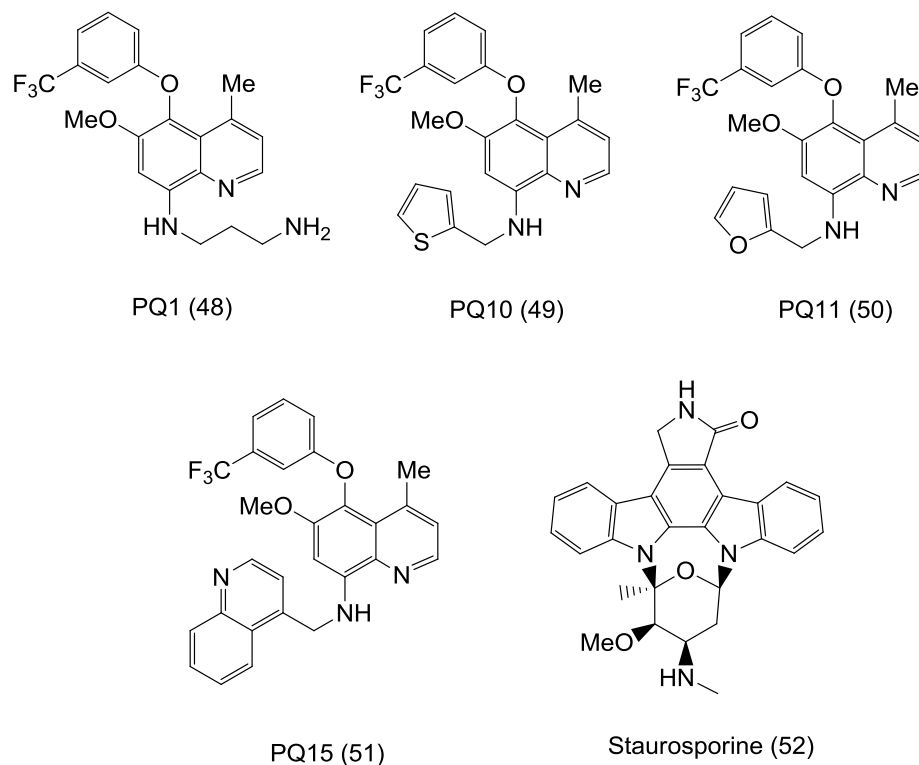


Figure 8: Structure of PQ1, PQ10, PQ11, PQ15, and staurosporine.

2.2 Background

PKCs are known to have at least twelve isozymes and on the basis of their mode of activation and similarities in amino acid sequences are grouped under three subfamilies: classical PKCs (cPKC: PKC α , PKC β I, PKC β II, and PKC γ) are activated by calcium, diacylglycerol (DAG) and phosphatidylserine (PS); novel PKCs (nPKC: PKC δ , PKC ϵ , PKC η , PKC θ and PKC μ) are activated by DAG and PS but are insensitive towards calcium; and atypical PKCs

(aPKC; PKC ζ and PK λ) are insensitive towards both calcium and DAG but can be activated by 3-phosphoinositides (PIP₃).^{9,17,18}

The single polypeptide chain of PKC is composed of an N-terminal regulatory domain (~ 20 - 40 kDa) linked to a highly conserved C-terminal catalytic domain (~ 45 kDa) by a proteolytically labile hinge region (V3) as shown in Figure 9.¹⁹ The regulatory domain in PKCs, consisting of C1 and C2 regions is diverse and on the basis of this domain PKC isozymes are classified into three subfamilies as mentioned above. The catalytic domain, consisting of C3 and C4 regions is highly conserved among the isozymes. In classical PKCs (cPKCs), C1 region contains two duplicated cysteine rich zinc finger motifs located towards the N-terminal and functions as a DAG or PS binding site, C2 region contains the recognition site for acidic lipids and calcium binding, and C3 and C4 regions are the ATP and substrate binding sites, respectively.¹⁹⁻²¹ Novel PKCs (nPKCs) also have similar C1, C2, C3 and C4 regions; however, the C2 region lacks calcium binding sites and is located towards the N-terminal as shown in Figure 9.^{19,20} Atypical PKCs (aPKCs) differ from the classical and novel PKCs by having structurally different C1 region as well as lacking functional C2 region.^{19,20} The C1 region in all the isozymes is preceded by a pseudosubstrate that resembles a PKC substrate but contains alanine and not serine or threonine in the phosphoacceptor site.²² In the absence of activators, the pseudosubstrate binds to the substrate binding site of C4 region and keeps the enzyme in autoinhibitory (inactive) state.²³

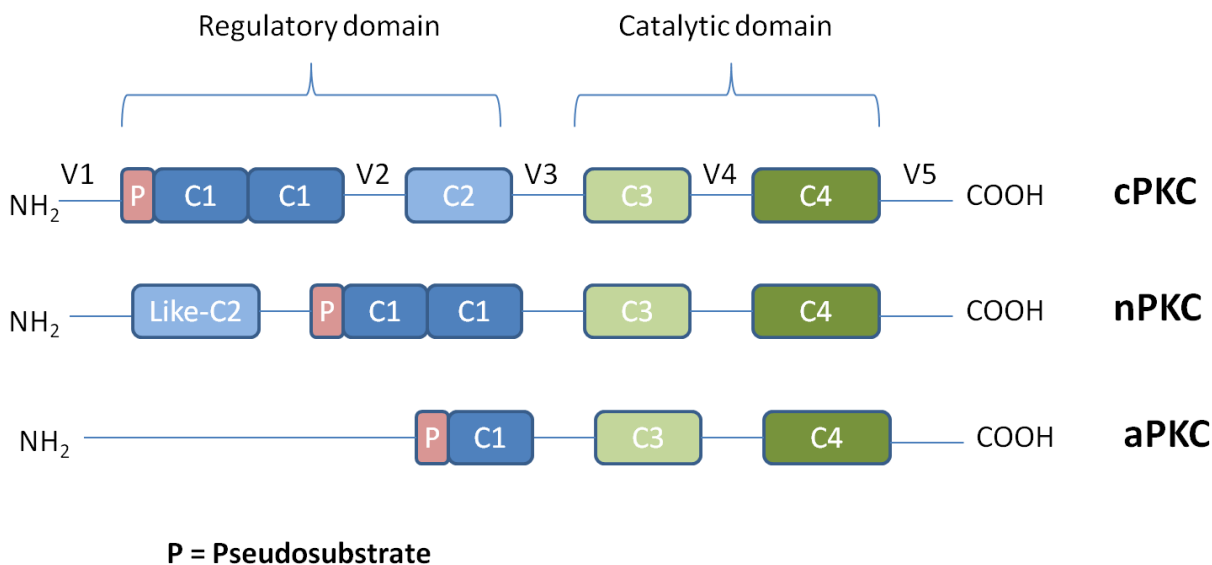


Figure 9: Schematic representation showing the conserved regions (C1 - C4) and variable regions (V1 - V5) in all three classes of PKC isozymes.¹⁹

2.2.1 PKC as a target in cancer therapy

There is a plethora of literatures in which PKCs have been related to cancer. The first ground breaking evidence was published in the early 1980s that identified PKC as a receptor for phorbol esters, natural tumor-promoting compounds, and highlighted PKC as one of the most intensively studied enzyme in anticancer research.^{7,24} Phorbol esters have been previously linked to promote the formation of skin tumors on mice treated with mutagenic agent.

PKCs have wide range of downstream signaling pathways and many of them are unknown. The most important downstream signaling pathway activated by PKC is the MEK-ERK, and the other probable cancer related downstream targets are glycogen synthases kinase-3 beta (GSK-3 β), nuclear factor kappa beta (Nf κ B), P-glycoprotein, etc.^{8,9} PKC α is known to activate mitogen activated protein kinase kinase kinase (MAP-KKK or Raf1), a serine/threonine

kinase by phosphorylation which in turn activates mitogen activated protein kinase kinase (MAP-KK; MEK1 and 2). The activated MEK1/2 further activates mitogen activated protein kinase (MAP-K; ERK 1 and 2) by phosphorylation. Finally, ERK phosphorylates several downstream proteins resulting in the transcription of genes involved in cell proliferation.⁸

The expression level and function of various PKC isozymes during cancer progression are found to vary depending on the cell and cancer type; furthermore, the PKC isozymes substrate-overlapping specificities have made it difficult to pin point functions of individual isozymes. For example, PKC α may act as tumor promoter or as a tumor suppressor: down-regulation of PKC α has been demonstrated in basal cell carcinoma and colon cancers,^{25,26} up- or down-regulation of PKC α has been described in hematological malignancies,²⁷ and up-regulation of PKC α has been found in prostate,²⁸ endometrial, and high-grade urinary cancer.²⁹ Similarly, PKC β expression is found to be upregulated in prostate²⁸ and colon cancers³⁰ and downregulated in bladder cancers.³¹ However, PKC δ activity in many cases is linked to induce apoptosis, probably through the release of mitochondrial cytochrome c and increase in the expression and stability of p53 (tumor suppressor), pro-apoptotic signals as a result of PKC δ activation.³²⁻³⁴ In general, majority of the studies have demonstrated that increased PKC α/β expressions is associated with increased motility, invasion, anti-apoptotic activity, and drug resistance in cancer cells; the effect is reversed by inhibiting PKCs activities.⁹ Importantly, only few cases of mutations have been reported in PKC which might aid in the designing of nonresistant anticancer drugs by targeting a specific isozyme culprit in the process.¹⁸ Since many studies have linked PKC during cancer progression, therapies targeting PKC or specific PKC isozyme could be effective in the cure of cancers.^{8,9,35}

2.2.2 PKC and breast cancer

Breast cancer, a heterogeneous disease, is one of the most common cancers in women. Breast cancer comprises of about 22.9% of all cancers diagnosed in women and is a leading cause of women deaths worldwide.³⁶ Less than 10% of the breast cancers have been related to be hereditary and are linked with mutation of tumor suppressor genes such as BRCA1 and BRCA2, whereas majority of breast cancers develop sporadically with the risk factors that include age, lifestyle, hormonal exposure, and environmental factors like pollution.³⁷ Estrogen is a major steroid hormone in female endocrine system and is required for the normal growth and development of the body. In addition, estrogen is vital for the development of secondary sexual character as well as in reproduction; however, high level of estrogen in the body has been linked to rapid cell proliferation in breast tissues leading to breast cancer.³⁸

Increase in the PKC level is correlated to the increased resistance and metastatic potential of human breast cancer cells.³⁹ In a study conducted among nine patients having breast cancer, the PKC expression was found to be significantly higher in the human breast cancer tumor cells as compared to the normal breast tissues of the same patients.⁴⁰ PKC expression was found to be significantly higher in several estrogen receptor negative (ER⁻) human breast cancer cells as compared to estrogen receptor positive (ER⁺) human breast cancer cells which inversely correlates between the expression of PKC and estrogen receptors in the cancer cells.⁴¹ *In vitro* studies, human breast cancer cells treated with phorbol ester downregulated PKC expression and inhibited cell growth; whereas, removal of phorbol ester from the medium upregulated PKC expression and resumed cell growth, suggesting that PKC is necessary for cell growth.^{42,43} These studies suggest the role of PKC as a potential targets in breast cancer therapy.

2.2.3 Gap junction and cancer

Gap junctions are transmembrane hydrophilic channels that connect the cytoplasm of adjacent cells and allow the passage of molecules such as water, cAMP, inositol triphosphate (IP₃), glucose, and calcium that are smaller than 1200 Daltons.⁴⁴ In normal cells gap junctions are present in very high-density clusters known as gap junctional plaques and are the only specializations in cell membranes for intercellular communication between adjacent cells.⁴⁵ Unlike normal cells that can communicate intercellularly through the gap junction, cancer cells lack or have defective gap junctions,⁴⁶ and are unable to receive intercellular signals such as required for apoptosis thus preventing cell death.

Gap junctions are formed when connexon of one cell docks with a connexon of the adjacent cell and each connexon is composed of six proteins of connexin family such as Cx43 and Cx32.^{47,48} Most of the connexins with the exception of Cx26 are phosphoproteins and are phosphorylated by several kinases including mitogen-activated protein kinase (MAPK), protein kinase C (PKC), and protein kinase A (PKA).⁴⁷

2.2.4 Inhibition of gap junction intercellular communication by PKC

PKCs have been related in the inhibition of gap junctional intercellular communication (GJIC) by inhibiting gap junctional channels.^{49,50} The inhibition of gap junctional channel is either induced by cell trauma such as sudden drop in pH and increase in Ca²⁺ level or physiological regulators like connexin phosphorylation.⁵¹ The higher the expression of phosphorylated form of connexin, the lower is gap junctional intercellular communication (GJIC). Phosphorylation of connexin mostly occurs on the serine residues of the C-terminal.⁵² Many studies suggest the phosphorylation of Cx43 through PKC dependent pathways. Mutation

of Ser-368 in Cx43 partially prevented the decrease in intercellular gap junctional communication (CJIC) when treated with PKC in the presence of phorbol ester, a known activator of PKC, indicating Ser-368 as a major site for PKC phosphorylation.^{53,54}

Restoration of gap junction in cancer cells can allow the access of small anticancer drugs as well as apoptosis signals deep into the cancer tissues causing cells death. Inhibition of PKC might be crucial in restoring gap junctions, enhancing gap junctional intercellular communication and inducing apoptosis, leading to the possible treatment of cancer. Substituted quinolines (PQs) are known to inhibit PKC phosphorylation of Cx43 by disrupting the interactions between Cx43 and Nedd4, an E3 ubiquitin ligase, resulting in the maintenance of gap junctions.¹² The structural similarities between PQs and several known PKC inhibitors like MT477, chelerythrine chloride, and dequalinium in having common quinoline moiety and H7 in having closely related isoquinoline moiety might be linked to the PKC inhibition properties of PQs. The structures of MT477, dequalinium, H7, chelerythrine chloride, and other known PKC inhibitors are highlighted in Figure 10.

2.2.5 PKC inhibitors and cancer

The role of PKC in cancer supports the notion that it could be potential therapeutic target in treating cancers. Several PKC inhibitors are known and some are currently employed in human clinical trials either as a single agent or in combination with other anti-cancer drugs. Approaches to inhibit PKC by small molecules are based on their binding to catalytic domain (ATP binding site) or regulatory domain (diacylglycerol or calcium binding site) of PKC. Known PKC inhibitors including safinol, calphostin C, miltefosine, bryostatin 1, curcumin, staurosporine and its synthetic analogs (midostaurin (PKC412), Go6850, Ro318220, Ro320432,

enzastaurin (LY317615), sotrastaurin (AEBO71), ruboxistaurin (LY333531), and UCN-01 (7-hydroxystaurosporine)), tamoxifen, dequalinium, MT477, H7, chelerythrine chloride, ingenol-3-angelate, and sangivamycin are highlighted in Figure 10.

Sphingosine, a sphingolipid, is a potent and selective inhibitor of PKC and acts on the regulatory domain of PKC.⁵⁵ Safingol, a saturated homologue of sphingosine, was the first PKC inhibitor to enter clinical trial in combination with doxorubicin.⁵⁶ It has entered phase I clinical trial in combination with cisplatin for the treatment of advanced solid tumors.⁵⁷

Calphostin C, a perylenequinone, is a natural product derived from fungus *Cladosporium cladosporioides* and is a potent and highly selective inhibitor of PKC showing preference over cAMP-dependent protein kinase and tyrosine-specific protein kinase.⁵⁸ Calphostin C has been found to induce apoptosis in broad spectrum of cancer cell lines;⁵⁹ however, its use has been limited to preclinical studies only.

Miltefosine, an alkylphosphocholine, has shown antitumor activities that might be due to its ability to inhibit PKC. Phase II clinical study of miltefosine in topical treatment to cutaneous breast cancer metastases has showed some activity with little systemic toxicity.⁶⁰

Bryostatin 1 is a macrocyclic lactone isolated from *Bugula neritina*, a marine bryozoans.⁶¹ The short-term exposure to bryostatin 1 is found to activate cPKC and nPKC, whereas the long-term exposure inhibits PKC activity.⁶² Phase II studies of bryostatin 1 in combination with paclitaxel has shown enhanced response of paclitaxel in advanced esophageal and gastroesophageal junction adenocarcinoma and in advanced esophageal as gastroesophageal junction cancer.^{63,64} Moreover, combination of bryostatin 1 with vincristine in phase II studies was effective in patients with aggressive B-cell non-Hodgkin lymphoma.⁶⁵

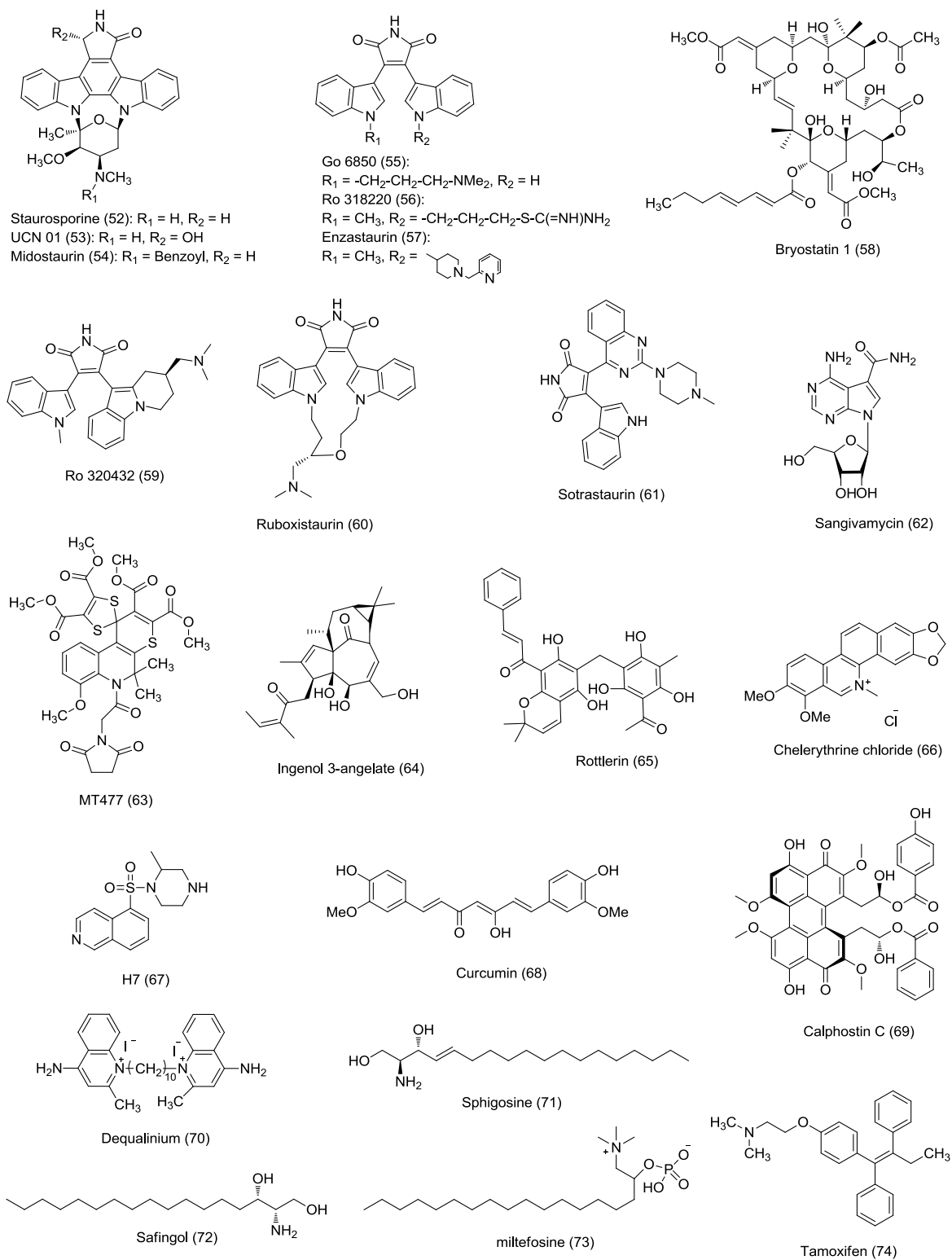


Figure 10: Structures of known PKC inhibitors.

Curcumin, commonly known as turmeric and used for yellow coloration in curry, is a natural polyphenol derived from the plant *Curcuma longa* and a potent inhibitor of PKC.⁶⁶ Anti-tumor activities of curcumin against a broad spectrum of cancers have been investigated in number of preclinical studies.³⁵ Phase I and phase II clinical studies has highlighted curcumin as a safe compound with possible therapeutic efficacy.³⁵

Chelerythrine chloride, a benzophenanthridine alkaloid derived from the plant *Chelidonium majus*, is a cell-permeable inhibitor of protein kinase C and do not inhibit protein tyrosine kinase, cAMP-dependent protein kinase, or calcium/calmodulin-dependent protein kinase.⁶⁷ Chelerythine chloride is also known to activate MAPK pathways, independent of PKC inhibition and inhibit binding of BclXL to Bak or Bad proteins stimulating apoptosis.⁶⁸

Ingenol-3-angelate (Ing3A), extracted from *Euphorbia peplus*, is currently in phase III clinical trials for treating actinic keratosis and phase II for non-melanoma skin cancer.^{69,70} H7, an isoquinoline sulphonamide, is one of the early used ATP site binding inhibitor of PKC and also inhibits cAMP- and cGMP-dependent protein kinases.^{71,72} Rottlerin, a natural product derived from *Mallotus philippinensis*, is a selective inhibitor of PKC δ showing preference over other cPKCs and nPKCs; however, it is also known to inhibit PKA and calmodulin kinase III.^{73,74} MT477, a novel thiopyranol[2,3-*c*]quinoline, is known to have activity against PKC isozymes and found to preferentially inhibit the proliferation of *K-ras*-mutated carcinoma as compared to non-Ras-mutated carcinoma.⁷⁵ In non-Ras- mutated cancer, MT477 is found to be a selective inhibitor of PKC α showing preference over PKC β I, PKC β II, and PKC γ isozymes.⁷⁶

Staurosporine, a natural product isolated from bacterium *Streptomyces staurosporeus* is a potent PKC inhibitor consisting of a sugar residue linked to a planar bis-indole carbazole.⁷⁷ It is the first reported PKC inhibitor that acts on the ATP binding site of the catalytic domain of PKC.

Lack of specificity of staurosporine towards kinases makes it highly toxic and has precluded it from clinical use. However, analogs of staurosporine including, midostaurin (PKC412) and UCN01 are more potent and specific inhibitors of PKC.

Midostaurin, an *N*-benzoylated staurosporine analog, was the first PKC inhibitor to be used in oncology clinical trials and known to be more selective than staurosporine towards PKCs inhibitions; however it also inhibits other kinases like inert domain receptor KDR, VEGF-R2, PDGF, and c-kit.⁷⁸ Phase I studies of midostaurin in combinations with 5-fluorouracil, paclitaxel and carboplatin, and gemcitabine and cisplatin has highlighted that midostaurin can be safely used for treating certain cancers.^{79,80} However, midostaurin failed to demonstrate significant clinical activities in phase II trials.

UCN01, an analog of staurosporine preferably suppresses the activities of cPKCs as compared to other PKC isozymes.⁸¹ UCN01 is in clinical trials for leukemia, non-small cell lung cancer (NSCLC) and lymphoma.³⁵

Enzastaurin (LY317615) is a potent inhibitor of PKC β .⁸² Enzastaurin was found to be effective in phase I and II trials in the patient with recurrent high-grade gliomas.⁸³ Phase III study conducted to compare the efficacy of enzastaurin with lomustine in the treatment of patient with recurrent glioblastoma showed its better efficacy towards hematological profile; however, was less effective than lomustine.⁸⁴

Sotrastaurin (AEB071) is a potent and selective inhibitor of cPKCs and nPKCs and has found to have high immunodilatory effect via inhibition of early T cell activation.⁸⁵ It is currently in phase II clinical trial for the prevention of solid organ allograft rejection.⁸⁵

Since PQs are known to have anticancer activities with their structures closely resembling to that of several PKC inhibitors including MT477, dequalinium, chelerythrine chloride, and H7; therefore, PQs might also function as PKC inhibitors.

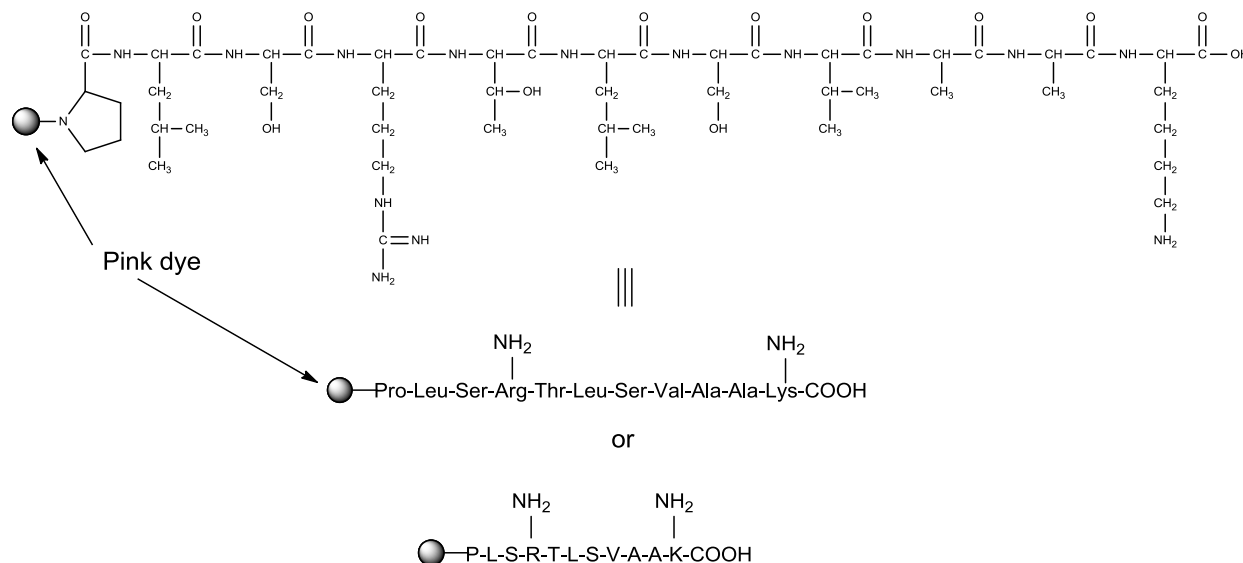
2.3 PKC inhibition by substituted quinolines (PQs)

2.3.1 Methods and materials

The PepTag® non-radioactive PKC assay kit (catalog # V5330) was purchased from Promega and PKC inhibition studies were carried out following the protocol published by Promega (technical bulletin #132) with minor modifications.

Protein Kinase C phosphorylation is determined by the use of fluorescent PepTag “C1 peptide” substrate consisting of eleven amino acids residues (amino acids sequence of C1 peptide; proline – leucine – serine – arginine – threonine – leucine – serine – valine – alanine – alanine – lysine). A dye molecule attached to the C1 peptide substrate imparts bright pink fluorescence to the peptide. At pH = 7.4, pH of the reaction, the C1 peptide in the nonphosphorylated state has a net +1 charge which changes to net -1 charge on PKC phosphorylation as illustrated in Figure 11.⁸⁶ In spite of having two serines (Ser-3, and Ser-7) and one threonine (Thr-9) residues in the amino acid sequence of C1 peptide only Ser-7 is phosphorylated; Ser-3, and Thr-9 are not typically phosphorylated due to steric hindrance.⁸⁷ The phosphorylated and nonphosphorylated C1 peptides can be separated by agarose gel electrophoresis, a method used to separate oppositely charged peptides or proteins (Figure 12). The use of non-radioactive assay is more rapid and convenient than the one that determines PKC activity by measuring the transfer of radioactive phosphate ($^{32}\text{PO}_4^{2-}$) group from the enzyme to

the substrate peptides or proteins.⁸⁸ During electrophoresis the nonphosphorylated peptide (+Ve charged) moves towards the negatively charged anode whereas the phosphorylated peptide (-Ve charged) moves toward the positively charged cathode and get separated as shown in Figure 12.



At pH = 7.4

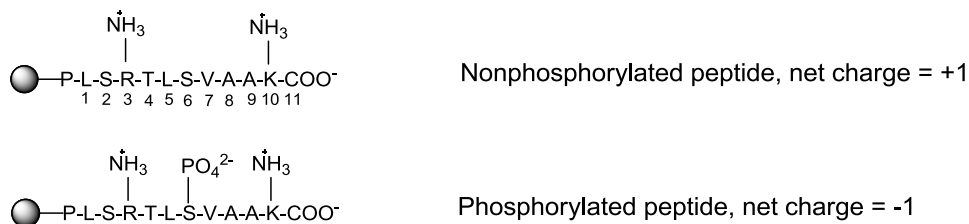


Figure 11: Amino acid sequence of C1 peptide and the change in net charge (+1) of nonphosphorylated peptide to the net charge of (-1) of phosphorylated peptide at pH = 7.4.

The phosphorylated and nonphosphorylated bands were visualized under UV light and the fluorescence intensities (pixel intensities) of the bands were quantified using Kodak Gel Logic 1500 Digital Imaging System and Imagequant 5.2 software; facilities provided by Dr.

Govindsamy Vedyappan laboratory, in the Division of Biology, Kansas State University. The ratio of the phosphorylated band intensity to the sum of the phosphorylated and nonphosphorylated band intensities was used as a measure of percentage phosphorylation of C1 peptide.⁸⁹

PepTag® assay kit for non-radioactive detection of protein kinase C consists of the following: PepTag® C1 peptide (0.4µg/µL in water), conjugated to a fluorescent molecule; PepTag® PKC reaction buffer having 100 mM 4-(2-hydroxyethyl)-1-piperazineethanesulfonic acid (HEPES), pH 7.4, 6.5 mM CaCl₂, 5 mM dithiothreitol (DTT), 50 mM MgCl₂, and 5mM adenosine triphosphate (ATP); PKC (25 µg/mL) having 20 mM tris(hydroxymethyl)aminomethane hydrochloride (C(CH₂OH)₃NH₂. HCl; Tris-HCl), pH 7.4, 2 mM ethylenediaminetetraacetic acid (EDTA), 1mM DTT, 10 mM K₃PO₄, 0.05% Triton® X-100 and 50% glycerol; gel solubilization solution (composition not supplied); and PKC activator solution having 1 mg/mL of phosphatidylserine (PS) in water; and peptide protection solution.

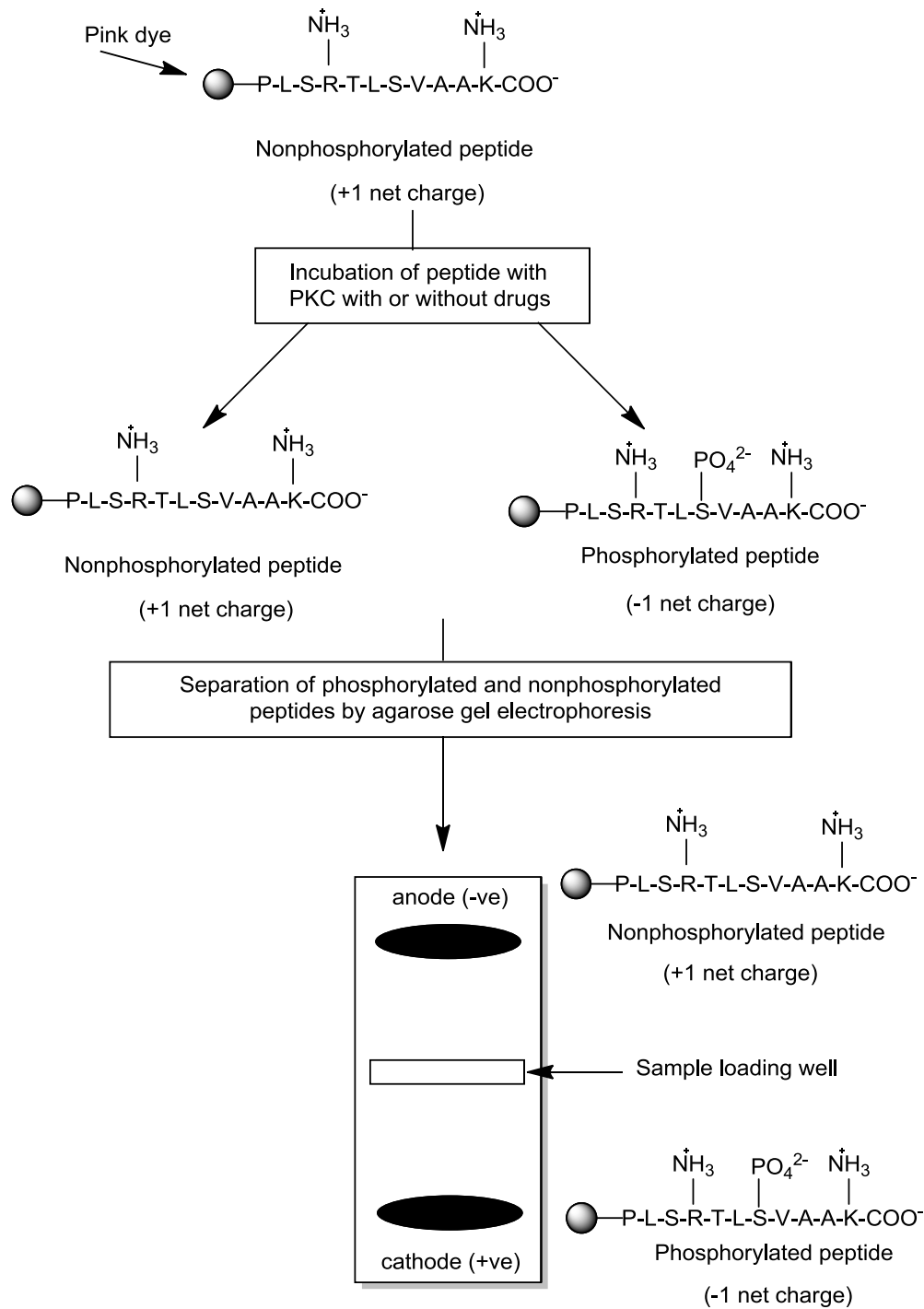


Figure 12: Schematic diagram showing the phosphorylation of C1 peptide by PKC and the separation of phosphorylated and nonphosphorylated C1 peptide by agarose gel electrophoresis. In the above figure, P = proline, L = leucine, S = serine, R = arganine, T = threonine, V = valine, A = alanine, and K = lysine.

2.3.2 Experimental

2.3.2.1 PKC inhibition studies

The inhibition of PKC phosphorylation was carried out following the protocol supplied by Promega (technical bulletin #132) with minor modifications. The negative control in the experiment consisted of C1 peptide but without PKC and PKC inhibitor (staurosporine or PQs); the positive control consisted of both C1 peptide and PKC but without PKC inhibitor; and the other experiments consisted of C1 peptide, PKC, and PKC inhibitor in varying concentrations. The inhibition of PKC phosphorylation by staurosporine or PQs in various concentrations was demonstrated by the decrease in the intensities of their respective phosphorylated bands as compared to the phosphorylated band of the positive control.

2.3.2.2 Preparation of agarose gel

To a solution of 50 mL of 50 mM Tris-HCl (pH 8.0) buffer was added 0.4 g of agarose, heated to boiling in a microwave till all of the agarose dissolved, cooled to about 60°C, and slowly added into a gel tray having required number of comb(s) placed in a mini horizontal electrophoresis apparatus.⁹⁰ Any bubbles formed in the solution were carefully removed with a pipette tip. On standing for 20 minutes the agarose solution solidified to a gel. Careful removal of the comb(s) gave desired number of wells for sample loading. The gel was covered with 50 mM Tris-HCl solution (pH 8.0) as a running buffer.

2.3.2.3 Preparation of reaction solutions

Each experiment (PKC inhibition studies) generally comprised of 7 reactions; one negative control, one positive control, and the remaining five with PKC inhibitor (staurosporine or PQs) in different concentrations. The procedure was based on Promega technical bulletin (#132) and is mentioned below:

1. Eight 1-mL microcentrifuge tubes were taken and labeled as mixture, negative control, positive control, and the remaining five as required PKC inhibitor concentrations.
2. In negative control, 6 μL of deionized water was added, whereas in positive control 3 μL (15 ng) of diluted PKC (PKC dilution solution comprises of 100 $\mu\text{g}/\text{mL}$ of bovine serum albumin (BSA) and 0.05% of Triton® X-100) and 3 μL of deionized water or 1:2 mixture of DMSO and deionized water (based on the solvent used for dissolving PKC inhibitors) was added.
3. In other five reactions, 3 μL (15 ng) of diluted PKC and 3 μL of drug solution of required concentration (each tube had different concentration of drug) in deionized water or 1:2 mixture of DMSO and deionized water were added. The reactions mentioned in points 2 and 3 of this section were then incubated at room temperature for 5 minutes.
4. In a tube labeled as mixture, 17.5 μL of PKC reaction buffer, 17.5 μL of PKC activator solution, 3.5 μL peptide protection solution, and 14 μL (5.6 μg) of C1 peptide were added at 0°C and incubated for 2 minutes in water bath maintained at 30°C. From the tube 7.5 μL of the solution were added to each tube labeled as negative control, positive control, and five reactions with varying drug concentrations. Each tube had 0.8 μg of C1 peptide in the total volume of 13.5 μL .

5. Negative control, positive control, and other five reactions with drug were incubated for 45 minutes in water bath maintained at 30°C.
6. The reaction was stopped by deactivating PKC enzyme by placing the tubes in boiling water for 10 minutes.
7. The tubes were then allowed to cool at room temperature and 0.5 μ L of 80% glycerol was added to each tubes. The samples were now ready to be loaded into the agarose gel for the separation of phosphorylated and nonphosphorylated peptides by horizontal gel electrophoresis.

2.3.2.4 Separation of phosphorylated and nonphosphorylated peptides by electrophoresis

Electrophoresis is a process of separation of molecules having different charge or size by the application of electric field. The samples from each tube (as described in section 2.3.2.3) were loaded in separate wells in the agarose gel placed in a horizontal gel electrophoresis chamber and electrophoresis was carried for 30 minutes at 100 V. As the net +1 charge in a nonphosphorylated C1 peptide is changed to a net -1 charge after phosphorylation,⁸⁶ on electrophoresis the nonphosphorylated peptides (+Ve charged) move towards the negatively charged electrode (anode) and the phosphorylated peptides (-Ve charged) move towards the positively charged electrode (cathode) and separate from each other.

2.3.2.5 Quantification of phosphorylated and nonphosphorylated bands

The gel after electrophoresis was removed from the electrophoresis chamber, photographed under UV by Kodak Gel Logic 1500 Digital Imaging System,⁹¹ and quantification of both phosphorylated and nonphosphorylated bands were carried out by Imagequant 5.2

software (Molecular Dynamics/Amersham Biosciences),⁹² using the facilities in Dr. Govindasamy Vedyappan laboratory, in the Division of Biology, Kansas State University. Quantification of the bands by the use of Imagequant 5.2 software is referred as photoimaging analysis in this chapter. For the quantification, the tiff image file of the gel was inverted (bands are black and background is white, opposite to the normal picture) and background correction was done to minimize noise. The obtained volumes of the bands (pixel intensities) were then used to determine the amounts of phosphorylated and non phosphorylated C1 peptide which is discussed in details in the following section. The accuracy of photoimaging analysis was tested by comparing the results with that of spectrofluorometric analysis, and was found to be similar. Thus the more convenient photoimaging analysis was carried out for the quantification of phosphorylated and nonphosphorylated C1 peptides in all performed experiments.

For spectrofluorometric analysis the bands were carefully incised with a clean and sharp razor and placed in a separate (labeled) 1 mL graduated micro centrifuge tubes. The gels in the tubes were heated on boiling water until they melted. After adjusting the volume in each tube to 250 μ L by the addition of deionized water (wherever necessary), 175 μ L of each solutions were transferred to different tubes containing 75 μ L of gel solubilization solution, 50 μ L of glacial acetic acid, and 400 μ L of deionized water, and vortexed. The solutions were then ready for spectrofluorometric analysis. The maximum intensities of the phosphorylated bands of positive control and reactions with different PKC inhibitor (PQs or staurosporine) concentration were compared from their respective emission spectra ($\lambda_{\text{max}} = 592$ nm; obtained with the excitation wavelength of 568 nm). The difference in the phosphorylation of peptide in the absence and presence of PKC inhibitors was calculated and inhibitions of PKC phosphorylation by the inhibitors were determined.

To minimize the effect of diffusion and overflowing of the lanes during the sample loading during gel electrophoresis, the sum of intensities or volumes of both phosphorylated and nonphosphorylated bands of each reaction were taken and considered to be the contribution of 0.8 μg of peptide that was initially added in each reaction. From this value the corrected amount of peptide phosphorylation and percentage of peptide phosphorylation were determined as mentioned in the second last and last columns of Tables 1, 2, and 3.

The correlation studies between the peptide phosphorylation and (a) the concentration of PKC (0 - 40 ng) and (b) time (15 to 60 minutes) were carried out before preceding the phosphorylation inhibition studies.

2.4 Results and discussions

2.4.1 Studies of the correlation between peptide phosphorylation verse (1) concentrations of PKC, and (2) time

Correlations between peptide phosphorylation verse (a) concentration of PKC, and (b) time were established before setting parameters for the experiments.

2.4.1.1 Correlation between peptide phosphorylation verses concentrations of PKC

The phosphorylation of the substrate peptide (C1 peptide) increased linearly with the increase in the amount of PKC (0 - 40 ng) as determined by both spectrofluorometric (bottom left of Figure 13) and photoimaging analysis (bottom right of Figure 13). The percentage of C1 peptide phosphorylation with varying concentrations of PKC, as measured by both spectrofluorometric and photoimaging methods, are highlighted in Table 1 and 2, respectively. The amounts of PKC required to phosphorylate 50 % of the C1 peptide were found to be 29 ng

and 30 ng from spectrofluorometric and photoimaging analysis, respectively. Results obtained from both methods were similar with an average difference of 4%. The use of 15 ng of PKC produced about 30% of C1 peptide phosphorylation; therefore, 15 ng of PKC was used in the following experiments to study the inhibition of PKC phosphorylation by staurosporine and PQs.

Table 1: Percentage phosphorylation of C1 peptide with varying amounts of PKC (0, 5, 15, 20, 30, and 40 ng) as determined by spectrofluorometric analysis

Amount of PKC (ng)	Maximum Intensity		A+B (Intensity due to 0.8 µg of C1 peptide)	Corrected amount of peptide phosphorylated (A', µg) (0.8× A/(A+B))	% Peptide phosphorylation (A' × 100/ 0.8) %
	Phosphorylated peptide (A)	Non phosphorylated peptide (B)			
0	0	3014204	3014204	0	0
5	207960	2719242	2927202	0.057	7.1
15	978600	2508340	3486940	0.225	28.1
20	1199304	1960410	3159714	0.304	38
30	1937402	1725586	3662988	0.423	52.9
40	2246314	1444880	3491194	0.514	64.3

Table 2: Percentage phosphorylation of C1 peptide with varying amounts of PKC (0, 5, 15, 20, 30, and 40 ng) as determined by photoimaging analysis

Amount of PKC (ng)	Volume (Pixel Intensity)		A+B (Intensity due to 0.8 µg of C1 peptide)	Corrected amount of peptide phosphorylated (A', µg) (0.8× A/(A+B))	% Peptide phosphorylation (A' × 100/ 0.8) %
	Phosphorylated peptide (A)	Non phosphorylated peptide (B)			
0	0	129513	129513	0	0
5	17595	133628	151223	0.093	11.63
15	80358	148940	229298	0.280	35
20	91876	134506	226382	0.325	40.58
30	110573	104745	215318	0.411	51.35
40	140443	94755	235198	0.478	60

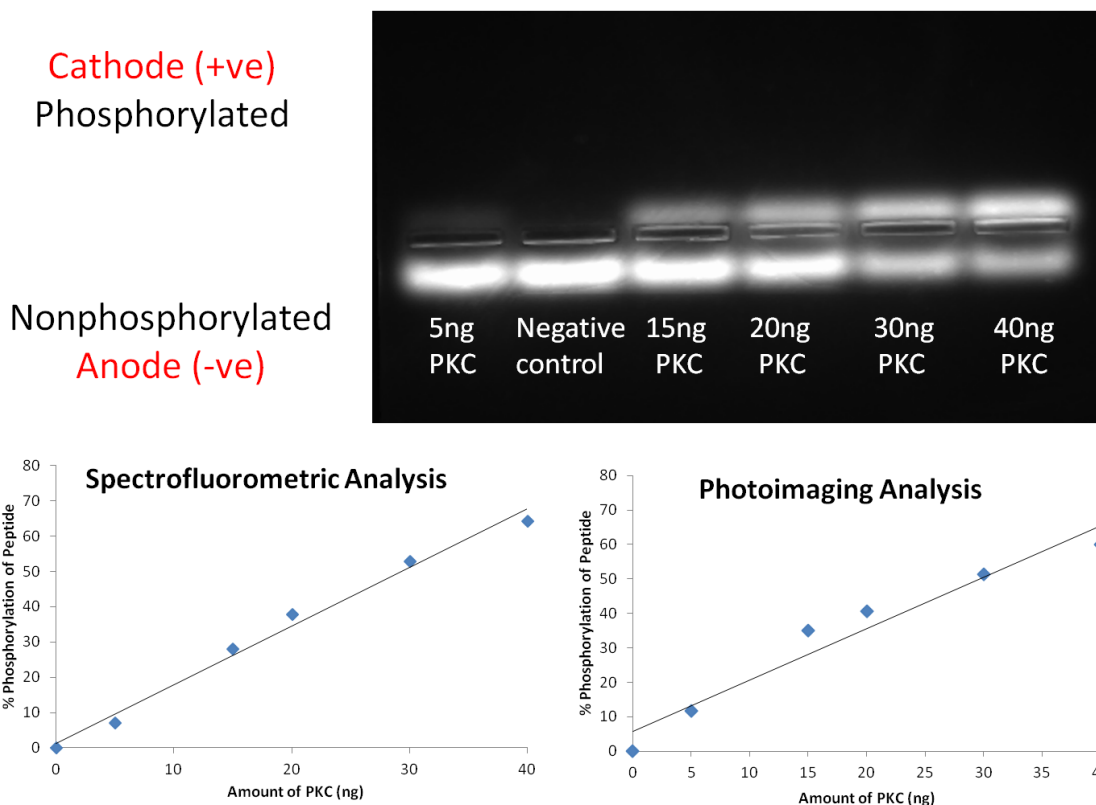


Figure 13: Gel image and graphs of C1 peptide phosphorylation with the amount of PKC. The amount of PKC used ranged from 0 - 40 ng (top). The negative control refers to no PKC (0 ng). The linear correlation of peptide phosphorylation vs. amount of PKC in nanograms (ng) was established by the spectrofluorometric (bottom left) and photoimaging (bottom right) methods. The results obtained in both cases were similar with an average difference of ~ 4%.

2.4.1.2 Correlation between the changes in peptide phosphorylation over time (15 - 60 min)

The percentage of peptide phosphorylation with respect to time was studied to find out the appropriate reaction time for the preceding experiments. For this 15 ng of PKC and 0.8 μ g of C1 peptide were used in each reaction (four reactions) and the first, second, third, and fourth reaction were stopped at 15, 30, 45, and 60 minutes respectively by deactivating PKC enzyme by placing the reaction on boiling water for 10 minutes. The reactions were then loaded into the sample loading wells in agarose gel for the separation of both phosphorylated and non phosphorylated peptides by horizontal gel electrophoresis. Percentage of C1 peptide

phosphorylation over time is summarized in Table 3, whereas the gel image and the corresponding graph are highlighted in Figure 14.

Table 3: Percentage phosphorylation of C1 peptide with varying time (15 - 60 minutes)

Time (minutes)	Volume (Pixel Intensity)		A+B (Intensity due to 0.8 μ g of C1 peptide)	Corrected amount of peptide phosphorylated (A', μ g) ($0.8 \times A/(A+B)$)	% Peptide phosphorylation ($A' \times 100/0.8$) %
	Phosphorylated peptide (A)	Non phosphorylated peptide (B)			
0	0	452529	452529	0	0
15	212081	430388	642469	0.264	33
30	182748	321058	503806	0.290	36.3
45	265429	412429	677858	0.313	39.2
60	281580	360734	642314	0.350	43.8

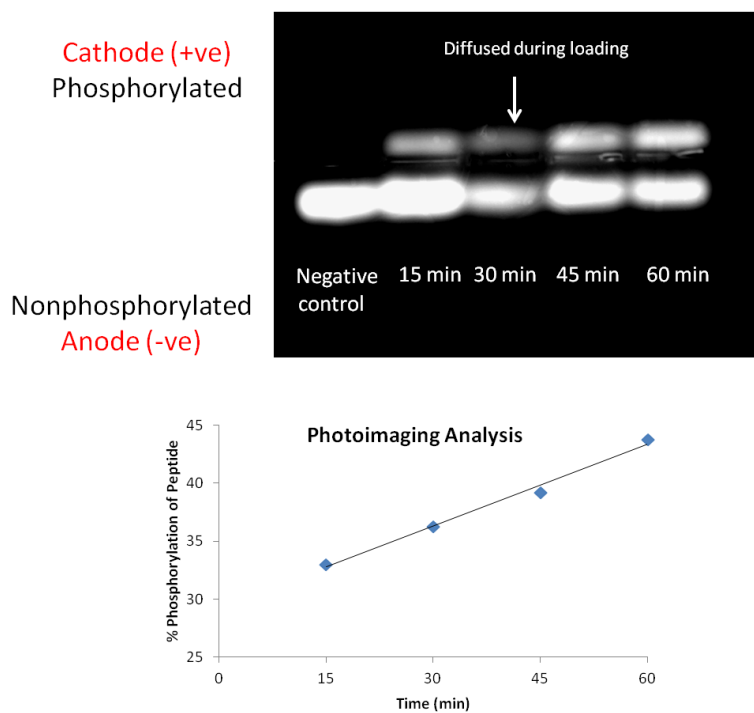


Figure 14: Gel image and linear correlation between percentage phosphorylation of C1 peptide catalyzed by PKC (15 ng) over time (15 - 60 min). Diffusion on loading 30 min reaction caused the decrease in the pixel intensities of both phosphorylated and non-phosphorylated bands which was corrected as shown in Table 3.

Percentage phosphorylation of C1 peptide with PKC showed a linear correlation with time within the experimental range from 15 to 60 minutes as shown in Figure 14. For each reaction the incubation time could be chosen between 15 to 60 minutes; however, 45 minutes incubation time was chosen for the phosphorylation experiments. Longer incubation time (> hour) was avoided since PKC is labile at room temperature.

2.4.2 Inhibition of PKC phosphorylation by staurosporine

Staurosporine is a natural product isolated from bacterium *Streptomyces staurosporeus* by Omura et al in 1977.⁷⁷ Staurosporine molecule consists of a sugar residue, with a unique stereochemical arrangement, linked to a planar bis-indole carbazole unit.

Initially, staurosporine was found to have biological activities ranging from anti-fungal to anti-hypertensive; however, elaborated studies highlighted staurosporine as a potent, but not selective inhibitor of various protein kinases including PKC with IC₅₀ values in nanomolar range.^{93,94} The higher affinity of staurosporine towards the adenosine triphosphate (ATP) binding site on the catalytic domain of PKC prevents the binding of ATP to the PKC, thus inhibiting PKC.⁹⁴ Lack of specificity of staurosporine towards kinases makes it highly toxic and has precluded it from clinical use. Staurosporine has an ability to drive virtually all mammalian cells to apoptosis; therefore, the role of staurosporine is virtually restricted in research to induce apoptosis.

Staurosporine was used as a positive compound to study the inhibition of PKC phosphorylation. The inhibition of PKC phosphorylation was carried out as per the protocol supplied by Promega and as explained in section 2.3 of this chapter. The gel image, percentage of C1 peptide phosphorylation catalyzed by PKC, and the percentage of PKC inhibition in the

absence and presence of various concentrations of staurosporine is highlighted in Figure 15. IC_{50} value of staurosporine towards the inhibition of PKC phosphorylation was found to be 33 nM (Figure 20); however, IC_{50} value of 22 nM has been previously reported by Wilkinson et al.⁹⁵

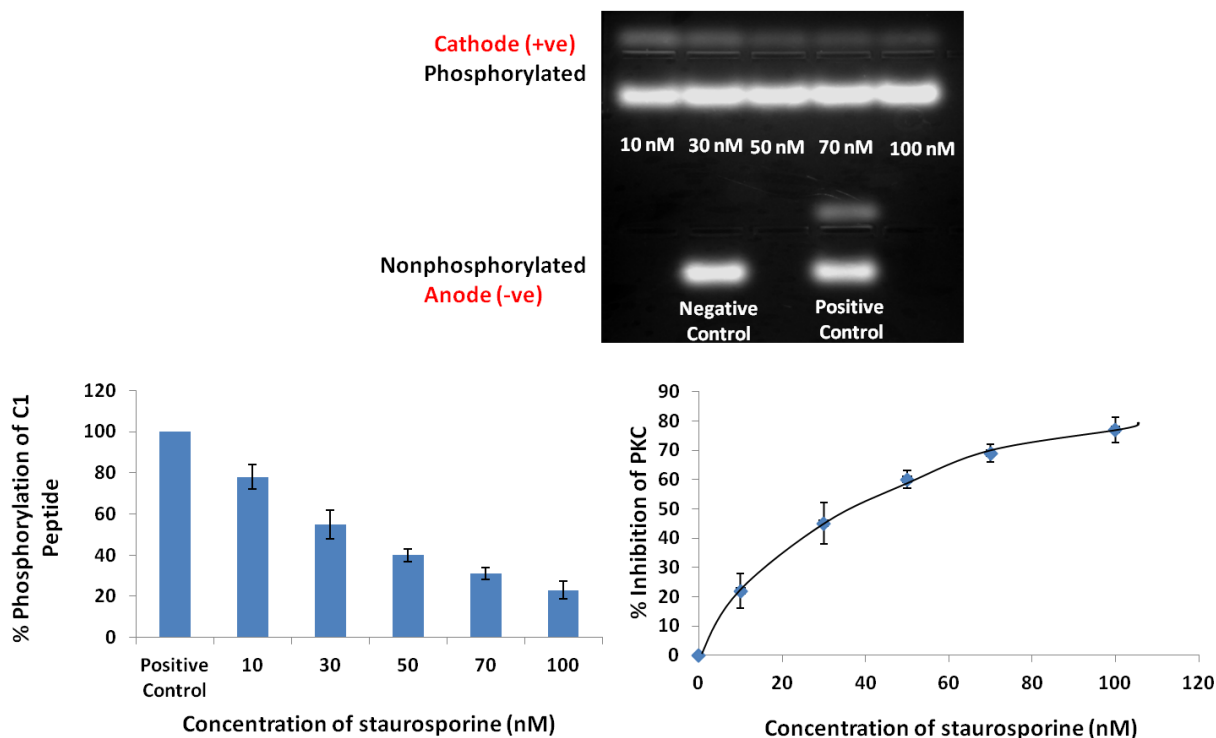


Figure 15: Gel image, percentage of C1 peptide phosphorylation catalyzed by PKC, and percentage inhibition of PKC phosphorylation in the presence and absence of staurosporine. All the reactions have 0.8 μ g of C1 peptide and 15 ng of PKC. In the negative and positive control there is no staurosporine whereas other reactions have different concentrations of staurosporine as mentioned in the graphs. The graphs are provided with (\pm) standard error obtained from three separate experiments.

2.4.3 Inhibition of PKC phosphorylation by PQs (PQ1, PQ10, PQ11, and PQ15)

Polysubstituted quinolines, abbreviated as PQ's, were synthesized by Jianyu Lu, in Hua's laboratory, following the literature procedure previously reported.¹¹ Structures of PQ compounds examined for the inhibition of PKC phosphorylation, in this chapter, are listed in previous

Figure 8. These PQ compounds are known to have anti-breast cancer activities. Among the PQ compounds, PQ1 and PQ11 have IC_{50} values of 119 nM and 15.6 nM in T47D cancer cells and are potential compounds for developing anticancer drugs.¹¹ PQ10 was less active against T47D cell line with IC_{50} value of 3.7 μ M.¹¹

N-(3-Aminopropyl)-6-methoxy-4-methyl-5-(3-(trifluoromethyl)phenoxy)quinolin-8-amine (PQ1), a potent anticancer drug was found to induce apoptosis in cancer cells by enhancing or restoring gap junction intercellular communication (GJIC); moreover, PQ1 had no effect on gap junction intercellular communication (GJIC) in normal cells.¹³ PQ1 was found to inhibit the phosphorylation of Cx43, gap junction protein and increased the expression of active caspase-3, suggesting its role as apoptosis inducing agent.¹³ *In vivo* studies indicated that PQ1 suppressed the xenograft tumor growth of T47D cells in nude mice.¹³ Combinational treatment of PQ1 and tamoxifen lowered the effective dose of tamoxifen in T47D cells.¹³

Since PKC is linked in the catalysis of phosphorylation of gap junction protein Cx43, the effect of PQ1 on PKC phosphorylation was studied. The PKC phosphorylation inhibition studies highlighted PQ1 as a potent PKC inhibitor with IC_{50} value of 35 nM (Figure 20), and its activity was comparable to that of staurosporine (IC_{50} value of 33 nM) as measured in the previous section. The gel image, percentage of C1 peptide phosphorylation catalyzed by PKC, and percentage inhibition of PKC in the presence and absence of PQ1 is highlighted in Figure 16.

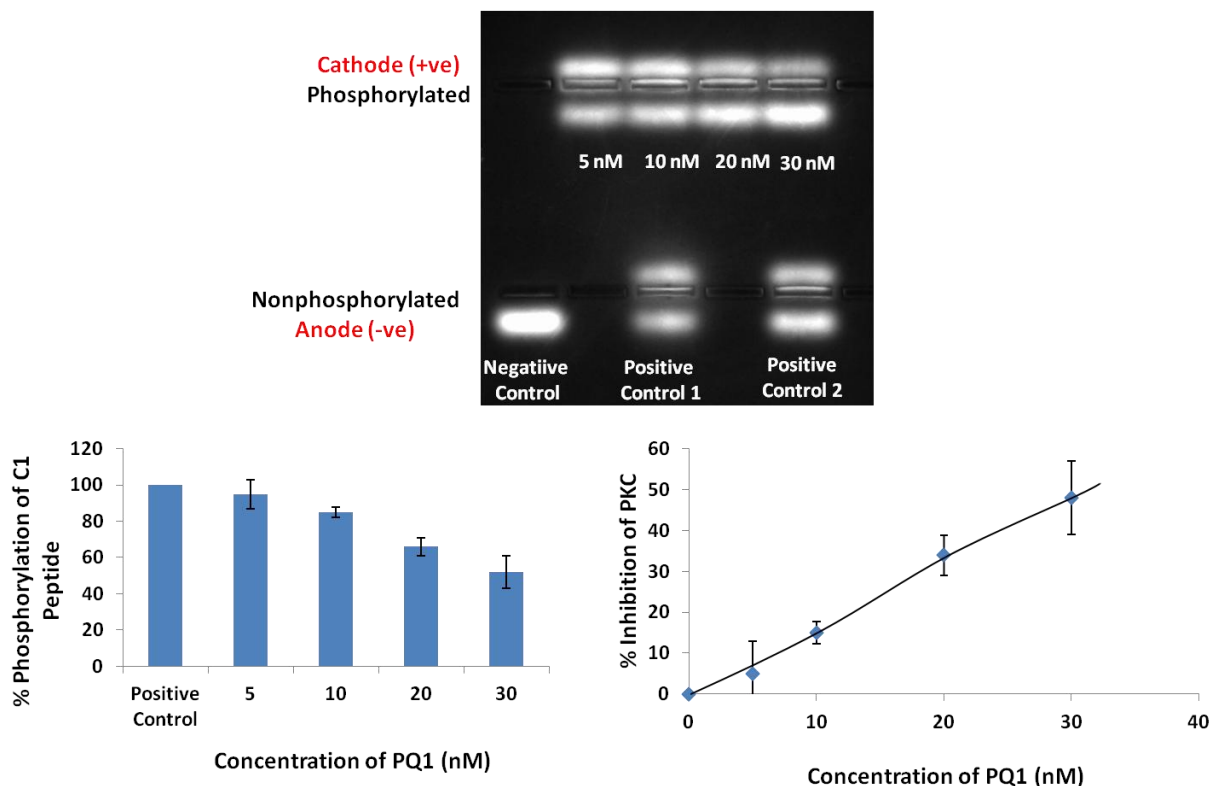


Figure 16: Gel image, percentage of C1 peptide phosphorylation catalyzed by PKC, and percentage inhibition of PKC phosphorylation in the absence and presence of PQ1. All the reactions have 0.8 μg of C1 peptide and 15 ng of PKC. In negative and positive control there is no PQ1 and others have varying concentrations of PQ1 as indicated in the graphs. The graphs are provided with (\pm) standard error obtained from three separate experiments.

N-(Furan-2-ylmethyl)-6-methoxy-4-methyl-5-(3-(trifluoromethyl)phenoxy)quinolin-8-amine (PQ11) was found to have much improved anticancer activities than PQ1.¹⁴ PQ11 was found to increase the expression of Cx43, a gap junctional protein, in T47D cells enhancing GJIC in the cells.¹⁴ PQ11 at 500 nM was known to enhance the GJIC by 1.7 and 16 folds as compared to PQ1 treated (under identical conditions) and nontreated T47D cells, respectively.¹⁴ Similarly, 100 nM of PQ11 and PQ1 inhibited the colony growth of T47D by 66% and 50 % respectively.¹⁴ *In vivo* studies showed that PQ11 treated nude mice grafted with T47D tumor had no tumor left after 7 injections of 1 μM PQ11 in 14 days.¹⁴ The increase in expression of

caspase-9 on cancer cells treated with PQ11 was linked to the role of PQ11 in the induction of apoptosis.¹⁴ These results demonstrate the potency of PQ11 in the development of potential anticancer drug.¹⁴ The inhibition of PKC phosphorylation by PQ11 was therefore studied and the corresponding IC_{50} value was obtained as 42.3 nM, which is slightly higher than that of PQ1 as shown in Figure 20. The higher IC_{50} value of PQ11, towards PKC inhibition, as compared to PQ1 is surprising but may be related to the difference in their cellular targets other than PKC. The gel image, percentage of C1 peptide phosphorylation catalyzed by PKC, and percentage inhibition of PKC phosphorylation in the absence (positive control) and presence of PQ11 is highlighted in Figure 17.

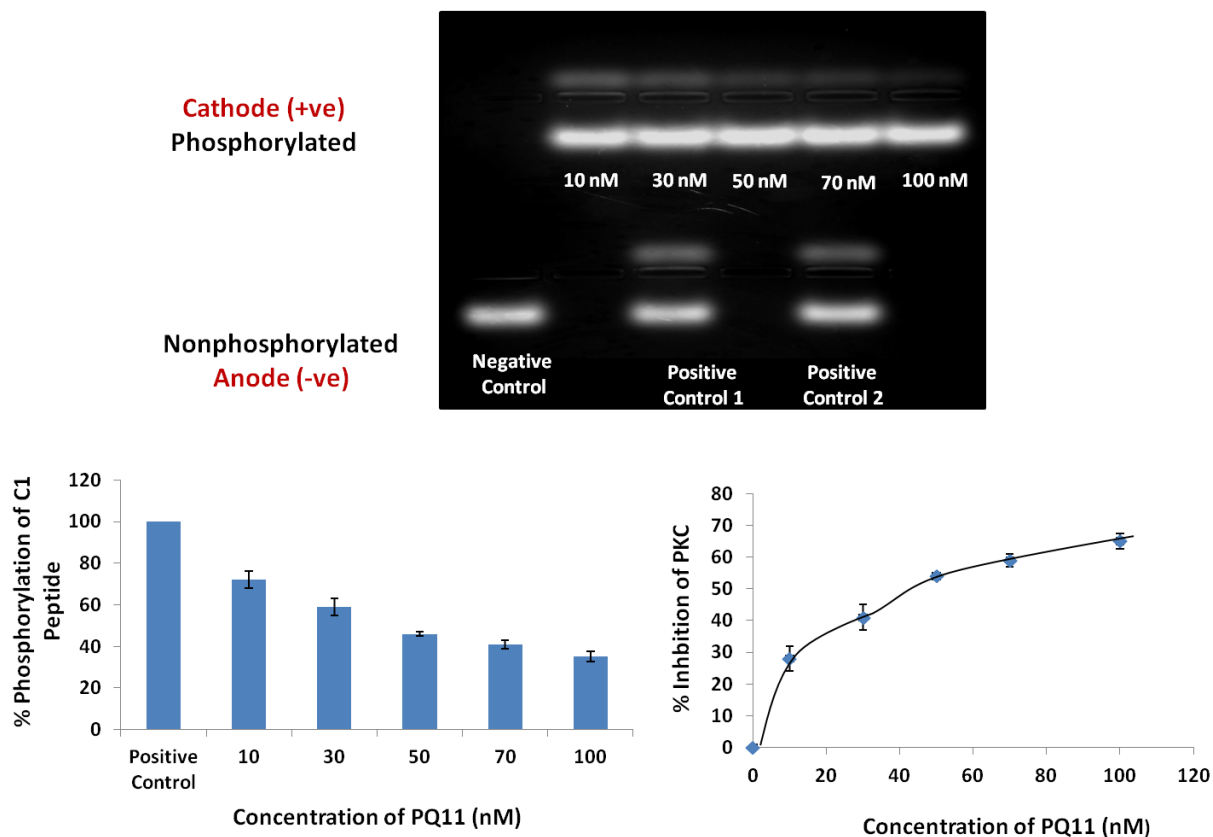


Figure 17: Gel image, percentage of C1 peptide phosphorylation catalyzed by PKC, and inhibition of PKC phosphorylation in the presence and absence of PQ11. All the reactions have 0.8 μ g of C1 peptide and 15 ng of PKC. In the negative and positive control there is no PQ11 and others have varying concentrations of PQ11 as indicated in the graphs. The graphs are provided with (\pm) standard error obtained from three separate experiments.

Another analog of PQ1, 6-methoxy-4-methyl-*N*-(quinolin-4-ylmethyl)-5-(3-trifluoromethyl)phenoxy)quinolin-8-amine (PQ15), was also found to have anticancer activities, but less potent than PQ1 and PQ11.¹² PQ15 was found to enhance gap junctional intercellular communication (GJIC) by inhibiting the PKC phosphorylation of Cx43, resulting in the decrease of cell proliferation and viability in T47D cells.¹² Moreover, PQ15 was found to downregulate the expression of α -survivin, a member of the inhibitor of apoptosis (IAP) family, increasing apoptosis and decreasing chemoresistance in T47D cells.¹² Alpha-survivin is overexpressed in

human cancer and might be associated to the prolonged life of cancer cells by increasing resistance to chemotherapy.⁹⁶ The inhibition of PKC phosphorylation by PQ15 was therefore studied and the corresponding IC₅₀ value of 216.3 nM was obtained, which was significantly higher than that of PQ1 and PQ11 as shown in Figure 20. The gel image, percentage of C1 peptide phosphorylation catalyzed by PKC, and inhibition of PKC phosphorylation in the absence (positive control) and presence of PQ15 is highlighted in Figure 18.

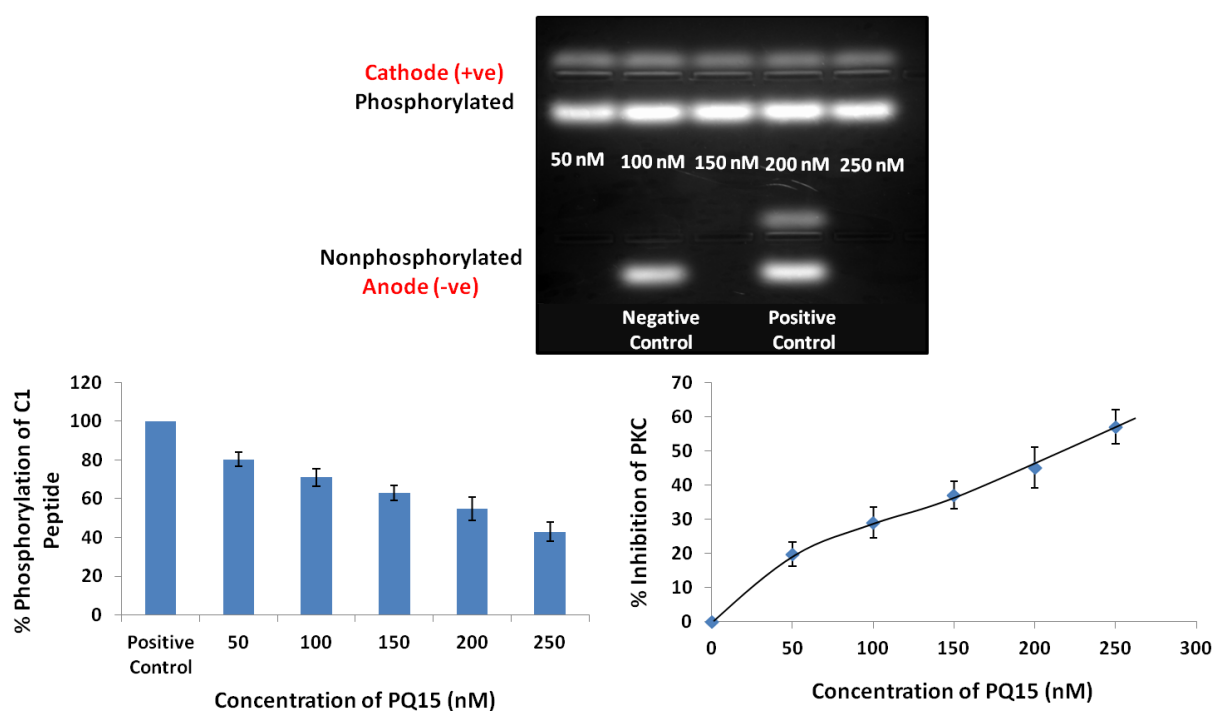


Figure 18: Gel image, percentage of C1 peptide phosphorylation catalyzed by PKC, and percentage inhibition of PKC in the absence and presence of PQ15. In the negative and positive control there is no PQ15 and others reactions have varying concentrations of PQ15 as indicated in the graphs. The graphs are provided with (\pm) standard error obtained from three separate experiments.

Among the compounds examined, 6-methoxy-4-methyl-*N*-(thiophen-2-ylmethyl)-5-(3-(trifluoromethyl)phenoxy)quinolin-8-amine (PQ10) did not show inhibition of PKC

phosphorylation within the studied concentration range of 1-20 μM . The gel image and percentage of C1 peptide phosphorylation by PKC in the absence (positive control) and presence of PQ10 in highlighted in Figure 19.

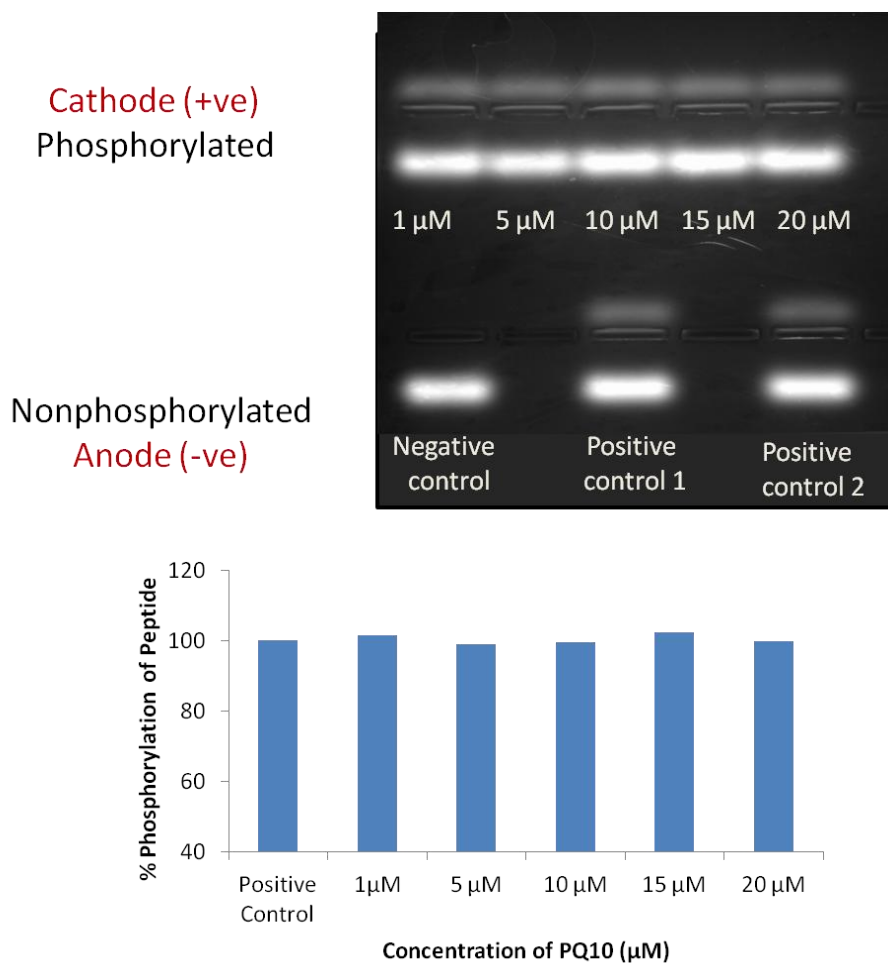


Figure 19: Gel image and percentage of C1 peptide phosphorylation by PKC in the absence and presence of PQ10. All the reactions have 0.8 μg of C1 peptide and 15 ng of PKC. In positive control there is no PQ10 and others have varying concentrations of PQ10 as indicated in the bar graphs. PQ10 shows no inhibition of PKC phosphorylation in the range of 1-20 μM . Only one experiment was carried out for PQ10.

The IC_{50} values of staurosporine, PQ1, PQ11, and PQ15 determined from PKC inhibition studies are summarized in Figure 20. A close structural resemblance of polysubstituted

quinolines (PQs) with that of several PKC inhibitors, including MT477, dequalinium, chelerythrine chloride, and M7 in having quinolines or isoquinoline moieties and with staurosporine and its analogs having closely related indole moiety might contribute to the PKC inhibition properties of PQs. However, the specificity of PQs towards PKC isozymes and other kinases has to be investigated.

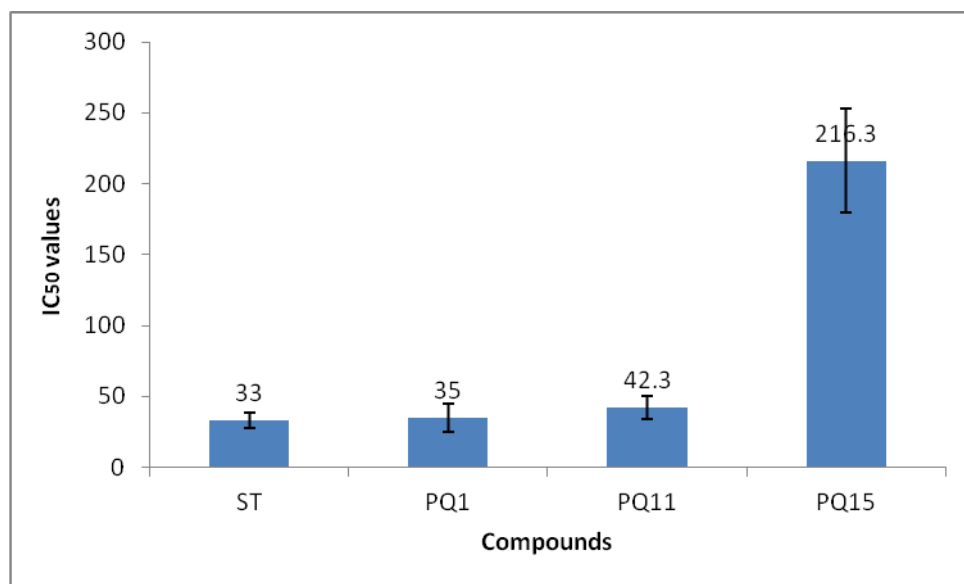


Figure 20: IC₅₀ values of staurosporine (ST), PQ1, PQ11, and PQ15. The values have been derived from three separate experiments for each compound and the bars are provided with (\pm) standard error.

2.5 Conclusions

Polysubstituted quinolines (PQs); PQ1, PQ11, and PQ15 known to have anti-breast cancer activities were evaluated for their role in the inhibition of PKC phosphorylation. The study indicated that PQ1, PQ11, and PQ15 were found to inhibit PKC phosphorylation with IC₅₀ values of 35, 42.3, and 216.3 nM, respectively. Moreover, PQ1 and PQ11 were found to be potent PKC inhibitor as comparable to staurosporine with IC₅₀ value of 33 nM. These results

indicate the possibility of developing PQ1 and PQ11 as possible anticancer drugs targeting PKC. However, it is still not known whether PQs are isozymes specific inhibitors of PKC or may even target other kinases.

2.6 References

- (1) Pearson, G.; Robinson, F.; Gibson, T. B.; Xu, B.-E.; Karandikar, M.; Berman, K.; Cobb, M. H. Mitogen-activated protein (MAP) kinase pathways: regulation and physiological functions. *Endocrine Reviews* **2001**, *22*, 153-183.
- (2) VanderZee, E. A.; Douma, B. R. K. Historical review of research on protein kinase C in learning and memory. *Prog. Neuro-Psychopharmacol. & Biol. Psychiat.* **1997**, *21*, 379-406.
- (3) Inoue, M.; Kishimoto, A.; Takai, Y.; Nishizuka, Y. Studies on a cyclic nucleotide-independent protein kinase and its proenzyme in mammalian tissues. II. Proenzyme and its activation by calcium-dependent protease from rat brain. *J. Biol. Chem.* **1977**, *252*, 7610-7616.
- (4) Takai, Y.; Kishimoto, A.; Inoue, M.; Nishizuka, Y. Studies on a cyclic nucleotide-independent protein kinase and its proenzyme in mammalian tissues. I. Purification and characterization of an active enzyme from bovine cerebellum. *J. Biol. Chem.* **1977**, *252*, 7603-7609.
- (5) Takai, Y.; Kishimoto, A.; Kikkawa, U.; Mori, T.; Nishizuka, Y. Unsaturated diacylglycerol as a possible messenger for the activation of calcium-activated, phospholipid-dependent protein kinase system. *Biochem. Biophys. Res. Commun.* **1979**, *91*, 1218-1224.
- (6) Carter, C. A.; Kane, C. J. Therapeutic potential of natural compounds that regulate the activity of protein kinase C. *Curr. Med. Chem.* **2004**, *11*, 2883-2902.

- (7) Castagna, M.; Takai, Y.; Kaibuchi, K.; Sano, K.; Kikkawa, U.; Nishizuka, Y. Direct activation of calcium-activated, phospholipid-dependent protein kinase by tumor-promoting phorbol esters. *J. Biol. Chem.* **1982**, *257*, 7847-7851.
- (8) Mackay, H. J.; Twelves, C. J. Protein Kinase C: a target for anticancer drugs? *Endocrine-Related Cancer* **2003**, *10*, 389-396.
- (9) Koivunen, J.; Aaltonen, V.; Peltonen, J. Protein kinase C (PKC) family in cancer progression. *Cancer Lett. (Amsterdam, Neth.)* **2006**, *235*, 1-10.
- (10) LaMontagne, M. P.; Blumbergs, P.; Smith, D. C. Antimalarials. 16. Synthesis of 2-substituted analogues of 8-[(4-amino-1-methylbutyl)amino]-6-methoxy-4-methyl-5-[3-(trifluoromethyl)phenoxy]quinoline as candidate antimalarials. *J. Med. Chem* **1989**, *32*, 1728-1732.
- (11) Shi, A.; Nguyen, T. A.; Battina, S. K.; Rana, S.; Takemoto, D. J.; Chiang, P. K.; Hua, D. H. Synthesis and anti-breast cancer activities of substituted quinolines. *Bioorg. Med. Chem. Lett.* **2008**, *18*, 3364–3368.
- (12) Bernzweig, J.; Heiniger, B.; Prasain, K.; Lu, J.; Hua, D. H.; Nguyen, T. A. Anti-breast cancer agents, quinolines, targeting gap junction. *Med. Chem.* **2011**, *7*, 448-453.
- (13) Gakhar, G.; Ohira, T.; Shi, A.; Hua, D. H.; Nguyen, T. A. Antitumor effect of substituted quinolines in breast cancer cells. *Drug Dev. Res.* **2008**, *69*, 526-534.
- (14) Heiniger, B.; Gakhar, G.; Prasain, K.; Hua, D. H.; Nguyen, T. A. Second-generation substituted quinolines as anticancer drugs for breast cancer. *Anticancer Res.* **2010**, *30*, 3927-3932.
- (15) Ding, Y.; Prasain, K.; Nguyen, T. D. T.; Hua, D. H.; Nguyen, T. A. The effect of PQ1 anti-breast cancer agent on normal tissues. *Anticancer Drugs* **2012**, *23*, 897-905.

- (16) Toullec, D.; Pianetti, P.; Coste, H.; Bellevergue, P.; Grand-Perret, T.; Ajakane, M.; Baudet, V.; Boissin, P.; Boursier, E.; Loriolle, F.; Duhamel, L.; Charon, D.; Kirilovsky, J. The bisindolylmaleimide GF 109203X is a potent and selective inhibitor of protein kinase C. *J. Biol. Chem.* **1991**, *266*, 15771-15781.
- (17) Schenk, P. W.; Snaar-Jagalska, B. E. Signal perception and transduction: the role of protein kinases. *Biochim. Biophys. Acta, Mol. Cell Res.* **1999**, *1449*, 1-24.
- (18) Griner, E. M.; Kazanietz, M. G. Protein kinase C and other diacylglycerol effectors in cancer. *Nature Reviews* **2007**, *7*, 281-294.
- (19) Newton, A. C. Protein kinase C: structure, function, and regulation. *J. Biol. Chem.* **1995**, *270*, 28495-28498.
- (20) Newton, A. C.; Johnson, J. E. Protein kinase C: a paradigm for regulation of protein function by two membrane-targeting modules. *Biochim. Biophys. Acta, Rev. Biomembr.* **1998**, *1376*, 155-172.
- (21) Bell, R. M.; Burns, D. J. Lipid activation of protein kinase C. *J. Biol. Chem.* **1991**, *266*, 4661-4664.
- (22) House, C.; Kemp, B. E. Protein kinase C contains a pseudosubstrate prototope in its regulatory domain. *Science (Washington, D. C., 1883)* **1987**, *238*, 1726-1728.
- (23) Dutil, E. M.; Newton, A. C. Dual role of pseudosubstrate in the coordinated regulation of protein kinase C by phosphorylation and diacylglycerol. *J. Biol. Chem.* **2000**, *275*, 10697-10701.
- (24) Kikkawa, U.; Takai, Y.; Tanaka, Y.; Miyake, R.; Nishizuka, Y. Protein kinase C as a possible receptor protein of tumor-promoting phorbol esters. *J. Biol. Chem.* **1983**, *258*, 11442-11445.

- (25) Neill, G. W.; Ghali, L. R.; Green, J. L.; Ikram, M. S.; Philpott, M. P.; Quinn, A. G. Loss of protein kinase C α expression may enhance the tumorigenic potential of Gli1 in basal cell carcinoma. *Cancer Res.* **2003**, *63*, 4692-4697.
- (26) Oster, H.; Leitges, M. Protein kinase C α but not PKC ζ suppresses intestinal tumor formation in *Apc*^{Min/+} mice. *Cancer Res.* **2006**, *66*, 6955-6963.
- (27) Lahn, M.; Sundell, K.; Koehler, G. The role of protein kinase C α in hematologic malignancies. *Acta Haematol.* **2006**, *115*, 1-8.
- (28) Koren, R.; Meir, D. B.; Langzam, L.; Dekel, Y.; Konichezky, M.; Baniel, J.; Livne, P. M.; Gal, R.; Sampson, S. R. Expression of protein kinase C isoenzymes in benign hyperplasia and carcinoma of prostate. *Oncol. Rep.* **2004**, *11*, 321-326.
- (29) Langzam, L.; Koren, R.; Gal, R.; Kugel, V.; Paz, A.; Farkas, A.; Sampson, S. R. Patterns of protein kinase C isoenzyme expression in transitional cell carcinoma of bladder relation to degree of malignancy. *Am. J. Clin. Pathol.* **2001**, *116*, 377-385.
- (30) Gokmen-Polar, Y.; Murray, N. R.; Velasco, M. A.; Gatalica, Z.; Fields, A. P. Elevated protein kinase C β II is an early promotive event in colon carcinogenesis. *Cancer Res.* **2001**, *61*, 1375-1381.
- (31) Varga, A.; Czifra, G.; Tallai, B.; Nemeth, T.; Kovacs, I.; Kovacs, L.; Biro, T. Tumor grade-dependent alterations in the protein kinase C isoform pattern in urinary bladder carcinomas. *Eur. Urol.* **2004**, *46*, 462-465.
- (32) Johnson, C. L.; Lu, D.; Huang, J.; Basu, A. Regulation of *p53* stabilization by DNA damage and protein kinase C. *Mol. Cancer Ther.* **2002**, *1*, 861-867.

- (33) Abbas, T.; White, D.; Kui, L.; Yoshida, K.; Foster, D. A.; Bargonetti, J. Inhibition of human *p53* basal transcription by down-regulation of protein kinase C δ . *J. Biol. Chem.* **2004**, *279*, 9970-9977.
- (34) Majumder, P. K.; Pandey, P.; Sun, X.; Cheng, K.; Datta, R.; Saxena, S.; Kharbanda, S.; Kufe, D. Mitochondrial translocation of protein kinase C δ in phorbol ester-induced cytochrome *c* release and apoptosis. *J. Biol. Chem.* **2000**, *275*, 21793-21796.
- (35) Marengo, B.; Ciucis, C. D.; Ricciarelli, R.; Pronzato, M. A.; Marinari, U. M.; Domenicotti, C. Protein kinase C: an attractive target for cancer therapy. *Cancers* **2011**, *3*, 531-567.
- (36) Ferlay, J.; Slin, H. R.; Bray, F. Estimates of worldwide burden of cancer 2008: GLOBOCAN 2008. *International Journal of Cancer* **2010**, *127*, 2893-2917.
- (37) Gray, J.; Evans, N.; Taylor, B.; Rizzo, J.; Walker, M. State of the evidence: the connection between breast cancer and the environment. *Int. J. Occup. Environ. Health* **2009**, *15*, 43-78.
- (38) Hilakivi-Clarke, L. Estrogens, BRCA1, and breast Cancer. *Cancer Research* **2000**, *60*, 4993-5001.
- (39) Blobe, G. C.; Obeid, L. M.; Hannun, Y. A. Regulation of protein kinase C and role in cancer biology. *Cancer Metastasis Rev.* **1994**, *13*, 411-431.
- (40) O'Brian, C. A.; Vogel, V. G.; Singletary, S. E.; Ward, N. E. Elevated protein kinase C expression in human breast tumor biopsies relative to normal breast tissue. *Cancer Res.* **1989**, *49*, 3215-3217.

- (41) Fabbro, D.; Kueng, W.; Roos, W.; Regazzi, R.; Eppenberger, U. Epidermal growth factor binding and protein kinase C activities in human breast cancer cell lines: possible quantitative relationship. *Cancer Res.* **1986**, *46*, 2720-2725.
- (42) Darbon, J. M.; Valette, A.; Bayard, F. Phorbol esters inhibit the proliferation of MCF-7 cells. Possible implication of protein kinase C. *Biochem. Pharmacol.* **1986**, *35*, 2683-2686.
- (43) Fabbro, D.; Regazzi, R.; Costa, S. D.; Borner, C.; Eppenberger, U. Protein kinase C desensitization by phorbol esters and its impact on growth of human breast cancer cells. *Biochem. Biophys. Res. Commun.* **1986**, *135*, 65-73.
- (44) Willecke, K.; Eiberger, J.; Degen, J.; Eckardt, D.; Romualdi, A.; Guldenagel, M.; Deutsch, U.; Sohl, G. Structural and functional diversity of connexin genes in the mouse and human genome. *Biol. Chem.* **2002**, *383*, 725-737.
- (45) Musil, L. S.; Goodenough, D. A. Biochemical analysis of connexin43 intracellular transport, phosphorylation, and assembly into gap junctional plaques. *The Journal of Cell Biology* **1991**, *115*, 1357-1374.
- (46) Eghbali, B.; Kessler, J. A.; Reid, L. M.; Roy, C.; Spray, D. C. Involvement of gap junction in tumorigenesis: transfection of tumor cells with connexin 32 cDNA retard growth *in vivo*. *Proc. Natl. Acad. Sci. USA* **1991**, *88*, 10701-10705.
- (47) Goodenough, D. A.; Goliger, J. A.; Paul, D. L. Connexins, connexons, and intercellular communication. *Annu. Rev. Biochem.* **1996**, *65*, 475-502.
- (48) Unger, V. M.; Kumar, N. M.; Gilula, N. B.; Yeager, M. Three-dimensional structure of a recombinant gap junction membrane channel. *Science* **1999**, *283*, 1176-1180.

- (49) Giepman, B. N. G. Gap junctions and connexin-interacting proteins. *Cardiovascular Research* **2004**, *62*, 233-245.
- (50) Bao, X.; Altenberg, G. A.; Reuss, L. Mechanism of regulation of the gap junction protein connexin 43 by protein kinase C-mediated phosphorylation. *Am. J. Physiol. Cell Physiol.* **2004**, *286*, 647-654.
- (51) Bruzzone, R.; White, T. W.; Paul, D. L. Connections with connexins: the molecular basis of direct intercellular signaling. *European Journal of Biochemistry* **1996**, *238*, 1-27.
- (52) Carystinos, G. D.; Bier, A.; Batist, G. The role of connexin-mediated cell-cell communication in breast cancer metastasis. *J. Mammary Gland Biol. Neoplasia* **2001**, *6*, 431-440.
- (53) Liu, T. F.; Johnson, R. G. Effects of TPA on dye transfer and dye leakage in fibroblasts transfected with a connexin 43 mutation at ser368. *Methods Find. Exp. Clin. Pharmacol.* **1999**, *21*, 387-390.
- (54) Lampe, P. D.; TenBroek, E. M.; Burt, J. M.; Kurata, W. E.; Johnson, R. G.; Lau, A. F. Phosphorylation of connexin43 on serine368 by protein kinase C regulates gap junctional communication. *J. Cell Biol.* **2000**, *149*, 1503-1512.
- (55) Hannun, Y. A.; Loomis, C. R.; Merrill, A. H.; Bell, R. M. Sphingosine inhibition of protein kinase C activity and of phorbol dibutyrate binding *in vitro* and in human platelets. *The Journal of Biological Chemistry* **1986**, *261*, 12604-12609.
- (56) Schwartz, G. K.; Ward, D.; Saltz, L.; Casper, E. S.; Spiess, T.; Mullen, E.; Woodworth, J.; Venuli, R.; Zervos, P.; Storniolo, A.-M.; Kelson, D. P. Pilot clinical/pharmacological study of the protein kinase C-specific inhibitor safinol alone and in combination with doxorubicin. *Clinical Cancer Research* **1977**, *3*, 537-543.

- (57) Dickson, M. A.; Carvajal, R. D.; Merrill, A. H.; Gonen, M.; Cane, L. M.; Schwartz, G. K. A phase I clinical trial of safinol in combination of cisplatin in advanced solid tumors. *Clinical Cancer Research* **2011**, *17*, 2484-2492.
- (58) Kobayashi, E.; Nakano, H.; Morimoto, M.; Tamaoki, T. Calphostin C (UCN-1028C), a novel microbial compound, is a highly potent and specific inhibitor of protein kinase C. *Biochem. Biophys. Res. Commun.* **1989**, *159*, 548-553.
- (59) Kaul, A.; Maltese, W. A. Killing of cancer cells by the photoactivatable protein kinase C inhibitor, calphostin C, involves induction of endoplasmic reticulum stress¹. *Neoplasia* **2009**, *11*, 823-834.
- (60) Smorenburg, C. H.; Seynaeve, C.; Bontenbal, M.; Planting, A. S.; Sindermann, H.; Verweij, J. Phase II study of miltefosine 6% solution as topical treatment of skin metastases in breast cancer patients. *Anticancer Drugs* **2000**, *11*, 2366-2373.
- (61) Pettit, G. R.; Herald, C. L.; Doubek, D. L.; Herald, D. L.; Arnold, E.; Clardy, J. Isolation and structure of bryostatin 1¹. *J. Am. Chem. Soc* **1982**, *104*, 6846-6848.
- (62) Philip, P. A.; Zonder, J. A. Pharmacology and clinical experience with bryostatin 1: a novel anticancer drug. *Expert Opin. Investig. Drug* **1999**, *8*, 2189-2199.
- (63) Ajani, J. A.; Jiang, Y.; Faust, J.; Chang, B. B.; Ho, L.; Yao, J. C.; Rousey, S.; Dakhil, S.; Cherny, R. C.; Craig, C.; Bleyer, A. A multi-center phase II study of sequential paclitaxel and bryostatin 1 (NSC 339555) in patients with untreated, advanced gastric or gastroesophageal junction adenocarcinoma. *Invest. New Drugs* **2006**, *24*, 353-357.
- (64) Ku, G. Y.; Ilson, D. H.; Schwartz, L. H.; Capanu, M.; O'Reilly, E.; Shah, M. A.; Kelsen, D. P.; Schwartz, G. K. Phase II trial of sequential paclitaxel and 1 h infusion of bryostatin

- 1 in patients with advanced esophageal cancer. *Cancer Chemother. Pharmacol.* **2008**, *62*, 875-880.
- (65) Barr, P. M.; Lazarus, H. M.; Cooper, B. W.; Schluchter, M. D.; Panneerselvam, A.; Jacobberger, J. W.; Hsu, J. W.; Janakiraman, N.; Simic, A.; Dowlati, A.; Remick, S. C. Phase II study of bryostatin 1 and vincristine for aggressive non-Hodgkin lymphoma relapsing after an autologous stem cell transplant. *Am. J. Hematol.* **2009**, *84*, 484-487.
- (66) Liu, J.-Y.; Lin, S.-J.; Lin, J.-K. Inhibitory effects of curcumin on protein kinase C activity induced by 12-*O*-tetradecanoyl-phorbol-13-acetate in NIH 3T3 cells. *Carcinogenesis* **1993**, *14*, 857-861.
- (67) Herbert, J. M.; Augereau, J. M.; Gleye, J.; Maffrand, J. P. Chelerythrine is a potent and specific inhibitor of protein kinase C. *Biochem. Biophys. Res. Commun.* **1990**, *172*, 993-999.
- (68) Chan, S.-L.; Lee, M. C.; Tan, K. O.; Yang, L.-K.; Lee, A. S. Y.; Flotow, H.; Fu, N. Y.; Butler, M. S.; Soejarto, D. D.; Buss, A. D.; Yu, V. C. Identification of chelerythrine as an inhibitor of BclXL function. *J. Biol. Chem.* **2003**, *278*, 20453-20456.
- (69) Anderson, L.; Schmieder, G. J.; Werschler, W. P.; Tschen, E. H.; Ling, M. R.; Stough, D. B.; Katsamas, J. Randomized, double-blind, double-dummy, vehicle-controlled study of ingenol mebutate gel 0.025% and 0.05% for actinic keratosis. *J. Am. Acad. Dermatol.* **2009**, *60*, 934-943.
- (70) Ogbourne, S. M.; Hampson, P.; Lord, J. M.; Parsons, P.; DeWitte, P. A.; Suhrbier, A. Proceedings of the first international conference on PEP005. *Anticancer Drugs* **2007**, *18*, 357-362.

- (71) Kawamoto, S.; Hidaka, H. 1-(5-isoquinolinesulfonyl)-s-methyl piperazine (H-7) is a selective inhibitor of protein kinase in rabbit platelets. *Biochem. Biophys. Res. Commun.* **1984**, *125*, 258-264.
- (72) Shen, G. X.; Way, K. J.; Jacobs, J. R. C.; King, G. L. In *Protein Kinase C Protocols*; Newton, A. C., Ed.; Humana Press: Totowa, New Jersey, **2003**; Vol. 233, p 397-422.
- (73) Gschwendt, M.; Muller, H. J.; Kielbassa, K.; Zang, R.; Kittstein, W.; Rincke, G.; Marks, F. Rottlerin, a novel protein kinase inhibitor. *Biochem. Biophys. Res. Commun.* **1994**, *199*, 93-98.
- (74) Mandil, R.; Ashkenazi, E.; Blass, M.; Kronfeld, I.; Kazimirsky, G.; Rosenthal, G.; Umansky, F.; Lorenzo, P. S.; Blumberg, P. M.; Brodie, C. Protein kinase C α and protein kinase C δ play opposite roles in the proliferation and apoptosis of glioma cells. *Cancer Res.* **2001**, *61*, 4612-4619.
- (75) Jasinski, P.; Zwolak, P.; Terai, K.; Dudek, A. Z. Novel Ras pathway inhibitor induces apoptosis and growth inhibition of *K-ras*-mutated cancer cells *in vitro* and *in vivo*. *Translational Research* **2008**, *152*, 203-212.
- (76) Jasinski, P.; Zwolak, P.; Terai, K.; Borja-Cacho, D.; Dudek, A. Z. PKC- α inhibitor MT477 slows tumor growth with minimal toxicity in *in vivo* model of non-Ras-mutated cancer via induction of apoptosis. *Invest. New Drugs* **2011**, *29*, 33-44.
- (77) Omura, S.; Iwai, Y.; Hirano, A.; Nakagawa, A.; Awaya, J.; Tsuchiya, H.; Takahashi, Y.; Masuma, R. A new alkaloid AM-2282 of *Streptomyces* origin. Taxonomy, fermentation, isolation and preliminary characterization. *J. Antibiot.* **1977**, *30*, 275-282.
- (78) Swannie, H. C.; Kaye, S. B. Protein kinase C inhibitors. *Current Oncology Reports* **2002**, *4*, 37-46.

- (79) Eder, J. P.; Garcia-Carbonero, R.; Clark, J. W.; Supko, J. G.; Puchalski, T. A.; Ryan, D. P.; Deluca, P.; Woznaik, A.; Campbell, A.; Rothermel, J.; LoRusso, P. A phase I trial of daily oral 4'-N-benzoyl-staurosporine in combination with protracted continuous infusion 5-fluorouracil in patients with advanced solid malignancies. *Invest. New Drugs* **2004**, *22*, 139-150.
- (80) Monnerat, C.; Henriksson, R.; LeChevalier, T.; Novello, S.; Berthaud, P.; Faivre, S.; Raymond, E. Phase I study of PKC412 (*N*-benzoyl-staurosporine), a novel oral protein kinase C inhibitor, combined with gemcitabine and cisplatin in patients with non-small-cell lung cancer. *Annals of Oncology* **2004**, *15*, 316-323.
- (81) Seynaeve, C. M.; Kazanietz, M. G.; Blumberg, P. M.; Sausville, E. A.; Worland, P. J. Differential inhibition of protein kinase C isozymes by UCN-01, a staurosporine analogue. *Molecular Pharmacology* **1994**, *45*, 1207-1214.
- (82) Teicher, B. A.; Alvarez, E.; Menon, K.; Esterman, M. A.; Considine, E.; Shih, C.; Faul, M. M. Antiangiogenic effects of protein kinase C β -selective small molecules. *Cancer Chemother. Pharmacol.* **2002**, *49*, 69-77.
- (83) Kreisl, T. N.; Kotliarova, S.; Butman, J. A.; Albert, P. S.; Kim, L.; Mushib, L.; Thornton, D.; Fine, H. A. A phase I/II trial of enzastaurin in patients with recurrent high-grade gliomas. *Neuro. Oncol.* **2010**, *12*, 181-189.
- (84) Wick, W.; Puduvalli, V. K.; Chamberlain, M.; vandenBent, M. J.; Carpentier, A. F.; Cher, L. M.; Mason, W.; Weller, M.; Hong, S.; Musib, L.; Liepa, A. M.; Thornton, D. E.; Fine, H. A. Phase III study of enzastaurin compared with lomustine in the treatment of recurrent intracranial glioblastoma. *Journal of Clinical Oncology* **2010**, *28*, 1168-1174.

- (85) Wagner, J.; Matt, P. v.; Sedrani, R.; Albert, R.; Cooke, N.; Ehrhardt, C.; Geiser, M.; Rummel, G.; Stark, W.; Strauss, A.; Cowan-Jacob, S. W.; Beerli, C.; Weckbecker, G.; Evenou, J.-P.; Zenke, G.; Cottens, S. Discovery of 3-(1*H*-Indol-3-yl)-4-[2-(4-methylpiperazin-1-yl)quinazolin-4-yl]-pyrrole-2,5-dione (AEB071), a potent and selective inhibitor of protein kinase C isotypes. *Journal of Medicinal Chemistry Letter* **2009**, *52*, 6193-6196.
- (86) Asghar, M.; Lokhandwala, M. F. Antioxidant supplementation normalizes elevated protein kinase C activity in the proximal tubules of old rats. *Experimental Biology and Medicine* **2004**, *229*, 270-275.
- (87) Information obtained from Heather M. Komars (PhD), Technical Service Scientist from Promega.
- (88) Lilienthal, E.; Kolanowski, K.; Becker, W. Development of a sensitive non-radioactive protein kinase assay and its application for detecting DYRK activity in *Xenopus laevis* oocytes. *BioMed Central Biochemistry* **2010**, *11*, 1-10.
- (89) Khaliulin, I.; Parker, J. E.; Halestrap, A. P. Consecutive pharmacological activation of PKA and PKC mimics the potent cardioprotection of temperature preconditioning. *Cardiovascular Research* **2010**, *88*, 324-333.
- (90) Stellwagen, N. C. Effect of pulsed and reversing electric fields on the orientation of linear and supercoiled DNA molecules in agarose gels. *Biochemistry* **1988**, *27*, 6417-6424.
- (91) McHenry, P. R.; Sears, J. C.; Herrick, M. P.; Chang, P.; Heckman-Stoddard, B. M.; Rybarczyk, M.; Chodosh, L. A.; Gunther, E. J.; Hilsenbeck, S. G.; Rosen, J. M.; Vargo-Gogola, T. P190B RhoGAP has pro-tumorigenic functions during MMTV-Neu mammary tumorigenesis and metastasis. *Breast Cancer Research* **2010**, *12*, 1-16.

- (92) Keates, S. E.; Kostman, T. A.; Anderson, J. D.; Bailey, B. A. Altered gene expression in three plant species in response to treatment with Nep1, a fungal protein that causes necrosis. *Plant Physiology* **2003**, *132*, 1610-1622.
- (93) Omura, S.; Sasaki, Y.; Iwai, Y.; Takeshima, H. Staurosporine, a potentially important gift from a microorganism. *J. Antibiot.* **1995**, *48*, 535-548.
- (94) Meggio, F.; Donella, D. A.; Ruzzene, M.; Brunati, A. M.; Cesaro, L.; Guerra, B.; Meyer, T.; Mett, H.; Fabbro, D.; Furet, P.; Dobrowolska, G.; Pinna, L. A. Different susceptibility of protein kinases to staurosporine inhibition. Kinetic studies and molecular bases for the resistance of protein kinase CK2. *Eur. J. Biochem.* **1995**, *234*, 317-322.
- (95) Wilkinson, S. E.; Parker, P. J.; Nixon, J. S. Isoenzyme specificity of bisindolylmaleimides, selective inhibitors of protein kinase C. *Biochem. J.* **1993**, *294*, 335-337.
- (96) Fukuda, S.; Pelus, L. M. Survivin, a cancer target with an emerging role in normal adult tissues. *Mol. Cancer Ther.* **2006**, *5*, 1087-1098.

Chapter 3. Distribution of PQ1 and PQ11 in tissues of mice and effect of PQ1 in normal tissues

3.1 Introduction

Cancer, a broad group of more than 100 diseases characterized by the unregulated growth and spread of abnormal cells in the body, has been listed as one of the most important public health problems in today's world. In 2008, an approximate of 12.6 million new cases of cancer were reported worldwide causing 7.6 million lives in the same year.¹ In 2011, about 1.6 million new cases of cancer were reported in the United States resulting in 0.6 million deaths in the same year.² In general, about 25% of all deaths in the United States is associated with cancer.² In the United States, breast cancer is the most common cancer in women and one in every eight women has a chance of getting breast cancer in her life time.²

Quinolines are known to have wide range of biological activities including antifungal,³ antibacterial,⁴ and antimalarial.⁵ Quinolines are also found to have anticancer activities such as by targeting tumor hypoxia,^{6,7} inhibiting topoisomerase,⁸ inhibiting tyrosine kinase,⁹ and reversing multidrug resistance.¹⁰ For example: irinotecan and topotecan, derivatives of camptothecin are used in the treatment of colorectal and ovarian cancer, respectively.¹¹ Amsacrine, another anticancer drug having a quinoline motif is used in the treatment leukemia and lymphomas in many countries.¹² The structures of camptothecin, irinotecan, topotecan, and amsacrine are highlighted in Figure 21.

Substituted quinolines (PQs), *N*-(3-aminopropyl)-6-methoxy-4-methyl-5-(3-(trifluoromethyl) phenoxy)quinolin-8-amine (PQ1) and *N*-(furan-2-ylmethyl)-6-methoxy-4-methyl-5-(3-(trifluoromethyl)phenoxy)quinolin-8-amine (PQ11) are potential anticancer drugs

with respective IC_{50} value of 119 and 15.6 nM in T47D cells.^{13,14} PQ1 and PQ11 are known to enhance gap junctional intercellular communication (GJIC) resulting in the decrease in cell viability and proliferation in cancer cells.^{13,15} The enhancement in GJIC in T47D cells by PQ1 and PQ11 is linked to the inhibition of PKC phosphorylation of Cx43, a gap junctional protein.^{13,15,16} The increase in gap junction activities is positively related to the increase in apoptosis and drug sensitivity in cancer cells.¹⁷ *In vivo* studies, PQ1 and PQ11 have demonstrated the attenuation of T47D xenograft tumors in nude mice up to 100%.^{13,15} As discussed in chapter two of this thesis, PQ1 and PQ11 are found to be potent inhibitors of PKC with IC_{50} values of 35 and 42.3 nM, respectively.

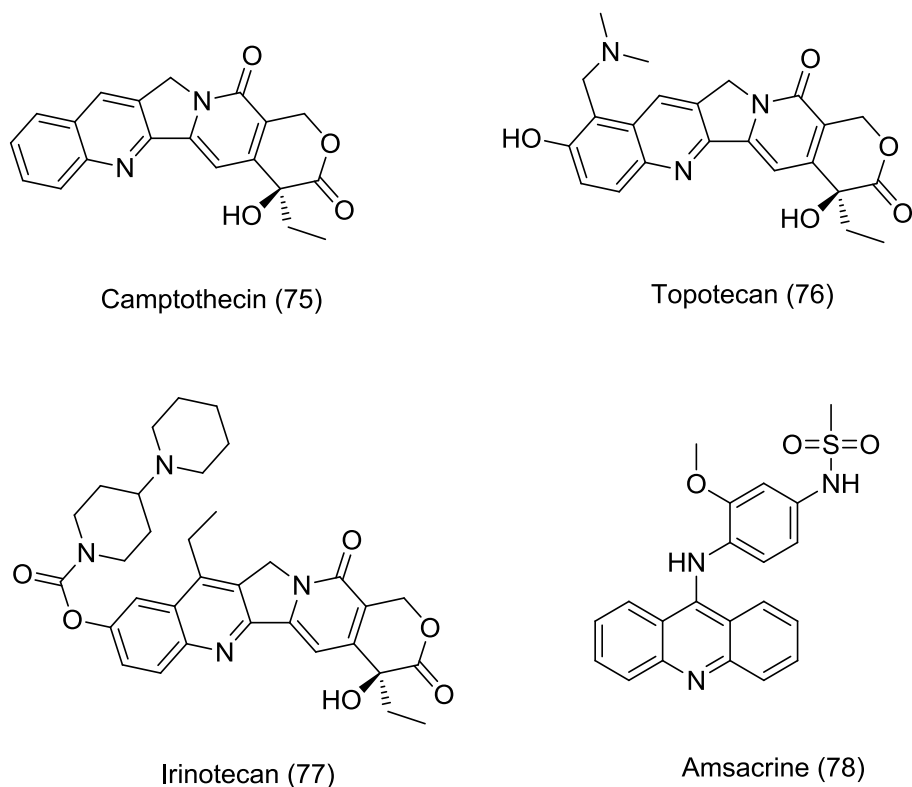


Figure 21: Structures of quinoline motif bearing anticancer drugs: camptothecin, topotecan, irinotecan, and amsacrine.

However, for a cancer drug to be effective, they must reach the targeted tissues in the body in concentrations sufficient to kill the cancer cells without producing cytotoxic or adverse effects in normal cells. In this chapter, the time dependent distribution of PQ1 and PQ11 in different organs of normal C57BL/6J mice and the effect of PQ1 on the normal organs are discussed. These studies are essential to establish PQ1 and PQ11 as potential candidates in the development of gap junctional or PKC targeting anticancer drugs by finding their possible toxicity and locating their presence in various tissues.

Oral gavage of PQ1 was conducted by Dr. Thu Annelise Nguyen and me, Intraperitoneal (IP) injection of PQ11 was done by Stephanie Shishido, and the effect of PQ1 in the normal tissues was studied by Ying Ding. Stephanie Shishido and Ying Ding are graduate students in Dr. Thu Annelise Nguyen group, College of Veterinary Medicine, Department of Diagnostic Medicine Pathobiology, Kansas State University.

3.2 Background

The mode of treatment of cancer is diverse including surgery, radiation, chemotherapy, hormone therapy, and targeted therapy. Surgery is carried out to remove the tumor from the body and is very effective for curing cancer that has not spread to other parts of the body. Radiation therapy uses high energy radiations to kill cancer cells by damaging their DNA. Cancer cells are known to grow and divide rapidly and chemotherapy is the most commonly used method to treat cancers by using chemicals capable of killing rapidly dividing cells in the body. In hormone therapy, a patient is treated with drugs that either prevent the cancer cell to come in contact with hormones that help the cancer cells to grow or activate the production of hormones that kill cancer cells. Finally, in targeted therapy drugs that block the growth and spread of cancer cells

by targeting specific culprit molecules in tumor growth and progression are used. In general the combination of different methods is used for the effective treatment of cancer.

Understanding how drugs behave in a biological system is a subject of prime importance in the treatment of various diseases. The circulatory system which comprises of blood and blood vessels is generally used to distribute drugs in several tissues in the body.

For systemic drug administration in research, the drugs are generally administered in the mice through three main routes that include oral gavage, intravenous injection, and intraperitoneal injection. In oral gavage, the drug in the form of solution is administered directly into the lower esophagus or stomach by the use of feeding needle. The feeding needle has a bulb tip which prevents the rupture of delicate tissues during the drug administration. The maximum volume that can be feed by oral gavage is 10 mL/Kg body weight of the mice.

Intraperitoneal (IP) injection of drug is one of the most frequently performed drug administration methods in mice. In this method the drug in the form of the solution is injected into the peritoneal cavity, a space that surrounds the abdominal organs. A small and thin needle is inserted into the abdominal cavity in the lower right quadrant to avoid the puncture of cecum and urinary bladder with the needle. For IP injection the volume of drug solution should not exceed 2 mL in an adult mouse.

Intravenous (IV) injection is used to administer the drug solution directly in the blood through veins. The vein in the tail of a mouse functions in thermoregulation and dilates on the rise in body temperature. Thus application of heat to the tail of the mouse causes venodilation making the veins easily accessible for IV administration. The maximum volume of drugs administration through IV should not exceed 0.5 mL in an adult mouse.

The drugs administered through oral gavage and IP injections must first diffuse into the blood stream. The blood then transports and distributes the drugs in various tissues in the body as shown in Figure 22.

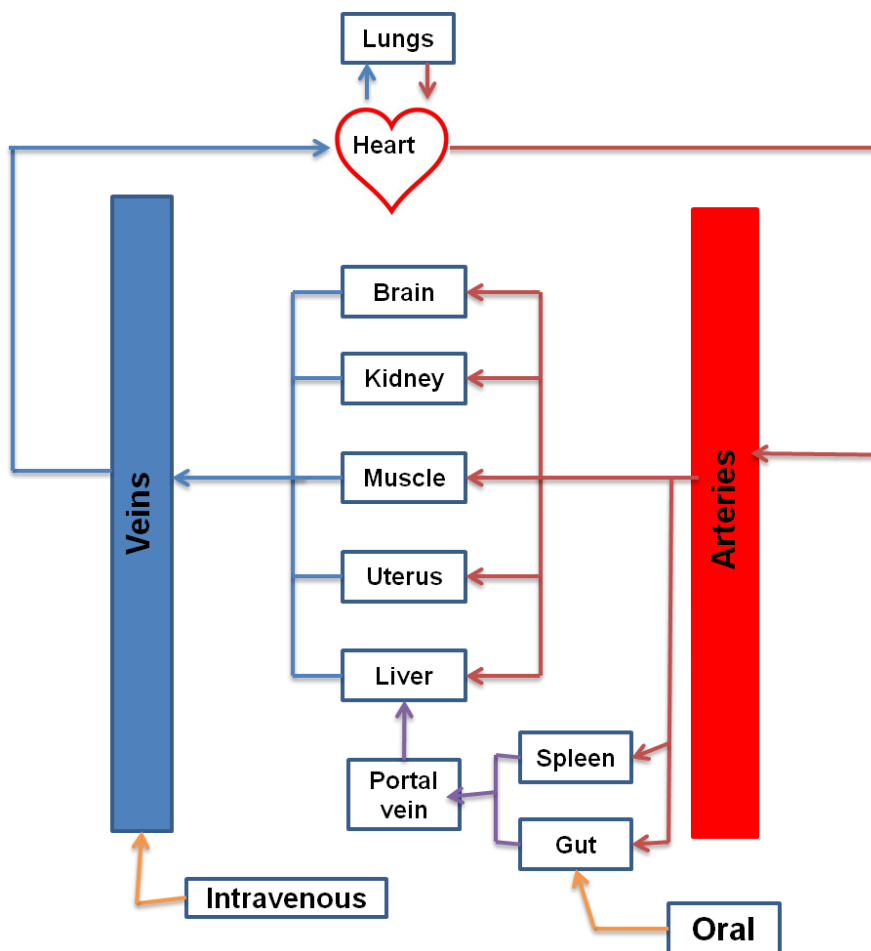


Figure 22: Schematic representation of blood circulation in mammals.

3.3 Experimental

Substituted quinolines, PQ1 and PQ11, were obtained as described by Shi et al.¹⁴ Oral gavage of PQ1, intraperitoneal (IP) injection of PQ11, and the effect of PQ1 in the mice tissues were studied in Dr. Annelise Nguyen laboratory. For PQ1 studies, each group consisted of four

female C57BL/6J mice and the distribution of PQ1 and its effect in normal tissues were studied at 1 hour, 12 hours, and 24 hours after the dosage of PQ1 by oral gavage. For PQ11, each group consisted of six female C57BL/6J mice and the tissue distribution of PQ11 was studied at 6 hours, 12 hours, 24 hours, and 36 hours after the dosage of PQ11 by intraperitoneal injection.

3.3.1 PQ1 and PQ11 administration and tissue collection

A dose of 25 mg/Kg (mice body weight) of PQ1 or PQ11 as their succinic acid salt dissolved in DMSO was administered to the mice. PQ1 was administered by oral gavage, whereas PQ11 was administered by IP injection. The distribution of PQ1 in the organs was analyzed in 1, 12, and 24 hour times from the exposure of PQ1. The animals were euthanized with CO₂ and sacrificed by cervical dislocation. The blood was immediately collected in a heparin-coated 1mL syringe by cardiac puncture. Various tissues including brain, heart, liver, lungs, uterus, and kidneys were obtained after immediate dissection of the animal and kept in vials over dry ice. The blood was centrifuged to collect plasma. All the tissues and plasma collected were stored at -78°C until further analysis was carried.

In case of PQ11, distribution of drug to the various tissues and plasma was evaluated in 6, 12, 24, and 36 hour times of the drug exposure. Similar method as applied for PQ1 was followed to collect plasma and tissue samples (liver, lungs, kidney, heart, spleen, uterus, gastro intestinal tract, and brain) from the mice.

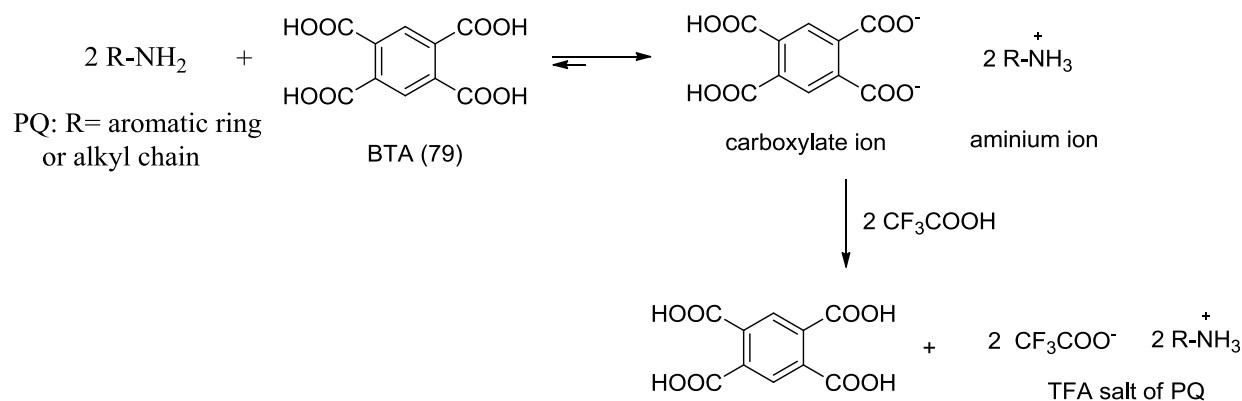
3.3.2 Extraction of PQ1 and PQ11 from organs and plasma

Organs were weighed and cut into small pieces followed by the addition of 4 mL of deionized water and 10 mL of 9:1 mixture of ethyl acetate and 1-propanol. Known volume of plasma samples were directly mixed with 4 mL of deionized water and 10 mL of a 9:1 mixture of ethyl acetate and 1-propanol. Sodium bicarbonate (10 mg) was added to the tissue or plasma solutions and were sonicated for 40 minutes and 10 minutes, respectively. The organic layer was separated from a separatory funnel. The aqueous layer was extracted twice with 10 mL of a 9:1 mixture of ethyl acetate and 1-propanol. The organic layers were combined, washed with 5 mL of brine, dried over anhydrous MgSO₄, and concentrated to dryness on a rotary evaporator. The residue was diluted with 1 mL of 1-propanol and filtered through a 0.2 µm filter disc (PTFE 0.2 µm, Fisherbrand) and analyzed using HPLC and mass spectrometry as described below.

3.3.3 Quantification of PQ1 and PQ11 using HPLC

HPLC analysis of PQ1 and PQ11 was carried out on a Varian Prostar 210 with a UV-Vis detector. A reverse phase column from Phenomenex (250 x 21.20 mm, 10 micron, S. No: 552581-1) was used for PQ1 analysis, whereas a C18 reverse phase column from Xper-chrom Aegis (S. No: 104117, 250 x 10 mm, 10 micron) was used for PQ11. For both PQ1 and PQ11, a flow rate of 5 mL/min and detection wavelength of 254 nm were used. A gradient elution of solvent A, containing deionized water and 0.01% of trifluoroacetic acid, and solvent B, containing acetonitrile and 0.01% of trifluoroacetic acid, was applied for the analysis.

Scheme 10: Schematic representation of the regeneration of BTA from the salt of BTA with PQ compounds



1,2,4,5-Benzenetetracarboxylic acid (BTA) was used as an internal standard to quantify the amount of PQ1 or PQ11 in the samples. BTA does not undergo amide formation reaction with PQ compounds (amine) at ambient temperature because (i) –OH group in carboxylic acid is a poor leaving group and (ii) BTA has a pKa ~ 3 that is lower as compared to the pKa of the aminium ions of aliphatic primary amine (pKa ~ 10) and aniline (pKa ~ 4.5) resulting in a very small amount of free amine (nucleophile) in the equilibrium as shown in Scheme 10. Moreover, the presence of 0.01% of trifluoroacetic acid (pKa = 0.52) in the solvents for HPLC regenerates BTA from its salt as shown in Scheme 10. Solutions of 100 μL of various mixtures of authentic PQ1 or PQ11 and BTA were injected into an HPLC instrument, the peak areas corresponding to PQ1 or PQ11 and BTA were integrated from the HPLC chromatogram, and the ratios of the peaks were obtained. The results of the ratios of HPLC peak areas and the ratios from PQ1 or PQ11 and BTA concentrations were plotted, and a linear correlation line was obtained from the graph. Hence, using this correlation diagram, the ratio of HPLC peak areas of PQ1 or PQ11 and BTA from tissue extract, and the added known amount of BTA to the tissue extract, the amount

of PQ1 or PQ11 in the tissue or plasma extract was determined. The eluant corresponding to the peak that had the same retention time as that of PQ1 or PQ11 from the injection of the tissue extract was collected, and its mass was determined using mass spectrometer. The mass spectrum acquired from the collected peak of PQ1 or PQ11 from the plasma or tissue extract was identical to that of the authentic PQ1 or PQ11 mass spectrum. Hence, the molecular identity of PQ1 and PQ11 in the tissue extract was verified by mass spectrometry. An Applied Biosystem API 2000 LS/MS/MS mass spectrometer was used in the analysis. The eluent corresponding to PQ1 or PQ11 peak from the HPLC was collected and injected into the mass spectrometer. A mass of 406 corresponding to M+1 of PQ1 or 429 corresponding to M+1 of PQ11 was found in their mass spectra and the fragmentation pattern of this M+1 mass is similar to that of the authentic PQ1 or PQ11 verifying the identity of PQ1 and PQ11.

The percentage distribution of PQ1 and PQ11 in the tissues was determined from the amount of PQ1 or PQ11 obtained in the organs compared to the total amount of the drugs administered to each mice. Similarly, the concentration of the drugs in the tissues was obtained by finding the number of moles of PQ1 or PQ11 in the given volume of the organs (mass of organs = volume of organs, density ~1).

3.4 Results and discussions

PQ1 and PQ11 are known to have anti-breast cancer activities in T47D cells by enhancing GJIC and inducing apoptosis; however, have no effect on normal human mammary epithelial cells (HMEC).^{13,15} It is therefore important to determine the distribution of these drugs in different tissues and study the toxicity of these compounds in the normal tissues. Since, the

studies on the effects of PQ11 on the normal tissues is ongoing, this chapter highlights the distribution of PQ1 and PQ11 in different tissues of normal mice and also discusses the effect of PQ1 in the normal tissues. Distribution of PQ1 in the mice tissues and its effect on the normal cells has been published recently and the results are summarized in this chapter.¹⁸ The effect of PQ1 on normal tissues was studied by Ying Ding in Dr. Annelise Nguyen laboratory.

3.4.1 Tissue distribution of PQ1

To examine the tissue distribution of PQ1 in different organs, a dose of 25mg/Kg of PQ1, was administered to C57BL/6J mice by oral gavage, a desirable and safe method for drugs administration. The main purpose of administering higher dose of PQ1 was to evaluate the toxicities of PQ1 in normal tissues.

PQ1 in the tissues was determined by plotting a calibration graph with the ratios of peak areas of PQ1 to BTA vs. molar ratios of PQ1 to BTA as mentioned in the experimental section of this chapter. The calibration graph for PQ1 is shown in Figure 23.

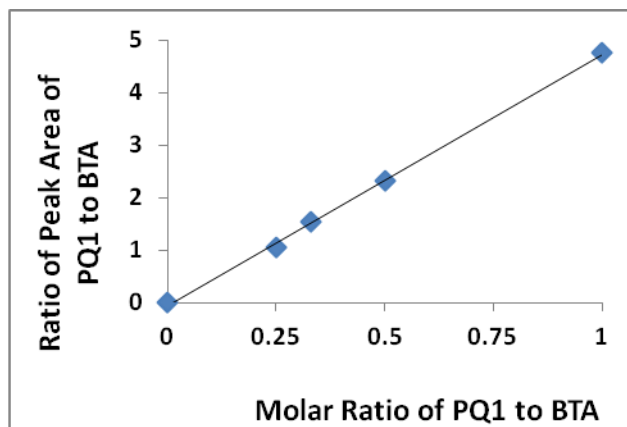


Figure 23: Correlation of ratios of peak areas of authentic BTA and PQ1 from HPLC chromatogram and molar ratios of PQ1 and BTA injected. Solutions of 100 μL of various mixtures of authentic PQ1 and BTA were injected into an HPLC, the peak areas corresponding to PQ1 and BTA were integrated from the HPLC chromatogram, and the ratios of the peaks were obtained. The results of the ratios of HPLC peak areas and the ratios from PQ1 and BTA concentrations were plotted, and a linear correlation line was obtained from the graph.

The amount of PQ1 in the tissues extract was calculated by determining the peak areas ratio of PQ1 to BTA and determining the number of moles of PQ1 from the correlation graphs, as the number of moles of BTA added to the tissue extract was known. HPLC chromatograms of the tissues extract injected with a known amount of BTA showed a peak at 28.8 minutes which had the same retention time compared to the authentic PQ1 as shown in Figure 24. The representative mass spectrum of eluant corresponding to the peak at 28.8 min is highlighted in Figure 31.

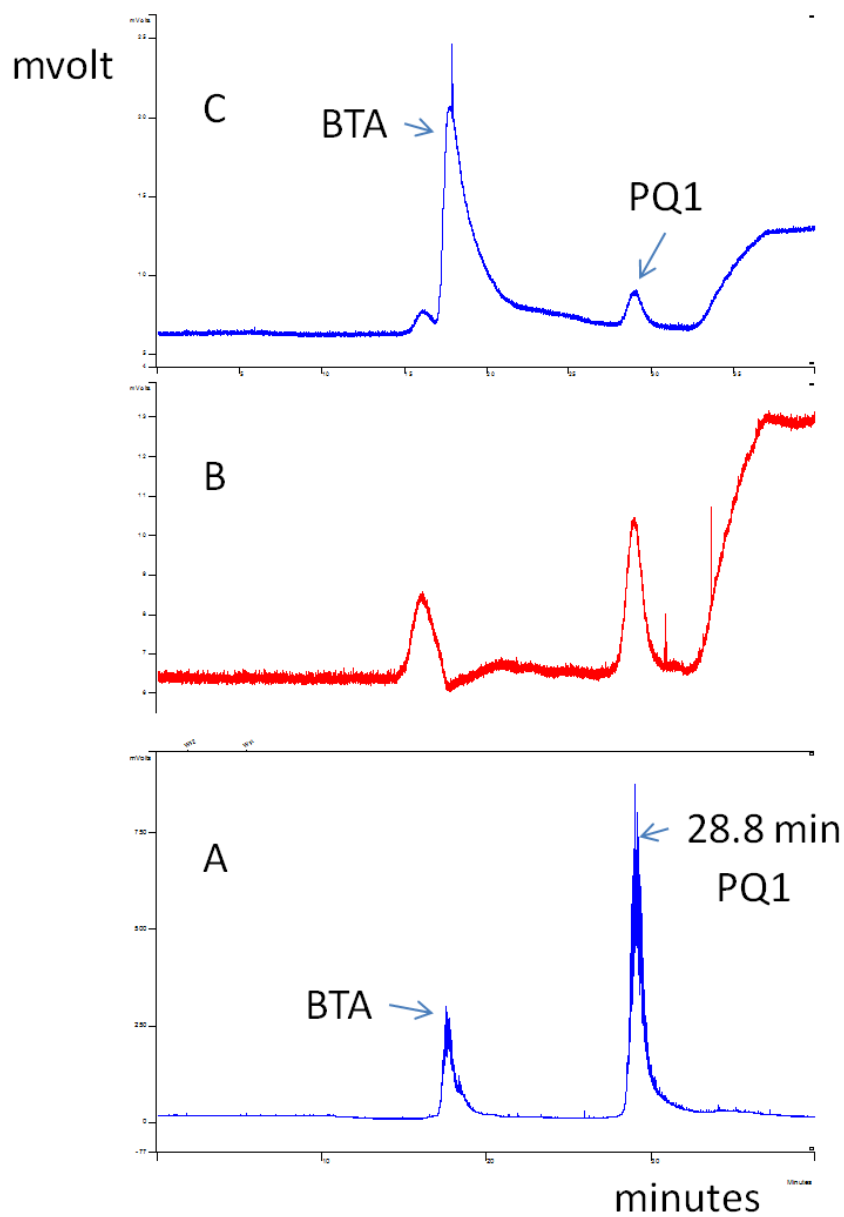


Figure 24: Representative HPLC chromatograms of PQ1 and BTA. 24A is the HPLC chromatogram of 1:1 mol ratio of BTA and authentic PQ1. 24B is the HPLC chromatogram of the tissue extract. 24C is the HPLC chromatogram of the tissue extract with known amount of BTA. The peak at 28.8 min retention time in 24C had the same mass as authentic PQ1 which was confirmed by mass spectrometry.

The percentage of PQ1 distribution to the organs was calculated by defining the amount of PQ1 administered as 100%, and the values are highlighted in Figure 25.

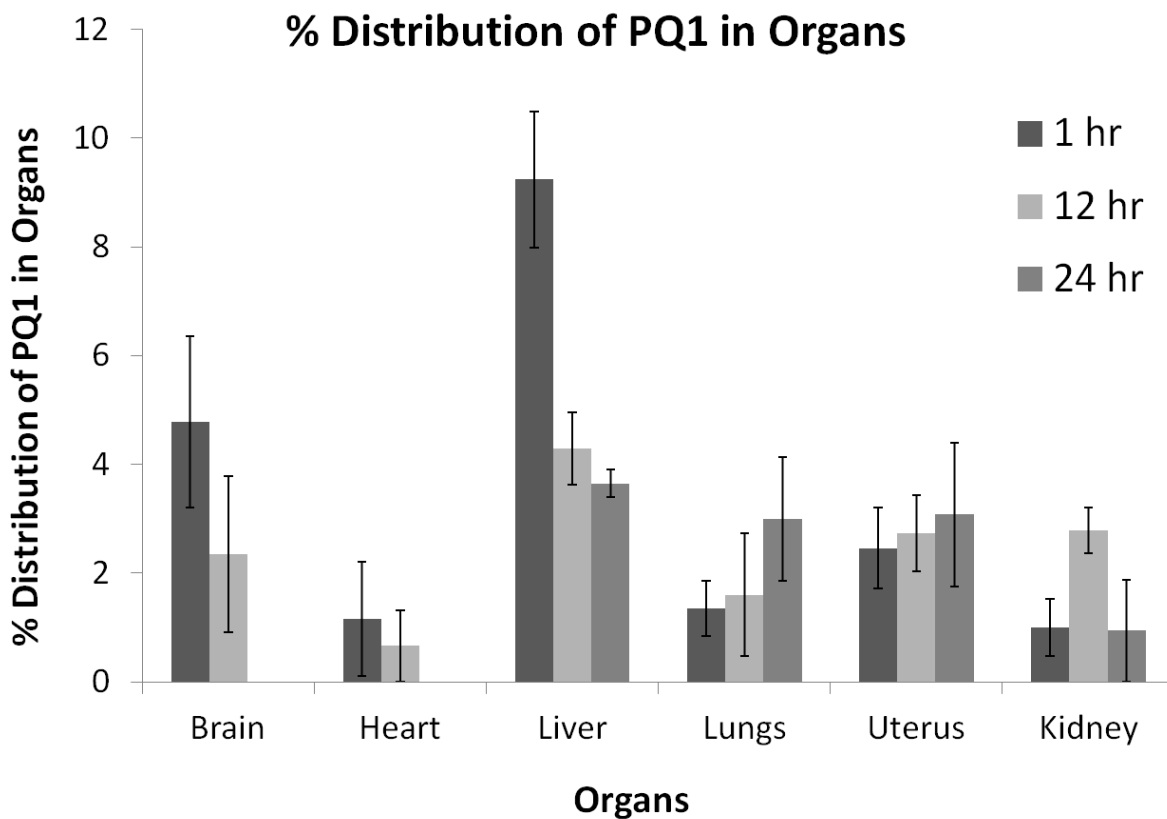


Figure 25: Percentage distribution of PQ1 in various tissues in female C57BL/6J mice in 1, 12, and 24 hours of PQ1 exposure. Each mouse was administered with 25 mg/Kg of PQ1 and the amount of PQ1 administered to each animal is defined as 100%. Data of each experiment was obtained from at least 3 mice and the bars are provided with (\pm) standard error.

In one hour from the oral administration of the drug, PQ1 was detected in the major organs including brain, heart, lungs, liver, kidneys, and uterus. Liver and brain had the highest distribution of PQ1 with the respective percentage distribution of 9.2% and 4.8% of the total PQ1 administered to the mice. The distribution of PQ1 in the brain suggests its efficacy to penetrate the blood brain barrier, which is generally difficult in cases of many drugs. Uterus,

heart, lungs, and kidneys were found to have 2.5%, 1.2%, 1.4%, and 1 % of the total PQ1 administered to the mice, respectively. In 12 hour time of the drug administration, the percentage of PQ1 distribution decreased in liver to 4.3%, brain to 2.4 %, and heart to 0.7% but increased in kidneys to 2.8%. This indicates the shift of drug to the kidney from where it is excreted. However, the amount of PQ1 in lungs and uterus remained consistent. Finally, in 24 hour time of the drug administration, the amount of PQ1 decreased to 3.7% in liver, 0.9% in kidney, whereas brain and heart had no detectable amount of PQ1 in 24 hours. The PQ1 distribution in uterus was found to remain consistent even in 24 hours; moreover, there was an increase of PQ1 in the lungs to 3% in 24 hours. These results show that PQ1 can be absorbed, distributed to major tissues, and metabolized in various tissues or excreted out from the body of mice.

For a cancer drugs to be effective, they must reach the targeted tissues in the body in concentrations sufficient to kill the cancer cells. Therefore, concentrations of PQ1 in the organs were also evaluated at 1, 12, and 24 hour times of the drug administration (Figure 26). Since the concentration of drugs depends on the volume of the organs, the organs having higher percentage of drug distribution but greater volume such as liver may have lower drug concentration compared to the organs which have smaller volume. PQ1 is reported to have IC_{50} value of 119 nM in T47D breast cancer cells, and has shown to suppress the xenograft tumor growth of T47D cells in nude mice by 70% in six days with one injection of 1 μ M.¹³

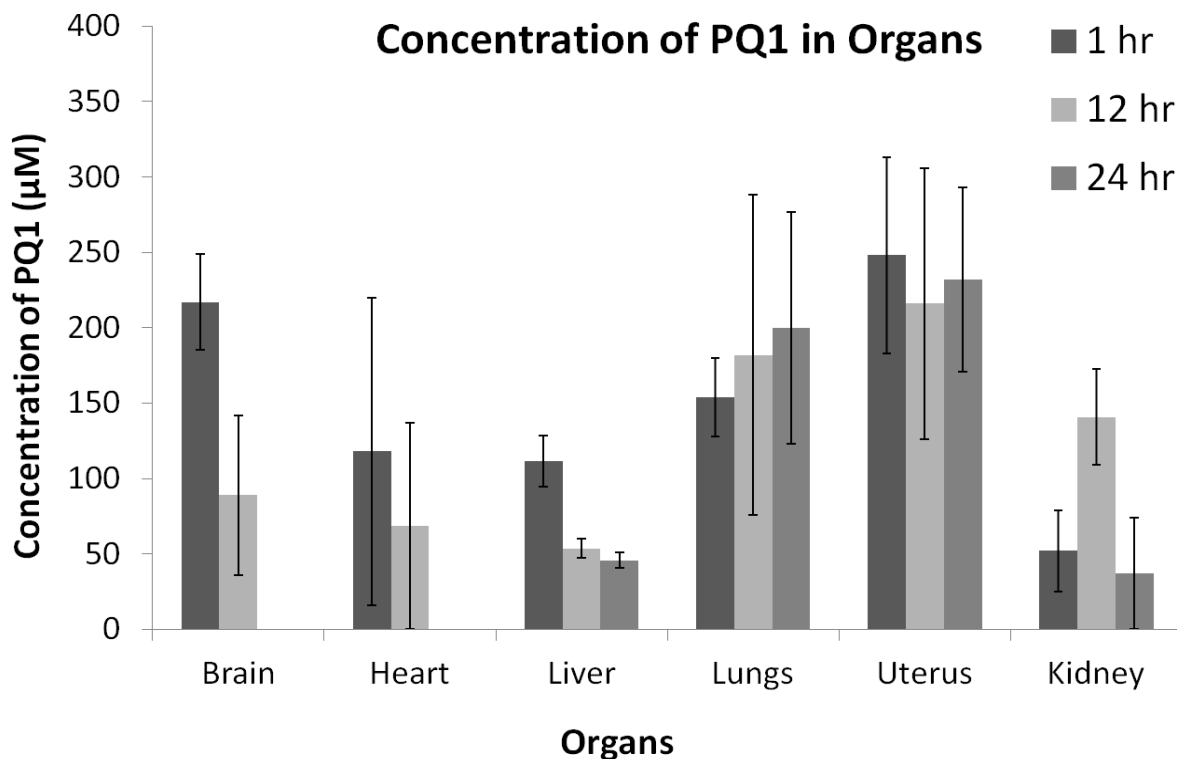


Figure 26: Concentration of PQ1 (μM) in various tissues in 1, 12, and 24 hours of the drug exposure. The concentration of PQ1 was calculated by determining the number of mmol of PQ1 per unit volume of the organs (density of organ = 1). Each bar represents the average concentration of PQ1 measured in at least three mice and is provided with (\pm) SE.

In one hour, the concentrations of PQ1 in the organs analyzed were higher than $100 \mu\text{M}$ with the exception of kidney which had $52 \mu\text{M}$, values more than 50 times higher than the effective dosage. The highest concentration of PQ1 in the organs evaluated was $248 \mu\text{M}$ in uterus, followed by $217 \mu\text{M}$ in brain, $154 \mu\text{M}$ in lungs, $118 \mu\text{M}$ in heart, and $115 \mu\text{M}$ in liver. The concentration of PQ1 in the uterus remained consistent even after 12 and 24 hours of the drugs administration. In brain and heart, the concentration of PQ1 decreased to $89 \mu\text{M}$ and $68 \mu\text{M}$ respectively in 12 hours; however, no detectable amount of PQ1 was observed in these organs in 24 hours. In liver, 12 hours from the drug administration, the concentration of PQ1 was

reduced to 54 μM and remained almost consistent till 24 hours (46 μM). The concentration of PQ1 in lungs and kidney was found to increase to 182 μM and 141 μM respectively in 12 hours. The concentration of PQ1 was found to further increase to 200 μM in the lungs in 24 hours but decrease in kidney to 37 μM .

3.4.2 Effect of PQ1 in normal tissues

PQ1 is known to have anti-breast cancer activity by enhancing gap junctional intercellular communications (GJIC) and probably inducing apoptosis.¹³ PQ1 was reported to inhibit 66% of T47D cells colony growth at 100 nM concentration; however, the same concentration had no effect on the normal human mammalian epithelial cells (HMEC), indicating its specificity towards cancer cells and producing no cytotoxic effect to normal cells.¹³ Although several molecules have been reported to modulate different levels of gap junctional proteins and GJIC, none of these molecules have been examined in clinical trials for the treatment of cancers. It is therefore important to study the effect of PQ1 in normal tissues to evaluate its potential towards the development of anti-breast cancer drugs targeting GJIC.

3.4.2.1 Effect of PQ1 on apoptosis in normal tissues

Apoptosis is a process of programmed cell death and is important in maintaining homeostasis in normal cells and tissues. The balance between both pro- and anti-apoptotic factors is crucial in maintaining normal cell cycle in an organism. Anticancer drugs that induce apoptosis in healthy cells may have several adverse effects.¹⁹ Therefore, to understand the effect of PQ1 on apoptosis in normal tissues, the expressions of survivin, an anti-apoptotic protein, and caspases, proapoptotic proteins were evaluated in both PQ1 treated and nontreated normal

tissues. The expressions of caspase-8 and cleaved caspase-3 expression were evaluated for proapoptotic proteins. Caspase-8 is linked to have a lead role in extrinsic apoptotic pathway, whereas cleaved caspase-3 is a common indicator of both extrinsic and intrinsic apoptotic pathways.²⁰

Survivin, a member of inhibitor of apoptosis (IAP) family is linked to inhibit caspase activation. In one hour from the administration of PQ1, the expression of survivin was found to increase in all the organs, except uterus, as compared to the normal organs from the nontreated mice. The level of survivin increased to 14% in liver, 28% in heart, and 44% in the lungs, which was consistent to the concentration of PQ1 found in these organs. Survivin expression was found to decrease by more than 25% in the uterus. The level of survivin in brain and kidney was found to be consistent as compared to the control (nontreated tissues) in the first hour but increased to 20% and 15% in 12 hours time, respectively. The expression level of survivin in nearly all organs was found to decrease to the same level as that of controls in 24 hours.

Since the cleaved caspase-3 was only detected in the uterus, liver, and lungs of PQ1 untreated animals, the expression of cleaved caspase-3 was only evaluated in these organs. In 12 hours from the administration of PQ1, the expression level of cleaved caspase-3 significantly decreased by 45% in uterus, 37% in liver, and 43% in lungs. The decrease in the expression of cleaved caspase-3 in these organs was consistent to the concentration of PQ1 found in these organs. Similarly, the expression of caspase-8, a key marker of extrinsic apoptotic pathway, was also evaluated. In 1 hour of the PQ1 administration, all the organs showed a decrease in the expression of caspase-8 ranging from 12% to 37% compared to untreated organs. In 24 hours from the drug administration, the expression of caspase-8 was found to decrease significantly in the organs like heart, lungs, liver, and uterus, by 40%, 43%, 43% and 55% respectively.

The increase in the expression of survivin and decrease in the expression of caspase-8 and cleaved caspase-3 in the normal tissues suggests the role of PQ1 as the suppresser of apoptosis, which is in contrary to the cancer cells, where it is found to induces apoptosis. Therefore, PQ1 as an anticancer drug might have double advantage, one by killing cancer cells inducing apoptosis, and the other by suppressing apoptosis in normal cells by inhibiting pro-apoptotic factor and activating anti-apoptotic proteins.

3.4.2.2 Effect of PQ1 on connexin in normal tissues

Connexin are gap junctional proteins. PQ1 was found to enhance GJIC by inhibiting the phosphorylation of Cx43.¹³ Therefore the expressions of Cx43 in the PQ1 treated and nontreated normal tissues were evaluated. Since Cx43 was detected in the heart, brain, and the lungs of the PQ1 non treated animals, the expressions of Cx43 was only studied in these organs. Interestingly, the expression of Cx43 was found to decrease in these organs. The expression of connexin was significantly lower at 24 hour time period, decreasing to 27% in brain, 69% heart, and 50% in lungs as compared to the controls from the PQ1 untreated animals. These studies indicated PQ1 to have an opposite role in normal cells as compared to the cancer cells and suggested that the function of PQ1 in normal cells may involve different mode of action compared to the previously studied in T47D cancer cells.

3.4.2.3 Histological analysis of normal tissues

The organs of PQ1 treated mice were accessed microscopically for observing histological changes if any had occurred to the organs. PQ1-treated liver of normal mice remained unchanged at 1, 12, and 24 hour times as compared to the control, indicating PQ1 produced no observable

toxicity to the mice. Similarly the tissues of heart, adrenal glands, kidney, and reproductive tract also did not show any changes as compared to the controls. Moreover, all the mice treated with PQ1 showed no evidence of hemorrhage or inflammatory cells.

3.4.3. Tissue distribution of PQ11

Since, the oral gavage method used to administer PQ1 in the mice had fluctuating results giving larger values of standard error; therefore, intraperitoneal injection of PQ11 was carried out to evaluate the distribution of PQ11 in different organs. A dose of 25mg/Kg (mice body weight) of PQ11 succinic acid salt in 100 μ L of DMSO was injected to C57BL/6J mice in the intraperitoneal cavity. The quantification of PQ11 in the tissues was carried out as mentioned in the experimental section of this chapter. The ratios of HPLC peak areas of PQ11 to BTA were plotted vs. the ratios of number of moles of PQ11 to BTA which produced a linear correlation calibration plot as shown in Figure 27. Since the amount of BTA injected with the tissue extract is known, the calibration graph was used to determine the amount of PQ11 in the tissues.

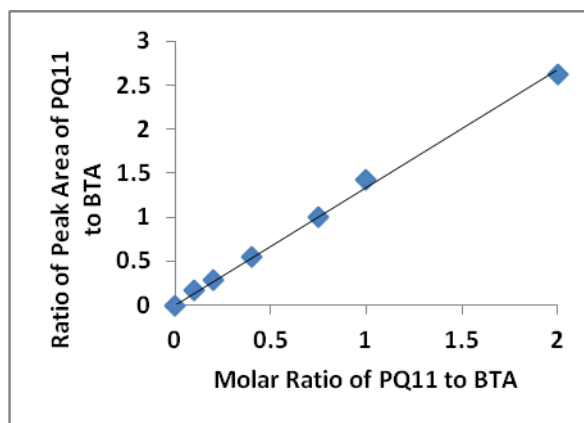


Figure 27: Correlation of ratios of peak areas of authentic BTA and PQ11 from HPLC chromatogram and molar ratios of PQ11 and BTA injected. Solutions of 100 μL of various mixtures of authentic PQ11 and BTA were injected into an HPLC, the peak areas corresponding to PQ11 and BTA were integrated from the HPLC chromatogram, and the ratios of the peaks were obtained. The results of the ratios of HPLC peak areas and the ratios from PQ11 and BTA concentrations were plotted, and a linear correlation line was obtained from the graph.

The HPLC chromatogram of the tissues extract with a known amount of BTA showed a peak at 9.5 minute which had the same retention time compared to the authentic PQ11 as shown in Figure 28. The eluant corresponding to the peak at 9.5 minute in Figure 28C had the same mass compared to the authentic PQ11, as confirmed by mass spectrometry. The amount of PQ11 in the tissues extract was then calculated by determining the peak areas ratio of PQ11 to BTA and determining the number of moles of PQ1 from the correlation graphs, as the number of moles of BTA added to the tissue extract was known. The representative mass spectrum of eluant corresponding to the peak at 9.5 min is highlighted in Figure 32.

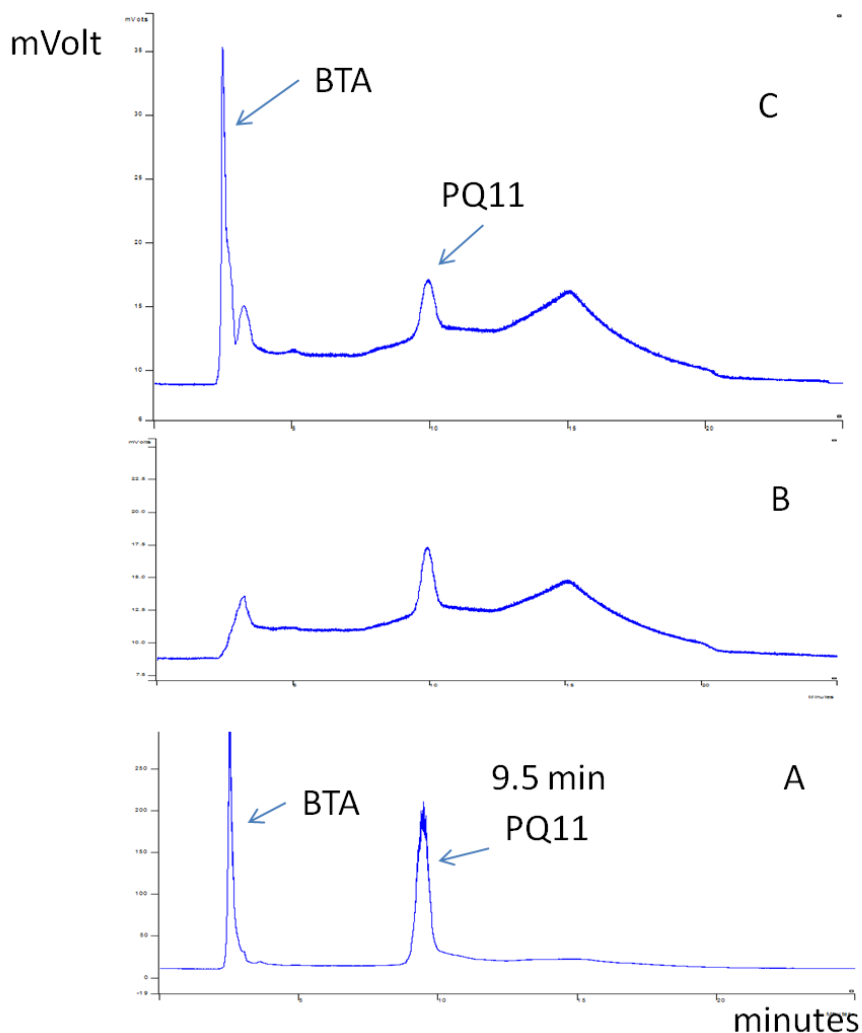


Figure 28: Representative HPLC chromatograms of PQ11 and BTA. 28A is the HPLC chromatogram of 1:1 mol ratio of BTA and authentic PQ11. 28B is the HPLC chromatogram of the tissue extract. 28C is the HPLC chromatogram of the tissue extract with known amount of BTA. The peak at 9.5 min retention time in 28C had the same mass as authentic PQ11 which was confirmed by mass spectrometry.

The percentage distribution of PQ11 in plasma and various organs in the body like liver, brain, kidney, gastro intestine (GI), spleen, uterus, and heart was evaluated at 6, 12, 24, and 36 hours after the administration of the compound. The percentage of PQ11 distribution in the organs was calculated by defining the amount of PQ11 administered as 100%. The percentage distribution of PQ11 in plasma and various organs in 6, 12, 24, and 36 hours are highlighted in

Figure 29. Since the volume of blood recovered from the PQ11 treated varied from animal to animal, the percentage of drugs distribution in plasma refers to that found in 200 μ L of the plasma analyzed. Interestingly, PQ11 was detected in all of the organs analyzed in 6 hours of the drug exposure. In 6 hour from the drug exposure, the percentage of drug recovered in the organs and plasma was 23% of the total PQ11 administrated. The highest percentage of PQ11 was found in liver (8.5%), followed by brain (3.3%), gastro intestinal tract (GI, 3.1%), lungs (2.2%), kidney (2%), uterus (1.27%), and heart (1.1%). In 200 μ L of the plasma analyzed, the percentage distribution of PQ11 was 1.1%. From the percentage distribution of drugs in the brain, PQ11 is also found to penetrate the blood brain barrier and accumulate in the brain as observed in PQ1.

Unlike PQ1, PQ11 showed better drug clearance from the organs as indicated by the gradual decrease of percentage drug distribution in 12, 24, and 36 hours of the drug administration. In 12 hour time of the drug administration, there was no detectable amount of PQ11 in the spleen, and the amount of PQ11 in other organs with the exception of gastro intestinal tract decreased rapidly ranging from 28% to 63%. The percentage distribution of PQ11 in gastro intestinal tract (GI) remained consistent at 6, 12, and 24 hours of the drugs administration but decreased significantly to 1.7 % at 36 hour time.

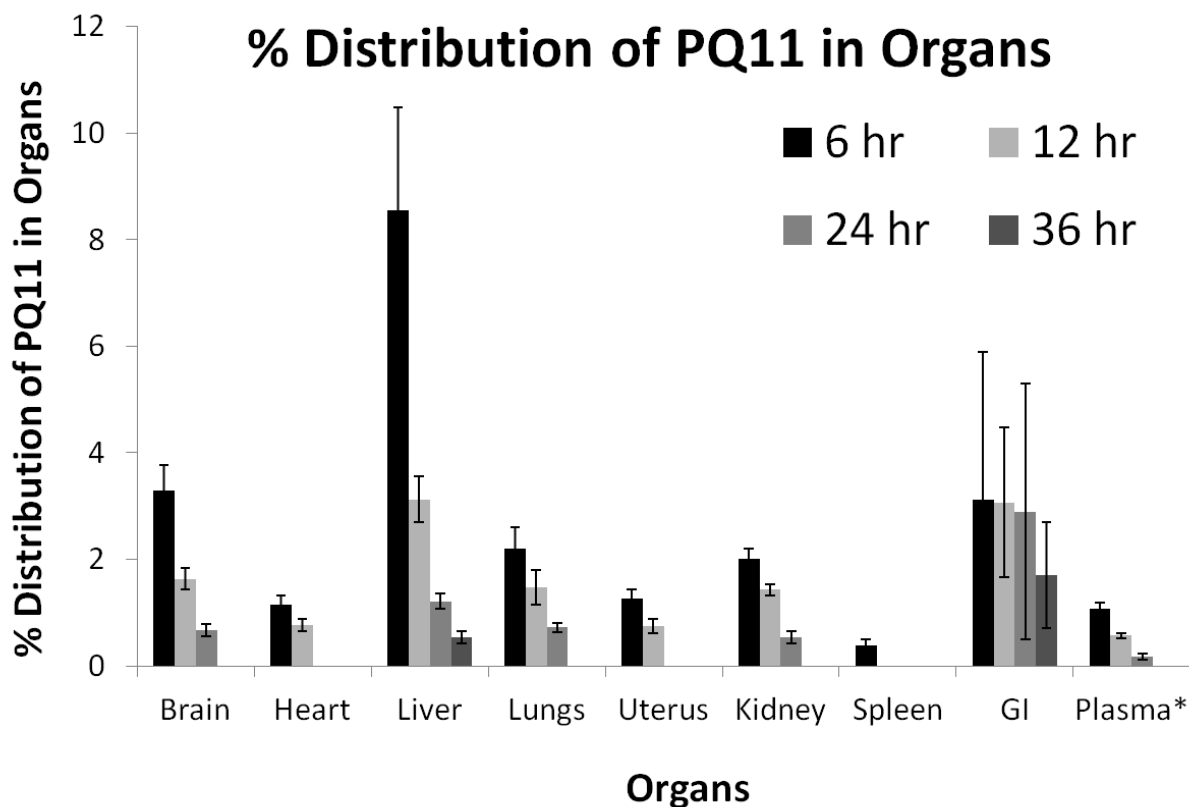


Figure 29: Percentage distribution of PQ11 in various tissues in female C57BL/6J mice in 6, 12, 24, and 36 hours of PQ11 exposure. Each mouse was administered with 25 mg/Kg of PQ11 and the amount of PQ1 administered to each animal is defined as 100%. The percentage distribution of PQ11 in plasma refers to that found in 200 μ L of the plasma analyzed. Data of each experiment was obtained from 6 mice and the bars are shown with (\pm) standard error.

The analysis showed that at 24 hours of the drugs administration, PQ11 could not be detected in the uterus and the heart indicating the rapid absorbance and clearance of PQ11 in these organs. At 24 hours from the drugs administration, GI and liver had 2.9% and 1.2% distribution of the drugs, whereas the percentage distributions of PQ11 in other organs were less than 1%. In 36 hours from the drugs administration, PQ11 was only found in GI (1.7%) and in liver (0.5%). The analysis showed PQ11 to have better pharmacokinetics as compared to PQ1. PQ11 was better absorbed, distributed, metabolized, and cleared from the body. The animals after 6, 12, 24, and 36 hours from the drugs administration were as active as before the

administration of PQ11, which indicated PQ11 to have no adverse effect to these animals. However, the effect of PQ11 in the normal tissues is being studied by Dr. Thu Annelise Nguyen and Stephanie Shishido. The preliminary studies, till to date has not indicate any toxicity effect to the normal cells. These data will be published in the near future.

PQ11 is reported to have IC_{50} value of 16 nM in T47D breast cancer cell, and has shown to suppress the xenograft tumor growth of T47D cells in nude mice by 100% in 14 days with one injection of 1 μ M (as per the volume of tumor) in every 2 days, in total seven injections.¹³ In 6 hours of the drugs administration, the concentrations of PQ11 in the organs analyzed were more than 40 times higher than its effective dose. The highest concentration of PQ11 was found in heart (107 μ M), followed by liver (98 μ M), lungs (91 μ M), uterus (82 μ M), brain (71 μ M), kidneys (70%). The concentration of PQ11 in the gastro intestinal tract and spleen was 36 μ M and 35 μ M, respectively. The concentration of PQ11 decreased gradually in all the organs, with the exception of GI tract, with time as shown in Figure 30. The concentration of the drugs in the GI tract remained consistent at 6, 12, and 24 hours from the PQ11 administration, however decreased to 15 μ M at 36 hours. The concentration of PQ11 in the organs was greatly reduced or even was zeroed at 24 hours of drugs administration. And finally at 36 hours the drugs was only detected in liver (5.2 μ M) and GI (15 μ M).

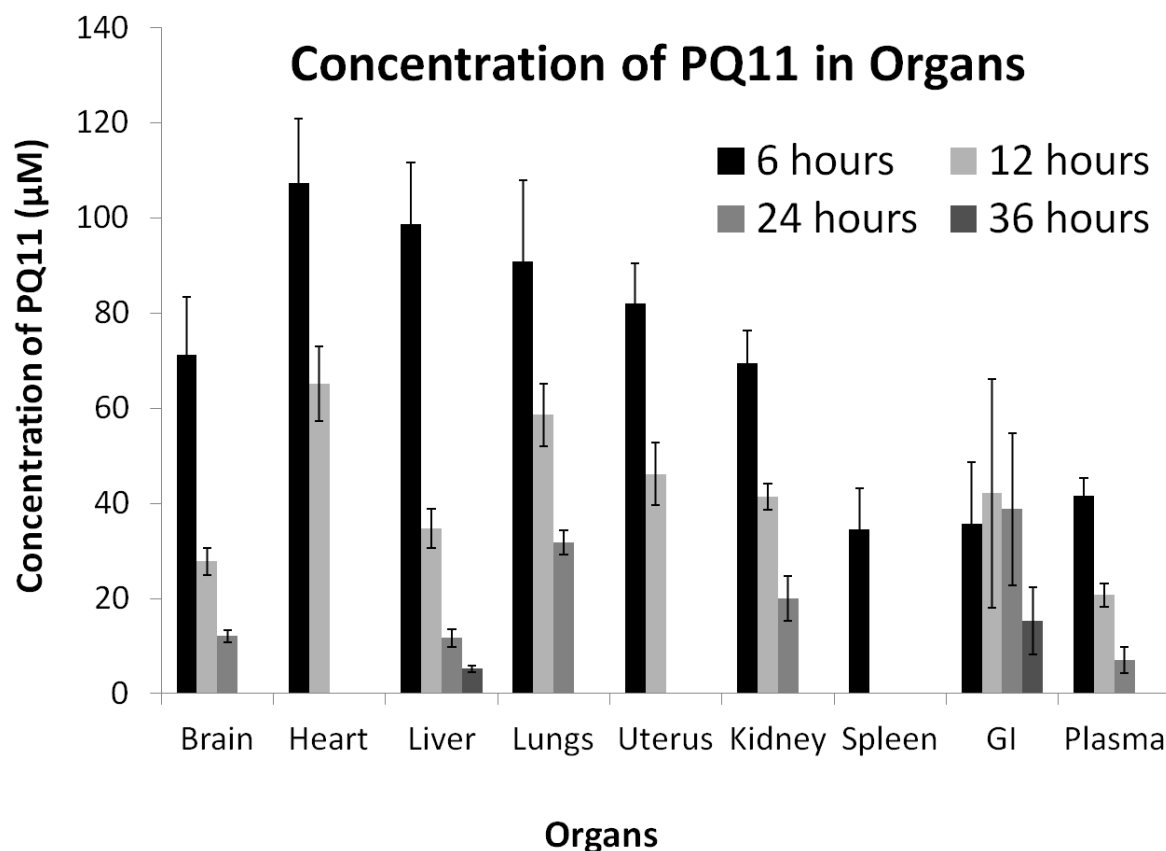


Figure 30: Concentration of PQ11 (μM) in various tissues in 6, 12, 24, and 36 hours of the drug exposure. The concentration of PQ11 was calculated by determining the number of mmol of PQ11 per unit volume of the organs (density of organ = 1). Each bar represents the average concentration of PQ11 measured from 6 mice and is provided with (\pm) SE.

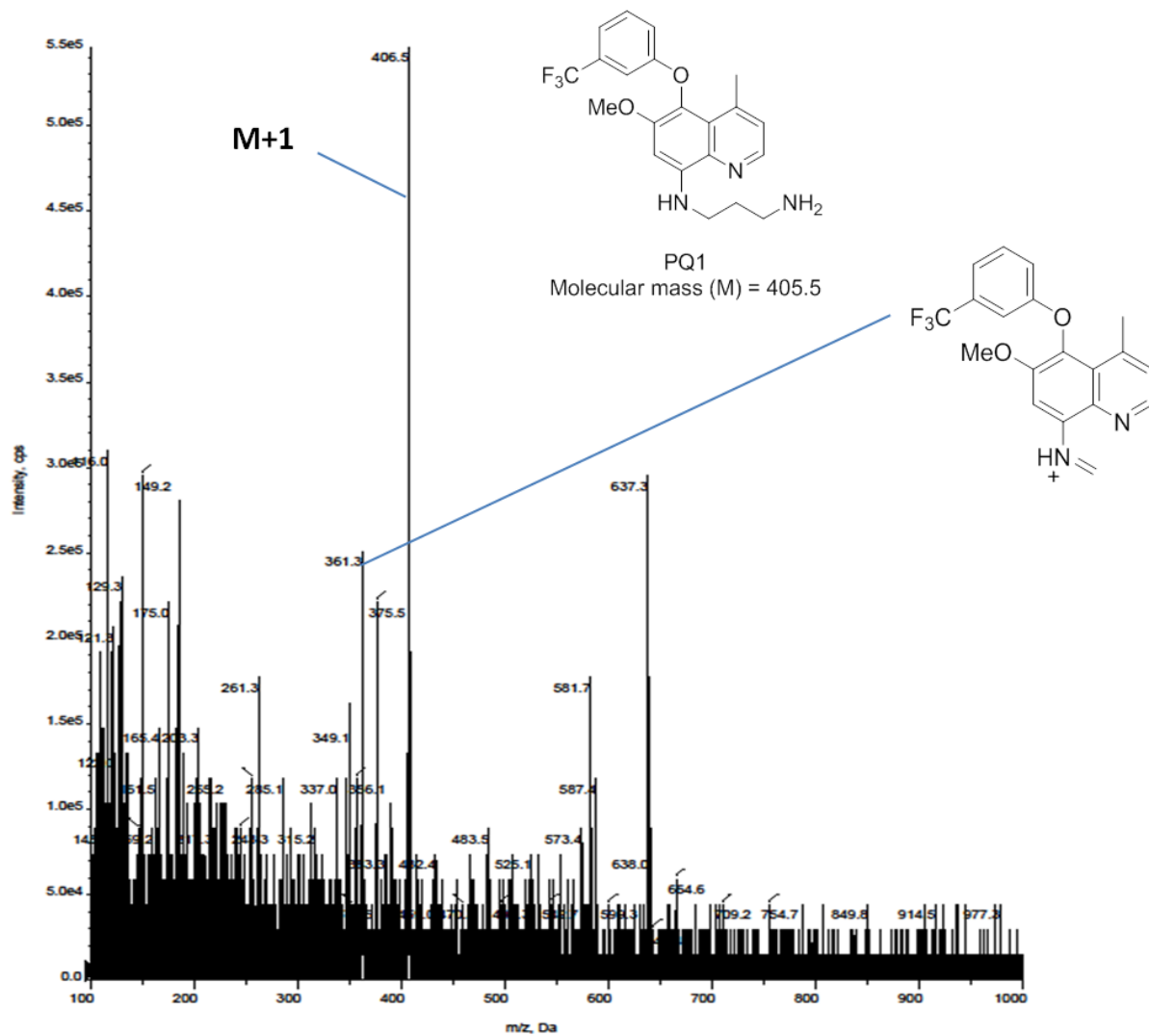


Figure 31: Mass spectrum of the eluant corresponding to the peak at 28.8 minutes (Figure 24C) which is identical to the authentic PQ1.

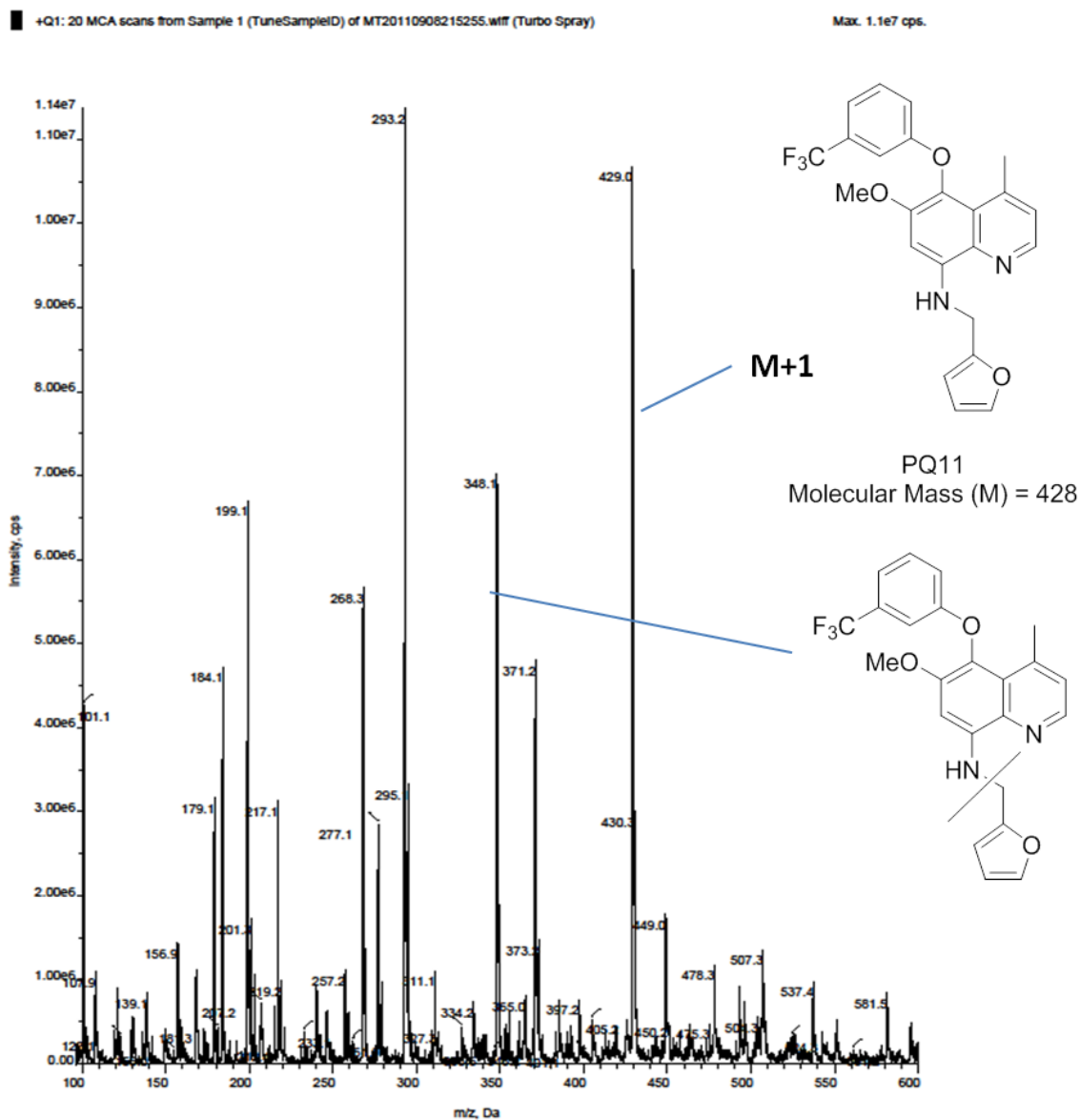


Figure 32: Mass spectrum of the eluant corresponding to the peak at 9.5 minutes (Figure 28C) which is identical to the authentic PQ11.

3.5 Conclusions

Substituted quinolines, PQ1 and PQ11 were distributed in the tissues following oral gavage and intraperitoneal injection, respectively. Both PQ1 and PQ11 were found to penetrate the blood brain barrier and collect in the tissues in significant amounts. These compounds were distributed in the tissues in the concentration that was more than 40 folds higher than their effective dose. The administration of PQ1 and PQ11 had no effect in the normal behavior of the animals indicating no short term adverse effects. PQ1 was found to increase the expression of survivin, an anti-apoptotic factor and decrease the expression of cleaved caspase-3 and caspase-8, pro-apoptotic proteins. These studies indicate that PQ1 had anti-apoptotic activities in normal cells, in contrast to the role of PQ1 in cancer cells, where it was known to induce apoptosis. PQ1 in normal T47D cells were found to decrease the expression of phosphorylated form of connexin 43 (Cx43) and increase the expression of Cx43 indicating its role as GJIC enhancing agent; however in normal tissue PQ1 was found to have opposite role and decreased the expression of Cx43. This concludes that PQ1 has opposing roles in cancer and normal cells. This property might add advantage to PQ1 which could be used to treat cancer cells by inducing apoptosis as well as prevents the adverse affect of apoptosis in the normal cells. The distribution of PQ11 in different normal tissues indicated that it was better cleared from the tissues as compared to PQ1; however, its effect on normal tissues is under investigation and will be published in the near future.

3.6 References

- (1) In *Global Cancer Facts and Figures*; Second ed.; American Cancer Society: Atlanta, **2011**, p 1-2.
- (2) In *Cancer Facts and Figures 2011*; American Cancer Society: Atlanta, **2011**, p 1-11.
- (3) Musiol, R.; Jampilek, J.; Buchta, V.; Silva, L.; Niedbala, H.; Podeszwa, B.; Palka, A.; Majerz-Maniecka, K.; Oleksynd, B.; Jaroslaw Polanska Antifungal properties of new series of quinoline derivatives. *Bioorg. Med. Chem.* **2006**, *14*, 3592-3598.
- (4) Appelbaum, P. C.; Jacobs, M. R. Recently approved and investigational antibiotics for treatment of severe infections caused by gram-positive bacteria. *Current Opinion in Microbiology* **2005**, *8*, 510-517.
- (5) Ridley, R. G. Medical need, scientific opportunity and the drive for antimalarial drugs. *Nature* **2002**, *415*, 686-693.
- (6) Milbank, J. B. J.; Stevenson, R. J.; Ware, D. C.; Chang, J. Y. C.; Tercel, M.; Ahn, G.-O.; Wilson, W. R.; Denny, W. A. Synthesis and evaluation of stable bidentate transition metal complexes of 1-(chloromethyl)-5-hydroxy-3-(5,6,7-trimethoxyindol-2-ylcarbonyl)-2,3-dihydro-1*H*-pyrrolo[3,2-*f*]quinoline (*seco*-6-azaCBI-TMI) as hypoxia selective cytotoxins. *Journal of Medicinal Chemistry* **2009**, *52*, 6822–6834.
- (7) Mooring, S. R.; Jin, H.; Devi, N. S.; Jabbar, A. A.; Stefan Kaluz; Liu, Y.; Meir, E. G. V.; Wang, B. Design and synthesis of novel small-molecule inhibitors of the hypoxia inducible factor pathway. *Journal of Medicinal Chemistry* **2011**, *54*, 8471–8489.
- (8) Peczynska-Czoch, W.; Pognan, F.; Kaczmarek, L.; Boratynski, J. Synthesis and structure-activity relationship of methyl-substituted indolo[2,3-*b*]quinolines: novel cytotoxic, DNA topoisomerase II Inhibitors. *Journal of Medicinal Chemistry* **1994**, *37*, 3503-3510.

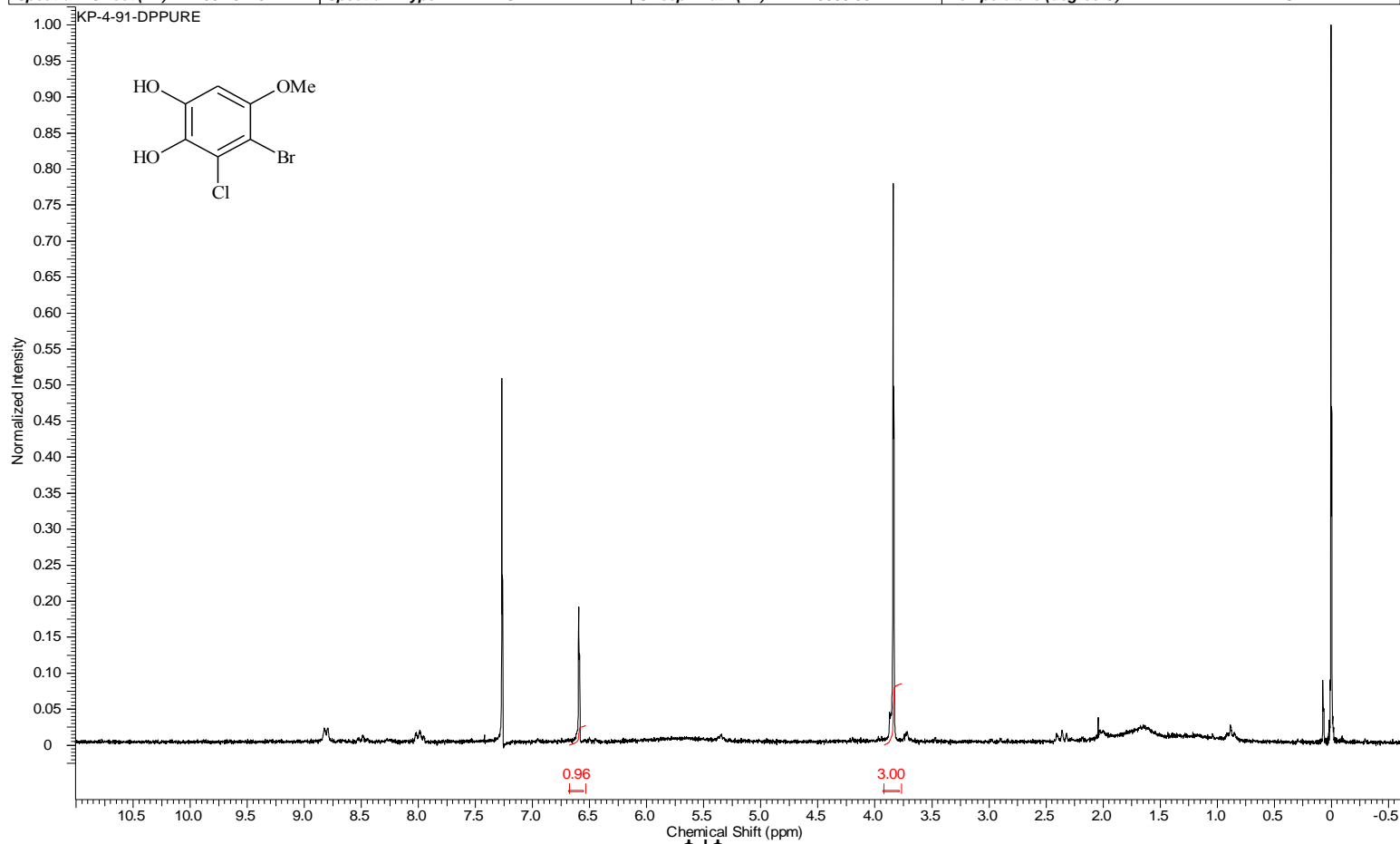
- (9) Gazit, A.; App, H.; McMahon, G.; Chen, J.; Levitzki, A.; Bohmer, F. D. Tyrphostins. 5. Potent inhibitors of platelet-derived growth factor receptor tyrosine kinase: structure-activity relationships in quinoxalines, quinolines, and indole tyrphostins. *Journal of Medicinal Chemistry* **1996**, *39*, 2170-2177.
- (10) Kawase, M.; Motohashi, N. New multidrug resistance reversal agents. *Curr. Drug Targets* **2003**, *4*, 31-43.
- (11) Du, W. Towards new anticancer drugs: a decade of advances in synthesis of camptothecins and related alkaloids. *Tetrahedron* **2003**, *59*, 8649–8687.
- (12) Ketron, A. C.; Denny, W. A.; Graves, D. E.; Osheroff, N. Amsacrine as a topoisomerase II poison: importance of drug–DNA interactions. *Biochemistry* **2012**, *51*, 1730-1739.
- (13) Gakhar, G.; Ohira, T.; Shi, A.; Hua, D. H.; Nguyen, T. A. Antitumor effect of substituted quinolines in breast cancer cells. *Drug Dev. Res.* **2008**, *69*, 526-534.
- (14) Shi, A.; Nguyen, T. A.; Battina, S. K.; Rana, S.; Takemoto, D. J.; Chiang, P. K.; Hua, D. H. Synthesis and anti-breast cancer activities of substituted quinolines. *Bioorg. Med. Chem. Lett.* **2008**, *18*, 3364-3368.
- (15) Heiniger, B.; Gakhar, G.; Prasain, K.; Hua, D. H.; Nguyen, T. A. Second-generation substituted quinolines as anticancer drugs for breast cancer. *Anticancer Res.* **2010**, *30*, 3927-3932.
- (16) Bernzweig, J.; Heiniger, B.; Prasain, K.; Lu, J.; Hua, D. H.; Nguyen, T. A. Anti-breast cancer agents, quinolines, targeting gap junction. *Med. Chem.* **2011**, *7*, 448-453.
- (17) Fernstrom, M. J.; Koffler, L. D.; Abou-Rjaily, G.; Boucher, P. D.; Shewach, D. S.; Ruch, R. J. Neoplastic reversal of human ovarian carcinoma cells transfected with connexin43. *Experimental and Molecular Pathology* **2002**, *73*, 54-60.

- (18) Ding, Y.; Prasain, K.; Nguyen, T. D. T.; Hua, D. H.; Nguyen, T. A. The effect of the PQ1 anti-breast cancer agent on normal tissues. *Anticancer Drugs* **2012**, *23*, 897–905.
- (19) Tamaki, T.; Naomoto, Y.; Kimura, S.; Kawashima, R.; Shirakawa, Y.; Shigemitsu, K.; Yamatsuji, T.; Haisa, M.; Gunduz, M.; Tanaka, N. Apoptosis in normal tissues induced by anti-cancer drugs. *J. Int. Med. Res.* **2003**, *31*, 6-16.
- (20) Elmore, S. Apoptosis: a review of programmed cell death. *Toxicol. Pathol.* **2007**, *35*, 495-516.

Appendix A: ^1H NMR, ^{13}C NMR, and IR spectra

Compound 22 ^1H NMR

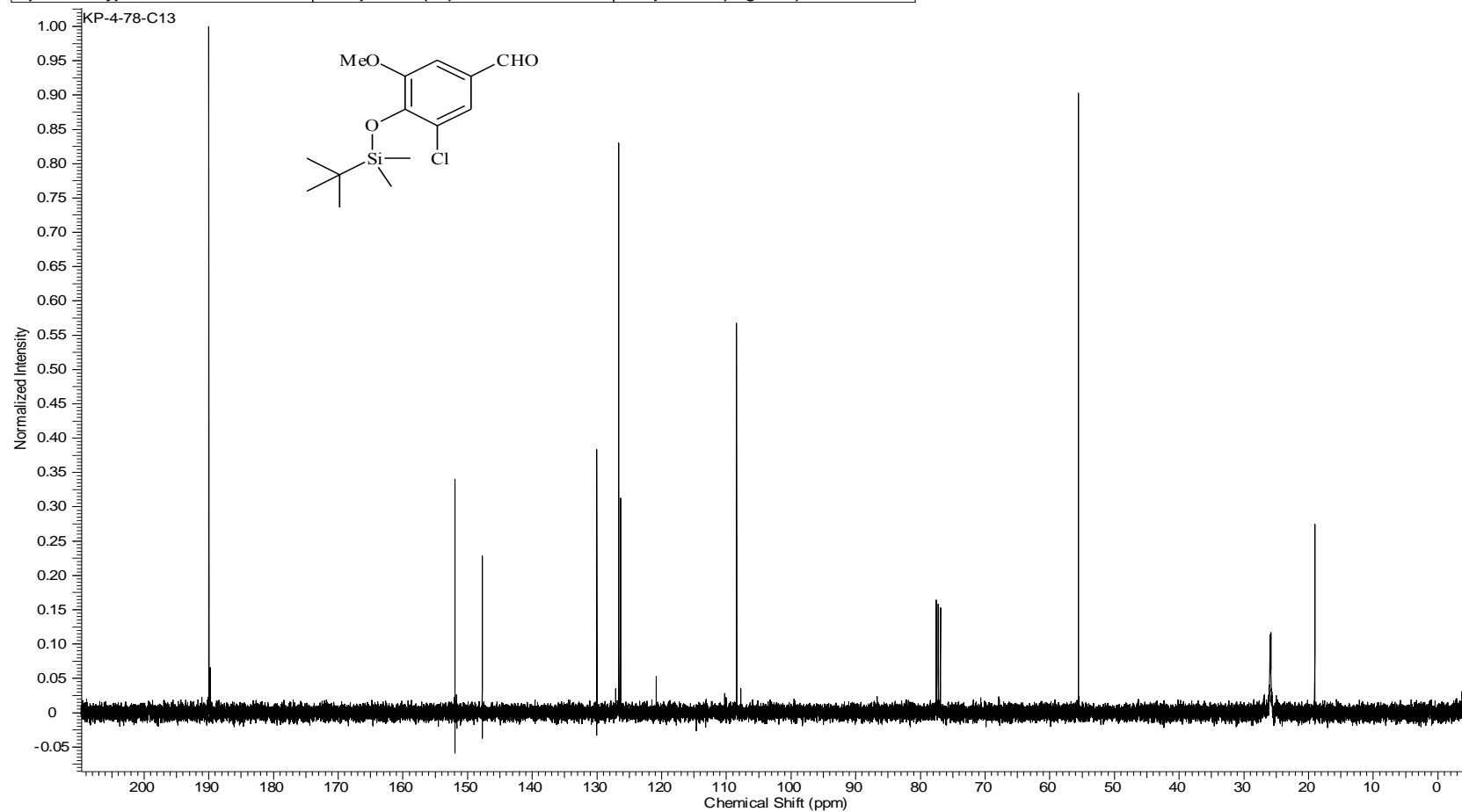
Acquisition Time (sec)	1.9945	Comment	STANDARD 1H OBSERVE		Date	May 14 2009	
Date Stamp	May 14 2009	File Name	C:\USERS\KESHAR\DESKTOP\NMR\BOOK 4\KP-4-91-DPPURE.FID\FID				
Frequency (MHz)	199.98	Nucleus	^1H	Number of Transients	36	Original Points Count	5984
Points Count	8192	Pulse Sequence	s2pul	Receiver Gain	40.00	Solvent	CHLOROFORM-d
Spectrum Offset (Hz)	1002.0226	Spectrum Type	STANDARD	Sweep Width (Hz)	3000.30	Temperature (degree C)	AMBIENT TEMPERATURE



Compound 22 ¹³C NMR

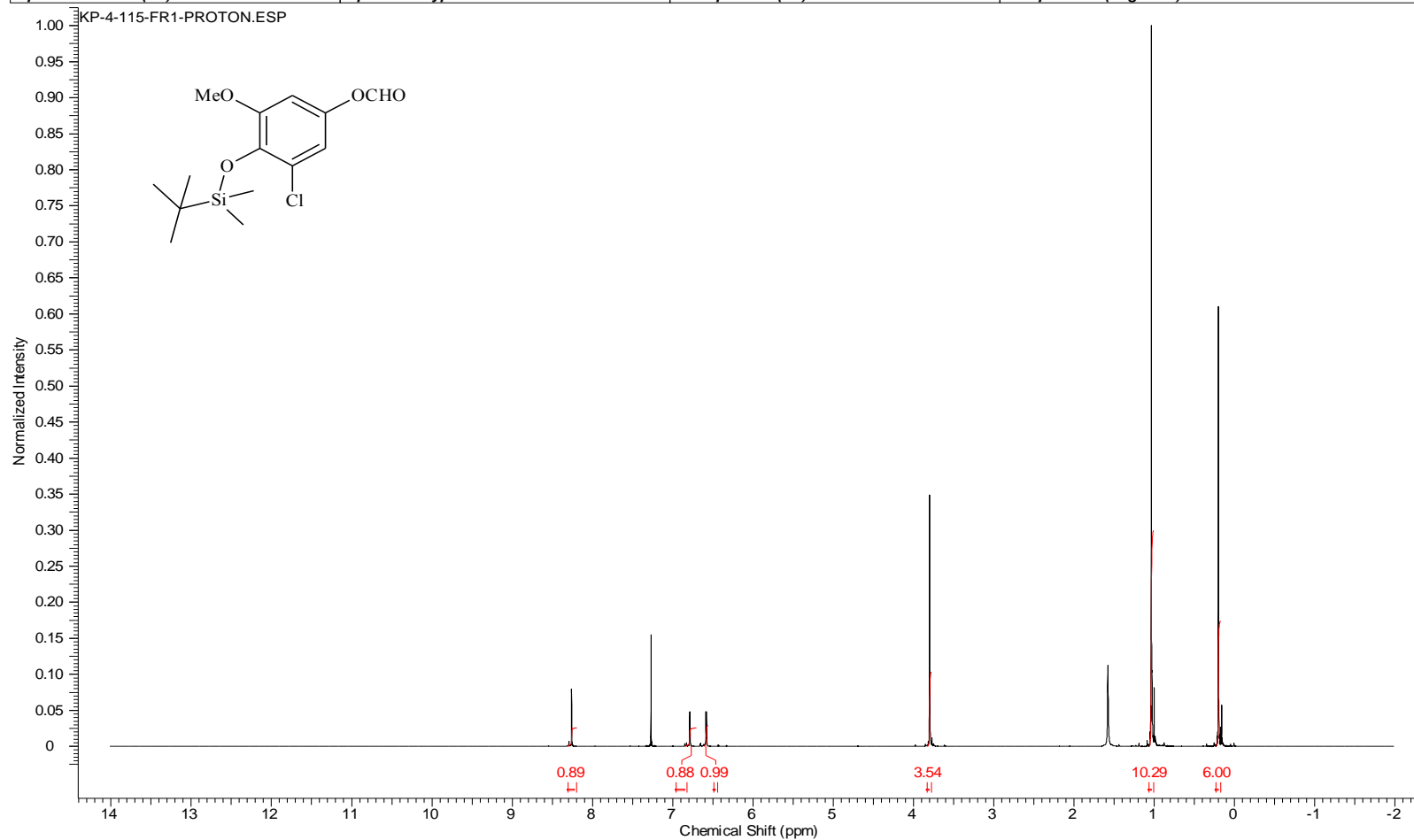
6/27/2012 3:30:36 PM

Acquisition Time (sec)	1.3005	Comment	Std proton	Date	Jul 13 2009	Date Stamp	Jul 13 2009
File Name	C:\USERS\KESHAR\DESKTOP\NMR\OTHERS\KP-4-78-C13\FID				Frequency (MHz)	100.53	
Nucleus	13C	Number of Transients	188	Original Points Count	31375	Points Count	32768
Pulse Sequence	s2pul	Receiver Gain	30.00	Solvent	acetone	Spectrum Offset (Hz)	11069.2324
Spectrum Type	STANDARD	Sweep Width (Hz)	24125.45	Temperature (degree C)	25.000		



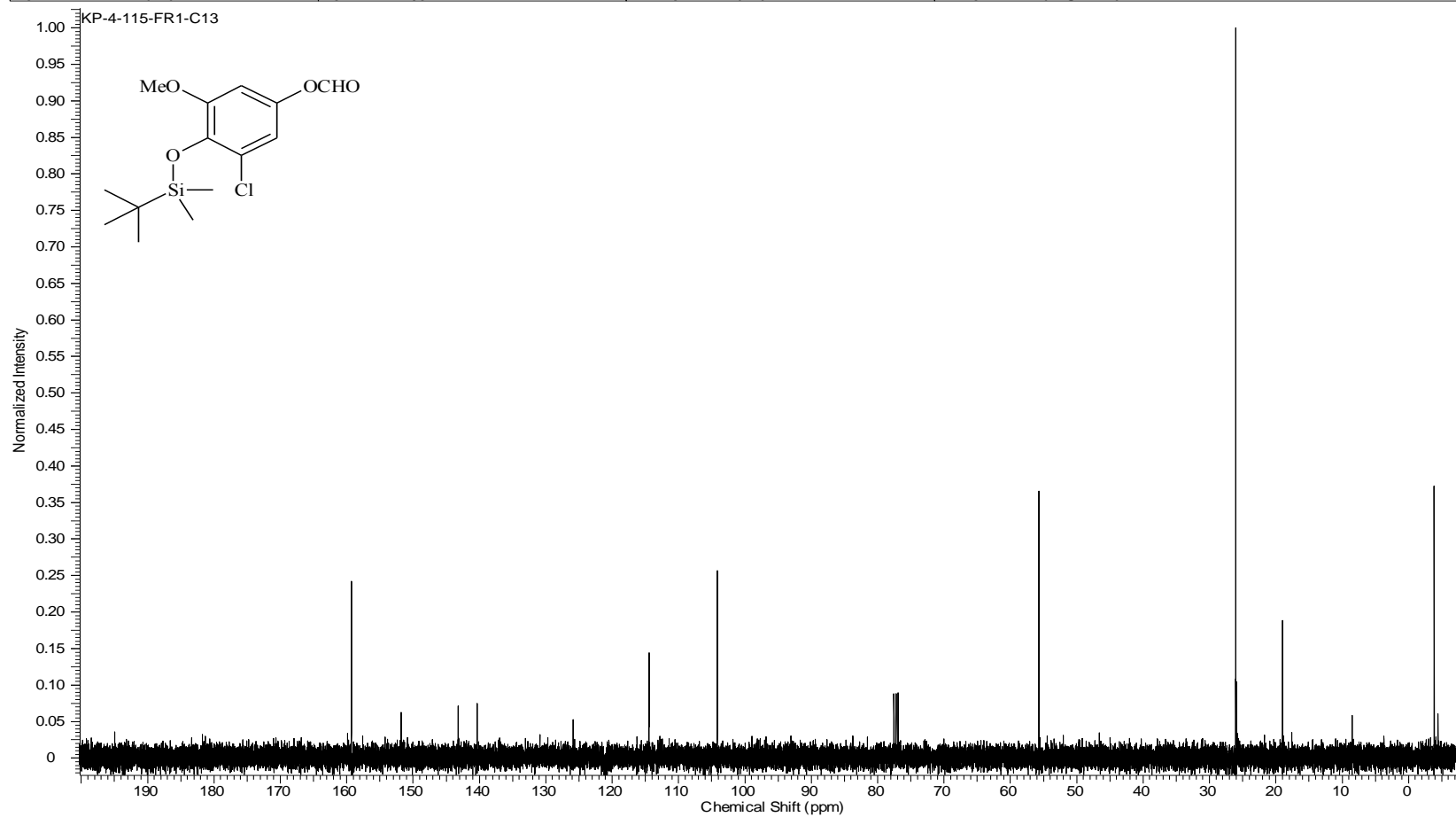
Compound 23 ¹H NMR

Acquisition Time (sec)	2.0487	Comment	Std proton	Date	Aug 15 2009	Date Stamp	Aug 15 2009
File Name	C:\USERS\KESHAR\KP-4-115-FR-1-Proton						
Frequency (MHz)	399.75	Nucleus	1H	Number of Transients	36	Original Points Count	13103
Points Count	16384	Pulse Sequence	s2pul	Receiver Gain	44.00	Solvent	CHLOROFORM-d
Spectrum Offset (Hz)	2403.9280	Spectrum Type	STANDARD	Sweep Width (Hz)	6395.91	Temperature (degree C)	25.000



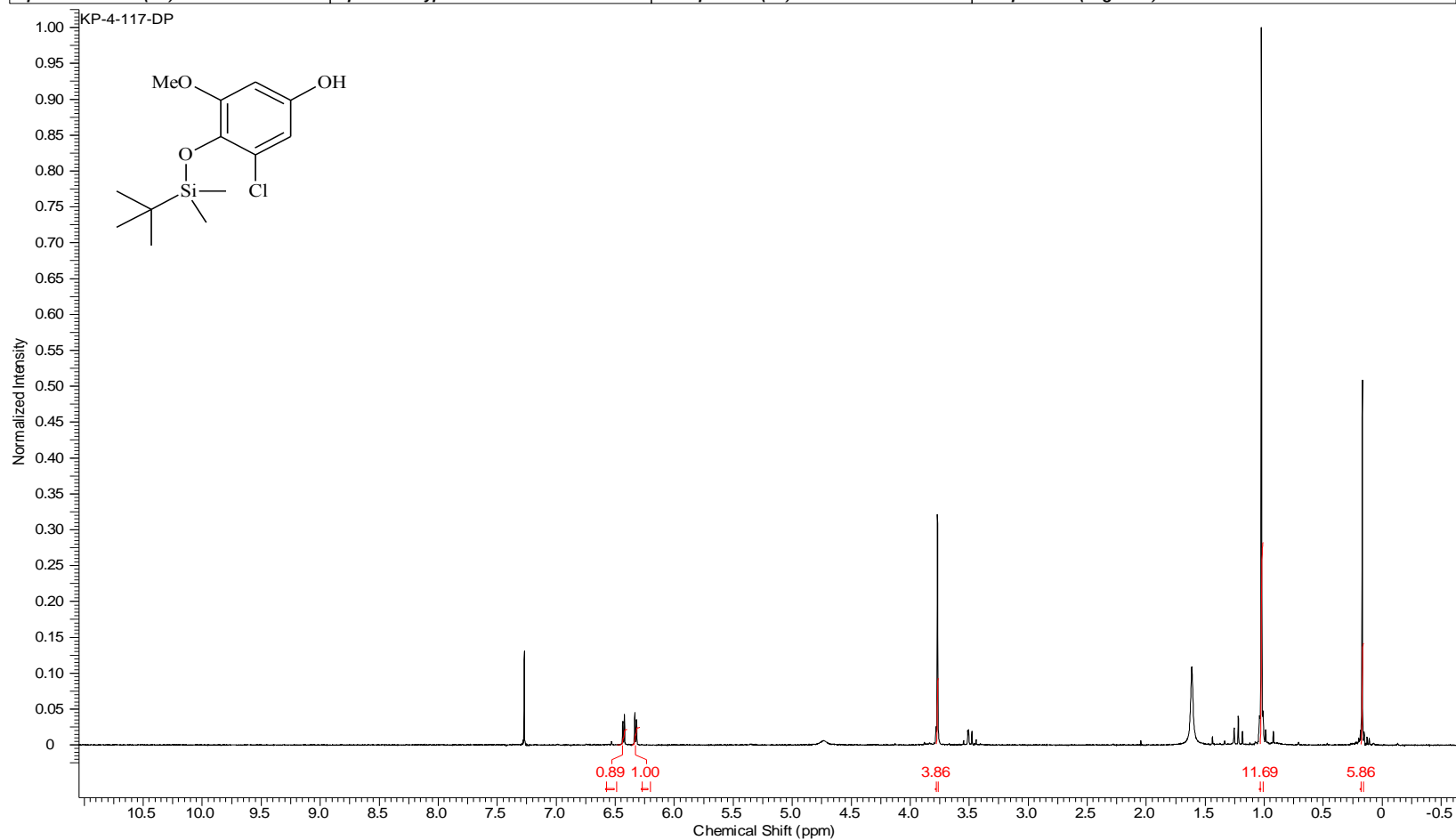
Compound 23 ¹³C NMR

Acquisition Time (sec)	1.3005	Comment	Std proton	Date	Jul 16 2009	Date Stamp	Jul 16 2009
File Name	C:\USERS\KESHAR\DESKTOP\NMR\OTHERS\KP-4-115-FR1-C13\FID			Frequency (MHz)	100.53		
Nucleus	¹³ C	Number of Transients	88	Original Points Count	31375	Points Count	32768
Pulse Sequence	s2pul	Receiver Gain	30.00	Solvent	CHLOROFORM-d		
Spectrum Offset (Hz)	10551.5918	Spectrum Type	STANDARD	Sweep Width (Hz)	24125.45	Temperature (degree C)	25.000



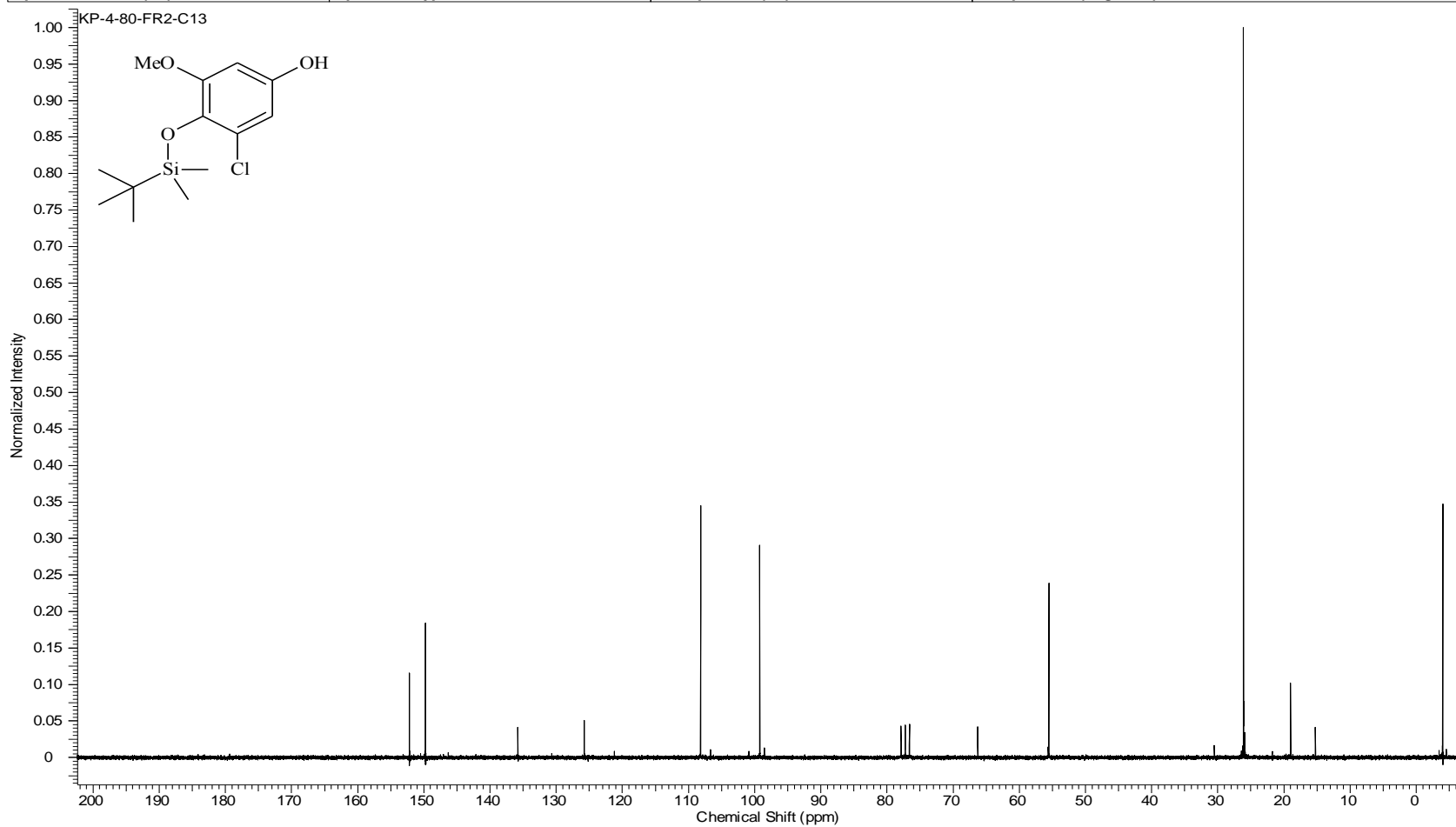
Compound 24 ¹H NMR

Acquisition Time (sec)	1.9945	Comment	STANDARD 1H OBSERVE		Date	Aug 16 2009	
Date Stamp	Aug 16 2009	File Name	C:\USERS\KESHAR\DESKTOP\NMR\BOOK 4\KP-4-117-DP.FID\FID				
Frequency (MHz)	199.98	Nucleus	1H	Number of Transients	36	Original Points Count	5984
Points Count	8192	Pulse Sequence	s2pul	Receiver Gain	40.00	Solvent	CHLOROFORM-d
Spectrum Offset (Hz)	1002.3889	Spectrum Type	STANDARD	Sweep Width (Hz)	3000.30	Temperature (degree C)	AMBIENT TEMPERATURE



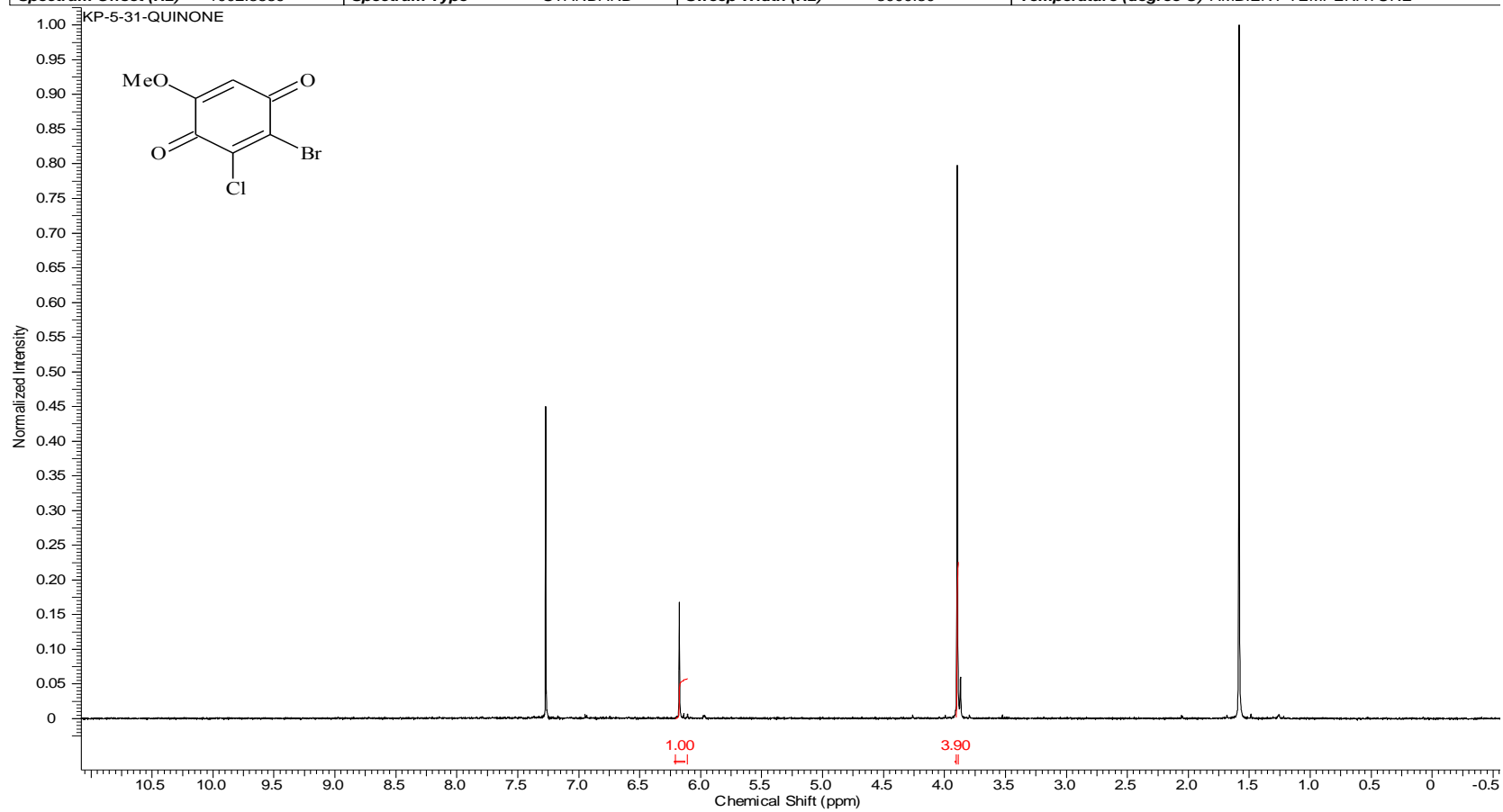
Compound 24 ¹³C NMR

Acquisition Time (sec)	1.4976	Comment	13C OBSERVE	Date	Sep 12 2009	Date Stamp	Sep 12 2009
File Name	C:\USERS\KESHAR\DESKTOP\NMR\LACCASE\KP-4-80-FR2-C13\FID			Frequency (MHz)	50.29		
Nucleus	13C	Number of Transients	4016	Original Points Count	18720	Points Count	32768
Pulse Sequence	s2pul	Receiver Gain	40.00	Solvent	CHLOROFORM-d		
Spectrum Offset (Hz)	4879.6978	Spectrum Type	STANDARD	Sweep Width (Hz)	12500.00	Temperature (degree C)	AMBIENT TEMPERATURE



Compound 19 ¹H NMR

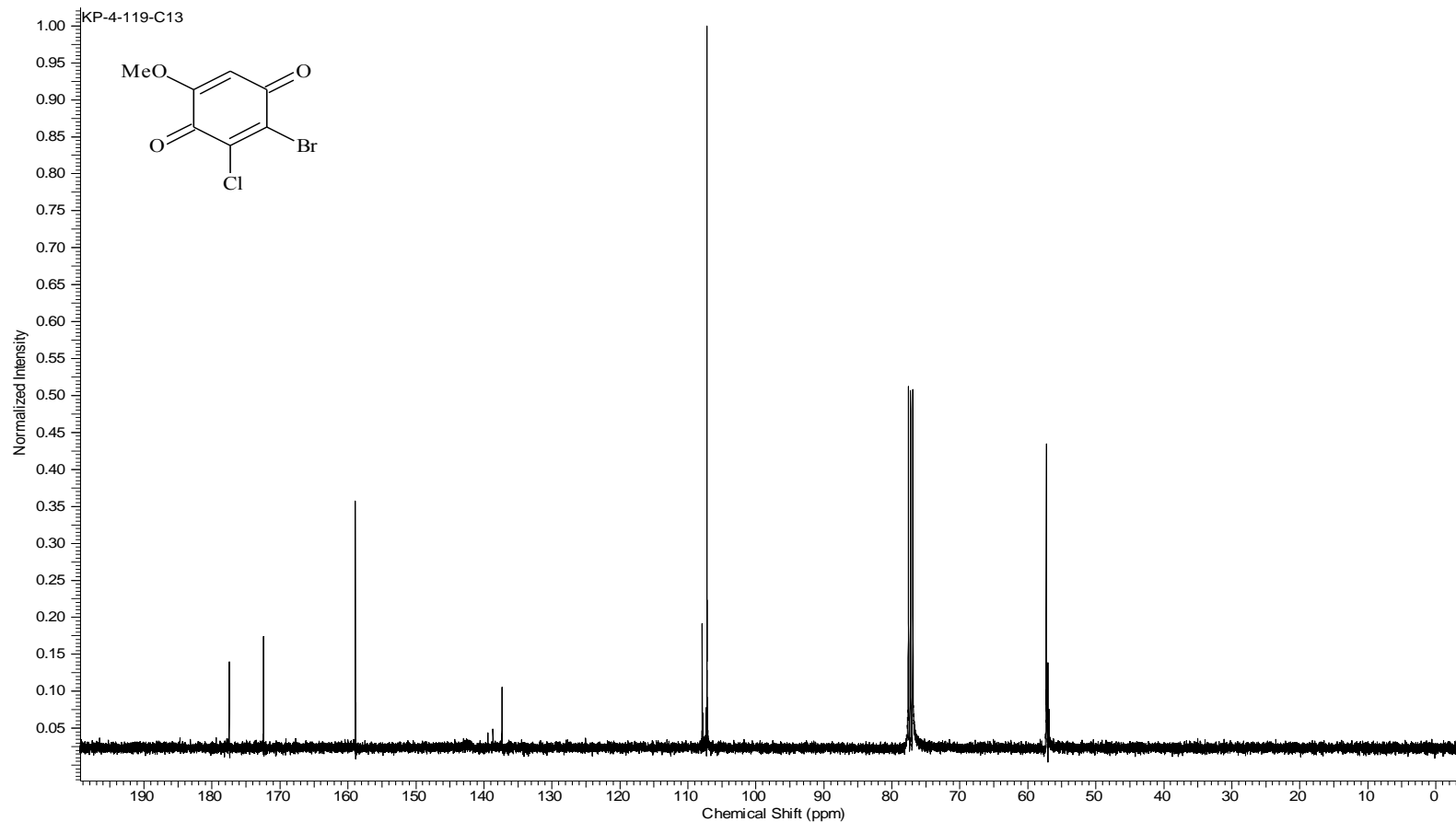
Acquisition Time (sec)	1.9945	Comment	STANDARD 1H OBSERVE		Date	Sep 17 2009	
Date Stamp	Sep 17 2009	File Name	C:\USERS\KESHAR\DESKTOP\NMR\BOOK 5\KP-5-31-QUINONE.FID\FID				
Frequency (MHz)	199.98	Nucleus	1H	Number of Transients	56	Original Points Count	5984
Points Count	8192	Pulse Sequence	s2pul	Receiver Gain	40.00	Solvent	CHLOROFORM-d
Spectrum Offset (Hz)	1002.3889	Spectrum Type	STANDARD	Sweep Width (Hz)	3000.30	Temperature (degree C)	AMBIENT TEMPERATURE



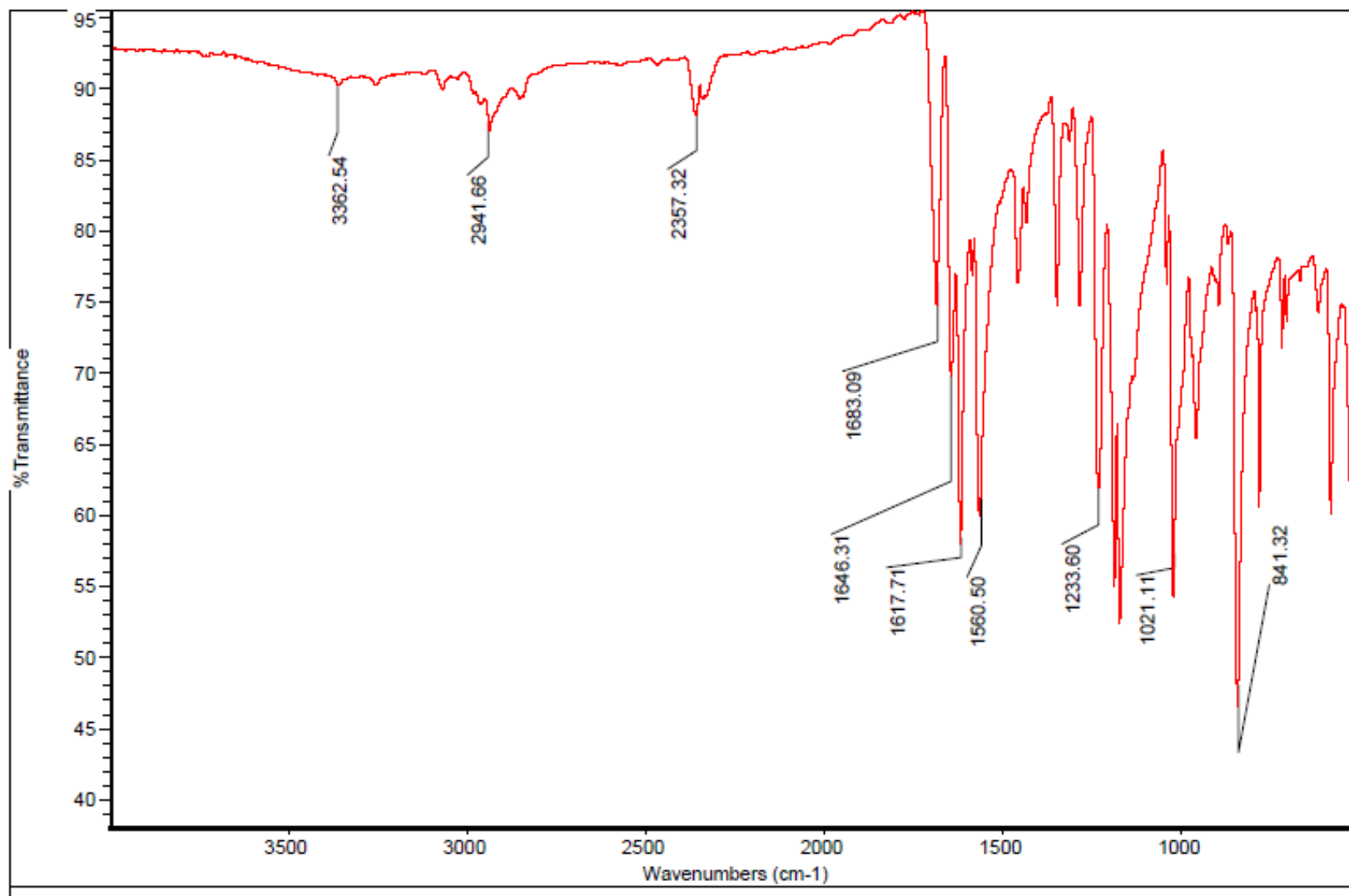
Compound 19 ¹³C NMR

6/27/2012 1:52:28 PM

Acquisition Time (sec)	1.3005	Comment	Std proton	Date	Oct 7 2009	Date Stamp	Oct 7 2009
File Name	C:\USERS\KESHAR\DESKTOP\NMR\LACCASE\KP-4-119-C13\FID				Frequency (MHz)	100.53	
Nucleus	13C	Number of Transients	9152	Original Points Count	31375	Points Count	32768
Pulse Sequence	s2pul	Receiver Gain	30.00	Solvent	CHLOROFORM-d		
Spectrum Offset (Hz)	10554.7441	Spectrum Type	STANDARD	Sweep Width (Hz)	24125.45	Temperature (degree C)	25.000

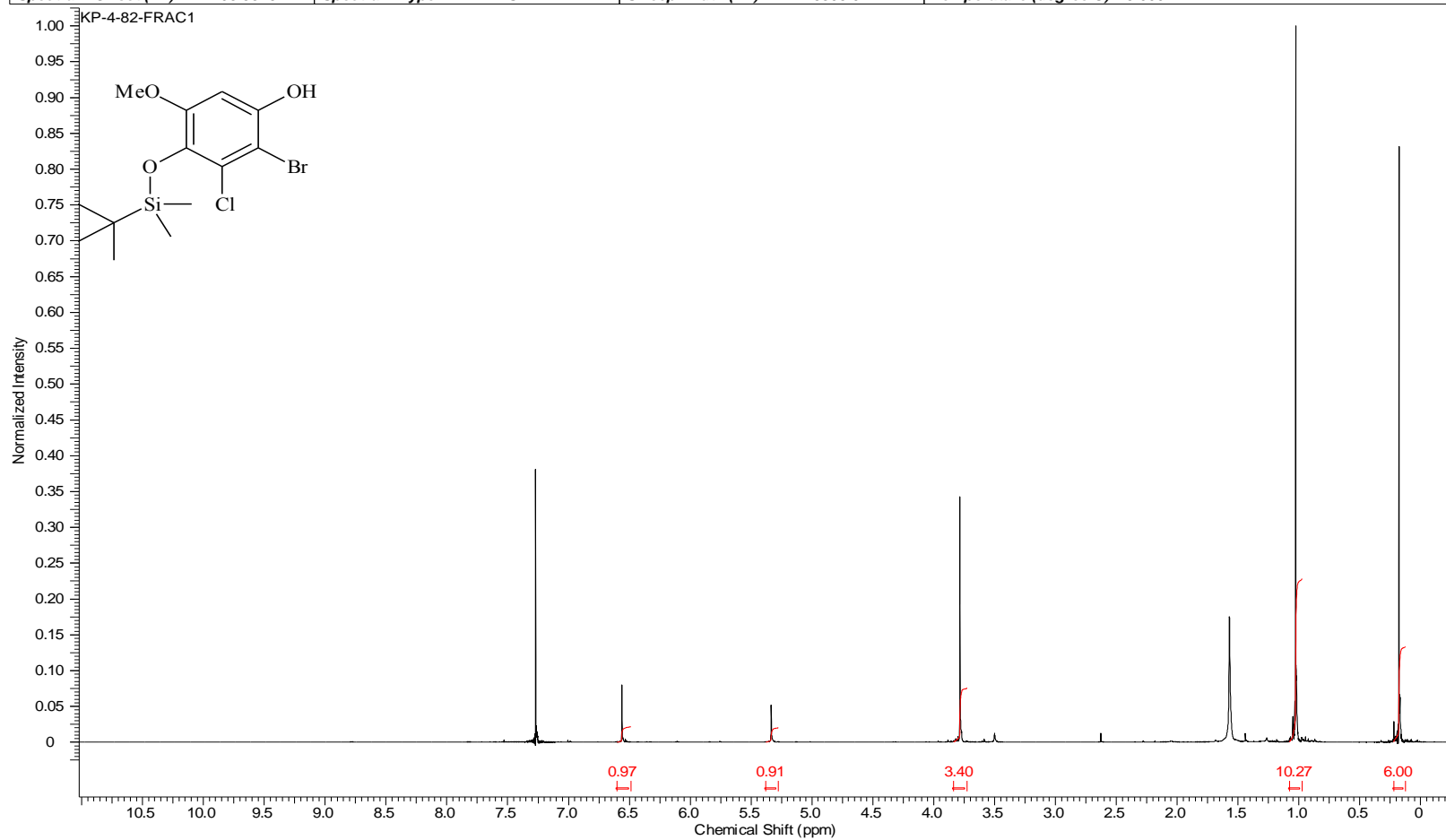


Compound 19 IR



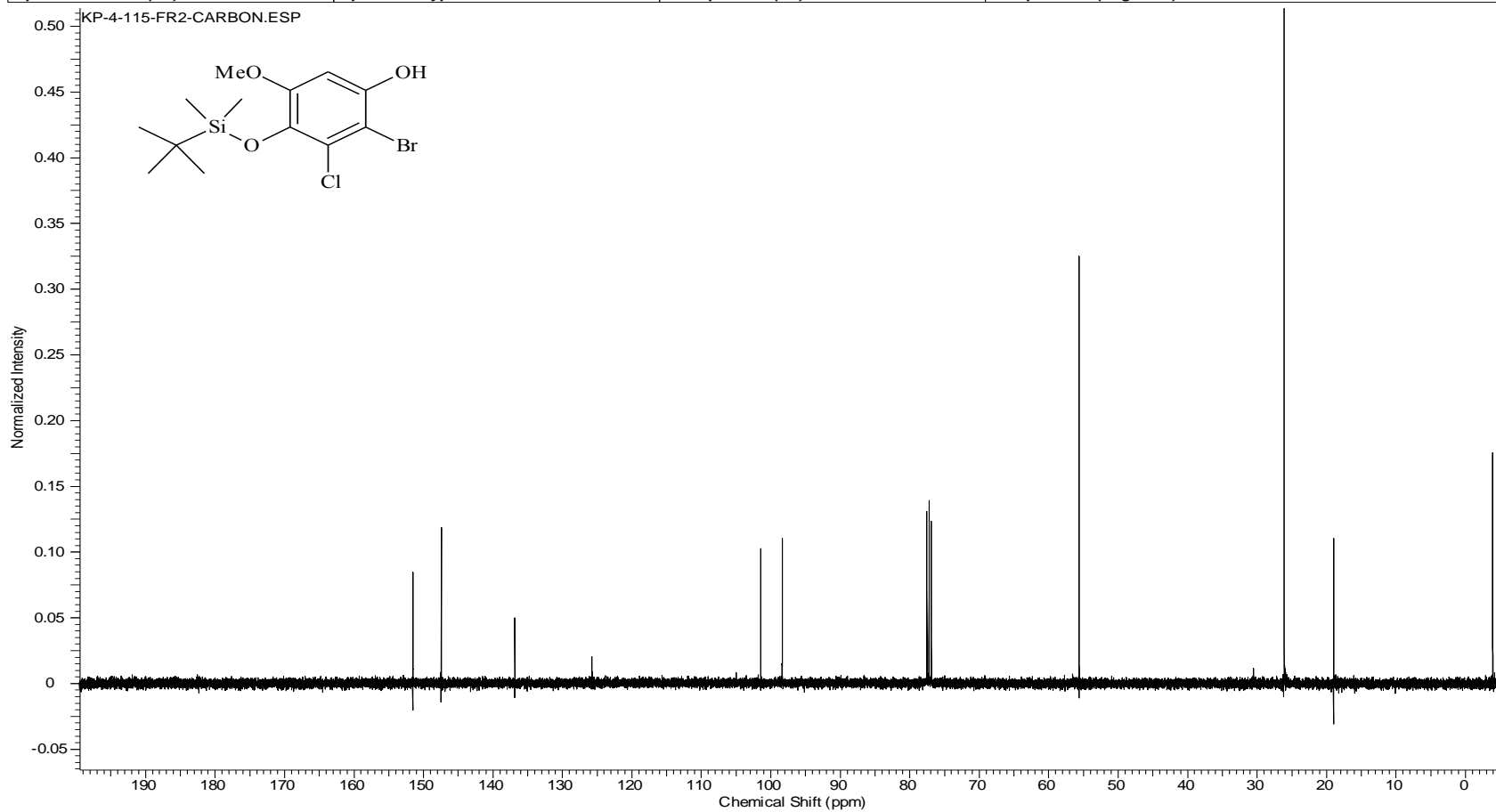
Compound 25 ¹H NMR

Acquisition Time (sec)	2.0487	Comment	Std proton	Date	Aug 15 2009	Date Stamp	Aug 15 2009
File Name	C:\USERS\KESHAR\DESKTOP\NMR\BOOK 4\KP-4-82-FRAC1.FID\FID			Frequency (MHz)	399.75		
Nucleus	1H	Number of Transients	24	Original Points Count	13103	Points Count	16384
Pulse Sequence	s2pul	Receiver Gain	54.00	Solvent	CHLOROFORM-d		
Spectrum Offset (Hz)	2403.5376	Spectrum Type	STANDARD	Sweep Width (Hz)	6395.91	Temperature (degree C)	25.000



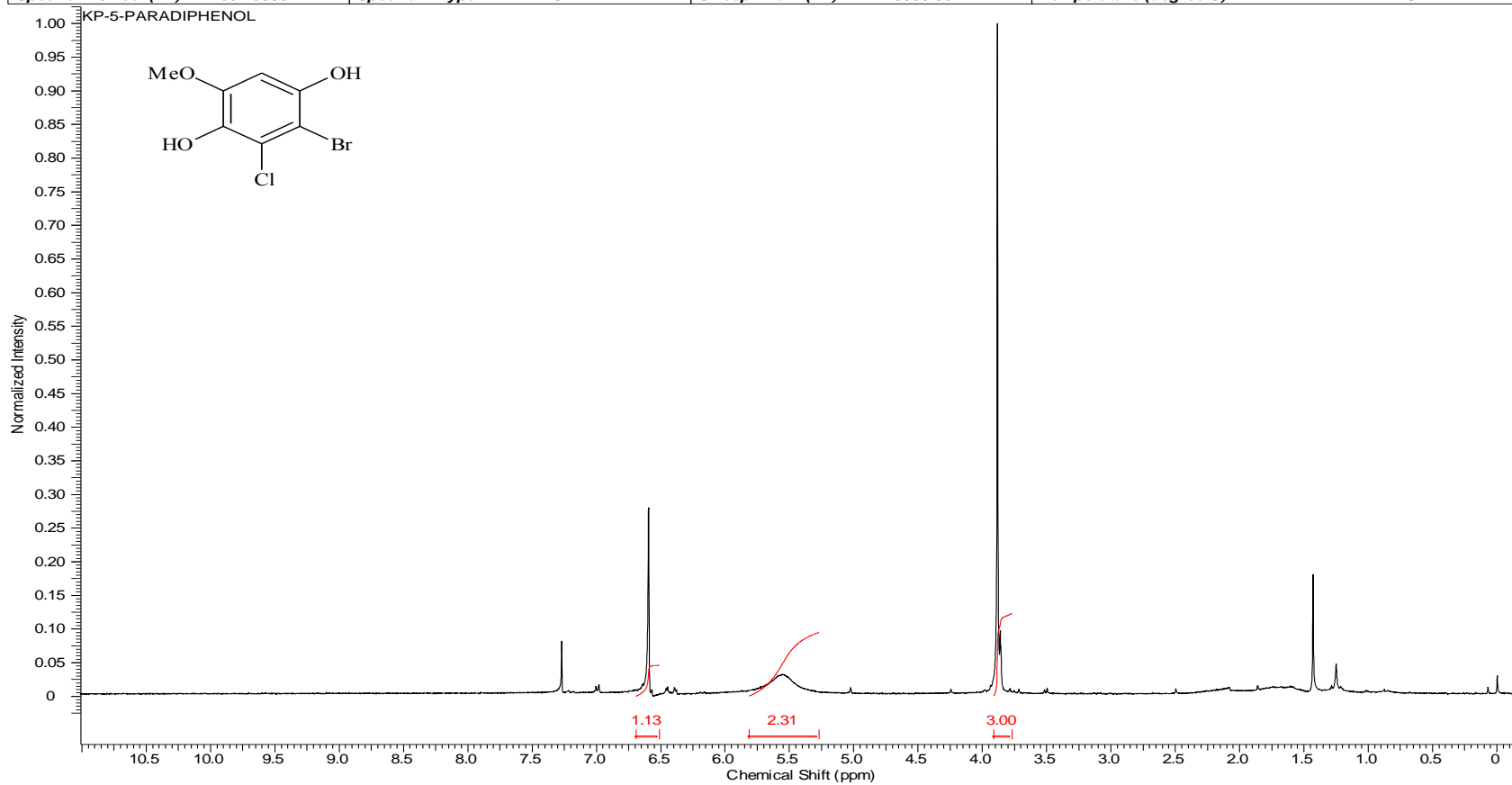
Compound 25 ¹³C NMR

Acquisition Time (sec)	1.3005	Comment	Std proton	Date	Oct 7 2009	Date Stamp	Oct 7 2009
File Name	C:\USERS\KESHAR\KP-4-115-FR2-Carbon			Frequency (MHz)	100.53		
Nucleus	¹³ C	Number of Transients	2112	Original Points Count	31375	Points Count	32768
Pulse Sequence	s2pul	Receiver Gain	30.00	Solvent	CHLOROFORM-d		
Spectrum Offset (Hz)	10554.9160	Spectrum Type	STANDARD	Sweep Width (Hz)	24125.45	Temperature (degree C)	25.000



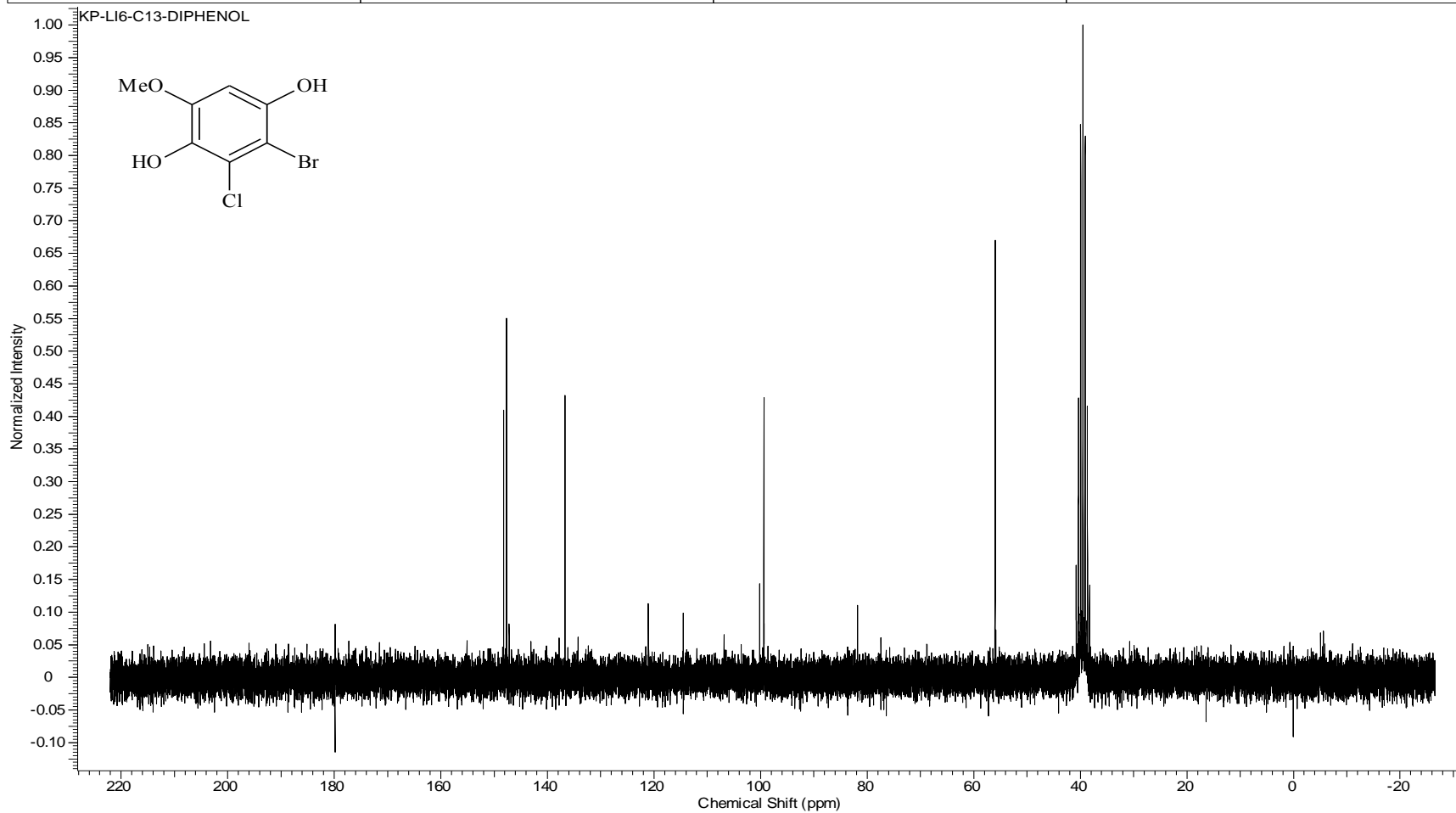
Compound 2 ¹H NMR

Acquisition Time (sec)	1.9945	Comment	STANDARD 1H OBSERVE		Date	Oct 1 2009	
Date Stamp	Oct 1 2009	File Name	C:\USERS\KESHAR\DESKTOP\NMR\BOOK 5\KP-5-PARADIPHENOL.FID\FID				
Frequency (MHz)	199.98	Nucleus	1H	Number of Transients	16	Original Points Count	5984
Points Count	8192	Pulse Sequence	s2pul	Receiver Gain	30.00	Solvent	CHLOROFORM-d
Spectrum Offset (Hz)	1002.3889	Spectrum Type	STANDARD	Sweep Width (Hz)	3000.30	Temperature (degree C)	AMBIENT TEMPERATURE

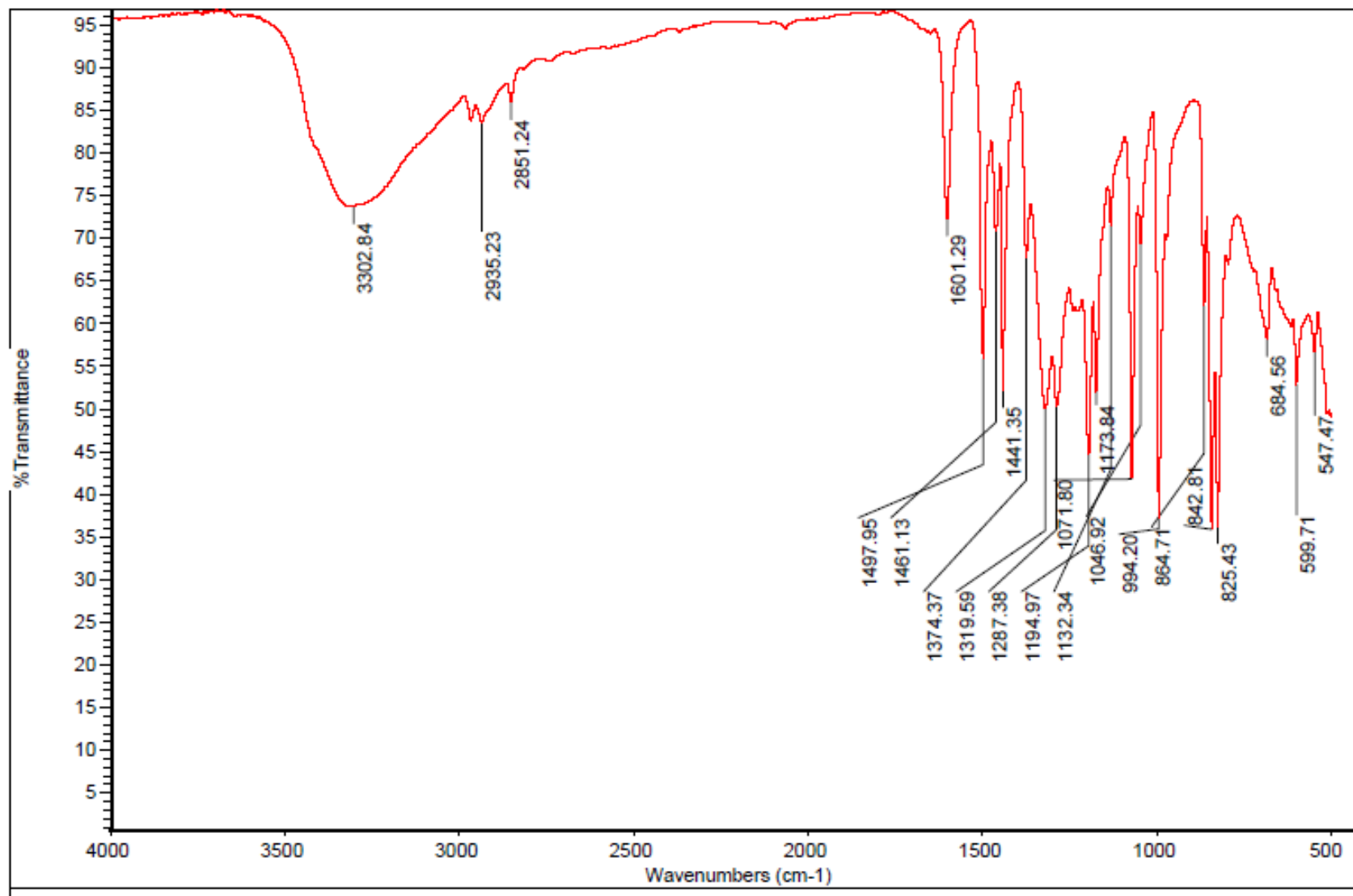


Compound 2 ¹³C NMR

Acquisition Time (sec)	1.4976	Comment	13C OBSERVE	Date	Oct 8 2009	Date Stamp	Oct 8 2009
File Name	C:\USERS\BOOK 6\KP-LI6-C13-DIPHENOL.FID\FID						
Frequency (MHz)	50.29	Nucleus	13C	Number of Transients	3680	Original Points Count	18720
Points Count	32768	Pulse Sequence	s2pul	Receiver Gain	40.00	Solvent	DMSO-d6
Spectrum Offset (Hz)	4915.7617	Spectrum Type	STANDARD	Sweep Width (Hz)	12500.00	Temperature (degree C)	AMBIENT TEMPERATURE

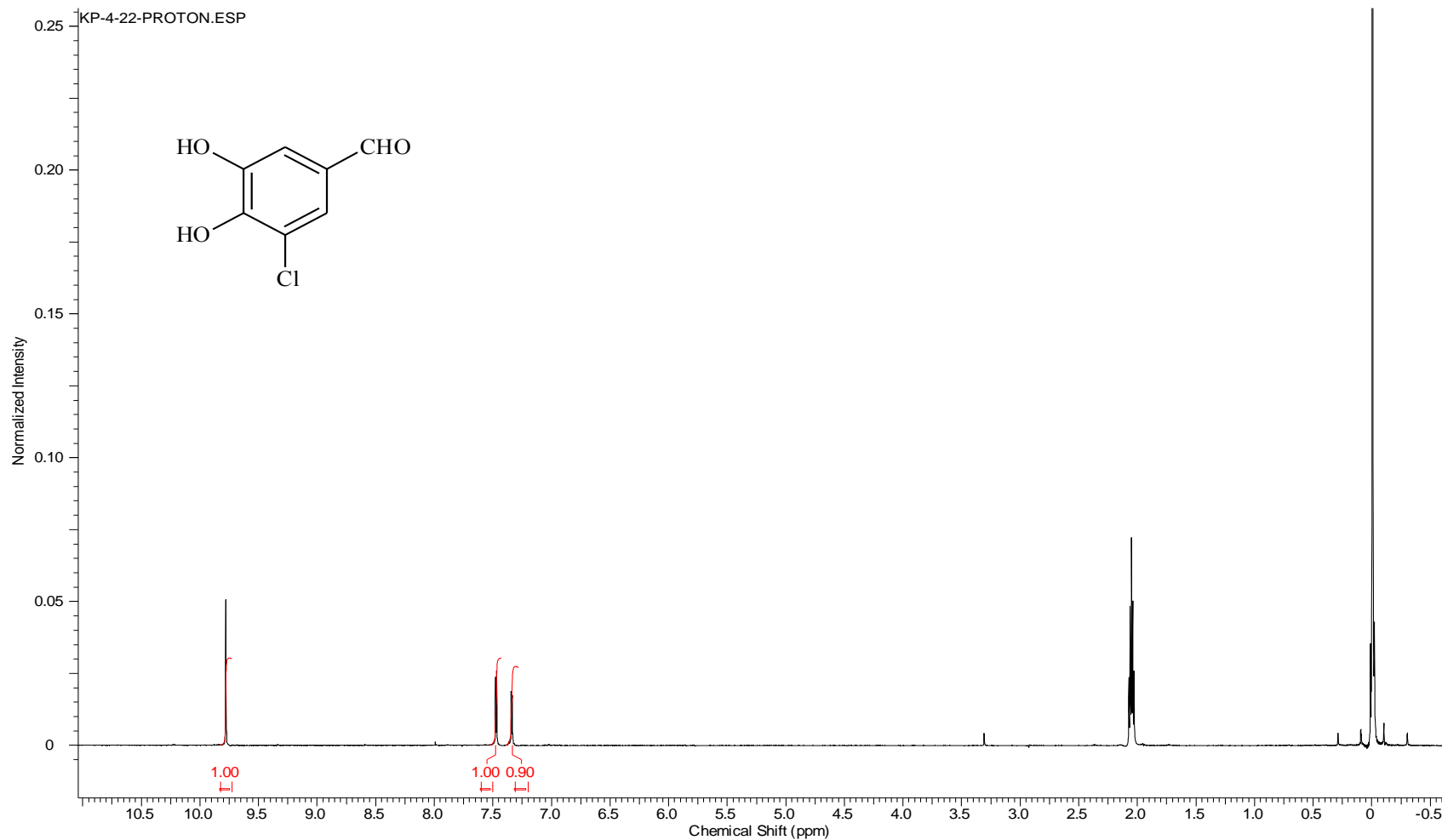


Compound 2 IR



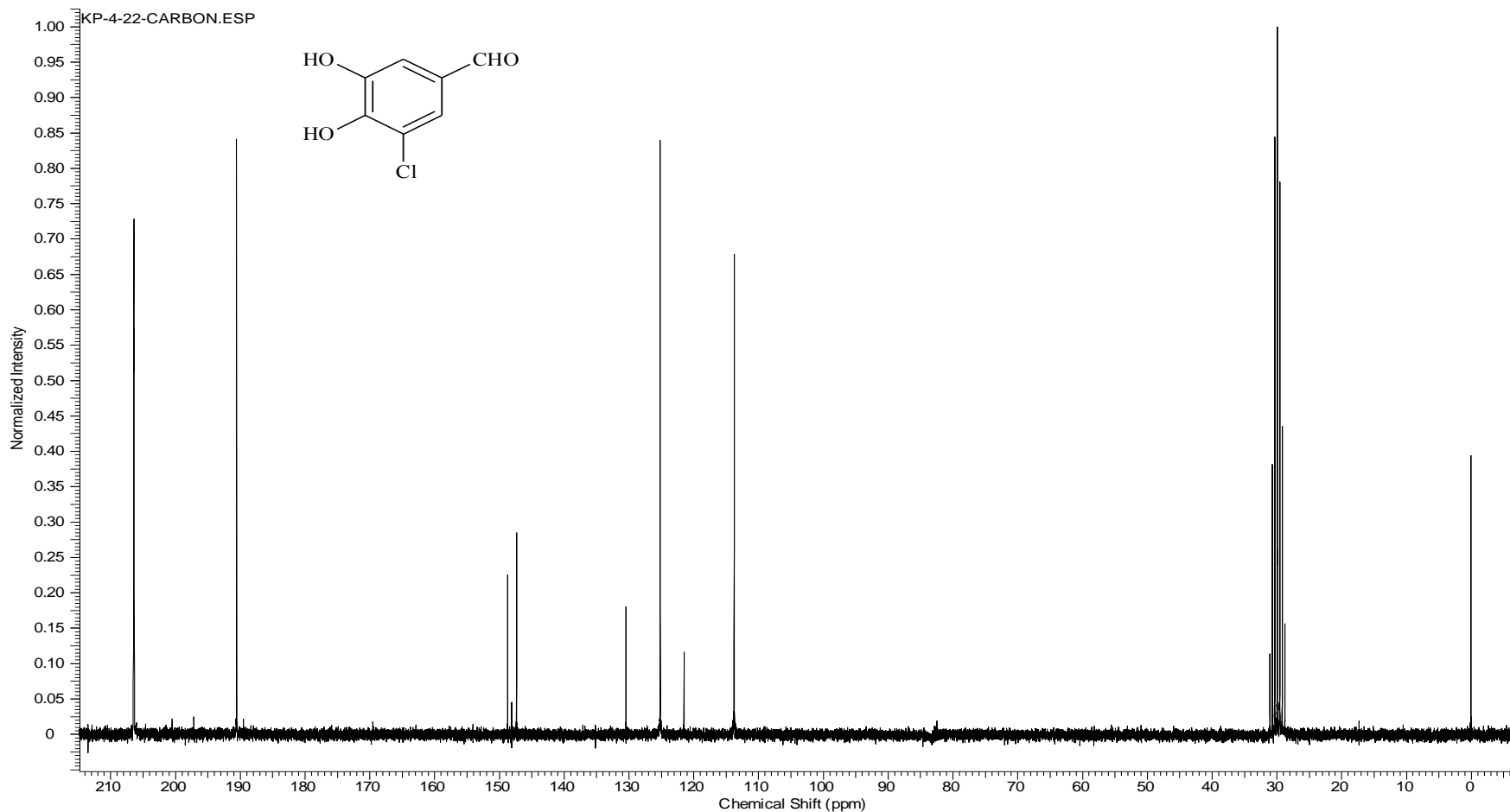
Compound 3 ¹H NMR

Acquisition Time (sec)	1.9945	Comment	STANDARD 1H OBSERVE		Date	Jul 19 2007	
Date Stamp	Jul 19 2007	File Name	C:\USERS\KESHAR\KP-4-22-Proton				
Frequency (MHz)	199.98	Nucleus	1H	Number of Transients	64	Original Points Count	5984
Points Count	8192	Pulse Sequence	s2pul	Receiver Gain	28.00	Solvent	Acetone
Spectrum Offset (Hz)	999.5056	Spectrum Type	STANDARD	Sweep Width (Hz)	3000.30	Temperature (degree C)	AMBIENT TEMPERATURE



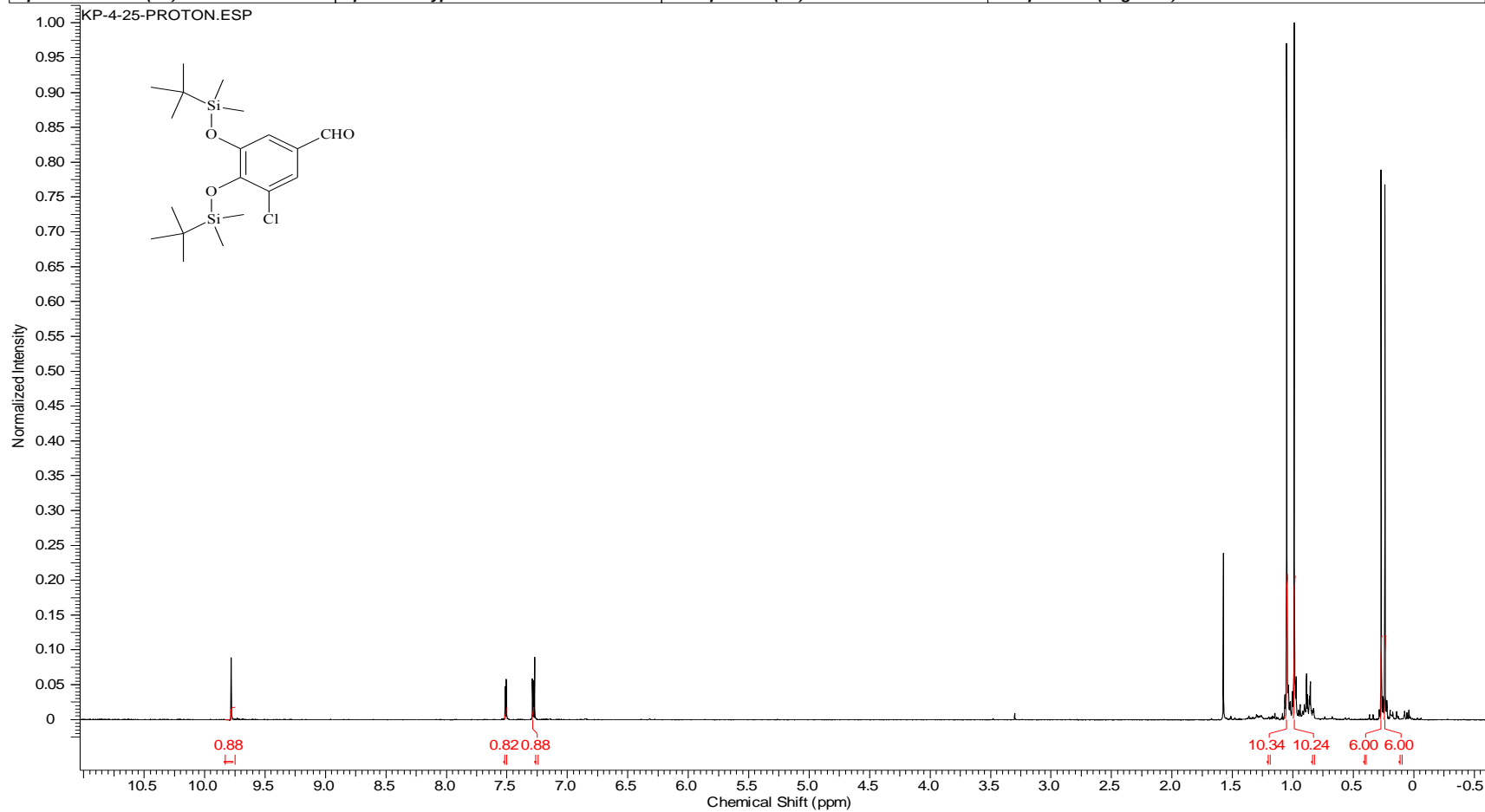
Compound 3 ¹³C NMR

Acquisition Time (sec)	1.4976	Comment	13C OBSERVE	Date	Aug 1 2007	Date Stamp	Aug 1 2007
File Name	C:\USERS\SKESHAR\KP-4-22-Carbon			Frequency (MHz)	50.29		
Nucleus	13C	Number of Transients	11897	Original Points Count	18720	Points Count	32768
Pulse Sequence	s2pul	Receiver Gain	40.00	Solvent	Acetone	Spectrum Offset (Hz)	4962.9824
Spectrum Type	STANDARD	Sweep Width (Hz)	12500.00	Temperature (degree C)	AMBIENT TEMPERATURE		



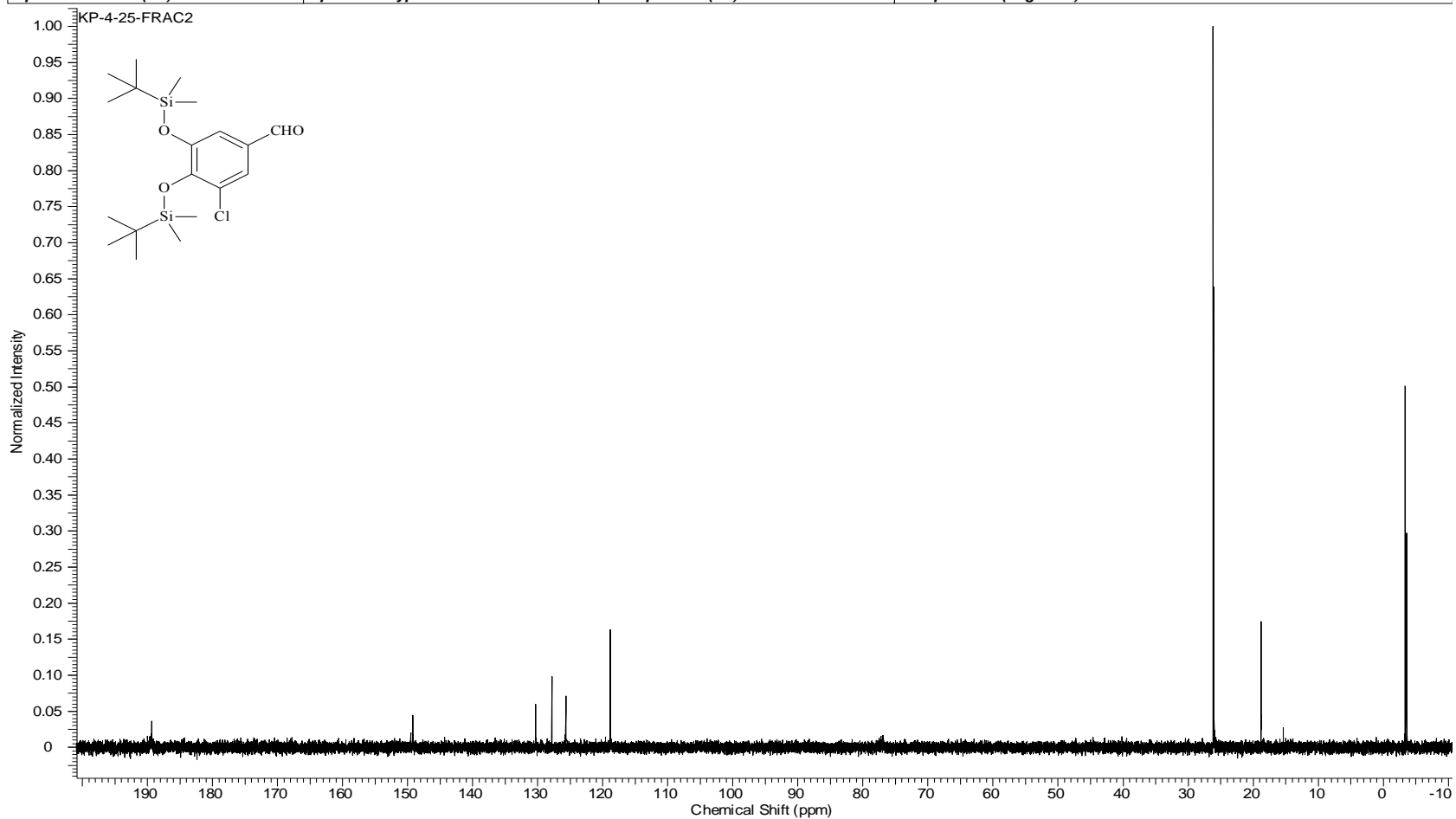
Compound 26 ¹H NMR

Acquisition Time (sec)	1.9945	Comment	STANDARD 1H OBSERVE		Date	Jul 20 2007	
Date Stamp	Jul 20 2007	File Name	C:\USERS\KESHAR\DESKTOP\NMR\HUIPING\HZ-9-82-AC.FID\FID				
Frequency (MHz)	199.98	Nucleus	1H	Number of Transients	32	Original Points Count	5984
Points Count	8192	Pulse Sequence	s2pul	Receiver Gain	28.00	Solvent	CHLOROFORM-d
Spectrum Offset (Hz)	1002.0226	Spectrum Type	STANDARD	Sweep Width (Hz)	3000.30	Temperature (degree C)	AMBIENT TEMPERATURE



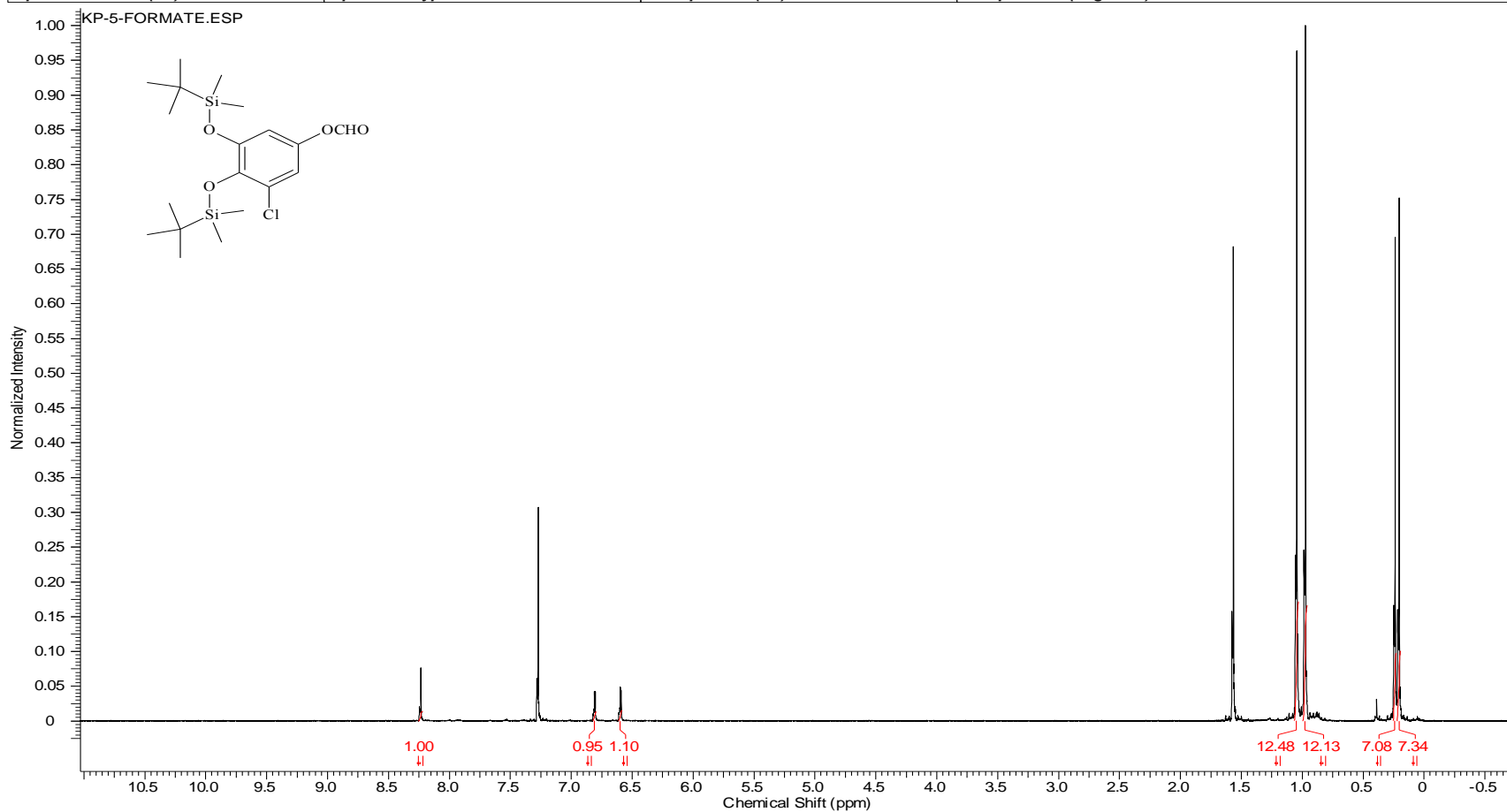
Compound 26 ¹³C NMR

Acquisition Time (sec)	1.2800	Comment	13C OBSERVE		Date	Aug 2 09	
Date Stamp	Aug 2 09	File Name	C:\USERS\KESHAR\DESKTOP\KP-4-25-FRAC2\FID		Frequency (MHz)	100.56	
Nucleus	13C	Number of Transients	96	Original Points Count	32000	Points Count	32768
Pulse Sequence	s2pul	Receiver Gain	60.00	Solvent	CHLOROFORM-d		
Spectrum Offset (Hz)	9502.9023	Spectrum Type	STANDARD	Sweep Width (Hz)	25000.00	Temperature (degree C)	27.000



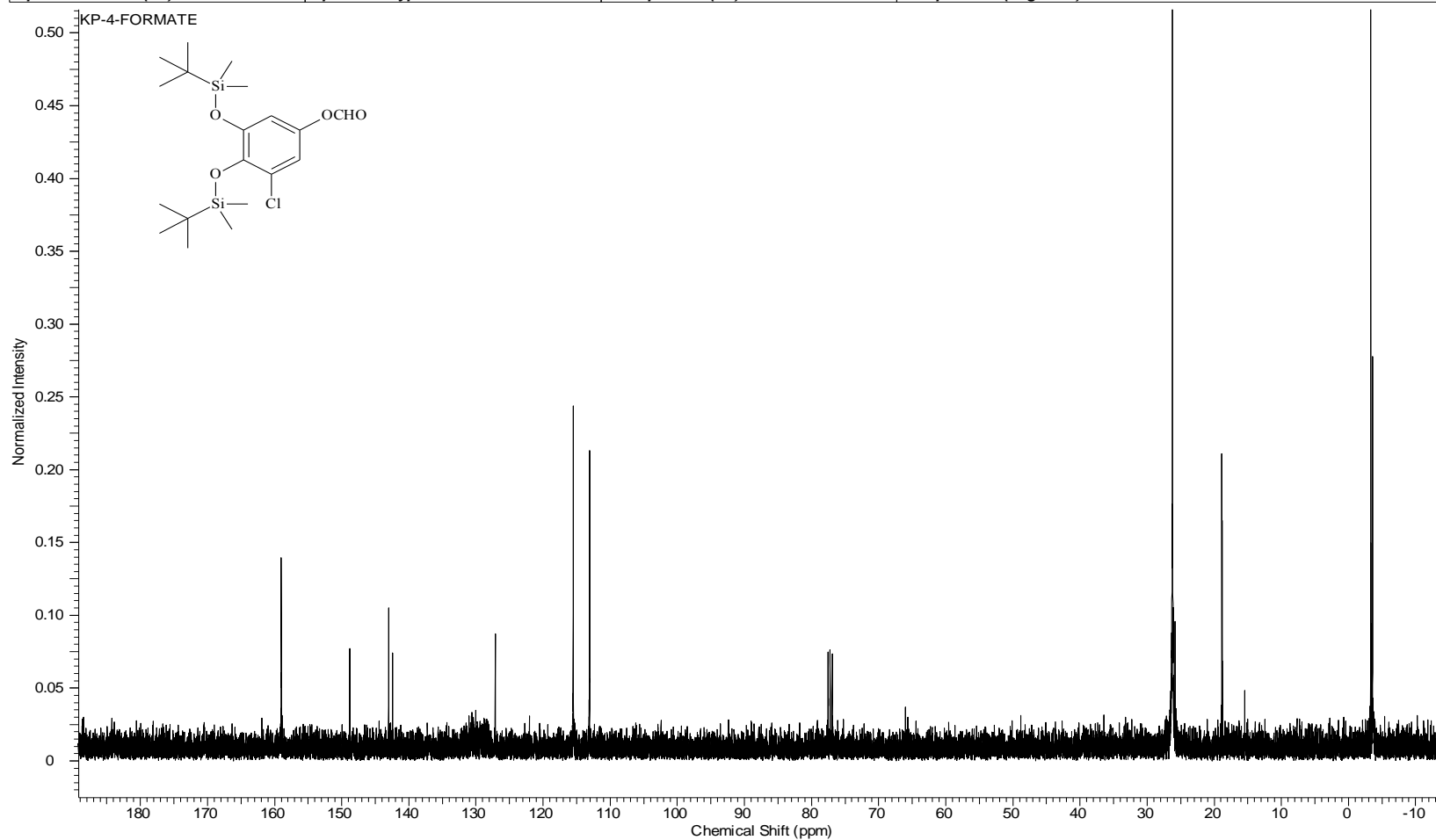
Compound 27 ¹H NMR

Acquisition Time (sec)	2.0486	Comment	Std proton	Date	Jul 21 2007	Date Stamp	Jul 21 2007
File Name	C:\USERS\KESHAR\KP-5-Formate			Frequency (MHz)	399.78		
Nucleus	1H	Number of Transients	4	Original Points Count	17199	Points Count	32768
Pulse Sequence	s2pul	Receiver Gain	44.00	Solvent	DEUTERIUM OXIDE		
Spectrum Offset (Hz)	3241.8862	Spectrum Type	STANDARD	Sweep Width (Hz)	8395.42	Temperature (degree C)	25.000



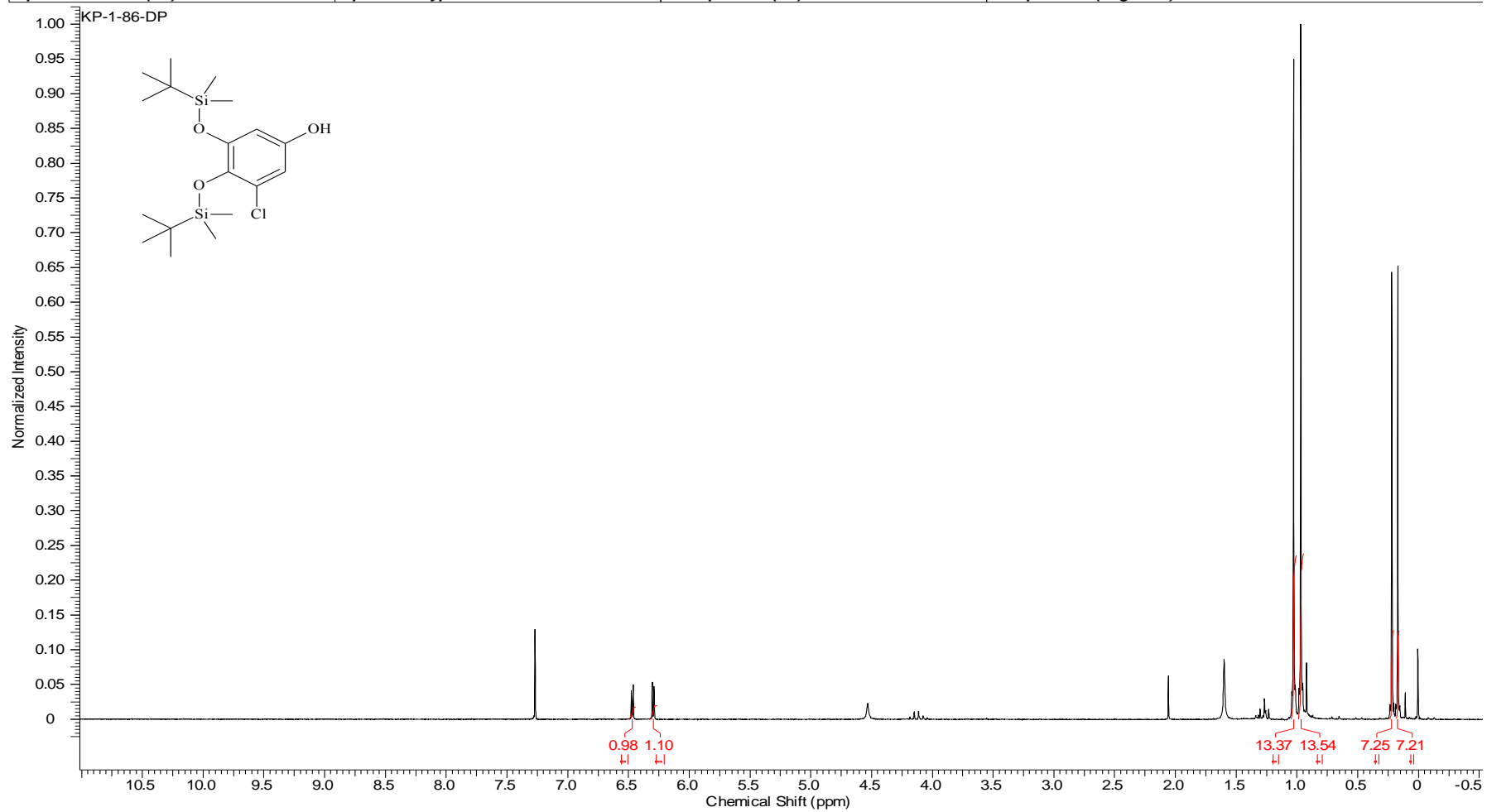
Compound 27 ¹³C NMR

Acquisition Time (sec)	1.2800	Comment	13C OBSERVE		Date	Aug 4 09	
Date Stamp	Aug 4 09	File Name	C:\USERS\KESHAR\DESKTOP\KP-4-FORMATE\FID		Frequency (MHz)	199.9	
Nucleus	13C	Number of Transients	128	Original Points Count	32000	Points Count	32768
Pulse Sequence	s2pul	Receiver Gain	60.00	Solvent	CHLOROFORM-d		
Spectrum Offset (Hz)	9512.8496	Spectrum Type	STANDARD	Sweep Width (Hz)	25000.00	Temperature (degree C)	25



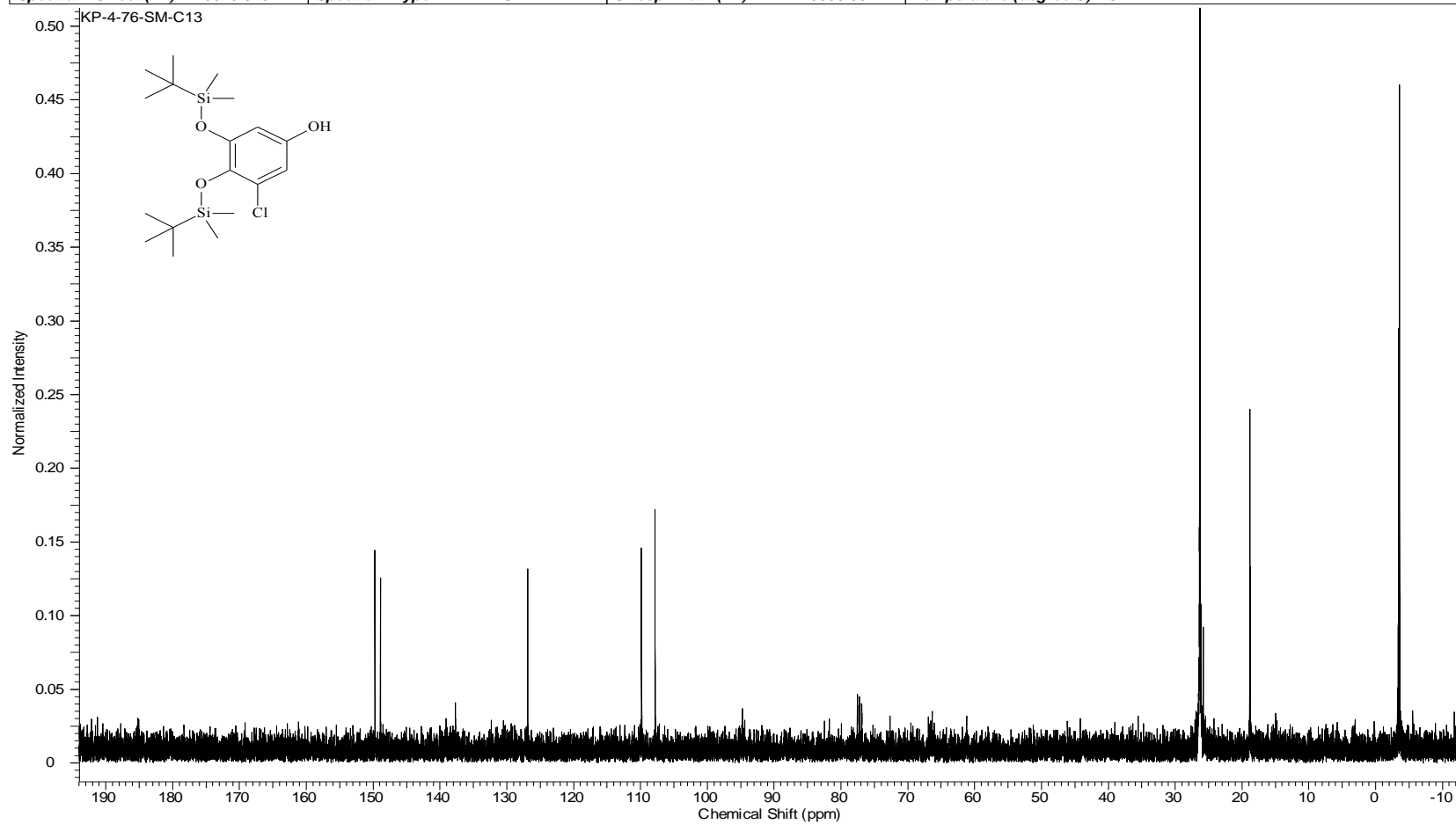
Compound 28 ¹H NMR

Acquisition Time (sec)	1.9945	Comment	STANDARD 1H OBSERVE		Date	Aug 2 2008	
Date Stamp	Aug 2 2008	File Name	C:\USERS\KESHAR\DESKTOP\NMR\BOOK 1\KP-1-86-DP.FID\FID				
Frequency (MHz)	199.98	Nucleus	1H	Number of Transients	32	Original Points Count	5984
Points Count	8192	Pulse Sequence	s2pul	Receiver Gain	34.00	Solvent	CHLOROFORM-d
Spectrum Offset (Hz)	1001.2900	Spectrum Type	STANDARD	Sweep Width (Hz)	3000.30	Temperature (degree C)	AMBIENT TEMPERATURE



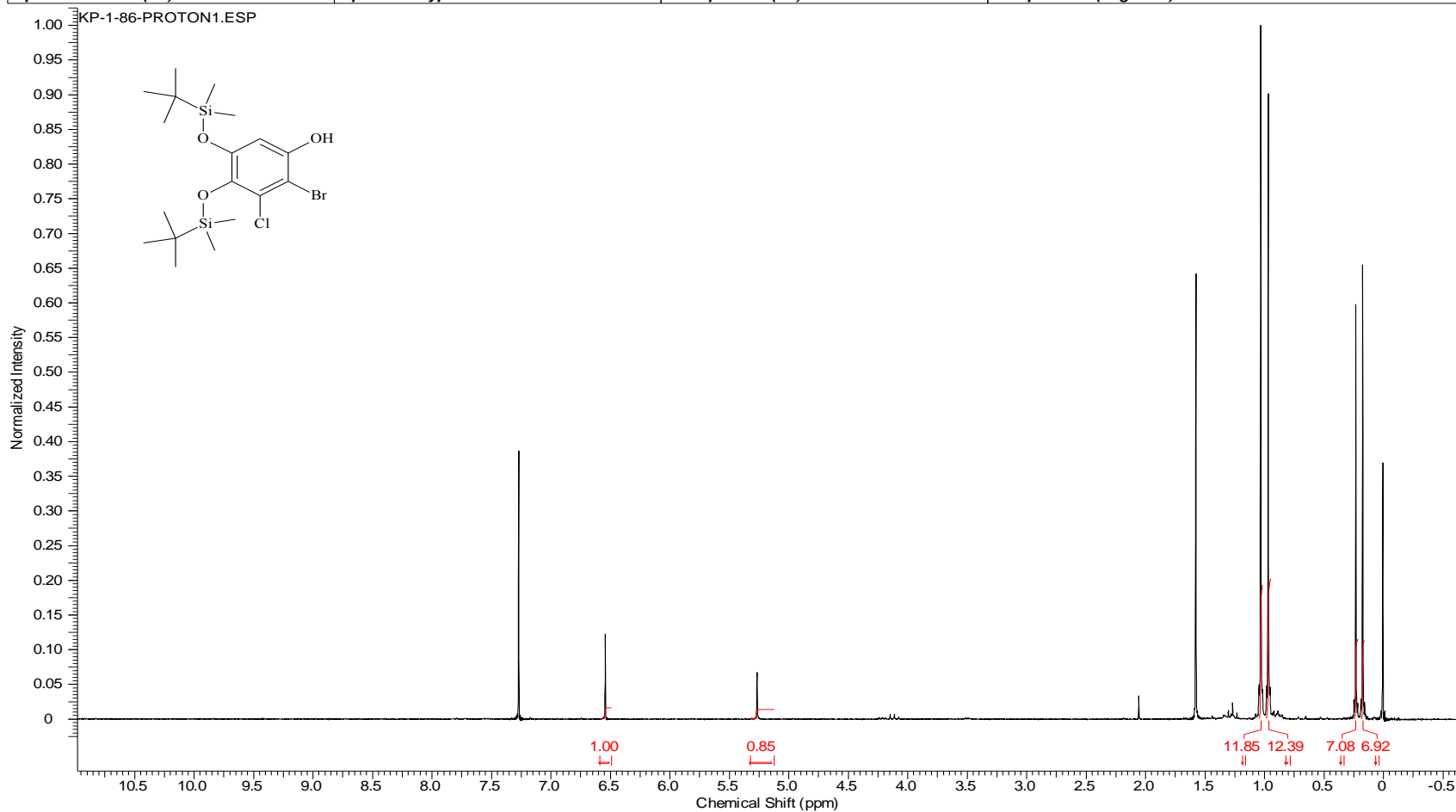
Compound 28 ¹³C NMR

Acquisition Time (sec)	1.2800	Comment	13C OBSERVE		Date	Jan 7 2009	
Date Stamp	Jan 7 2009	File Name	C:\USERS\KESHAR\DESKTOP\KP-4-76-SM-C13\FID		Frequency (MHz)	199.9	
Nucleus	13C	Number of Transients	128	Original Points Count	32000	Points Count	32768
Pulse Sequence	s2pul	Receiver Gain	60.00	Solvent	CHLOROFORM-d		
Spectrum Offset (Hz)	9513.0752	Spectrum Type	STANDARD	Sweep Width (Hz)	25000.00	Temperature (degree C)	25



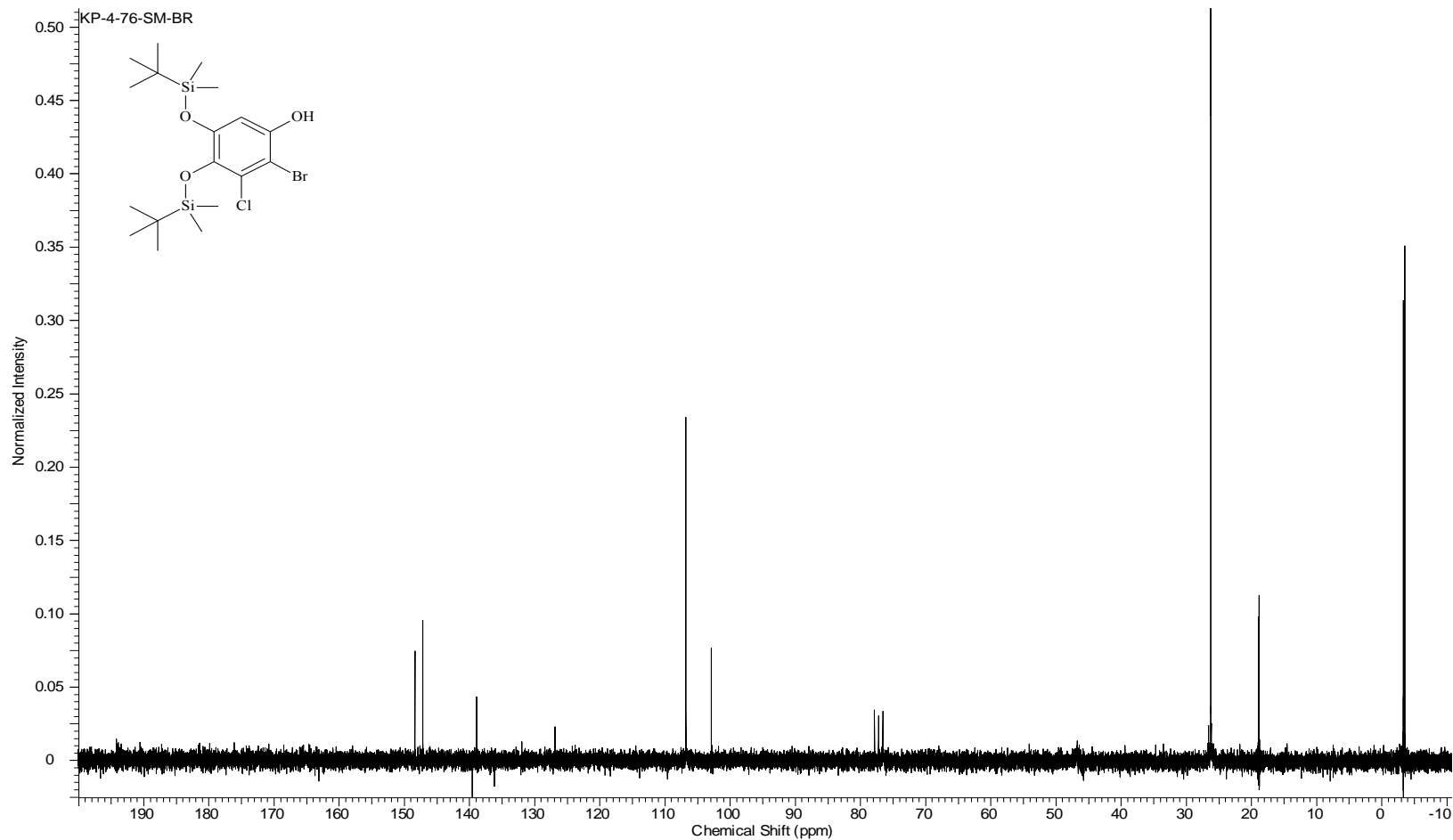
Compound 29 ¹H NMR

Acquisition Time (sec)	1.9945	Comment	STANDARD 1H OBSERVE		Date	Aug 6 2008	
Date Stamp	Aug 6 2008	File Name	C:\USERS\KESHAR\DESKTOP\NMR\BOOK 1\KP-1-86-DPCOLUMN.FID\FID				
Frequency (MHz)	199.98	Nucleus	1H	Number of Transients	64	Original Points Count	5984
Points Count	8192	Pulse Sequence	s2pul	Receiver Gain	39.00	Solvent	CHLOROFORM-d
Spectrum Offset (Hz)	1001.6563	Spectrum Type	STANDARD	Sweep Width (Hz)	3000.30	Temperature (degree C)	AMBIENT TEMPERATURE



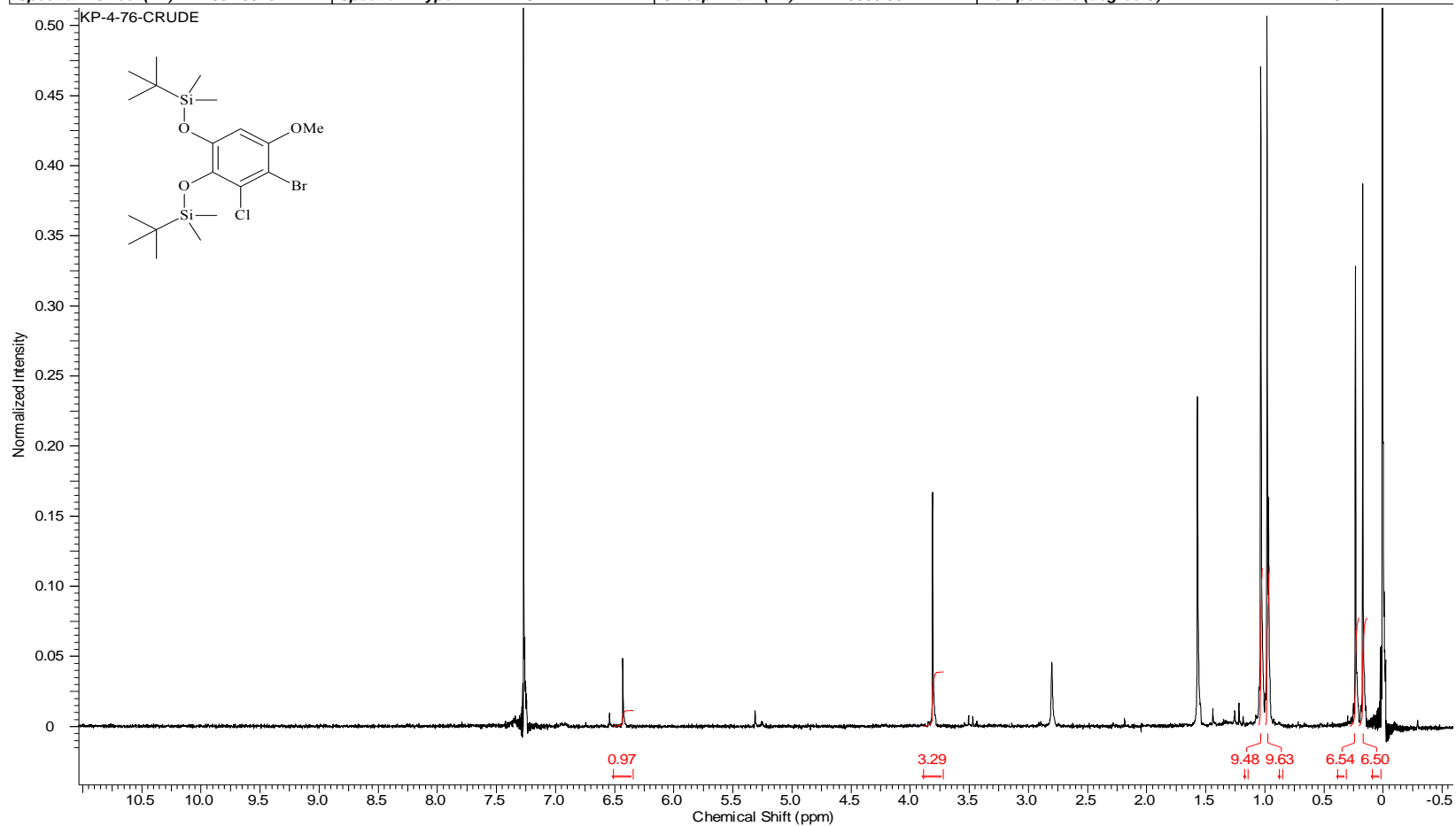
Compound 29 ¹³C NMR

Acquisition Time (sec)	1.4976	Comment	13C OBSERVE	Date	Sep 6 200	Date Stamp	Sep 6 2009
File Name	C:\USERS\KESHAR\DESKTOP\NMR\LACCASE\KP-4-76-SM-BR\FID			Frequency (MHz)	50.29		
Nucleus	13C	Number of Transients	320	Original Points Count	18720	Points Count	32768
Pulse Sequence	s2pul	Receiver Gain	40.00	Solvent	CHLOROFORM-d		
Spectrum Offset (Hz)	4880.4648	Spectrum Type	STANDARD	Sweep Width (Hz)	12500.00	Temperature (degree C)	AMBIENT TEMPERATURE



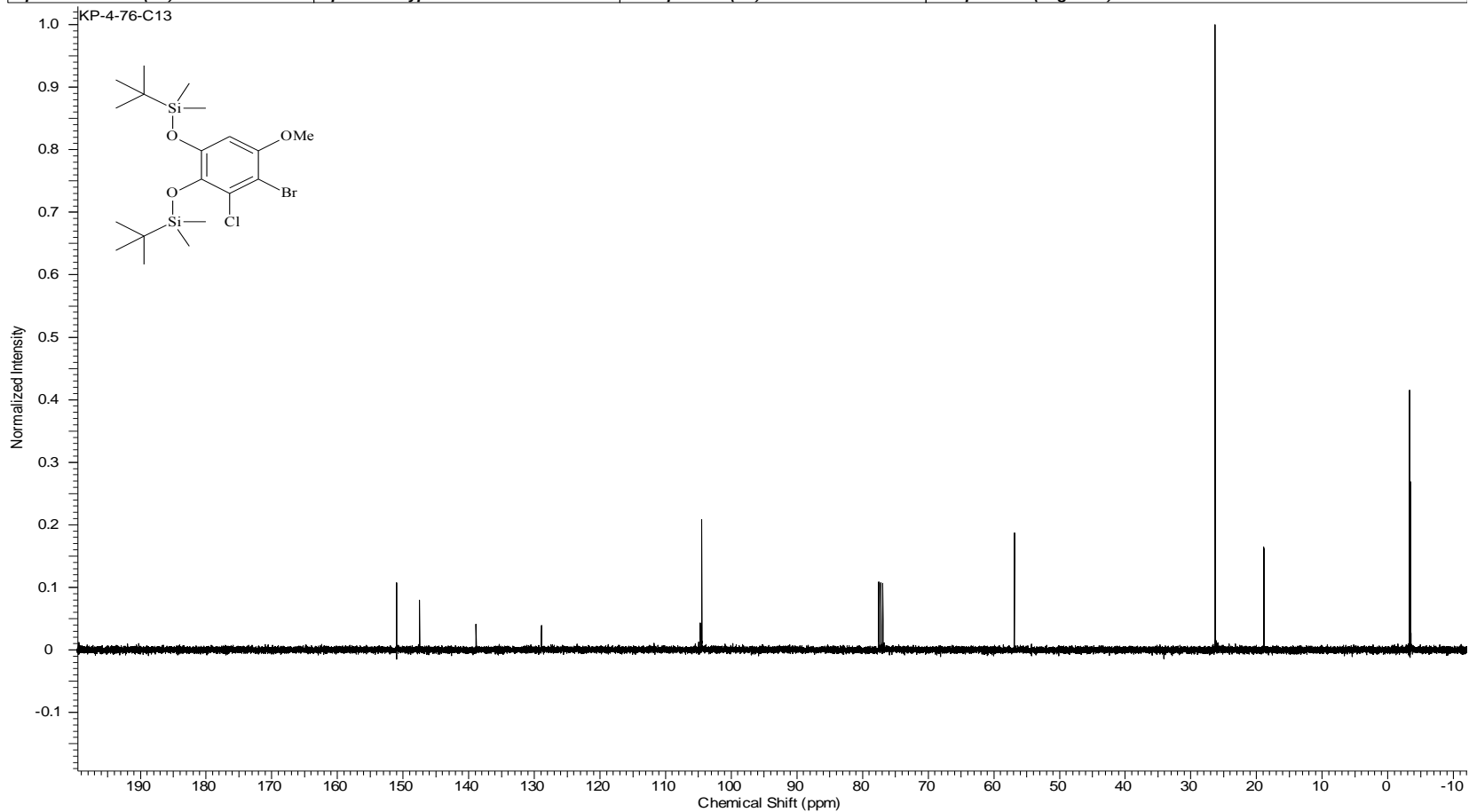
Compound 30 ¹H NMR

Acquisition Time (sec)	1.9945	Comment	STANDARD 1H OBSERVE		Date	Apr 21 2009	
Date Stamp	Apr 21 2009	File Name	C:\USERS\KESHAR\DESKTOP\NMR\BOOK 4\KP-4-76-CRUDE.FID\FID				
Frequency (MHz)	199.98	Nucleus	1H	Number of Transients	100	Original Points Count	5984
Points Count	8192	Pulse Sequence	s2pul	Receiver Gain	40.00	Solvent	CHLOROFORM-d
Spectrum Offset (Hz)	1002.3816	Spectrum Type	STANDARD	Sweep Width (Hz)	3000.30	Temperature (degree C)	AMBIENT TEMPERATURE



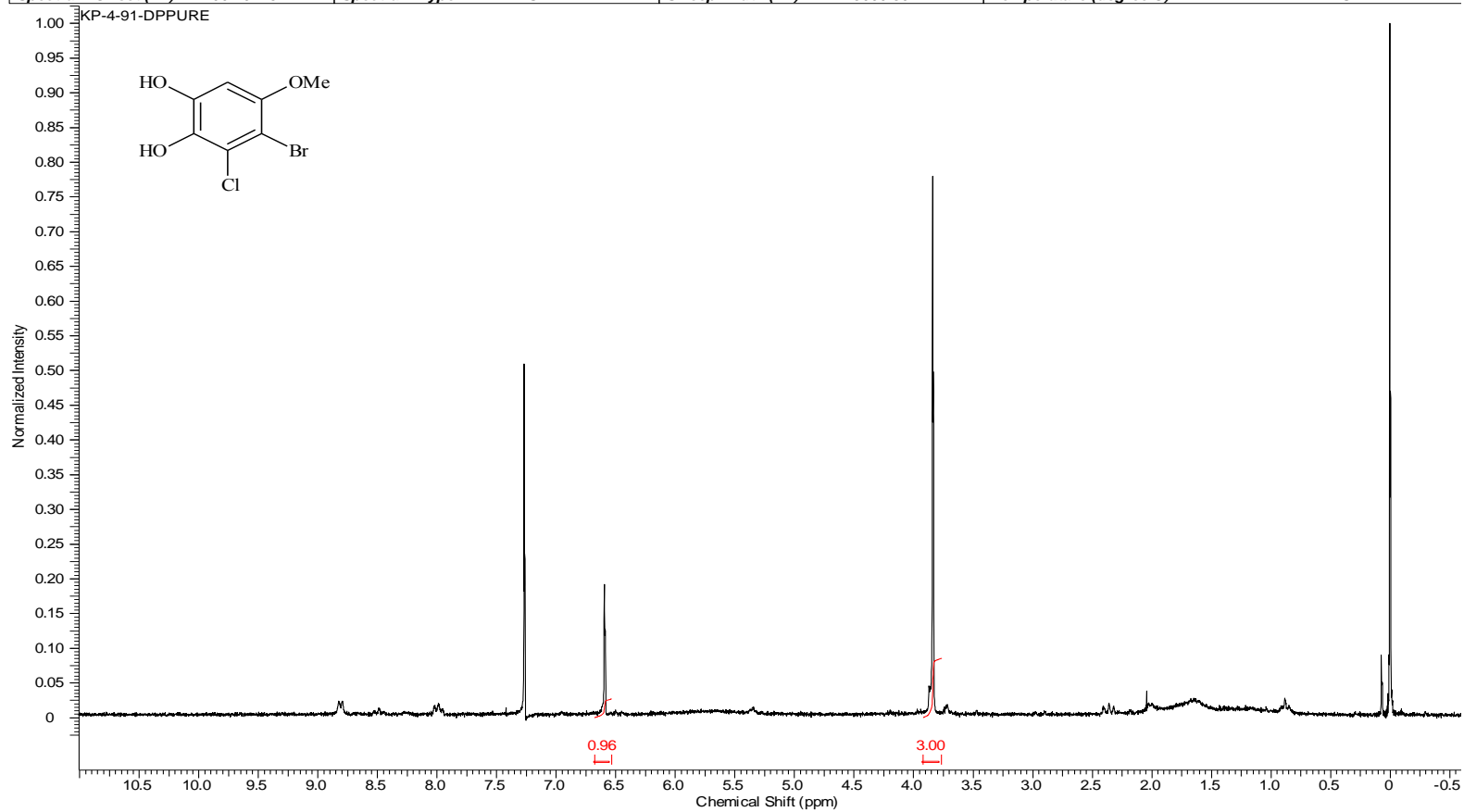
Compound 30 ¹³C NMR

Acquisition Time (sec)	1.3005	Comment	Std proton	Date	Oct 8 2009	Date Stamp	Oct 8 2009
File Name	C:\USERS\KESHAR\KP-4-76-C13			Frequency (MHz)	100.53		
Nucleus	13C	Number of Transients	1408	Original Points Count	31375	Points Count	32768
Pulse Sequence	s2pul	Receiver Gain	30.00	Solvent	CHLOROFORM-d		
Spectrum Offset (Hz)	10554.9160	Spectrum Type	STANDARD	Sweep Width (Hz)	24125.45	Temperature (degree C)	25.000



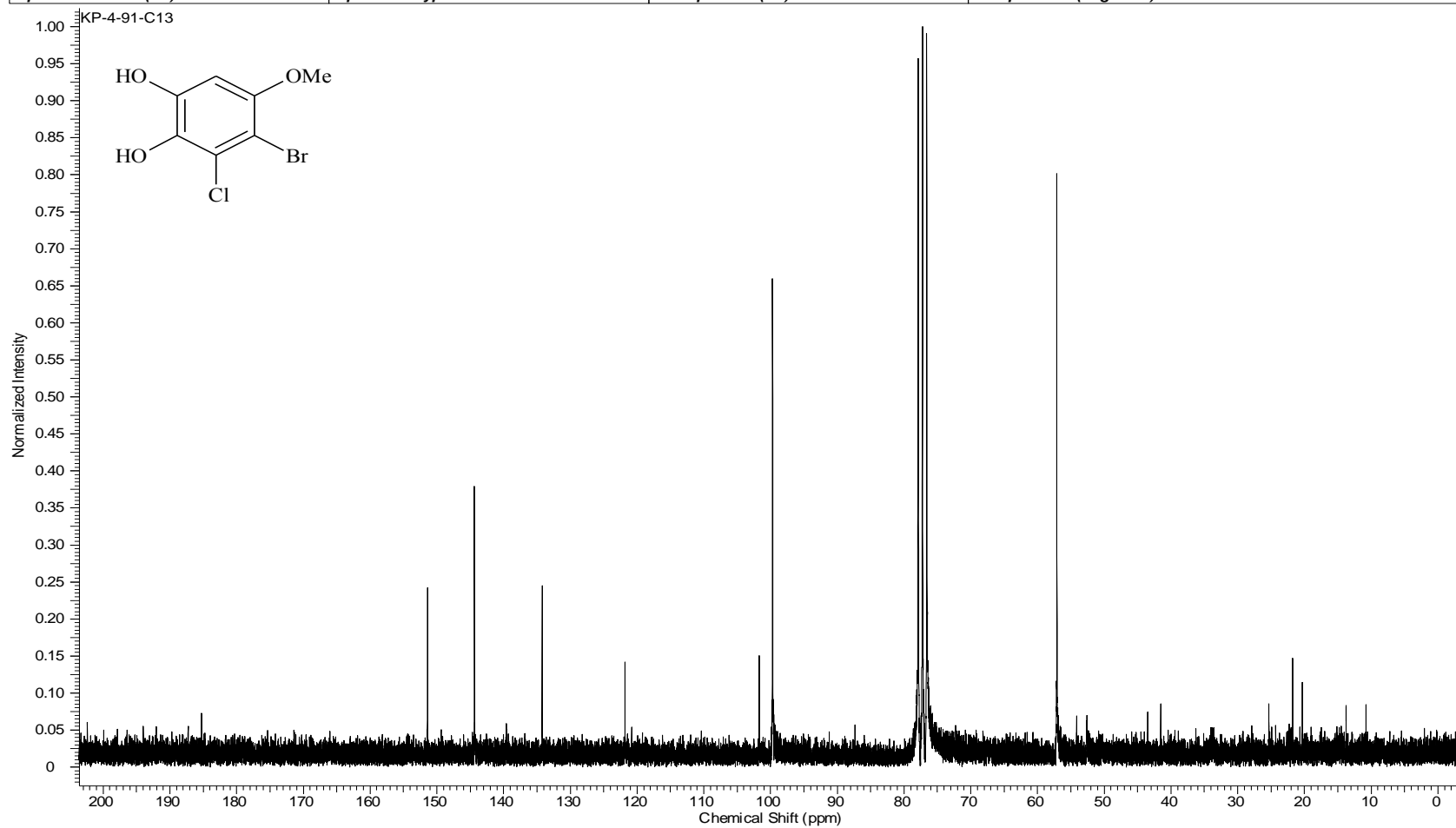
Compound 4 ¹H NMR

Acquisition Time (sec)	1.9945	Comment	STANDARD 1H OBSERVE		Date	May 14 2009	
Date Stamp	May 14 2009	File Name	C:\USERS\KESHAR\DESKTOP\NMR\BOOK 4\KP-4-91-DPPURE.FID\FID				
Frequency (MHz)	199.98	Nucleus	1H	Number of Transients	36	Original Points Count	5984
Points Count	8192	Pulse Sequence	s2pul	Receiver Gain	40.00	Solvent	CHLOROFORM-d
Spectrum Offset (Hz)	1002.0226	Spectrum Type	STANDARD	Sweep Width (Hz)	3000.30	Temperature (degree C)	AMBIENT TEMPERATURE

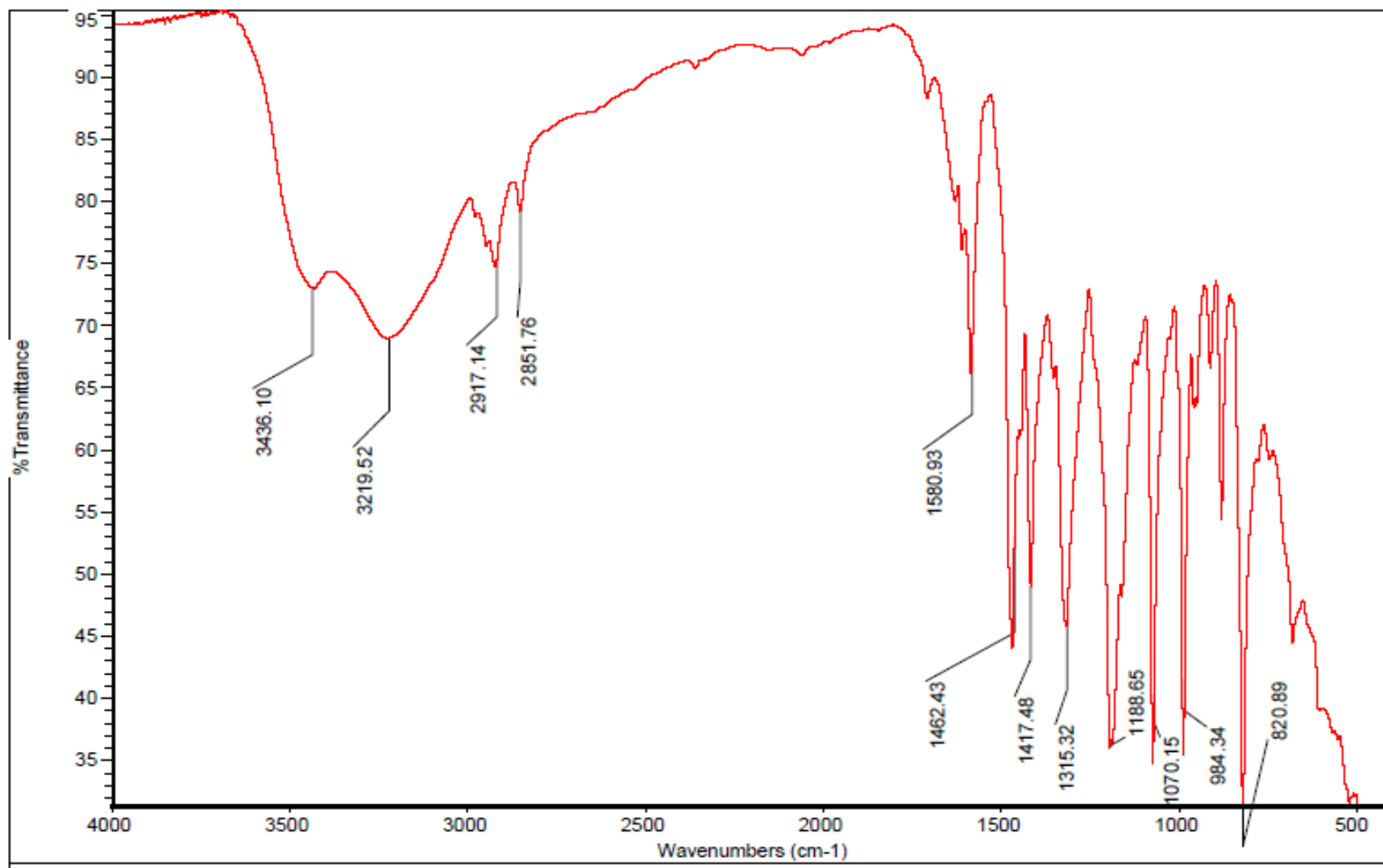


Compound 4 ¹³C NMR

Acquisition Time (sec)	1.4976	Comment	13C OBSERVE	Date	Oct 22 2009	Date Stamp	Oct 22 2009
File Name	C:\USERS\KESHAR\DESKTOP\NMR\LACCASE\KP-4-91-C13\FID			Frequency (MHz)	50.29		
Nucleus	13C	Number of Transients	17867	Original Points Count	18720	Points Count	32768
Pulse Sequence	s2pul	Receiver Gain	40.00	Solvent	CHLOROFORM-d		
Spectrum Offset (Hz)	4880.8467	Spectrum Type	STANDARD	Sweep Width (Hz)	12500.00	Temperature (degree C) AMBIENT TEMPERATURE	

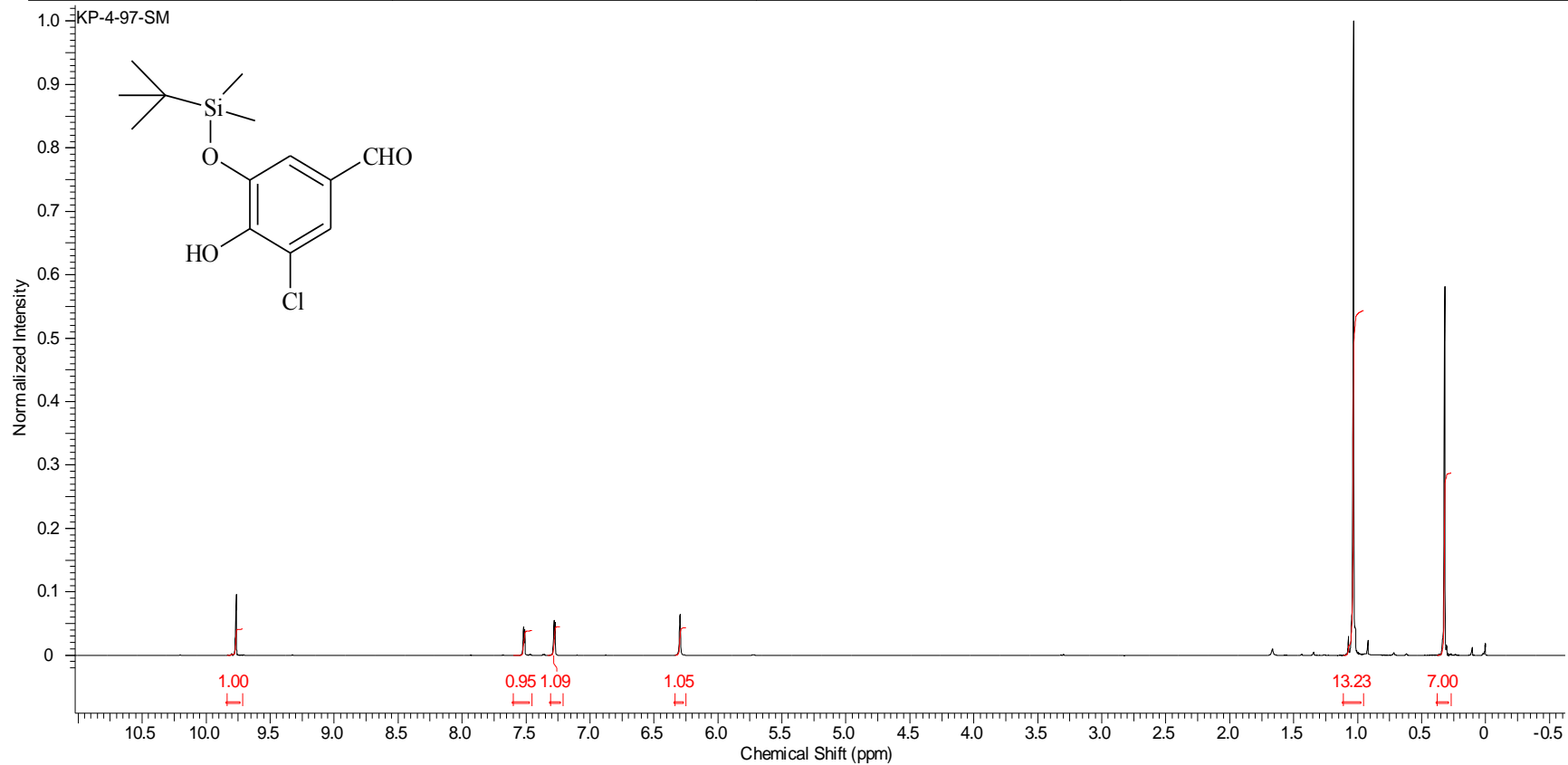


Compound 4 IR



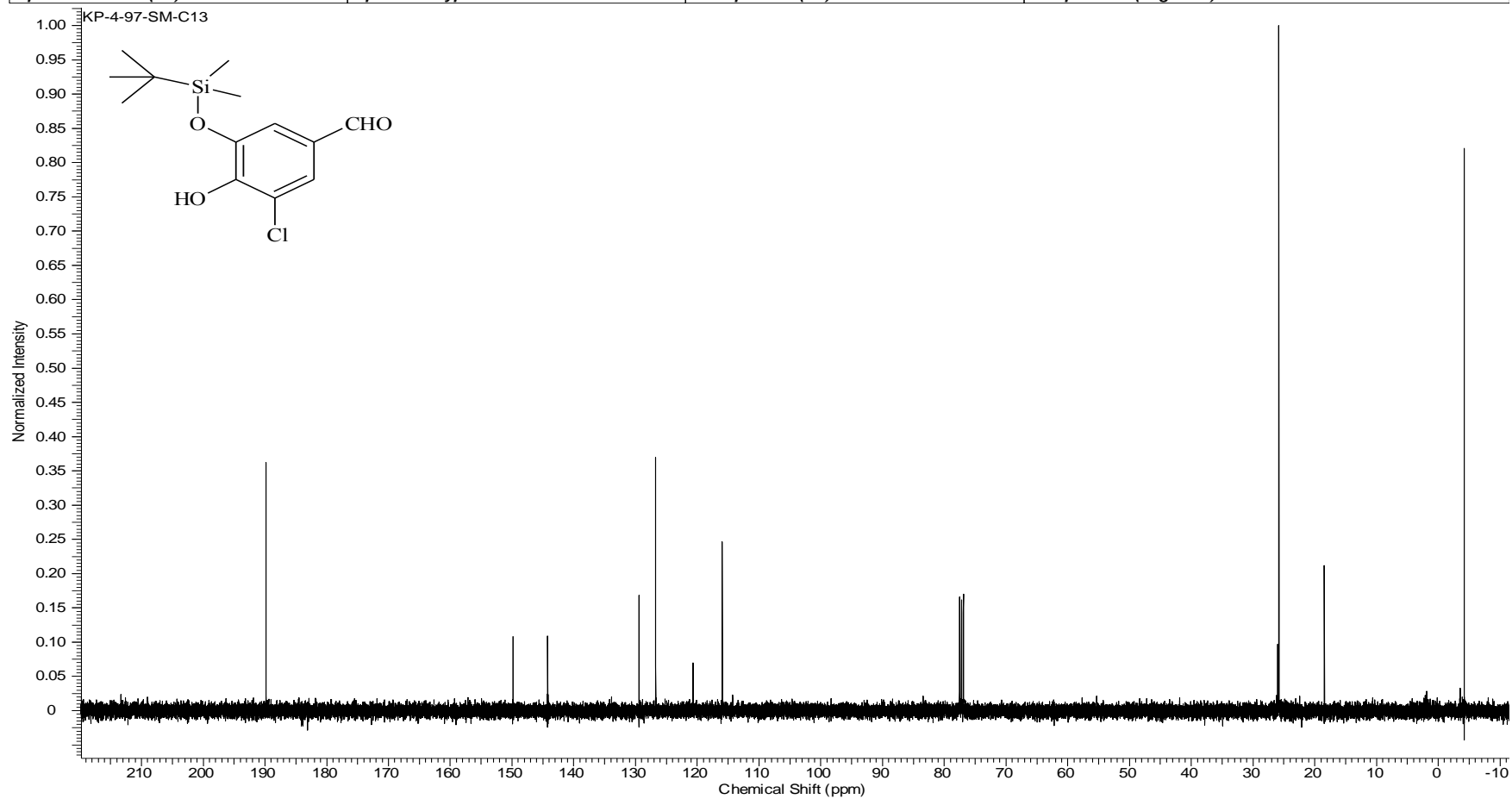
Compound 31 ¹H NMR

Acquisition Time (sec)	1.9945	Comment	STANDARD 1H OBSERVE		Date	Aug 4 2009	
Date Stamp	Aug 4 2009	File Name	C:\USERS\KESHAR\DOCUMENTS\PHD THESIS SUPPORT JUNE 28\NMR\LACCASE\KP-4-97-SM\FID				
Frequency (MHz)	199.98	Nucleus	1H	Number of Transients	64	Original Points Count	5984
Points Count	8192	Pulse Sequence	s2pul	Receiver Gain	18.00	Solvent	CHLOROFORM-d
Spectrum Offset (Hz)	1003.0914	Spectrum Type	STANDARD	Sweep Width (Hz)	3000.30	Temperature (degree C)	AMBIENT TEMPERATURE



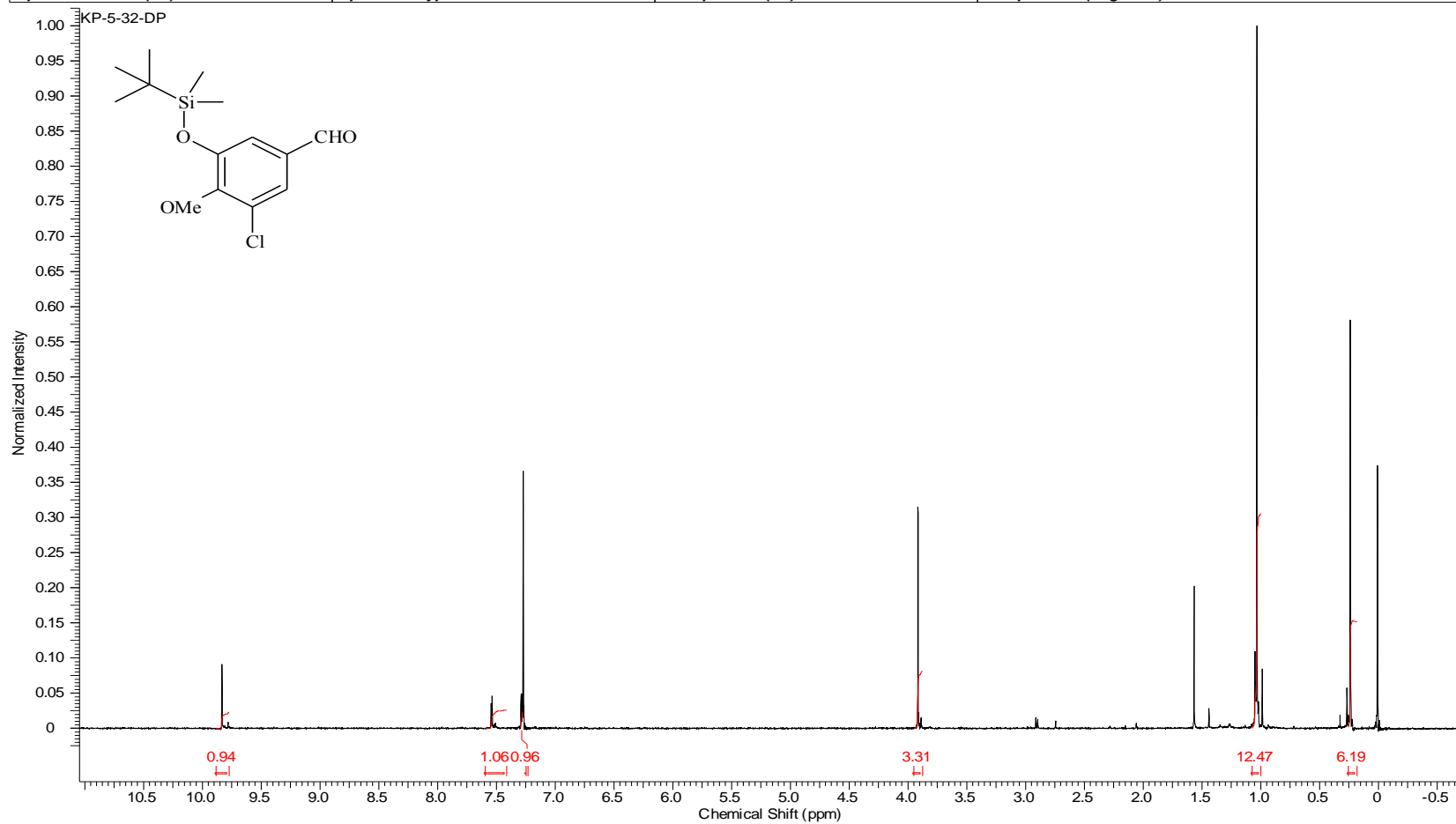
Compound 31 ¹³C NMR

Acquisition Time (sec)	1.3005	Comment	Std proton	Date	Aug 17 2009	Date Stamp	Aug 17 2009
File Name	C:\USERS\SKESHAR\DOCUMENTS\PHD THESIS SUPPORT JUNE 28\NMR\LACCASE\KP-4-97-SM-C13\FID						
Frequency (MHz)	100.53	Nucleus	13C	Number of Transients	640	Original Points Count	31375
Points Count	32768	Pulse Sequence	s2pul	Receiver Gain	30.00	Solvent	CHLOROFORM-d
Spectrum Offset (Hz)	10554.5117	Spectrum Type	STANDARD	Sweep Width (Hz)	24125.45	Temperature (degree C)	25.000



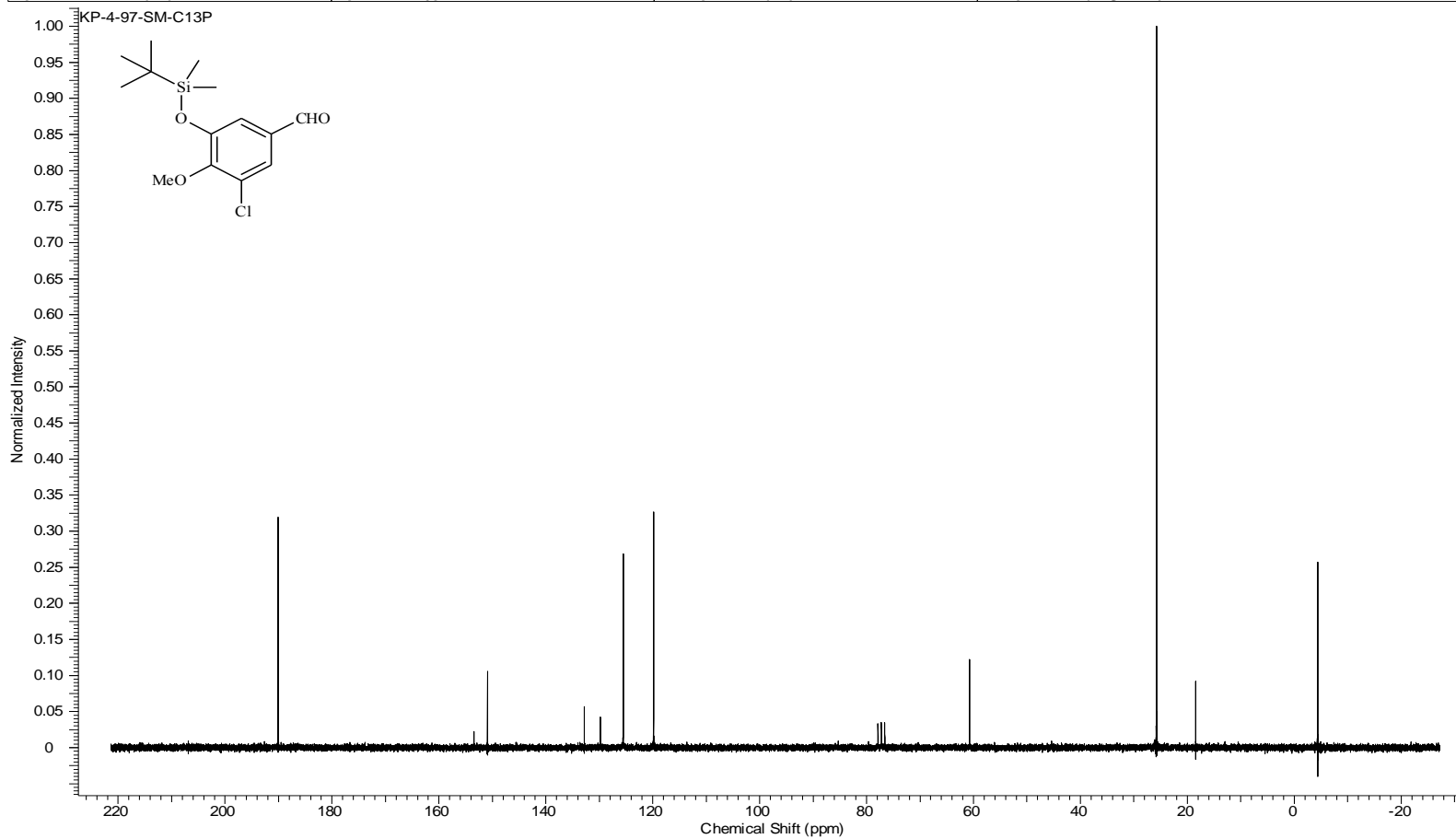
Compound 32 ¹H NMR

Acquisition Time (sec)	1.9945	Comment	STANDARD 1H OBSERVE		Date	Sep 18 2009	
Date Stamp	Sep 18 2009	File Name	C:\USERS\KESHAR\DESKTOP\NMR\BOOK 5\KP-5-32-DP.FID\FID				
Frequency (MHz)	199.98	Nucleus	1H	Number of Transients	44	Original Points Count	5984
Points Count	8192	Pulse Sequence	s2pul	Receiver Gain	40.00	Solvent	CHLOROFORM-d
Spectrum Offset (Hz)	1002.3889	Spectrum Type	STANDARD	Sweep Width (Hz)	3000.30	Temperature (degree C)	AMBIENT TEMPERATURE



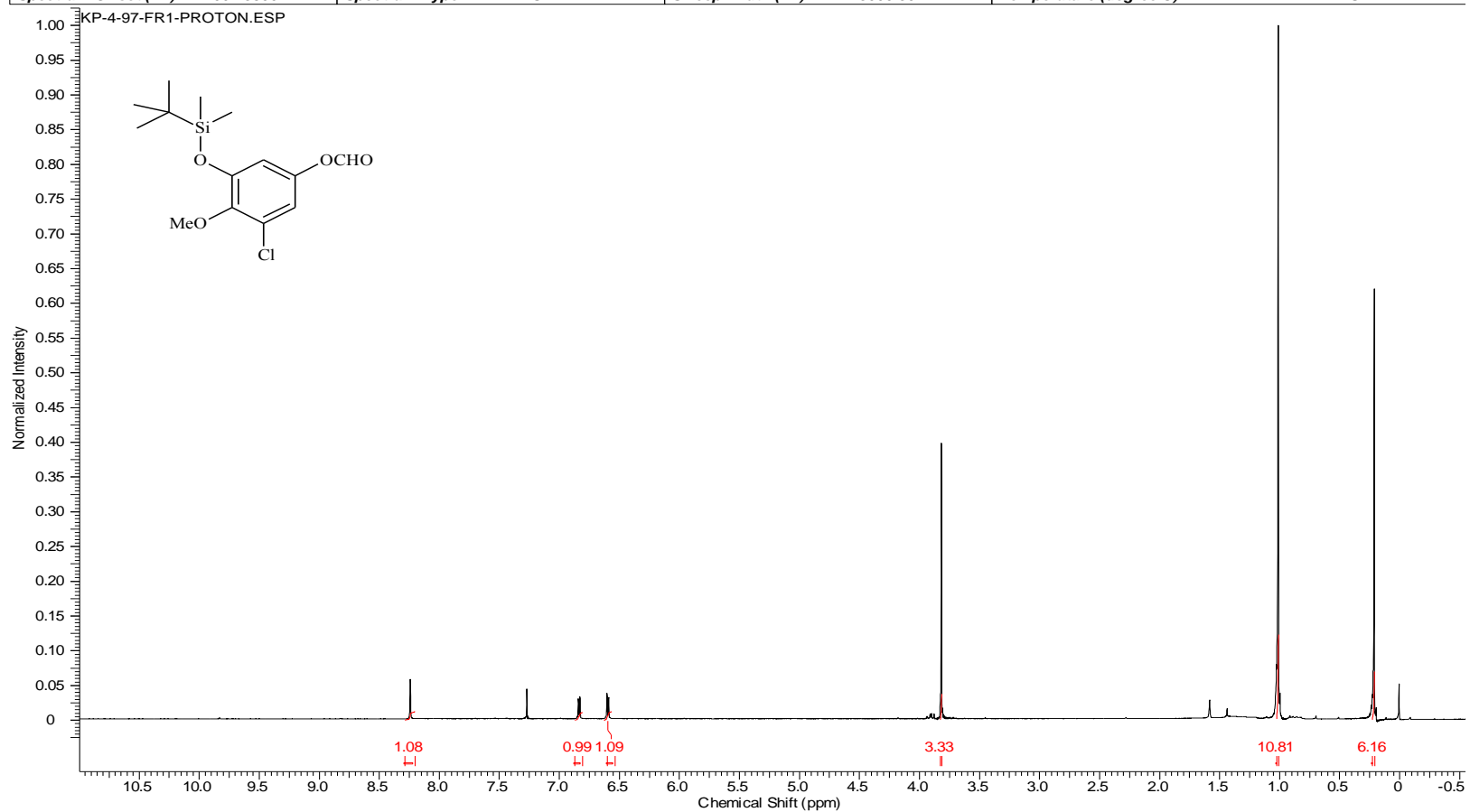
Compound 32 ¹³C NMR

Acquisition Time (sec)	1.4976	Comment	13C OBSERVE	Date	Aug 17 2009	Date Stamp	Aug 17 2009
File Name	C:\USERS\KESHAR\DESKTOP\NMR\LACCASE\KP-4-97-SM-C13P\FID			Frequency (MHz)	50.29		
Nucleus	13C	Number of Transients	752	Original Points Count	18720	Points Count	32768
Pulse Sequence	s2pul	Receiver Gain	40.00	Solvent	CHLOROFORM-d		
Spectrum Offset (Hz)	4880.0840	Spectrum Type	STANDARD	Sweep Width (Hz)	12500.00	Temperature (degree C) AMBIENT TEMPERATURE	



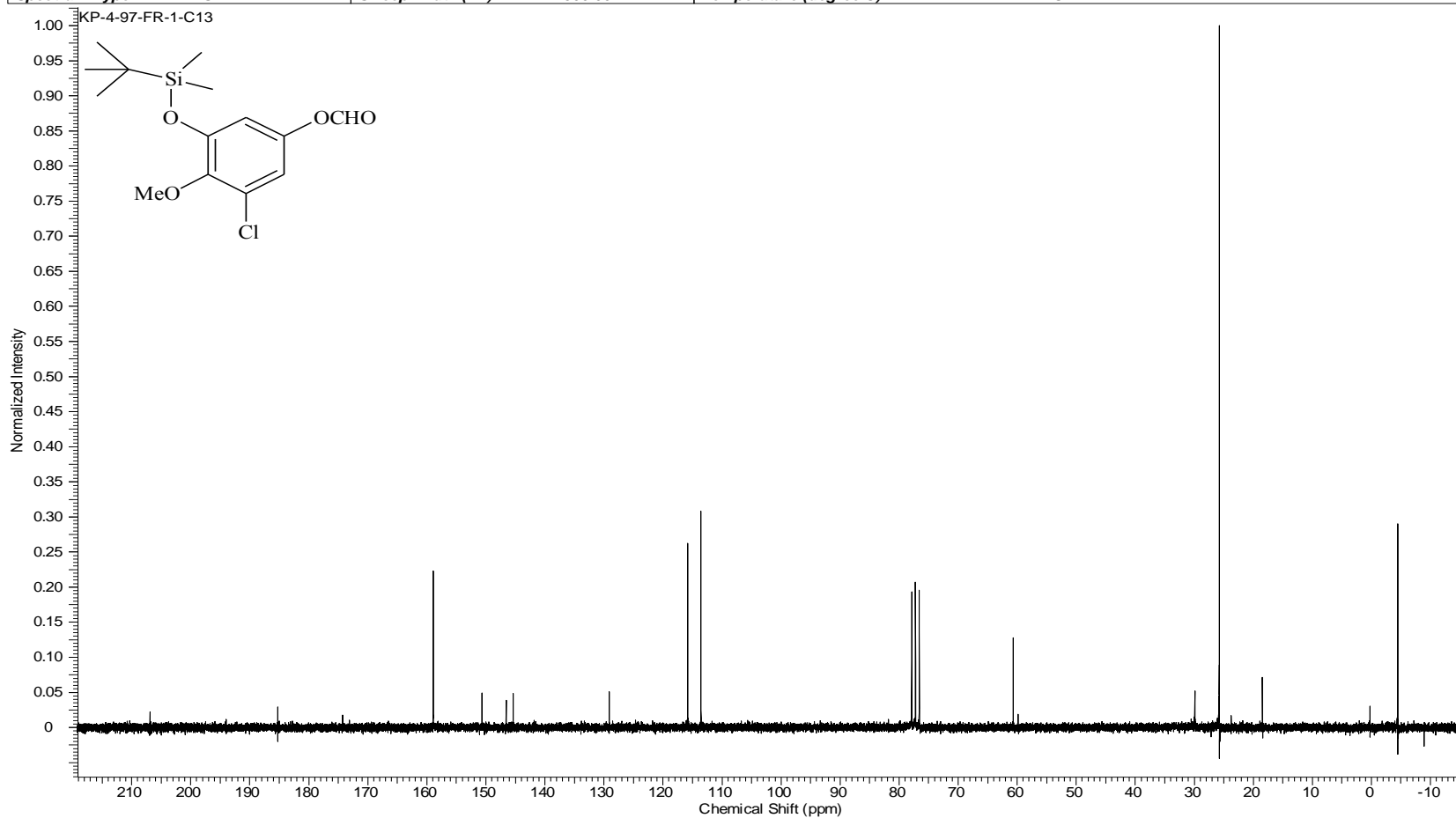
Compound 33 ¹H NMR

Acquisition Time (sec)	1.9945	Comment	STANDARD 1H OBSERVE		Date	Aug 27 2007	
Date Stamp	Aug 27 2007	File Name	C:\USERS\KESHAR\KP-4-97-Fr1-Proton				
Frequency (MHz)	199.98	Nucleus	1H	Number of Transients	64	Original Points Count	5984
Points Count	8192	Pulse Sequence	s2pul	Receiver Gain	28.00	Solvent	CHLOROFORM-d
Spectrum Offset (Hz)	1002.3890	Spectrum Type	STANDARD	Sweep Width (Hz)	3000.30	Temperature (degree C)	AMBIENT TEMPERATURE



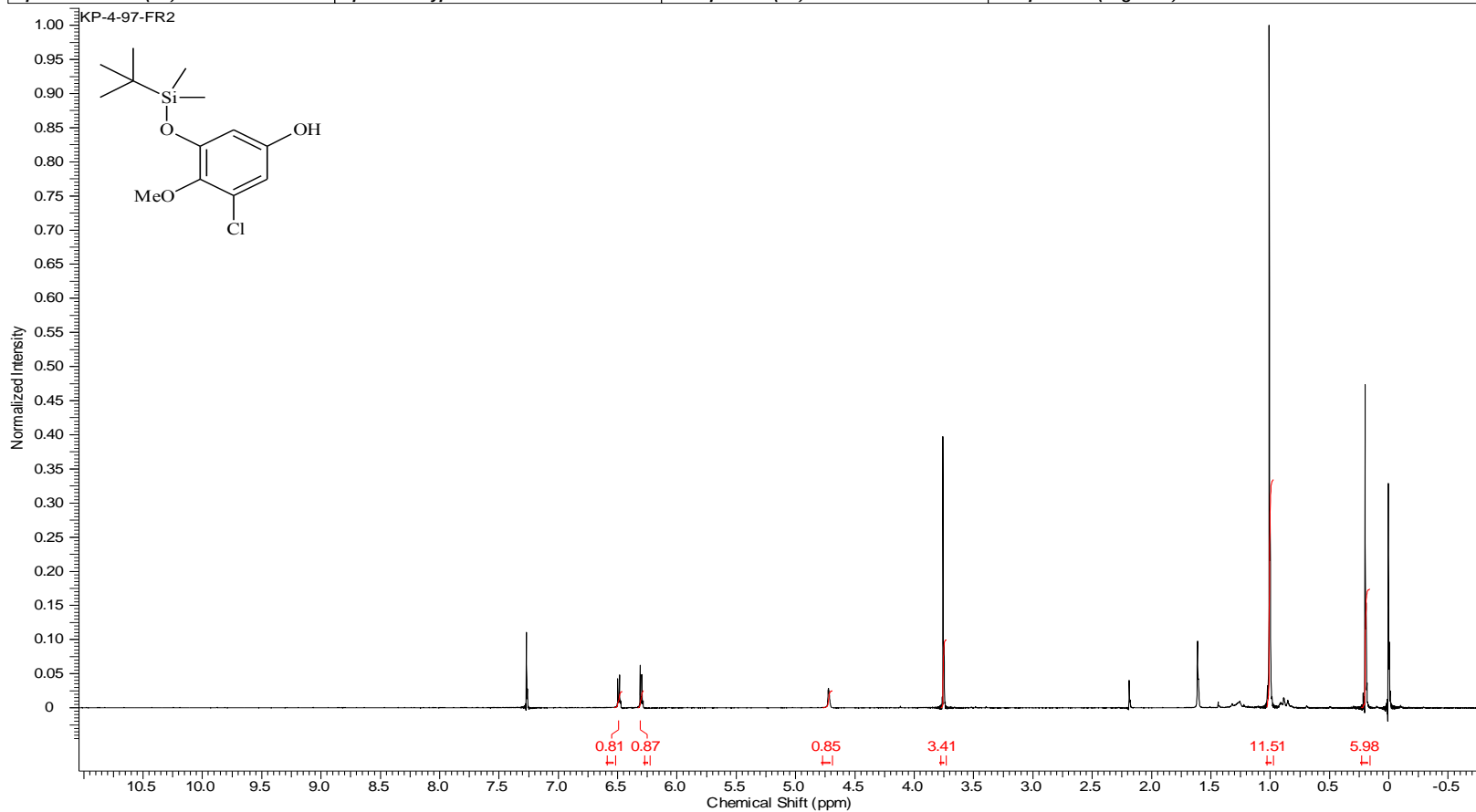
Compound 33 ¹³C NMR

Acquisition Time (sec)	1.4976	Comment	13C OBSERVE	Date	Sep 1 2009	Date Stamp	Sep 1 2009
File Name	C:\USERS\KESHAR\DOCUMENTS\PHD THESIS SUPPORT JUNE 28\NMR\LACCASE\KP-4-97-FR-1-C13\FID			Frequency (MHz)	50.29		
Nucleus	13C	Number of Transients	12208	Original Points Count	18720	Points Count	32768
Pulse Sequence	s2pul	Receiver Gain	40.00	Solvent	CHLOROFORM-d	Spectrum Offset (Hz)	4881.2285
Spectrum Type	STANDARD	Sweep Width (Hz)	12500.00	Temperature (degree C)	AMBIENT TEMPERATURE		



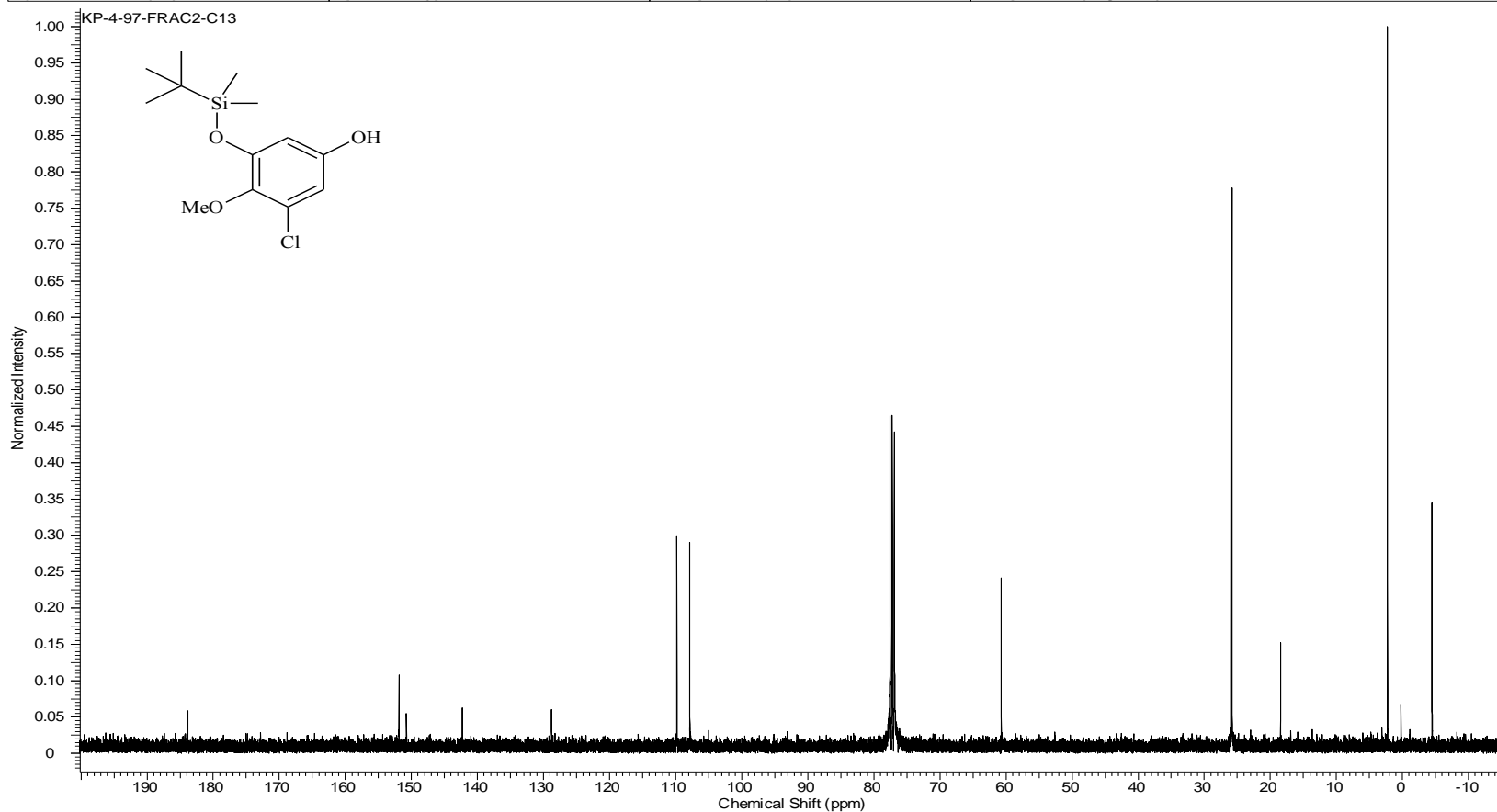
Compound 34 ¹H NMR

Acquisition Time (sec)	1.9945	Comment	STANDARD 1H OBSERVE		Date	Aug 27 2009	
Date Stamp	Aug 27 2009	File Name	C:\USERS\KESHAR\DESKTOP\NMR\LACCASE\KP-4-97-FR2\FID				
Frequency (MHz)	199.98	Nucleus	1H	Number of Transients	64	Original Points Count	5984
Points Count	8192	Pulse Sequence	s2pul	Receiver Gain	34.00	Solvent	CHLOROFORM-d
Spectrum Offset (Hz)	1001.6563	Spectrum Type	STANDARD	Sweep Width (Hz)	3000.30	Temperature (degree C)	AMBIENT TEMPERATURE



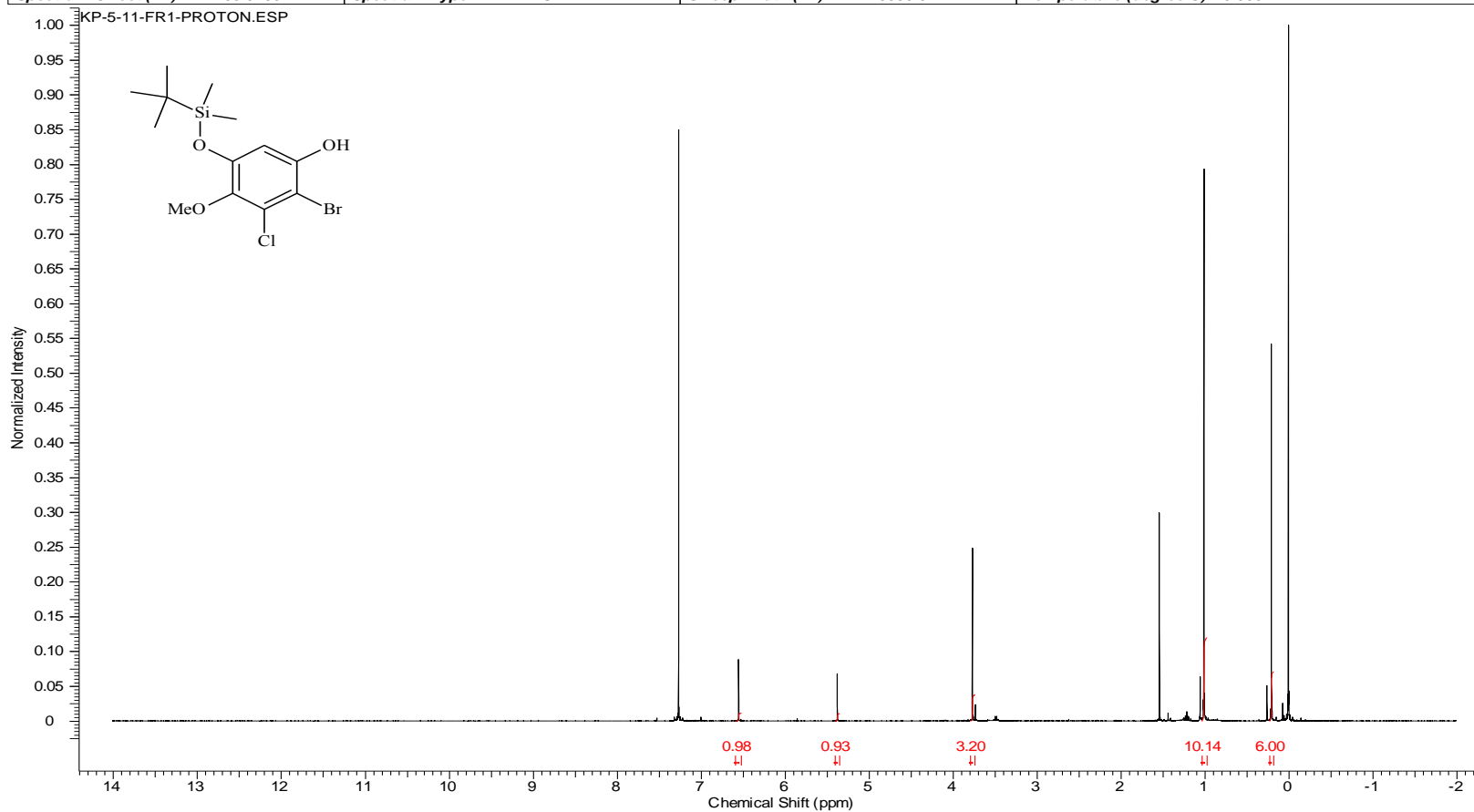
Compound 34 ¹³C NMR

Acquisition Time (sec)	1.3005	Comment	Std proton	Date	Aug 29 2009	Date Stamp	Aug 29 2009
File Name	C:\USERS\KESHAR\DESKTOP\NMR\LACCASE\KP-4-97-FRAC2-C13\FID			Frequency (MHz)	100.53		
Nucleus	13C	Number of Transients	1856	Original Points Count	31375	Points Count	32768
Pulse Sequence	s2pul	Receiver Gain	30.00	Solvent	CHLOROFORM-d		
Spectrum Offset (Hz)	10557.2520	Spectrum Type	STANDARD	Sweep Width (Hz)	24125.45	Temperature (degree C)	25.000



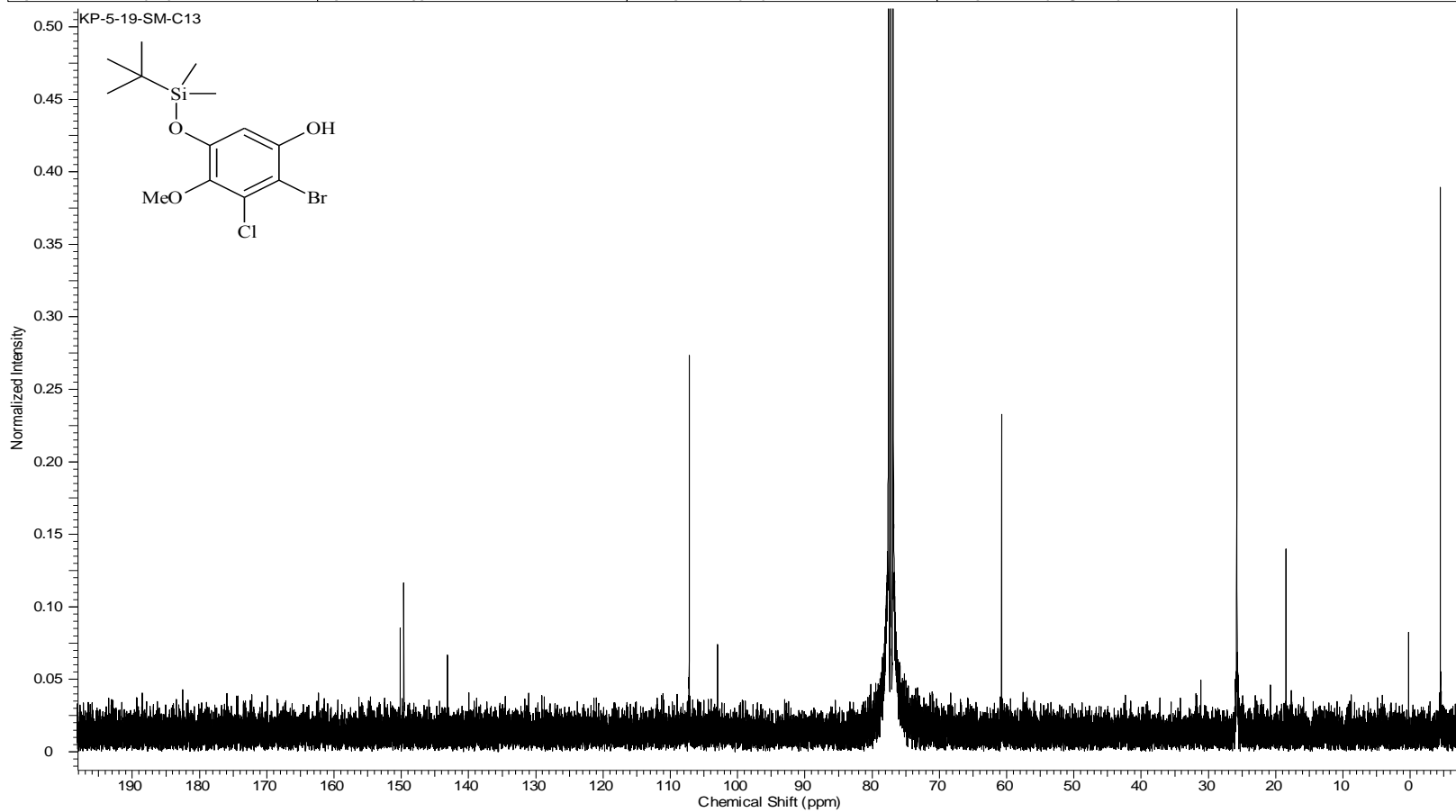
Compound 35 ¹H NMR

Acquisition Time (sec)	2.0487	Comment	Std proton	Date	Aug 26 2009	Date Stamp	Aug 26 2009
File Name	C:\USERS\KESHAR\KP-5-11-FR1-Proton						
Frequency (MHz)	399.75	Nucleus	1H	Number of Transients	44	Original Points Count	13103
Points Count	16384	Pulse Sequence	s2pul	Receiver Gain	60.00	Solvent	CHLOROFORM-d
Spectrum Offset (Hz)	2403.9280	Spectrum Type	STANDARD	Sweep Width (Hz)	6395.91	Temperature (degree C)	25.000



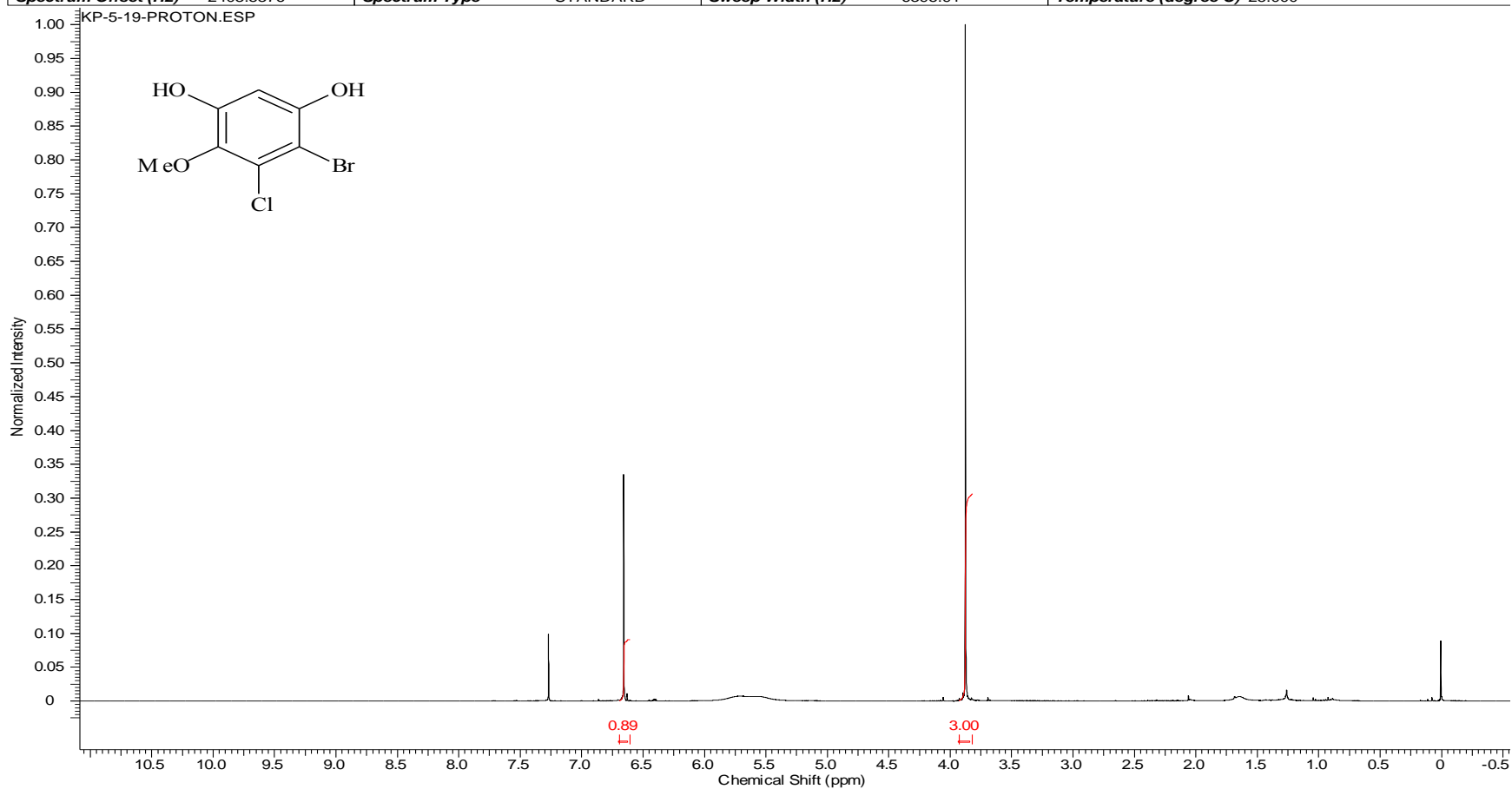
Compound 35 ¹³C NMR

Acquisition Time (sec)	1.3005	Comment	Std proton	Date	Sep 4 2009	Date Stamp	Sep 4 2009
File Name	C:\USERS\KESHAR\DESKTOP\NMR\LACCASE\KP-5-19-SM-C13\FID				Frequency (MHz)	100.53	
Nucleus	13C	Number of Transients	15226	Original Points Count	31375	Points Count	32768
Pulse Sequence	s2pul	Receiver Gain	30.00	Solvent	CHLOROFORM-d		
Spectrum Offset (Hz)	10555.8564	Spectrum Type	STANDARD	Sweep Width (Hz)	24125.45	Temperature (degree C)	25.000



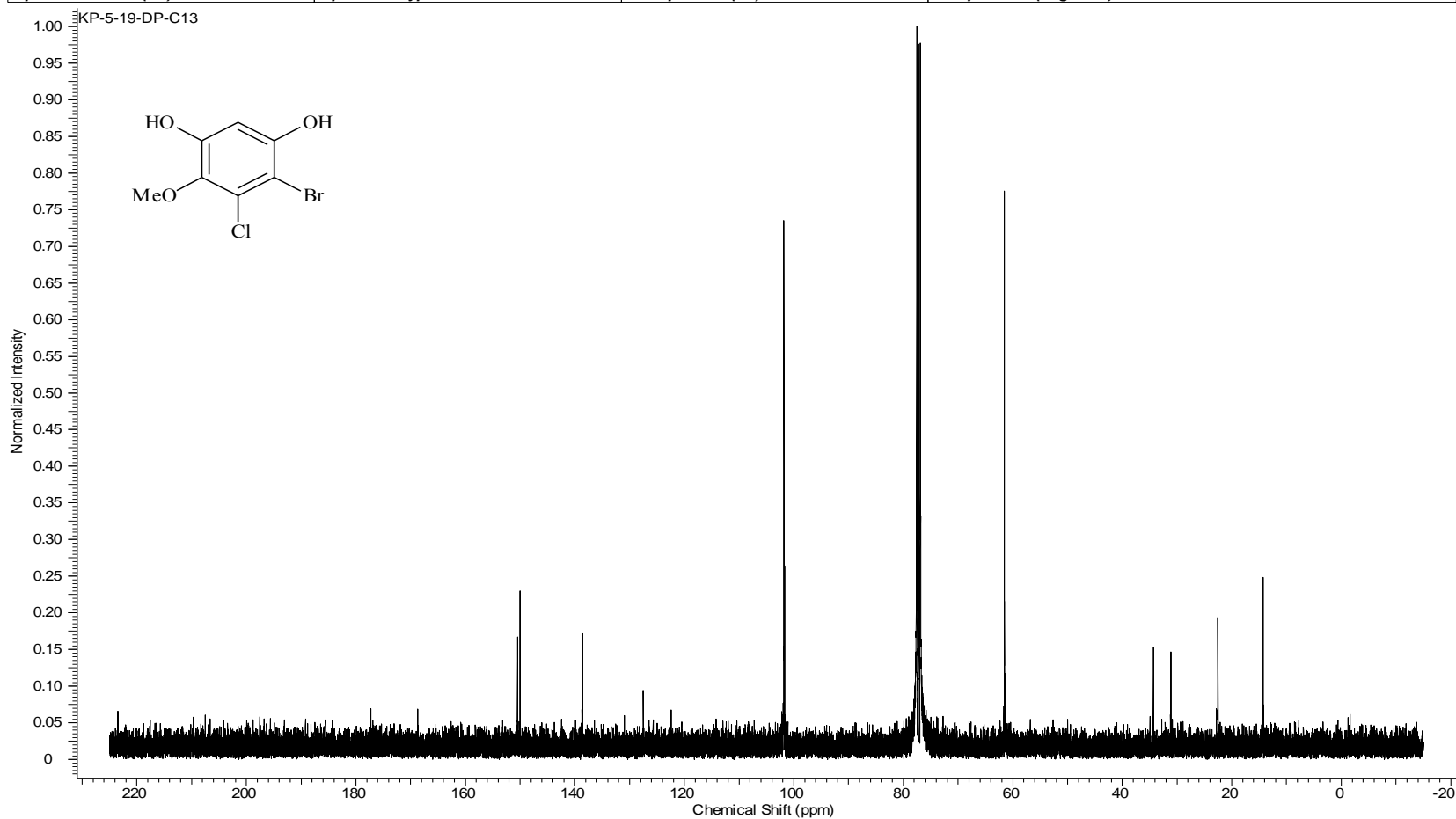
Compound 5 ¹H NMR

Acquisition Time (sec)	2.0487	Comment	Std proton	Date	Aug 27 2009	Date Stamp	Aug 27 2009
File Name	C:\USERS\KESHAR\KP-5-19-Proton						
Frequency (MHz)	399.75	Nucleus	1H	Number of Transients	20	Original Points Count	13103
Points Count	16384	Pulse Sequence	s2pul	Receiver Gain	42.00	Solvent	CHLOROFORM-d
Spectrum Offset (Hz)	2403.5376	Spectrum Type	STANDARD	Sweep Width (Hz)	6395.91	Temperature (degree C)	25.000

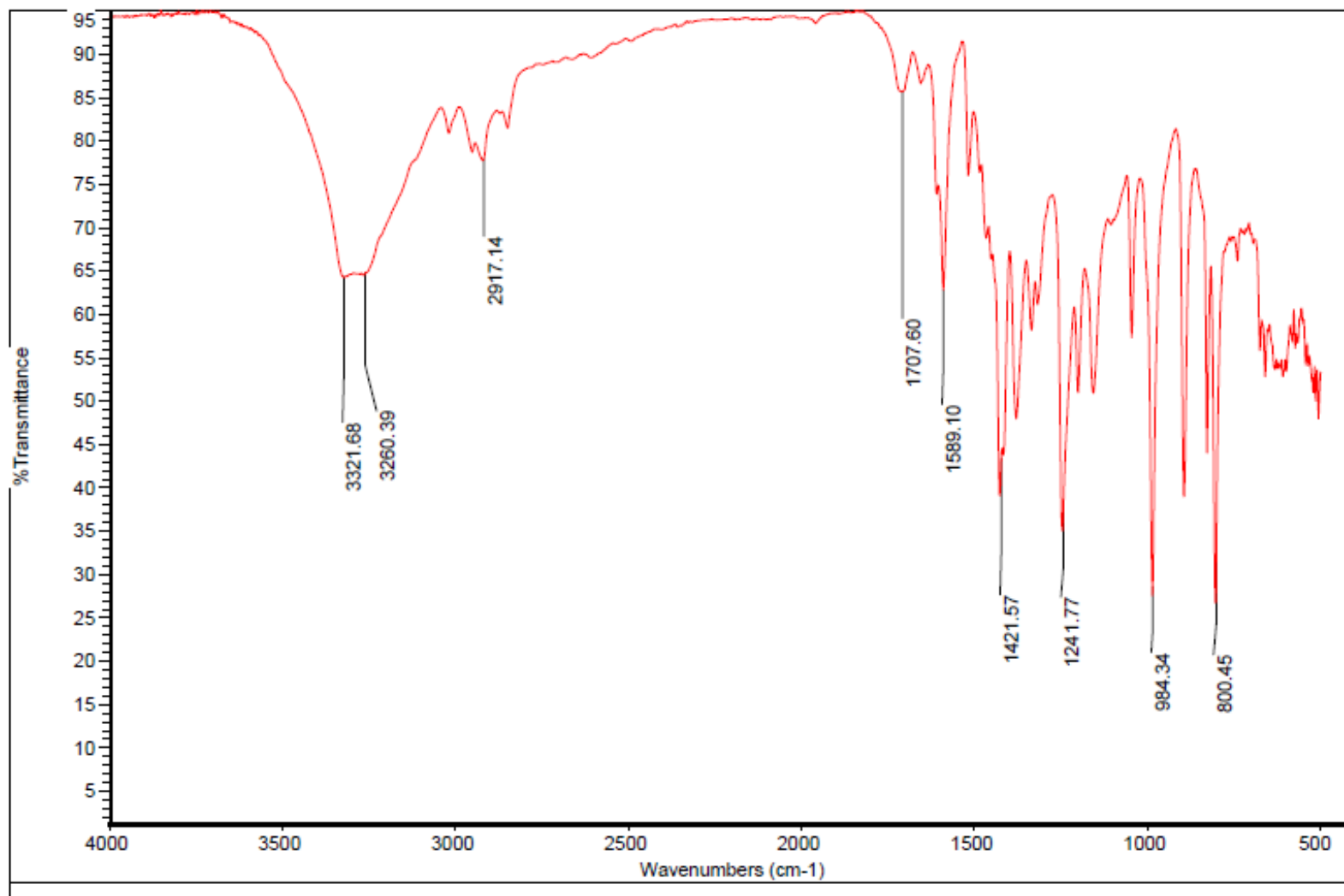


Compound 5 ¹³C NMR

Acquisition Time (sec)	1.3005	Comment	Std proton	Date	Oct 23 2009	Date Stamp	Oct 23 2009
File Name	C:\USERS\KESHAR\DESKTOP\NMR\LACCASE\KP-5-19-DP-C13\FID				Frequency (MHz)	100.53	
Nucleus	13C	Number of Transients	5696	Original Points Count	31375	Points Count	32768
Pulse Sequence	s2pul	Receiver Gain	30.00	Solvent	CHLOROFORM-d		
Spectrum Offset (Hz)	10554.3848	Spectrum Type	STANDARD	Sweep Width (Hz)	24125.45	Temperature (degree C)	25.000

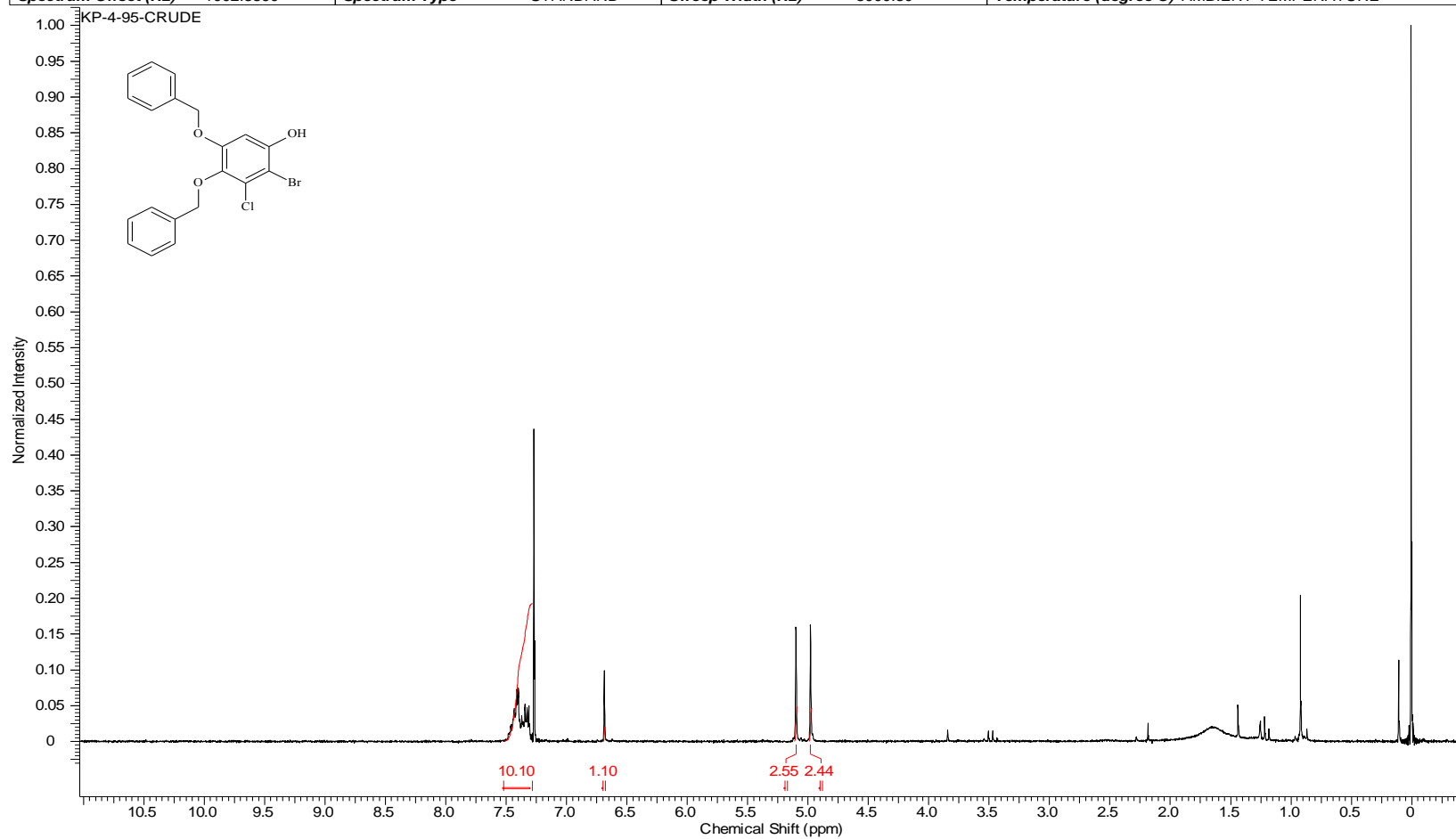


Compound 5 IR



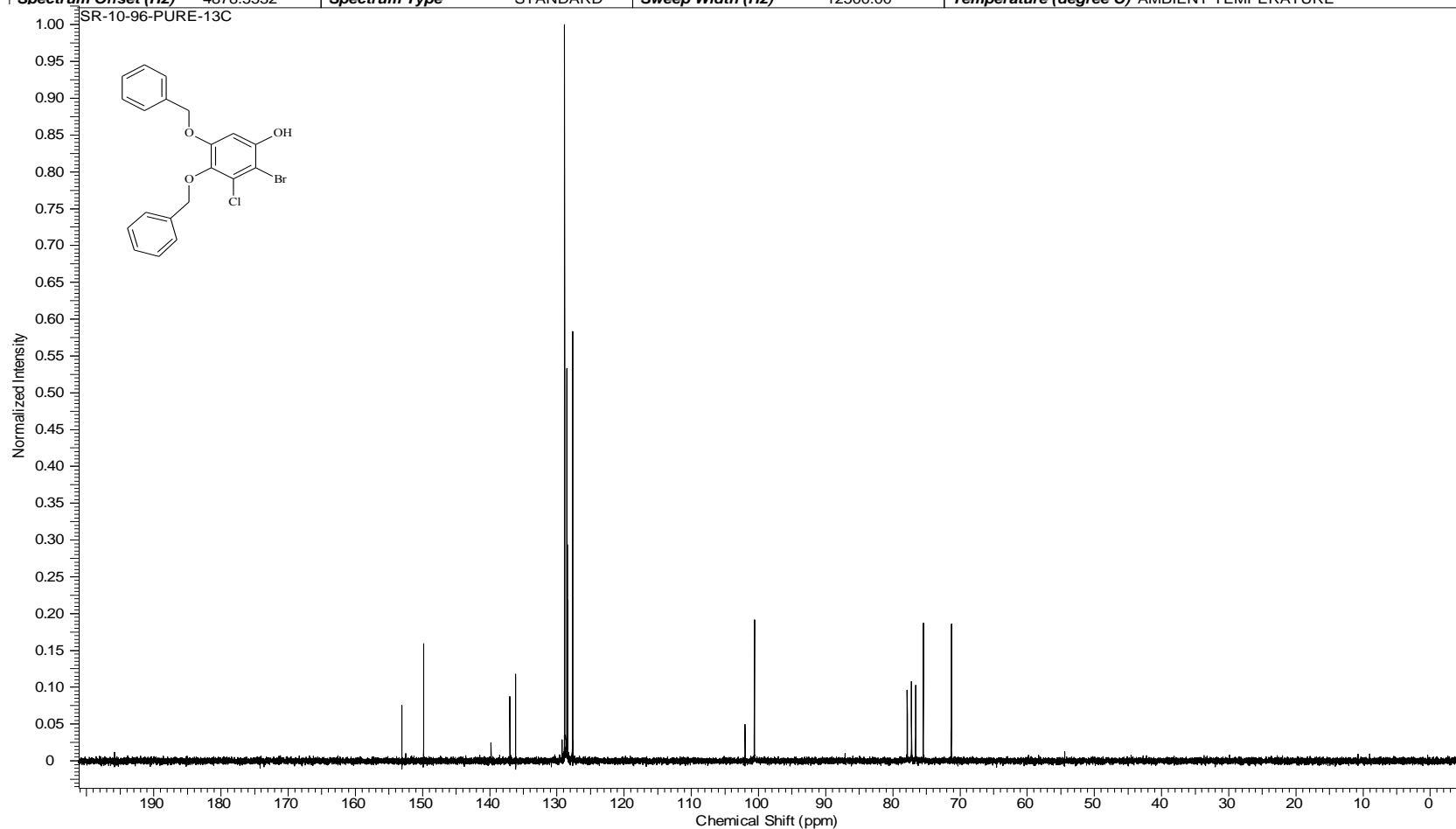
Compound 37 ¹H NMR

Acquisition Time (sec)	1.9945	Comment	STANDARD 1H OBSERVE		Date	May 19 2009	
Date Stamp	May 19 2009	File Name	C:\USERS\KESHAR\DESKTOP\NMR\BOOK 4\KP-4-95-CRUDE.FID\FID				
Frequency (MHz)	199.98	Nucleus	1H	Number of Transients	64	Original Points Count	5984
Points Count	8192	Pulse Sequence	s2pul	Receiver Gain	40.00	Solvent	CHLOROFORM-d
Spectrum Offset (Hz)	1002.3890	Spectrum Type	STANDARD	Sweep Width (Hz)	3000.30	Temperature (degree C)	AMBIENT TEMPERATURE



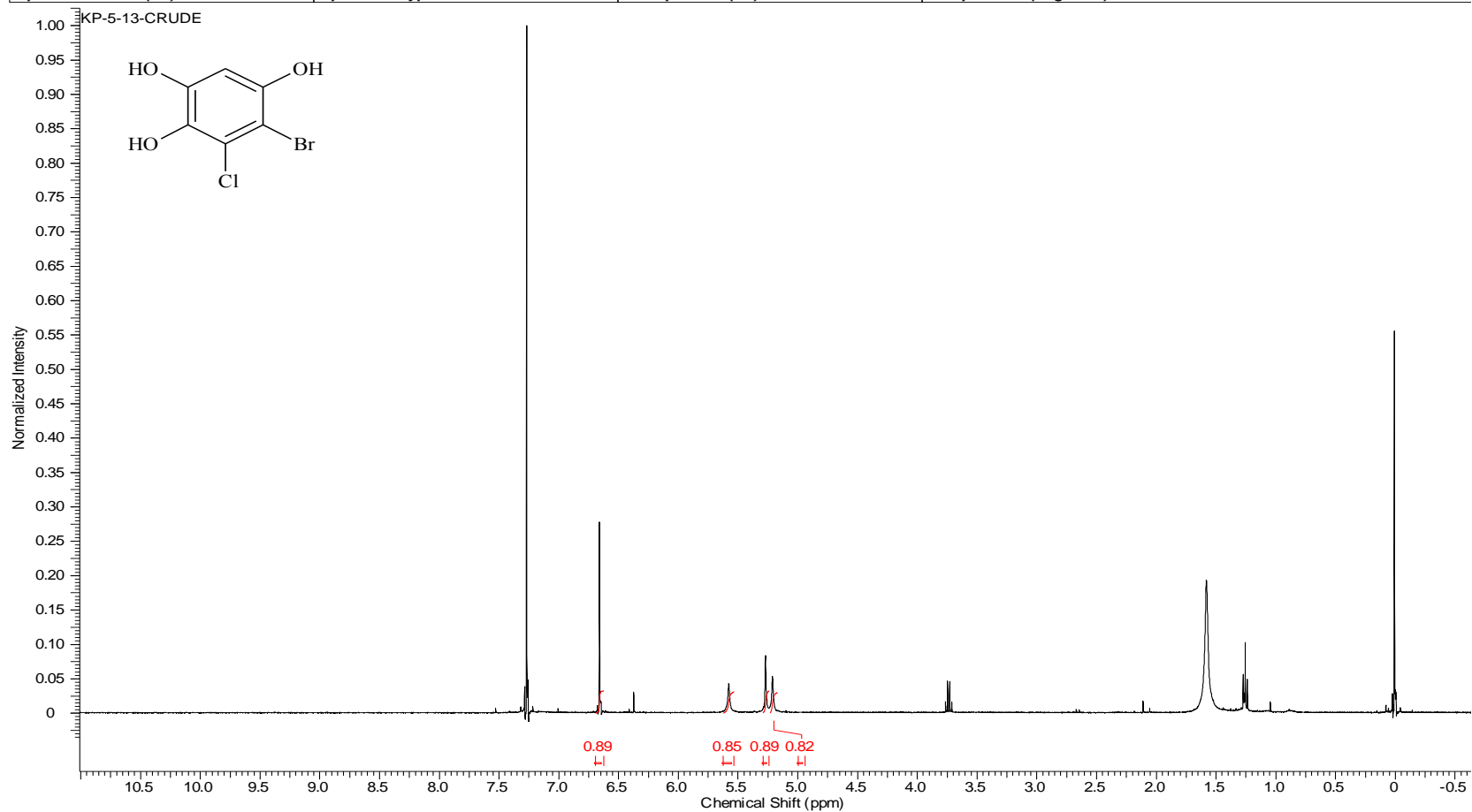
Compound 37 ¹³C NMR

Acquisition Time (sec)	1.4976	Comment	13C OBSERVE		Date	Jul 8 2009	
Date Stamp	Jul 8 2009	File Name	E:\KESHAR NMR REMAIN\SR-10-96-PURE-13C.FID\FID		Frequency (MHz)	50.29	
Nucleus	13C	Number of Transients	1872	Original Points Count	18720	Points Count	32768
Pulse Sequence	s2pul	Receiver Gain	40.00	Solvent	CHLOROFORM-d		
Spectrum Offset (Hz)	4878.5532	Spectrum Type	STANDARD	Sweep Width (Hz)	12500.00	Temperature (degree C)	AMBIENT TEMPERATURE



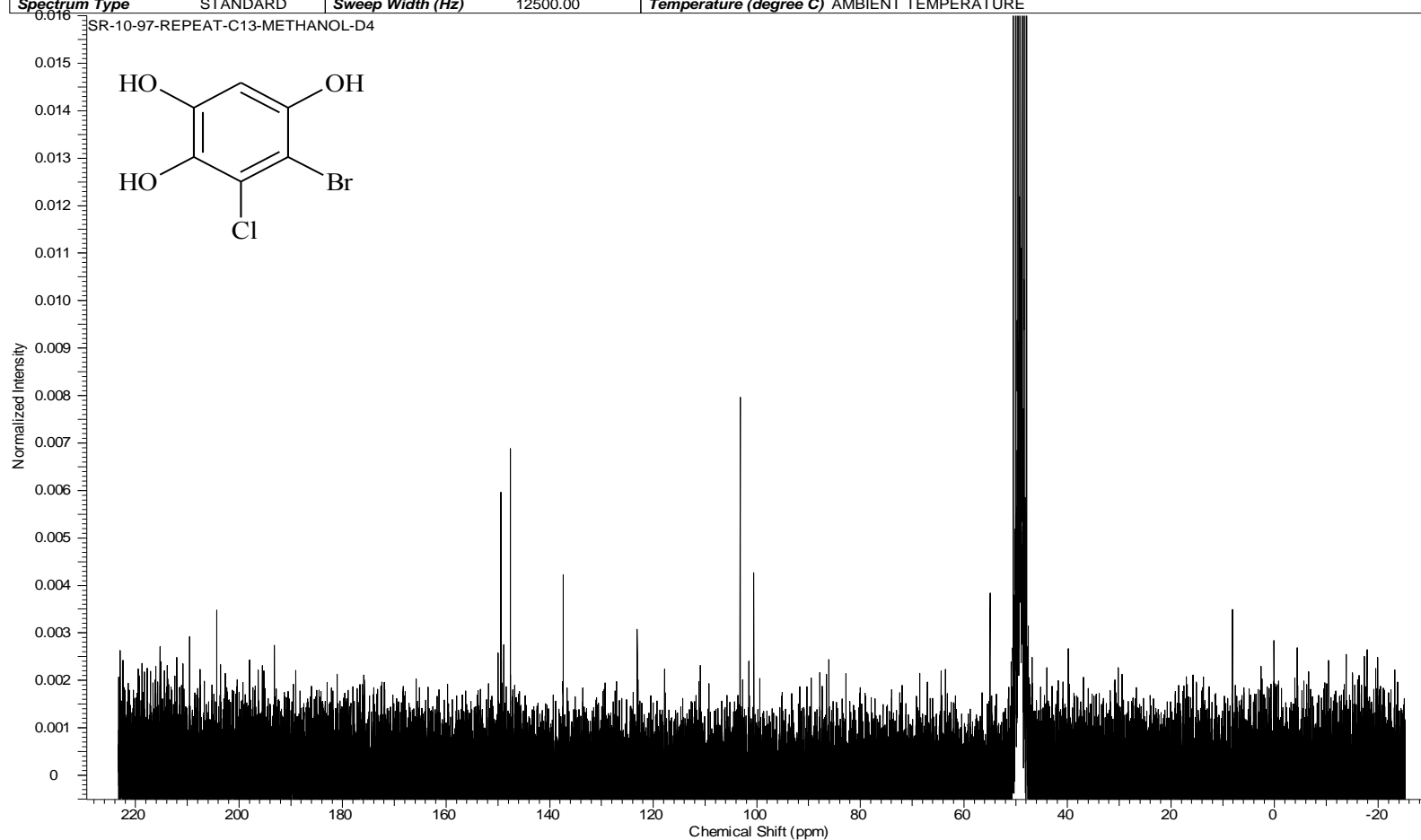
Compound 6 ¹H NMR

Acquisition Time (sec)	2.0487	Comment	Std proton	Date	Jul 7 2009	Date Stamp	Jul 7 2009
File Name	C:\USERS\KESHAR\DESKTOP\NMR\OTHERS\KP-5-13-CRUDE\FID			Frequency (MHz)	399.75		
Nucleus	1H	Number of Transients	4	Original Points Count	13103	Points Count	16384
Pulse Sequence	s2pul	Receiver Gain	46.00	Solvent	CHLOROFORM-d		
Spectrum Offset (Hz)	2403.9280	Spectrum Type	STANDARD	Sweep Width (Hz)	6395.91	Temperature (degree C)	25.000

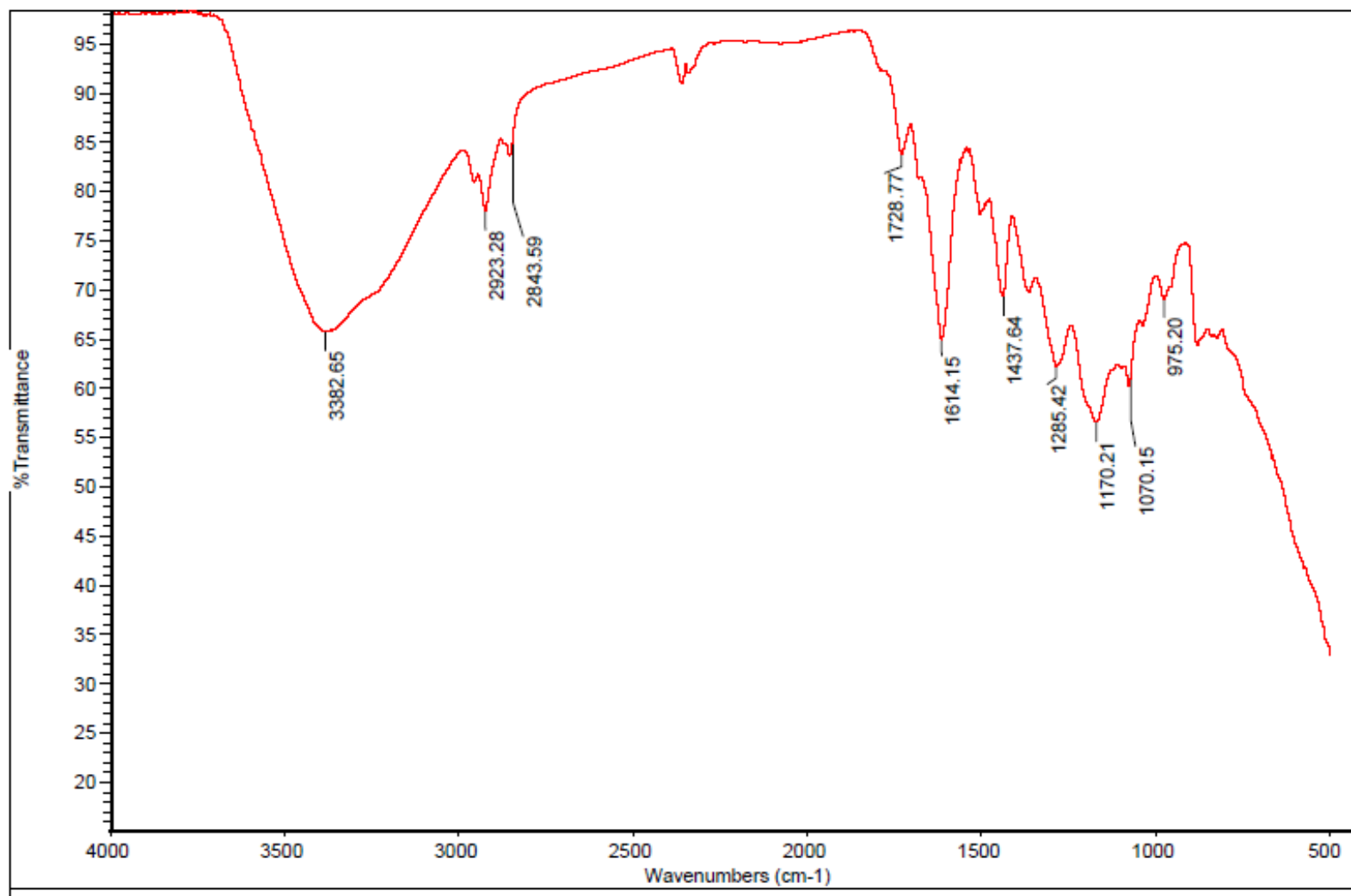


Compound 6 ¹³C NMR

Acquisition Time (sec)	1.4976	Comment	13C OBSERVE	Date	Jul 22 2009	Date Stamp	Jul 22 2009
File Name	E:\KESHAR NMR REMAIN\SR-10-97-REPEAT-C13-METHANOL-D4.FID\FID			Frequency (MHz)	50.29		
Nucleus	13C	Number of Transients	7048	Original Points Count	18720	Points Count	32768
Pulse Sequence	s2pul	Receiver Gain	40.00	Solvent	METHANOL-d4	Spectrum Offset (Hz)	4978.7695
Spectrum Type	STANDARD	Sweep Width (Hz)	12500.00	Temperature (degree C)	AMBIENT TEMPERATURE		

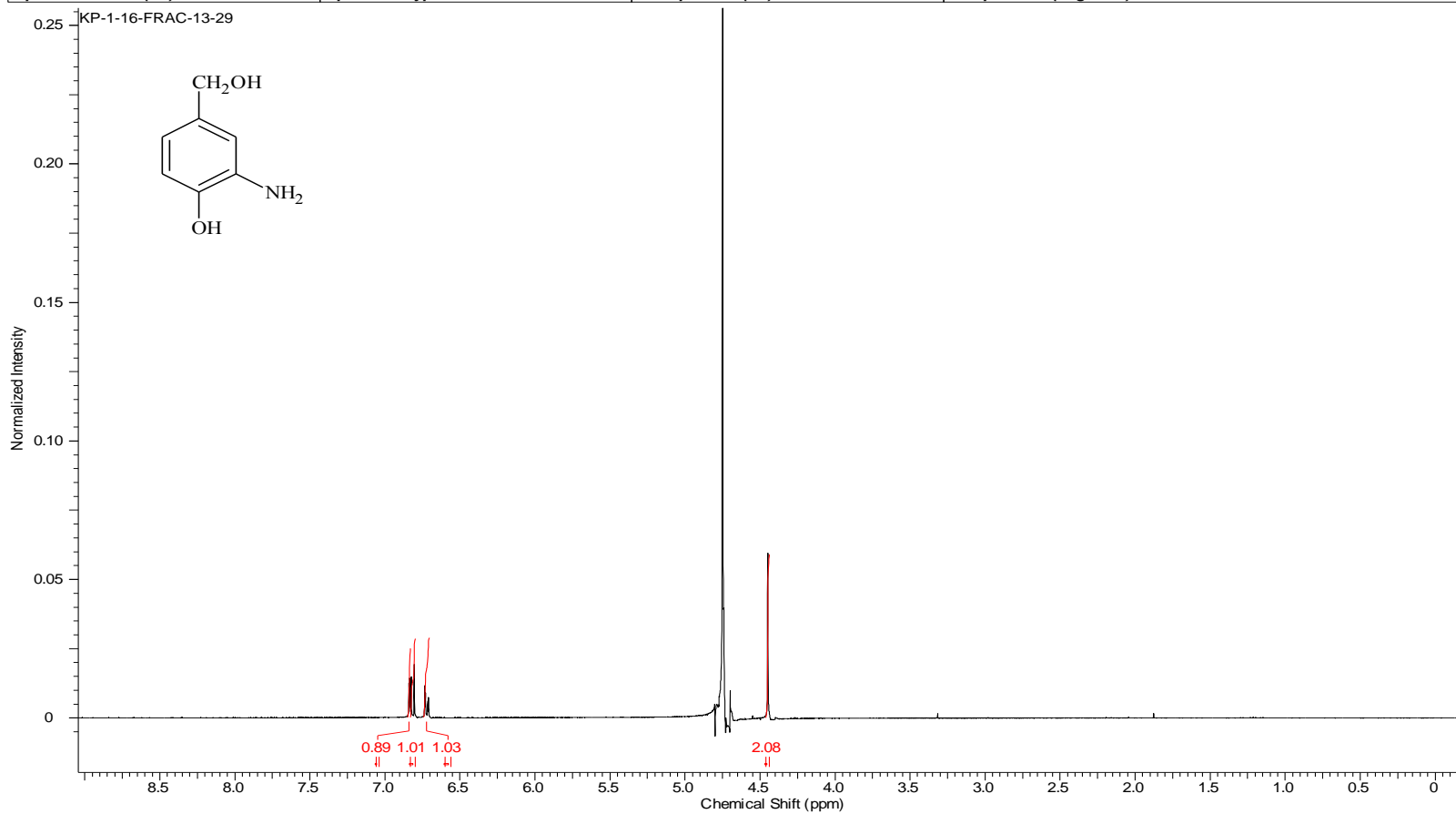


Compound 6 IR



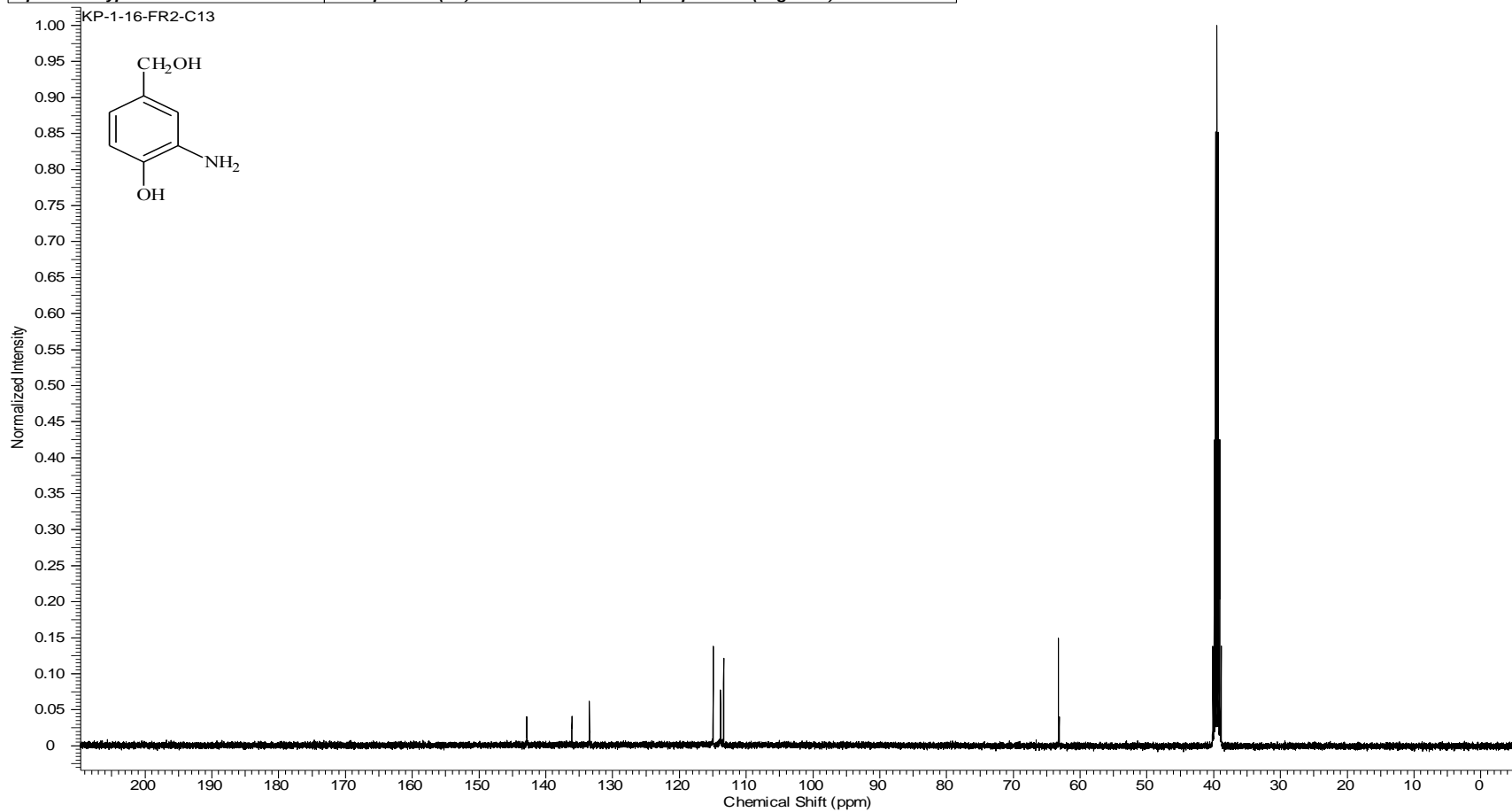
Compound 7 ¹H NMR

Acquisition Time (sec)	2.0487	Comment	Std proton	Date	Jun 2 2008	Date Stamp	Jun 2 2008
File Name	C:\USERS\KESHAR\DESKTOP\NMR\OTHERS\KP-1-16-FRAC-13-29.FID\FID			Frequency (MHz)	399.76		
Nucleus	1H	Number of Transients	32	Original Points Count	13103	Points Count	16384
Pulse Sequence	s2pul	Receiver Gain	50.00	Solvent	DEUTERIUM OXIDE		
Spectrum Offset (Hz)	2455.7793	Spectrum Type	STANDARD	Sweep Width (Hz)	6395.91	Temperature (degree C)	25.000

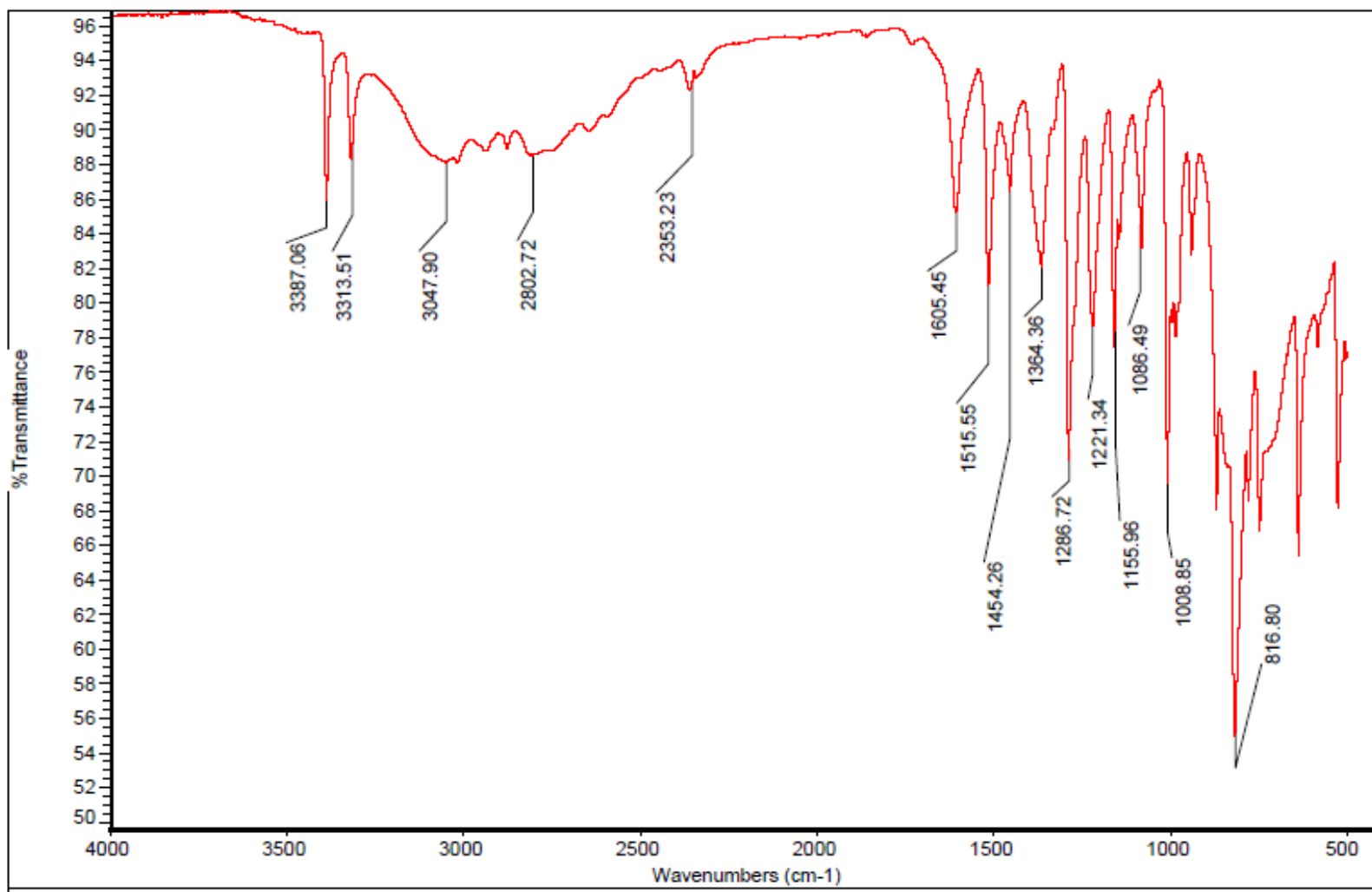


Compound 7 ¹³C NMR

Acquisition Time (sec)	1.3005	Comment	Std proton	Date	Jul 17 2009	Date Stamp	Jul 17 2009
File Name	C:\USERS\KESHAR\KP-1-16-FR2-C13\FID			Frequency (MHz)	100.53		
Nucleus	13C	Number of Transients	26396	Original Points Count	31375		
Pulse Sequence	s2pul	Receiver Gain	30.00	Solvent	DMSO-d6		
Spectrum Type	STANDARD	Sweep Width (Hz)	24125.45	Temperature (degree C)	25.000		

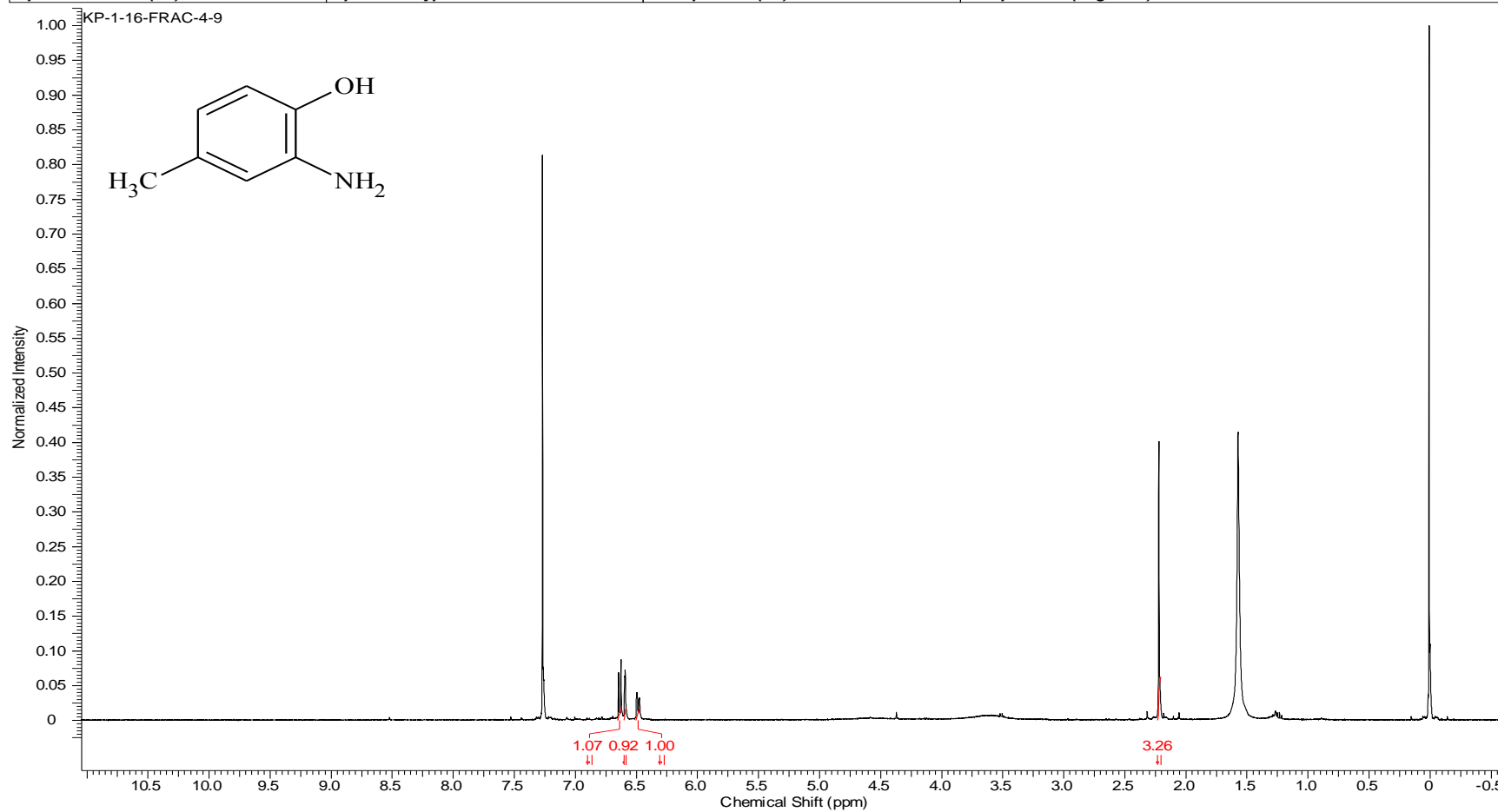


Compound 7 IR



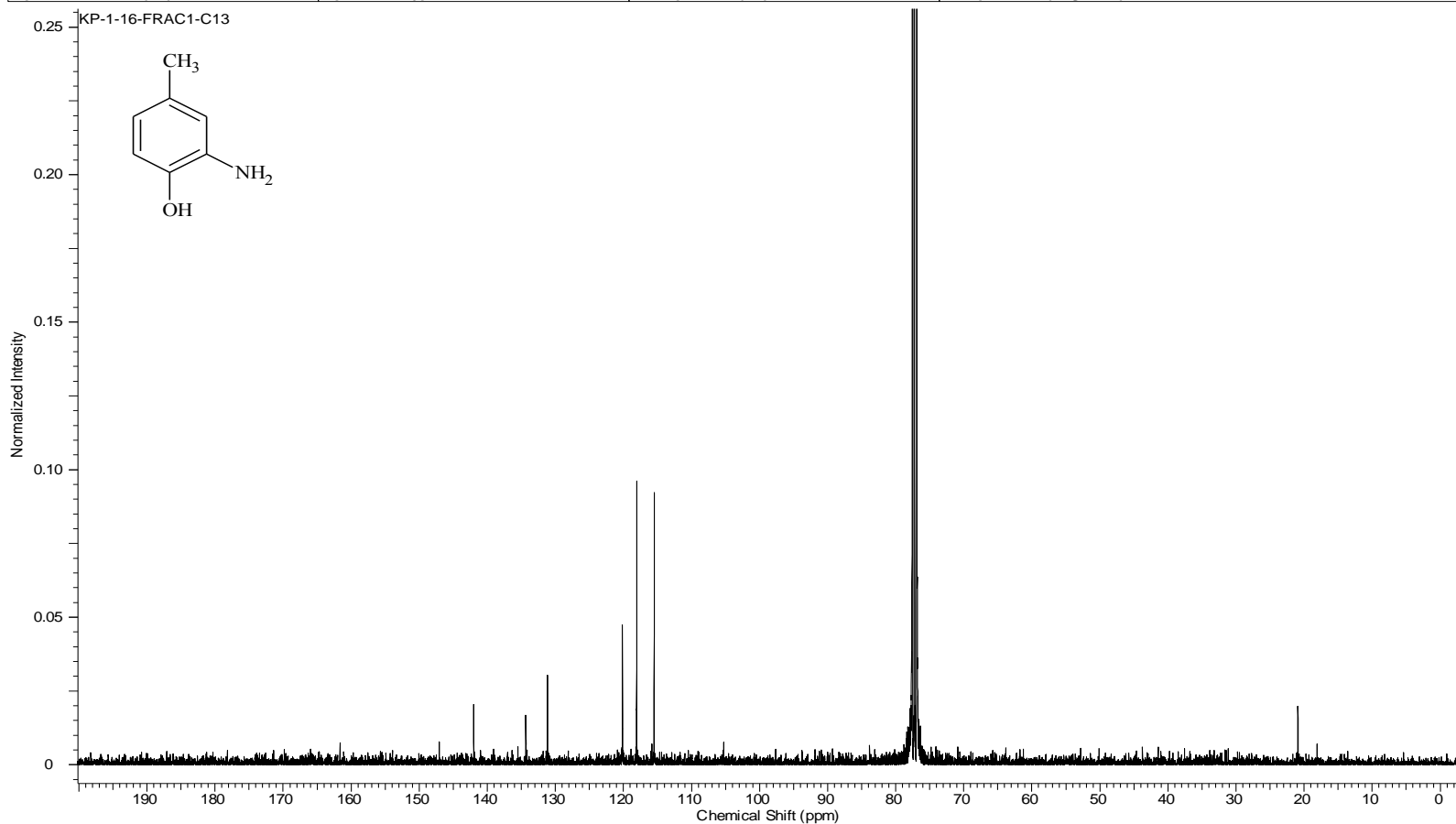
Compound 8 ¹H NMR

Acquisition Time (sec)	2.0487	Comment	Std proton	Date	Jun 2 2008	Date Stamp	Jun 2 2008
File Name	C:\USERS\KESHAR\DESKTOP\NMR\BOOK 1\KP-1-16-FRAC-4-9.FID\FID				Frequency (MHz)	399.76	
Nucleus	1H	Number of Transients	32	Original Points Count	13103	Points Count	16384
Pulse Sequence	s2pul	Receiver Gain	56.00	Solvent	CHLOROFORM-d		
Spectrum Offset (Hz)	2418.0771	Spectrum Type	STANDARD	Sweep Width (Hz)	6395.91	Temperature (degree C)	25.000

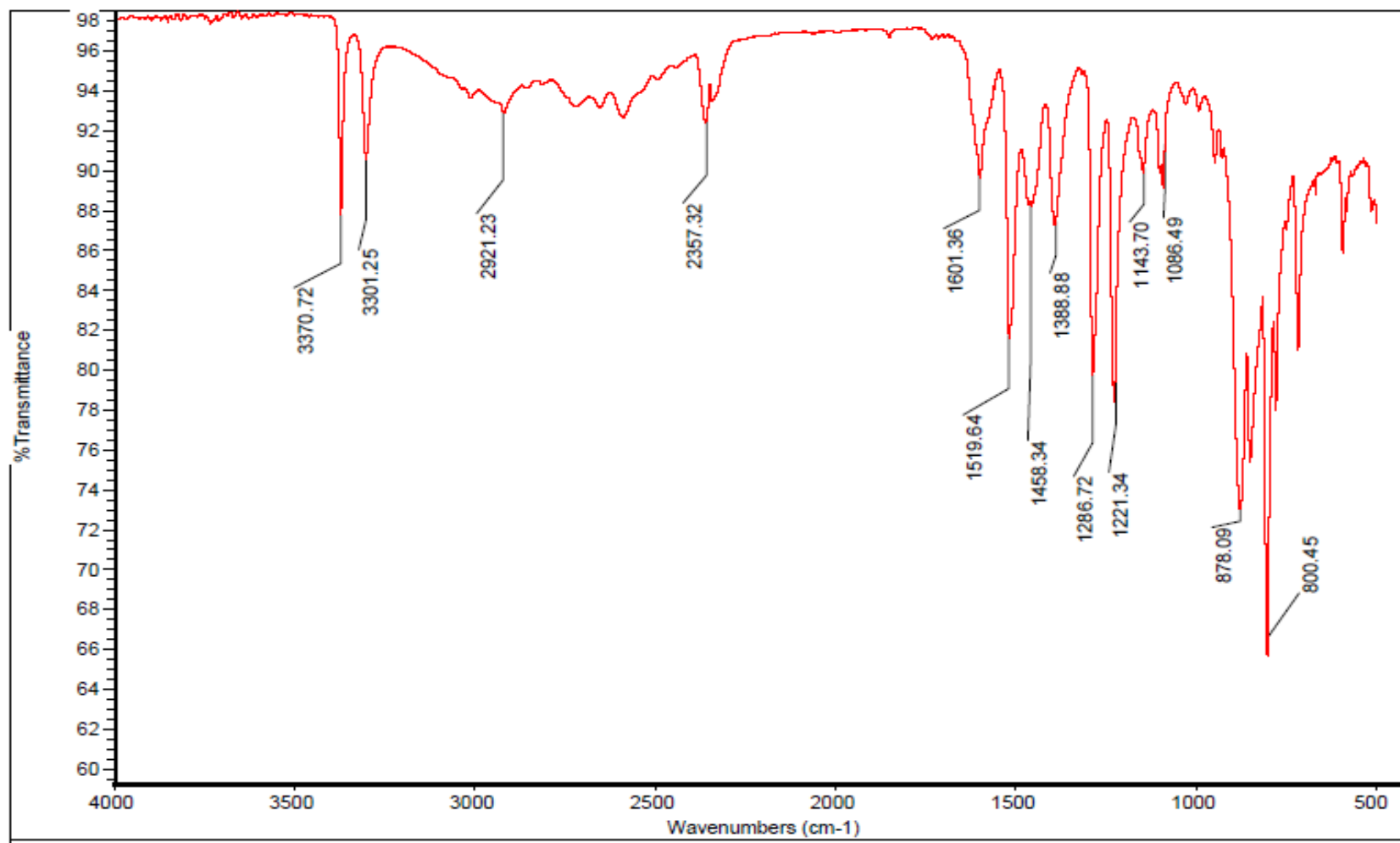


Compound 8 ¹³C NMR

Acquisition Time (sec)	1.3005	Comment	Std Carbon experiment		Date	Jun 28 2012	
Date Stamp	Jun 28 2012	File Name	C:\USERS\KESHAR\DESKTOP\KP-1-16-FRAC1-C13.FID\FID				
Frequency (MHz)	100.58	Nucleus	13C	Number of Transients	1664	Original Points Count	31413
Points Count	32768	Pulse Sequence	s2pul	Receiver Gain	20.00	Solvent	CHLOROFORM-d
Spectrum Offset (Hz)	10556.1475	Spectrum Type	STANDARD	Sweep Width (Hz)	24154.59	Temperature (degree C)	25.000

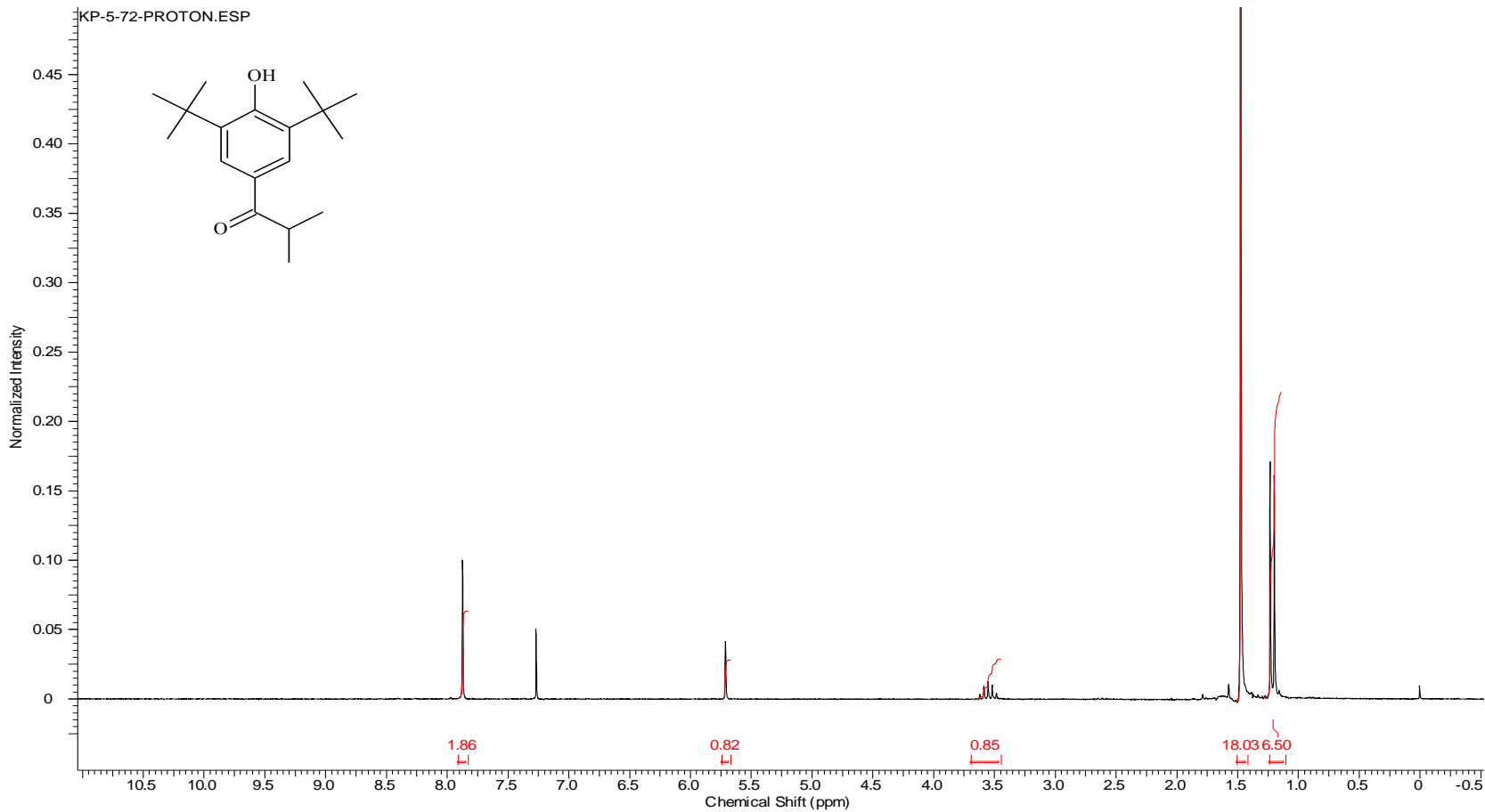


Compound 8 IR



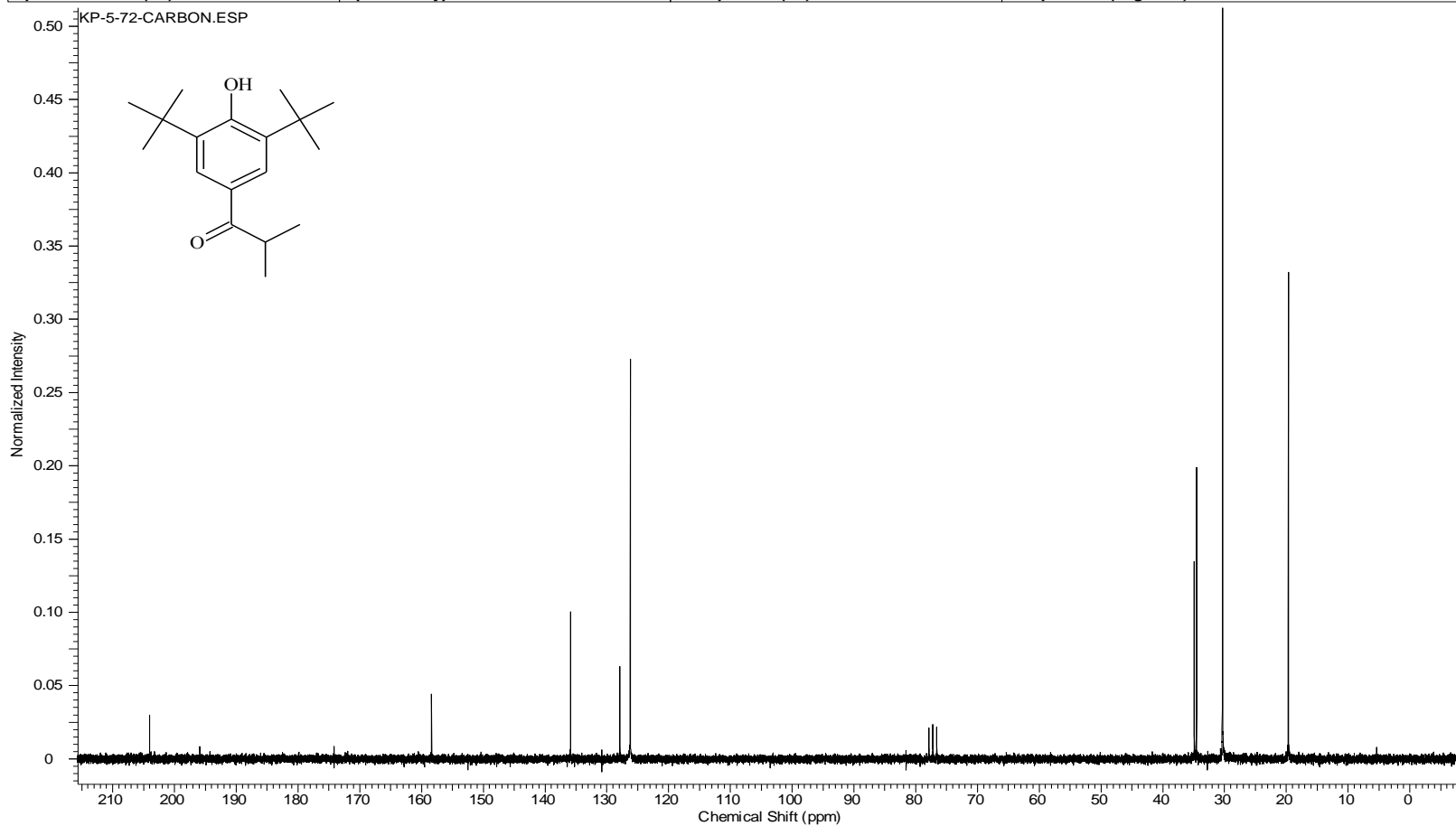
Compound 9 ¹H NMR

Acquisition Time (sec)	1.9945	Comment	STANDARD 1H OBSERVE		Date	Nov 16 2009	
Date Stamp	Nov 16 2009	File Name	C:\USERS\KESHAR\DESKTOP\NMR\BOOK 5\KP-5-72-DP.FID\FID				
Frequency (MHz)	199.98	Nucleus	1H	Number of Transients	32	Original Points Count	5984
Points Count	8192	Pulse Sequence	s2pul	Receiver Gain	34.00	Solvent	CHLOROFORM-d
Spectrum Offset (Hz)	1002.0226	Spectrum Type	STANDARD	Sweep Width (Hz)	3000.30	Temperature (degree C)	AMBIENT TEMPERATURE



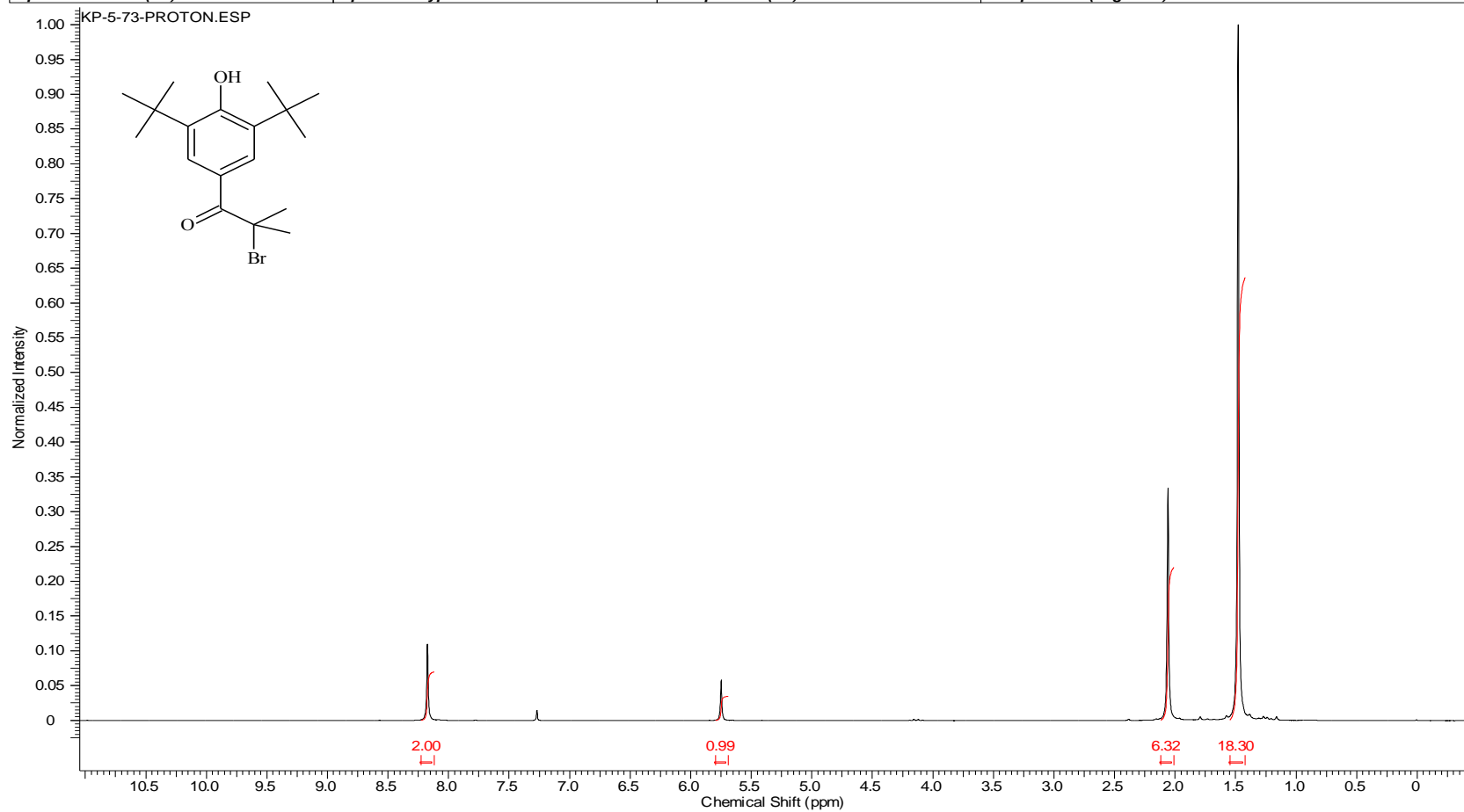
Compound 9 ¹³C NMR

Acquisition Time (sec)	1.4976	Comment	13C OBSERVE KP-5-72-Dp-C13		Date	Nov 18 2009	
Date Stamp	Nov 18 2009	File Name	C:\USERS\KESHAR\KP-5-72-Carbon				
Frequency (MHz)	50.29	Nucleus	13C	Number of Transients	384	Original Points Count	18720
Points Count	32768	Pulse Sequence	s2pul	Receiver Gain	40.00	Solvent	CHLOROFORM-d
Spectrum Offset (Hz)	4878.5537	Spectrum Type	STANDARD	Sweep Width (Hz)	12500.00	Temperature (degree C)	AMBIENT TEMPERATURE



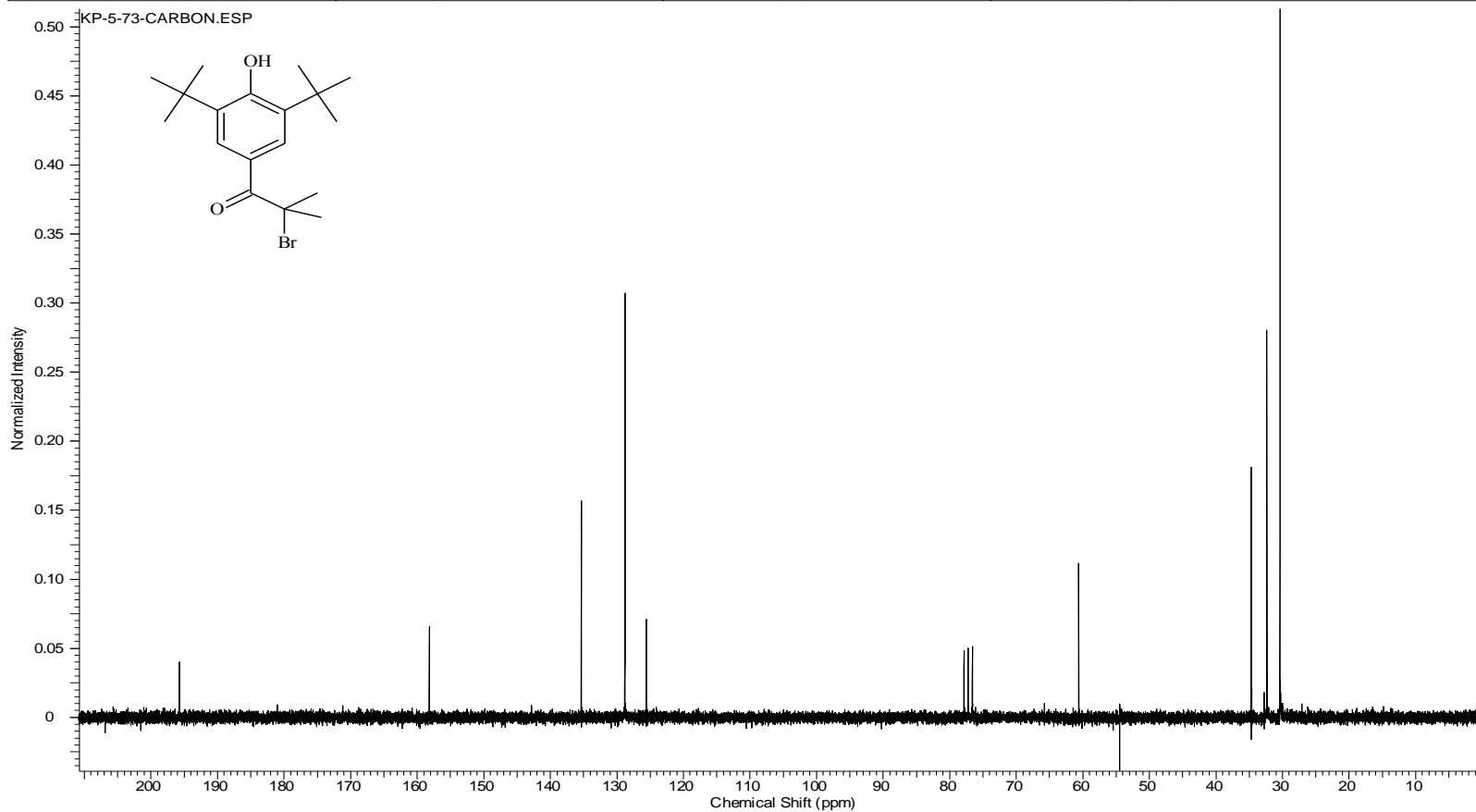
Compound 10 ¹H NMR

Acquisition Time (sec)	1.9945	Comment	STANDARD 1H OBSERVE		Date	Nov 17 2009	
Date Stamp	Nov 17 2009	File Name	C:\USERS\KESHAR\DESKTOP\NMR\BOOK 5\KP-5-73-DP.FID\FID				
Frequency (MHz)	199.98	Nucleus	1H	Number of Transients	96	Original Points Count	5984
Points Count	8192	Pulse Sequence	s2pul	Receiver Gain	18.00	Solvent	CHLOROFORM-d
Spectrum Offset (Hz)	1002.7551	Spectrum Type	STANDARD	Sweep Width (Hz)	3000.30	Temperature (degree C)	AMBIENT TEMPERATURE



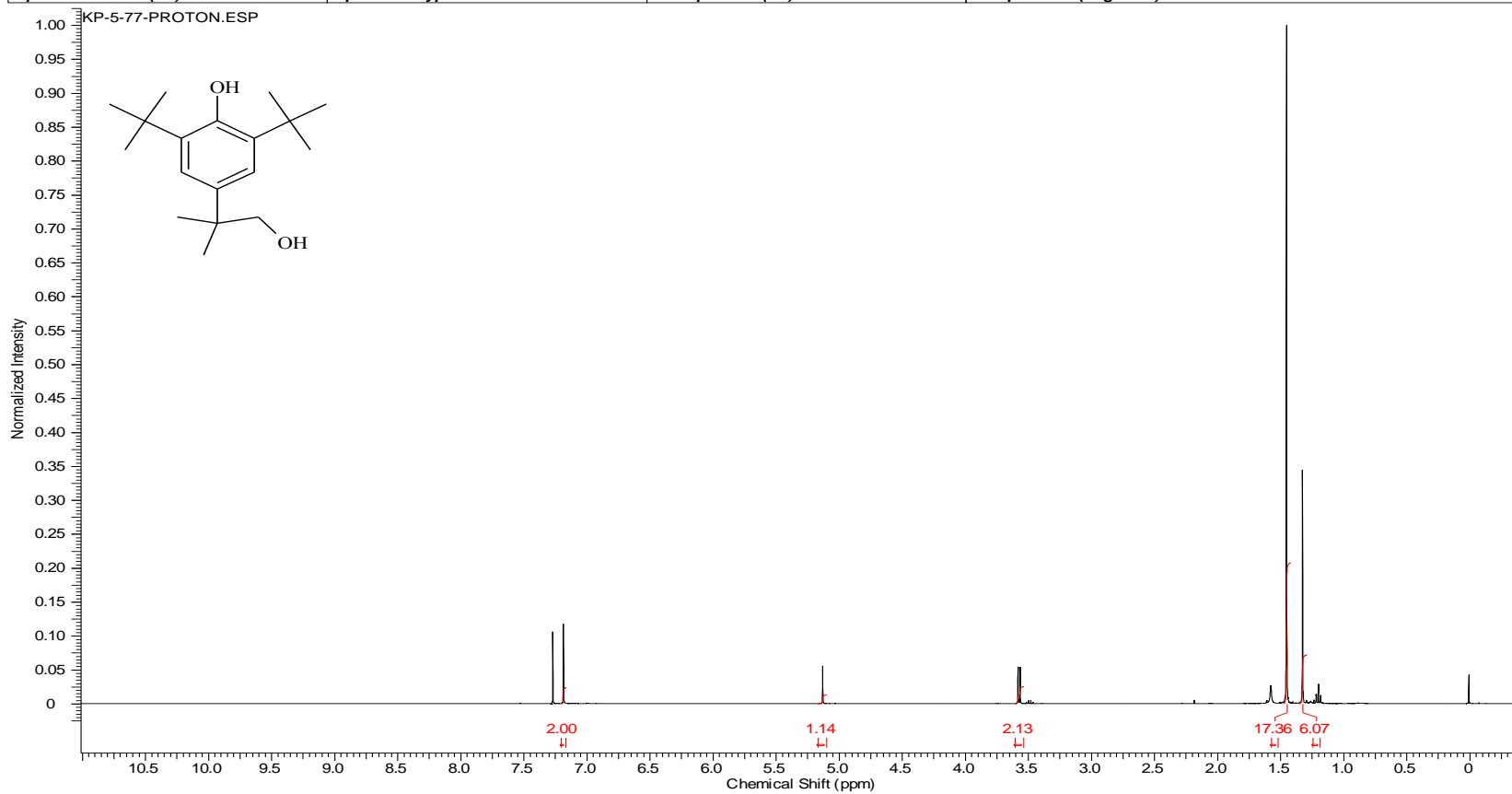
Compound 10 ¹³C NMR

Acquisition Time (sec)	1.4976	Comment	13C OBSERVE	Date	Nov 18 2009	Date Stamp	Nov 18 2009
File Name	C:\USERS\KESHAR\DESKTOP\NMR\BOOK 5\KP-5-73-DP-C13.FID\FID			Frequency (MHz)	50.29		
Nucleus	13C	Number of Transients	416	Original Points Count	18720	Points Count	32768
Pulse Sequence	s2pul	Receiver Gain	40.00	Solvent	CHLOROFORM-d		
Spectrum Offset (Hz)	4879.3164	Spectrum Type	STANDARD	Sweep Width (Hz)	12500.00	Temperature (degree C)	AMBIENT TEMPERATURE



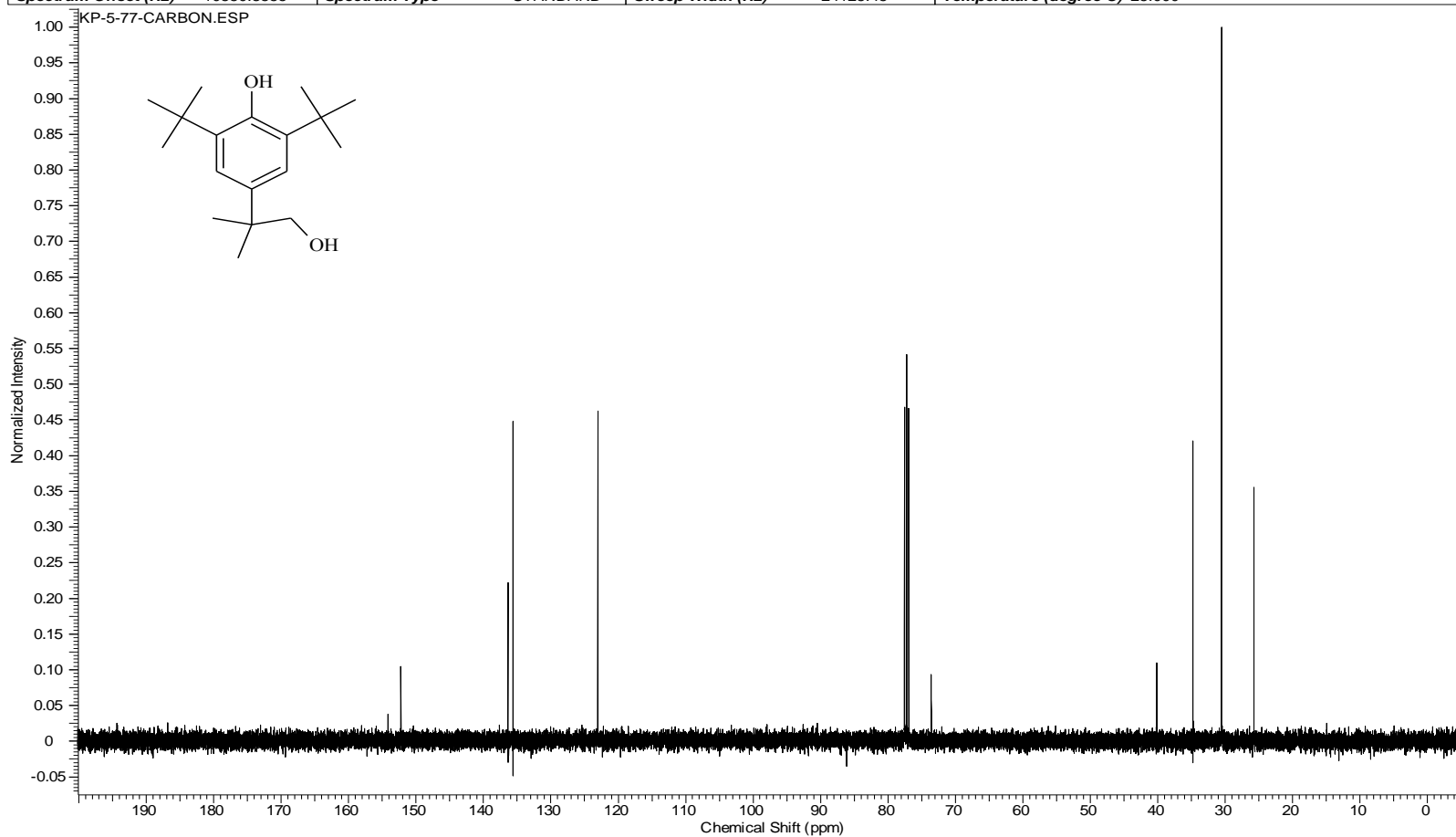
Compound 11 ¹H NMR

Acquisition Time (sec)	2.0487	Comment	Std proton	Date	Nov 23 2009	Date Stamp	Nov 23 2009
File Name	C:\USERS\KESHAR\DESKTOP\NMR\BOOK 5\KP-5-77-CRUDE.FID\FID			Frequency (MHz)	399.75		
Nucleus	1H	Number of Transients	8	Original Points Count	13103	Points Count	16384
Pulse Sequence	s2pul	Receiver Gain	48.00	Solvent	CHLOROFORM-d		
Spectrum Offset (Hz)	2404.7087	Spectrum Type	STANDARD	Sweep Width (Hz)	6395.91	Temperature (degree C)	25.000



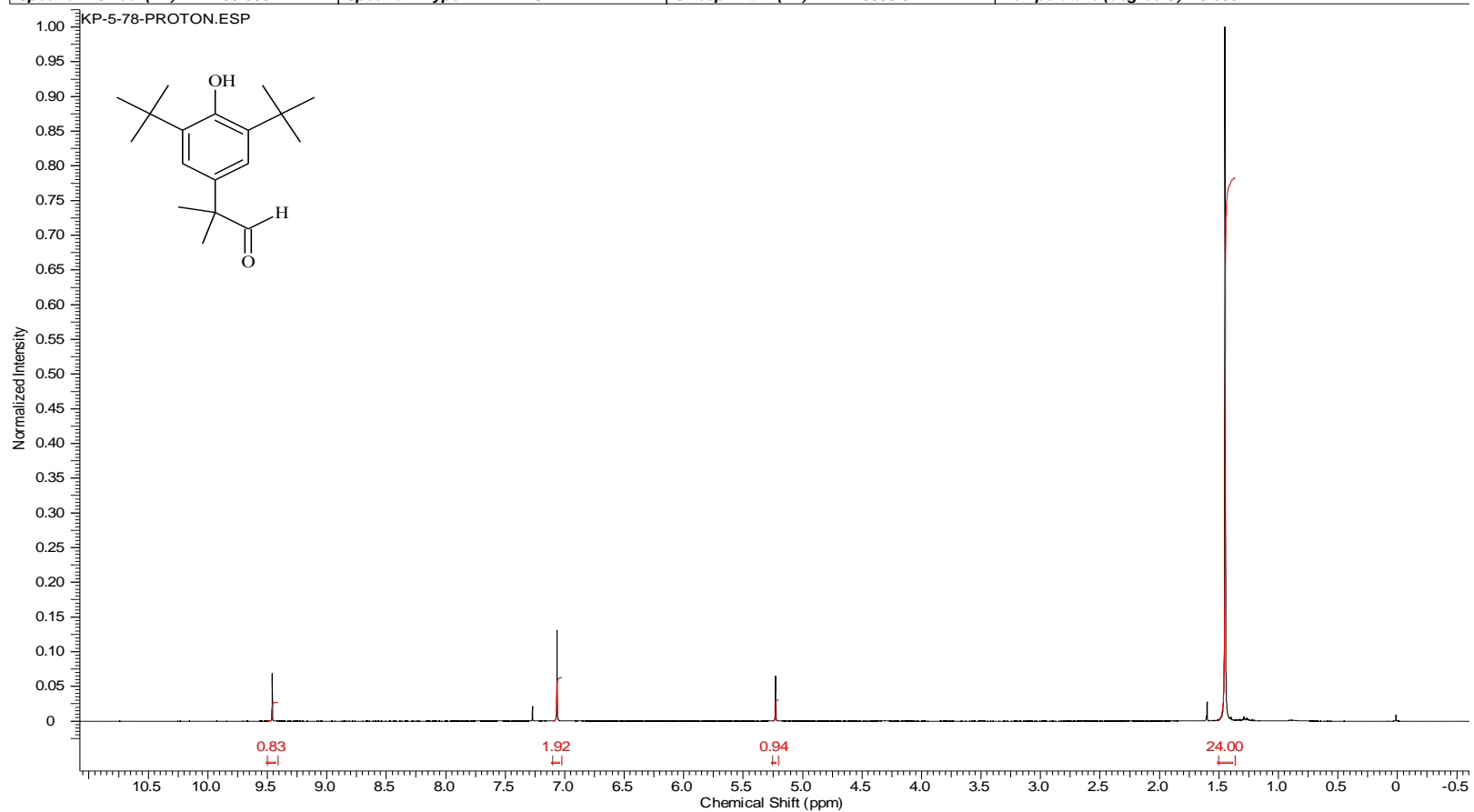
Compound 11 ¹³C NMR

Acquisition Time (sec)	1.3005	Comment	Std proton	Date	Nov 23 2009	Date Stamp	Nov 23 2009
File Name	C:\USERS\KESHAR\DESKTOP\NMR\BOOK 5\KP-5-77-C13.FID\FID			Frequency (MHz)	100.53		
Nucleus	13C	Number of Transients	512	Original Points Count	31375	Points Count	32768
Pulse Sequence	s2pul	Receiver Gain	30.00	Solvent	CHLOROFORM-d		
Spectrum Offset (Hz)	10550.8555	Spectrum Type	STANDARD	Sweep Width (Hz)	24125.45	Temperature (degree C)	25.000



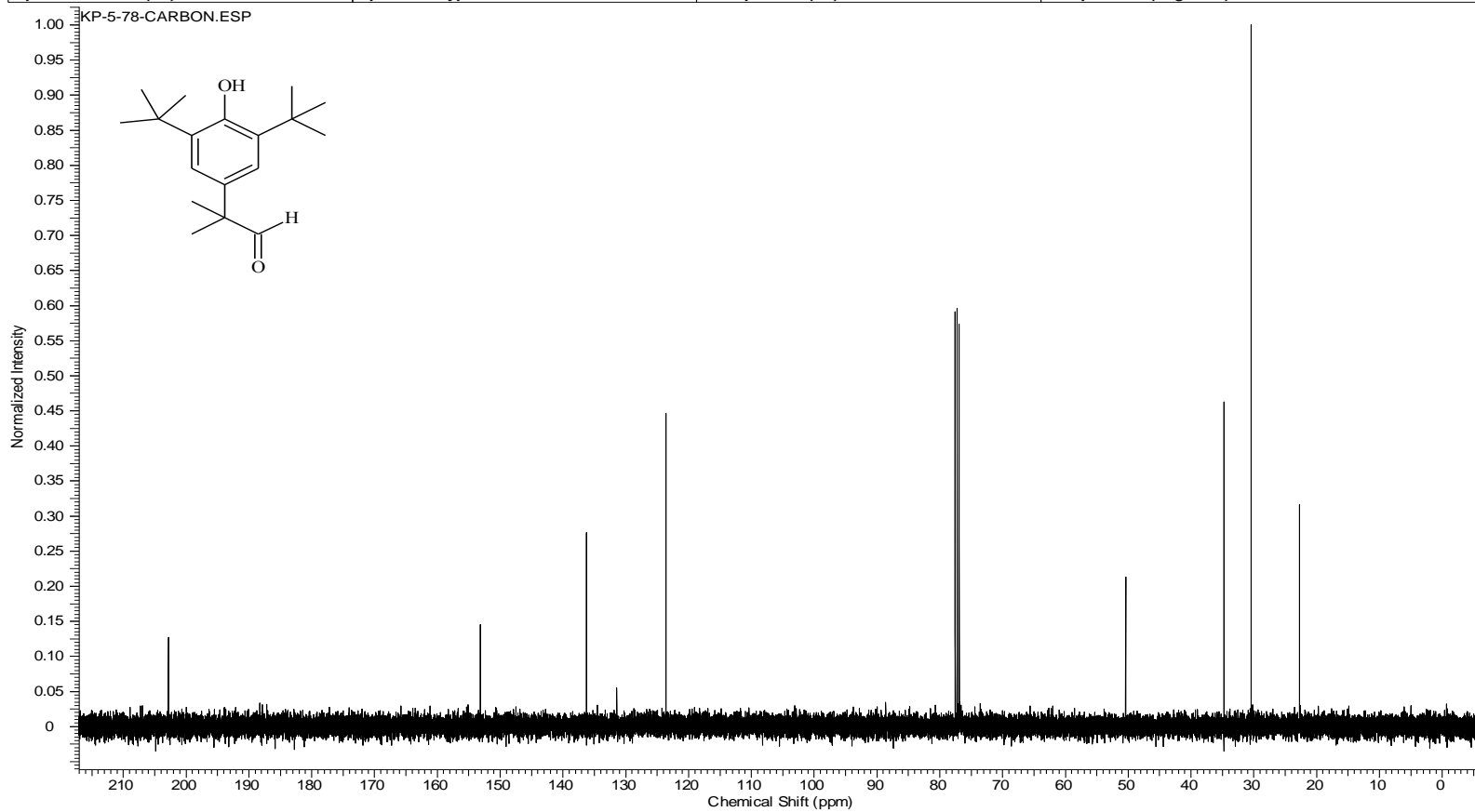
Compound 12 ¹H NMR

Acquisition Time (sec)	2.0487	Comment	Std proton	Date	Nov 24 2009	Date Stamp	Nov 24 2009
File Name	C:\USERS\KESHAR\DESKTOP\KESHAR NEW NMR BACKUP 2011\NMR BACK UP 4 AND 5\KP-5-78-DP.FID\FID						
Frequency (MHz)	399.75	Nucleus	1H	Number of Transients	4	Original Points Count	13103
Points Count	16384	Pulse Sequence	s2pul	Receiver Gain	36.00	Solvent	CHLOROFORM-d
Spectrum Offset (Hz)	2405.0991	Spectrum Type	STANDARD	Sweep Width (Hz)	6395.91	Temperature (degree C)	25.000

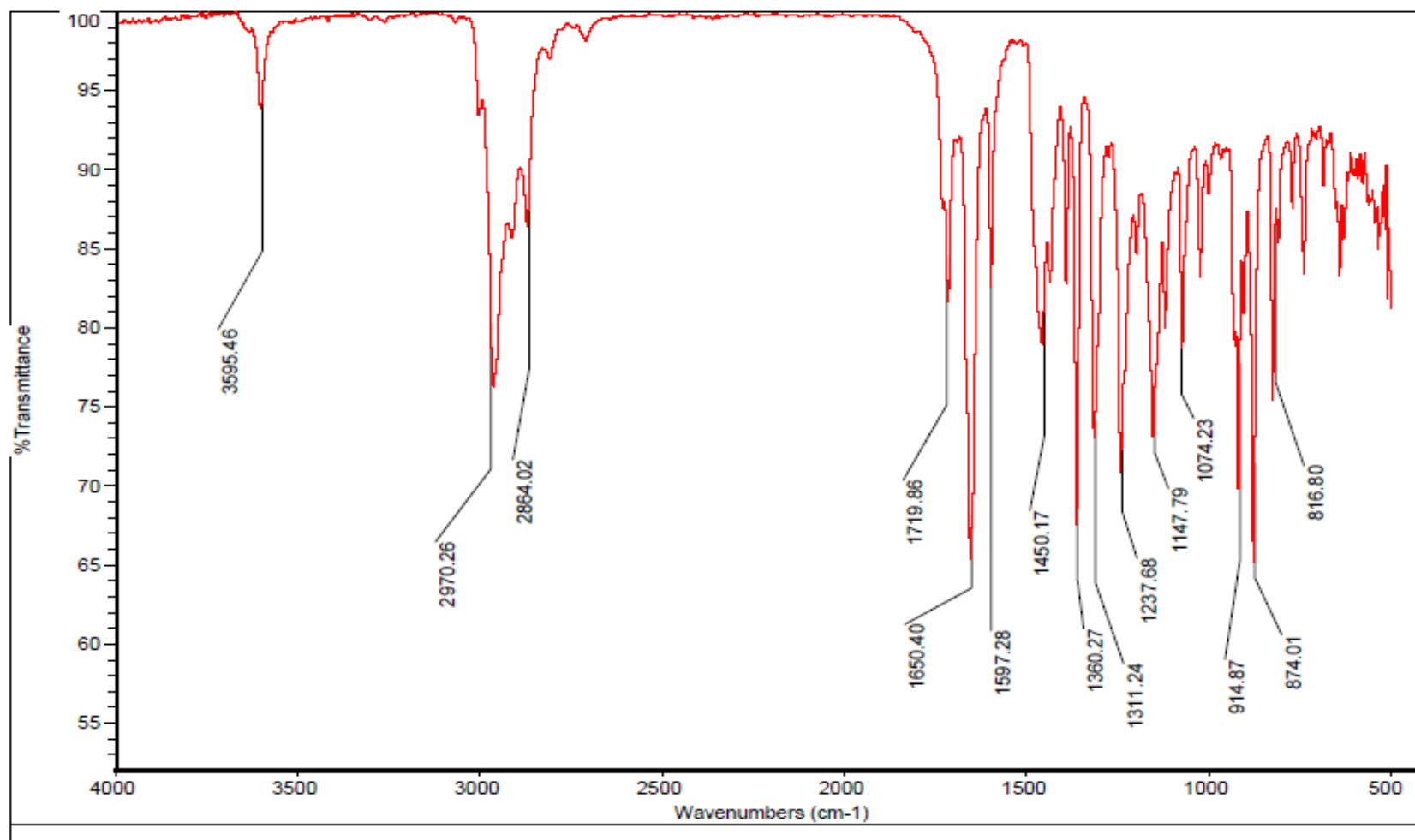


Compound 12 ¹³C NMR

Acquisition Time (sec)	1.3005	Comment	Std proton	Date	Nov 24 2009	Date Stamp	Nov 24 2009
File Name	C:\USERS\KESHAR\DOCUMENTS\KESHAR NMR\KESHAR\COPY OF KESHAR NOVA 3-16-2011\KESHAR\KP-5-78-C13.FID\FID						
Frequency (MHz)	100.53	Nucleus	13C	Number of Transients	448	Original Points Count	31375
Points Count	32768	Pulse Sequence	s2pul	Receiver Gain	30.00	Solvent	CHLOROFORM-d
Spectrum Offset (Hz)	10551.5918	Spectrum Type	STANDARD	Sweep Width (Hz)	24125.45	Temperature (degree C)	25.000

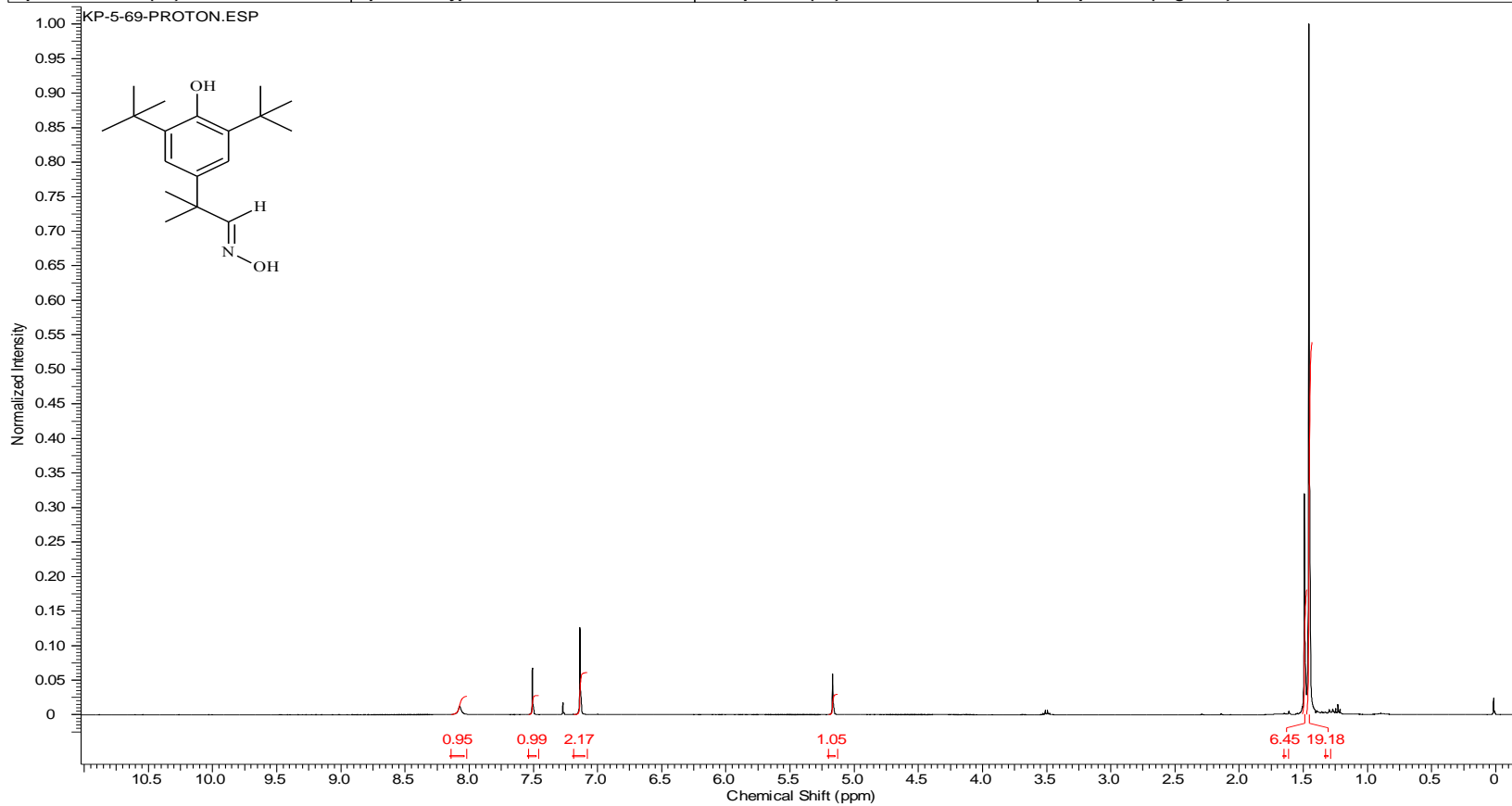


Compound 12 IR



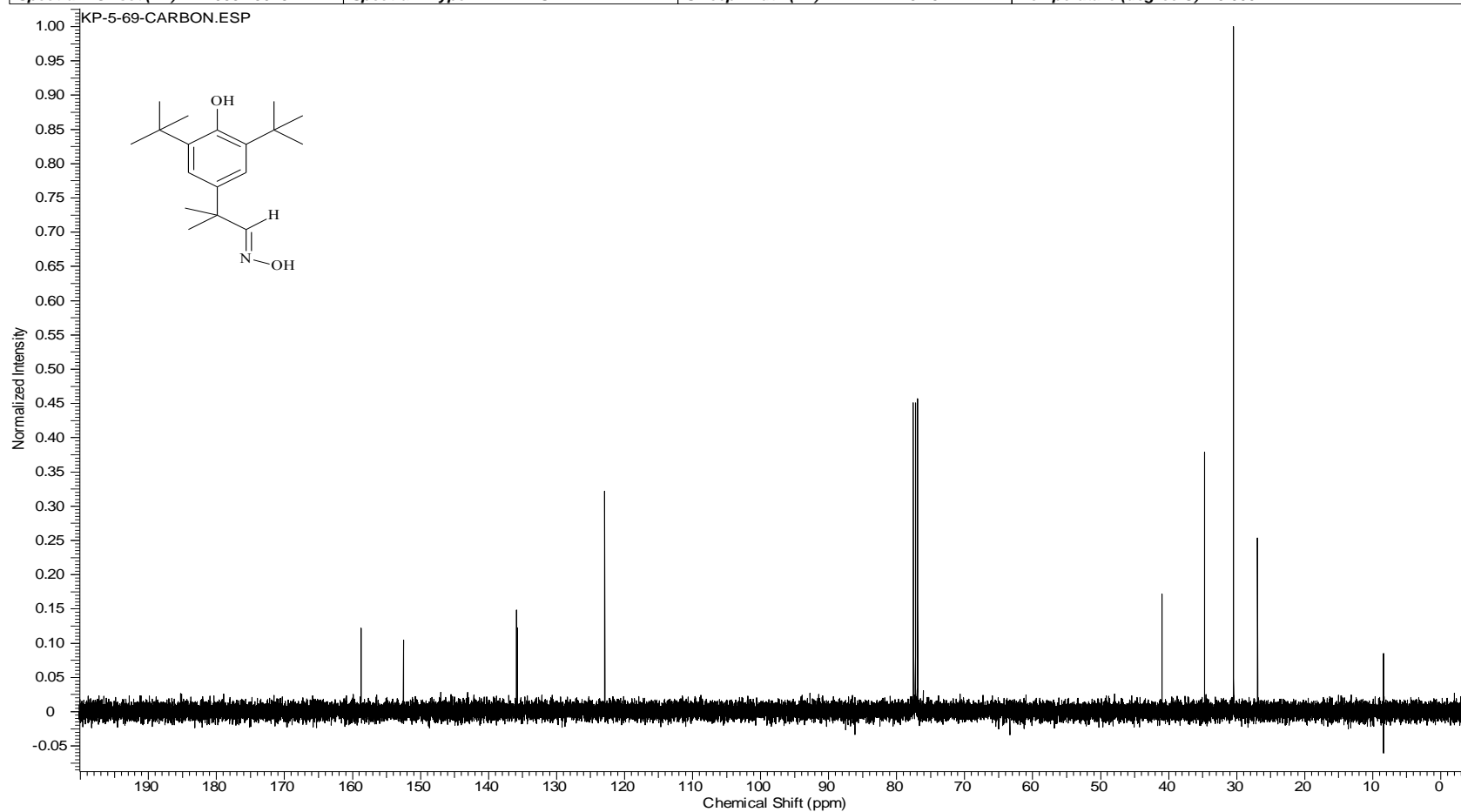
Compound 14 ¹H NMR

Acquisition Time (sec)	2.0487	Comment	Std proton	Date	Nov 25 2009	Date Stamp	Nov 25 2009
File Name	C:\USERS\KESHAR\KP-5-69-Proton						
Frequency (MHz)	399.75	Nucleus	1H	Number of Transients	16	Original Points Count	13103
Points Count	16384	Pulse Sequence	s2pul	Receiver Gain	32.00	Solvent	CHLOROFORM-d
Spectrum Offset (Hz)	2405.0991	Spectrum Type	STANDARD	Sweep Width (Hz)	6395.91	Temperature (degree C)	25.000

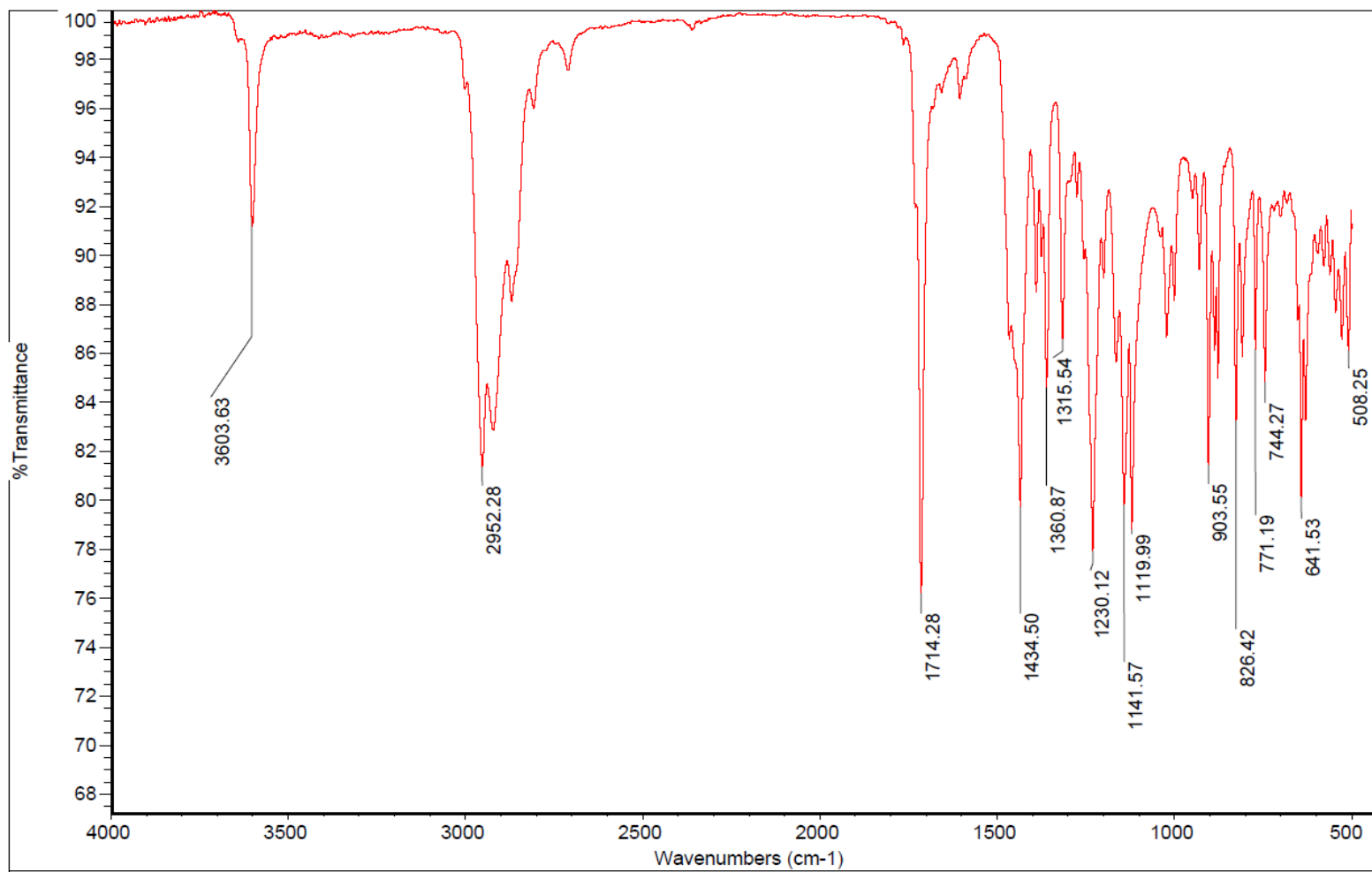


Compound 14 ¹³C NMR

Acquisition Time (sec)	1.3005	Comment	Std proton	Date	Nov 25 2009	Date Stamp	Nov 25 2009
File Name	C:\USERS\KESHAR\KP-5-69-Carbon						
Frequency (MHz)	100.53	Nucleus	13C	Number of Transients	544	Original Points Count	31375
Points Count	32768	Pulse Sequence	s2pul	Receiver Gain	30.00	Solvent	CHLOROFORM-d
Spectrum Offset (Hz)	10551.5918	Spectrum Type	STANDARD	Sweep Width (Hz)	24125.45	Temperature (degree C)	25.000

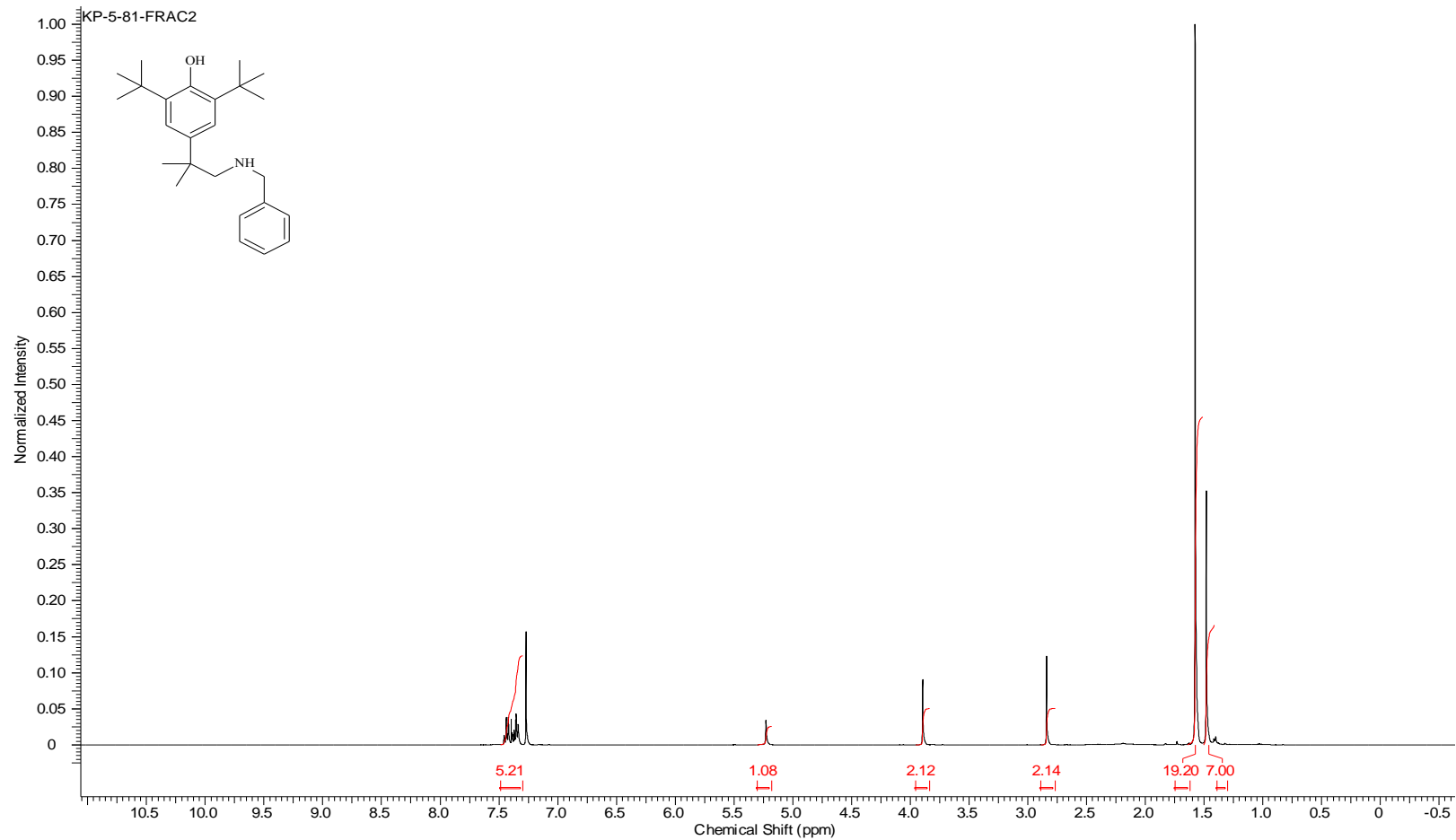


Compound 14 IR



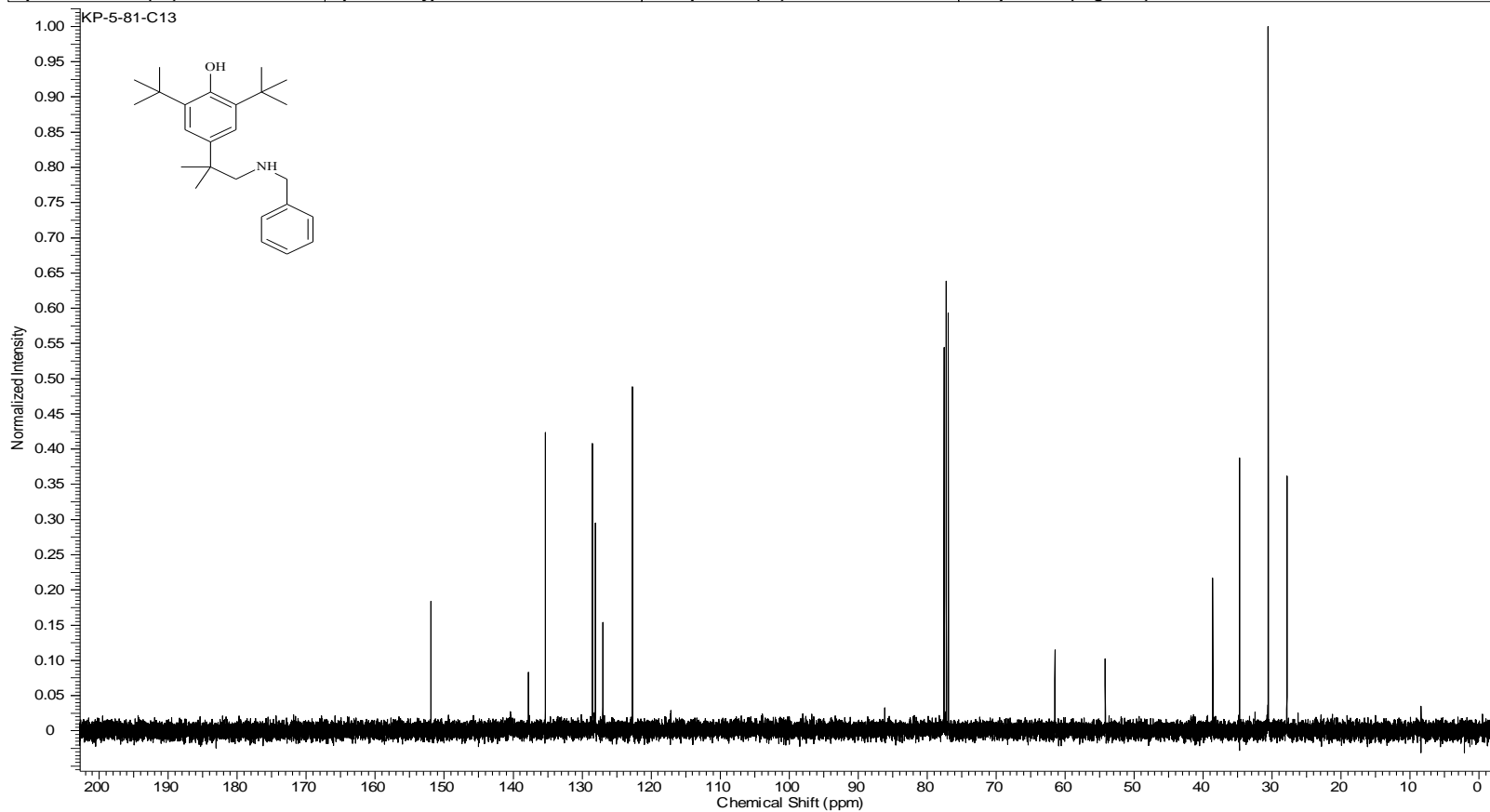
Compound 15 ¹H NMR

Acquisition Time (sec)	2.0487	Comment	Std proton	Date	Nov 29 2009	Date Stamp	Nov 29 2009
File Name	C:\USERS\KESHAR\DESKTOP\NMR\BOOK 5\KP-5-81-FRAC2.FID\FID				Frequency (MHz)	399.75	
Nucleus	1H	Number of Transients	20	Original Points Count	13103	Points Count	16384
Pulse Sequence	s2pul	Receiver Gain	32.00	Solvent	CHLOROFORM-d		
Spectrum Offset (Hz)	2454.6799	Spectrum Type	STANDARD	Sweep Width (Hz)	6395.91	Temperature (degree C)	25.000



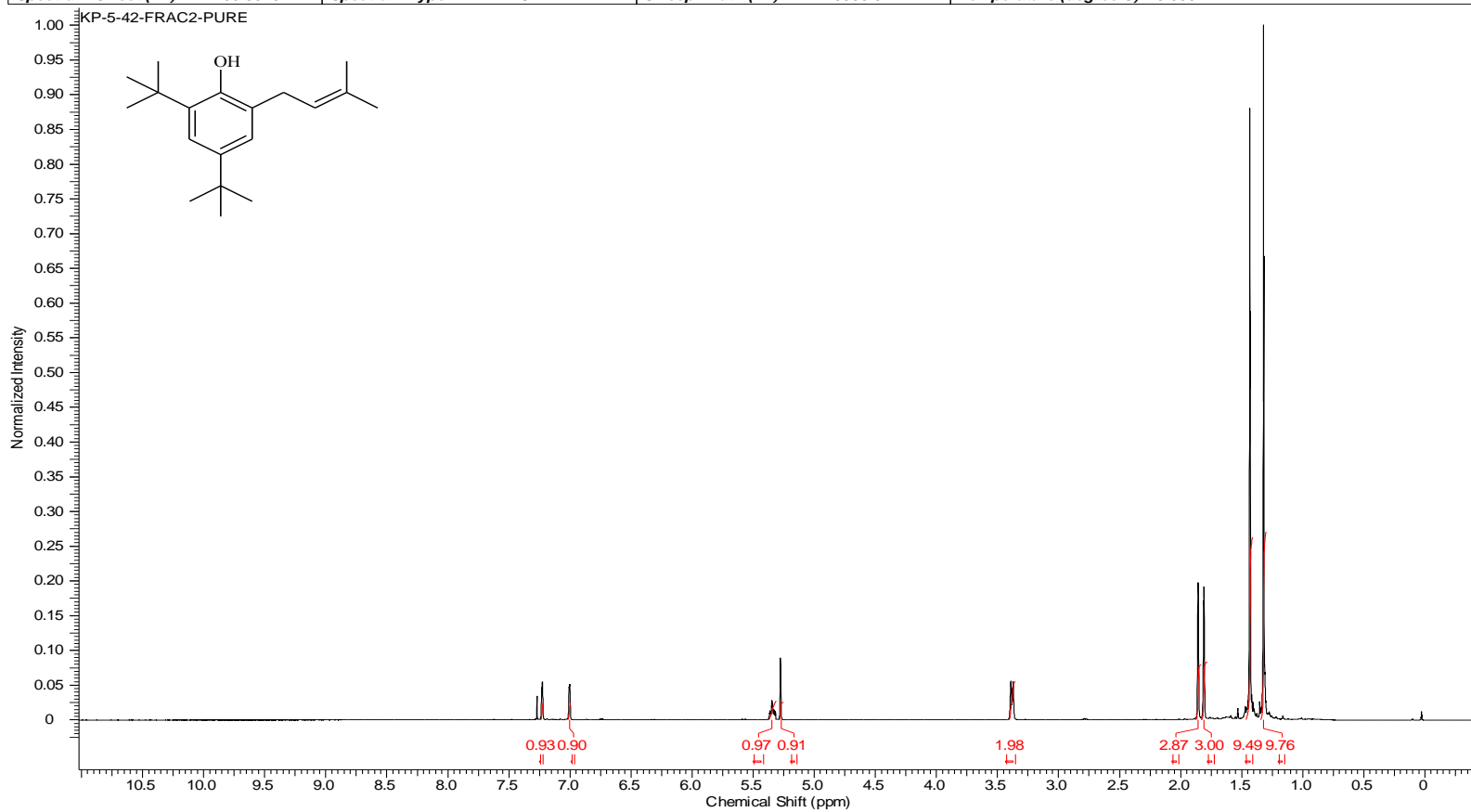
Compound 15 ¹³C NMR

Acquisition Time (sec)	1.3005	Comment	Std proton	Date	Nov 29 2009	Date Stamp	Nov 29 2009
File Name	C:\USERS\KESHAR\DESKTOP\NMR\BOOK 5\KP-5-81-C13.FID\FID			Frequency (MHz)	100.53		
Nucleus	13C	Number of Transients	1000	Original Points Count	31375	Points Count	32768
Pulse Sequence	s2pul	Receiver Gain	30.00	Solvent	CHLOROFORM-d		
Spectrum Offset (Hz)	10550.1191	Spectrum Type	STANDARD	Sweep Width (Hz)	24125.45	Temperature (degree C)	25.000



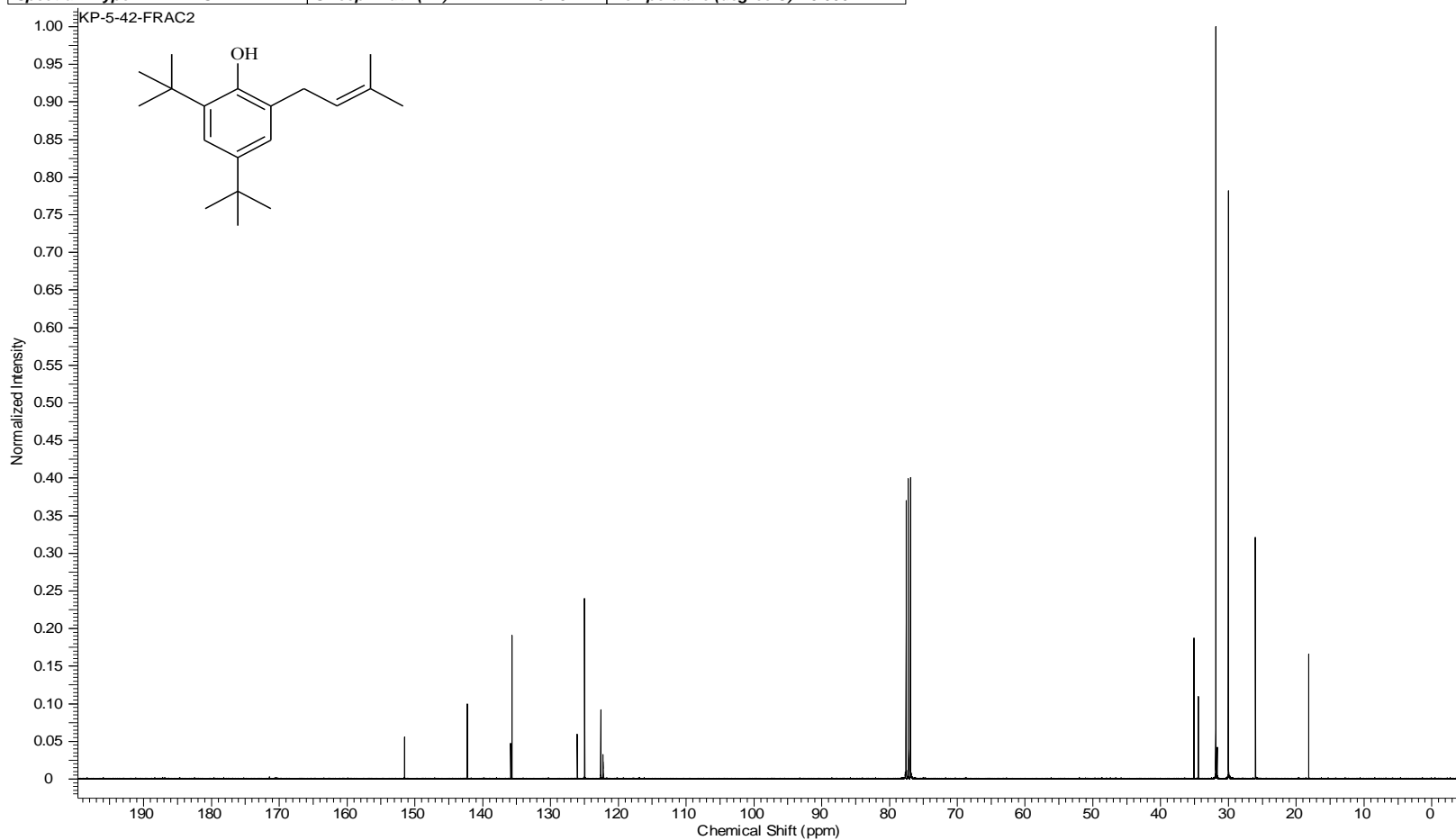
Compound 16 ¹H NMR

Acquisition Time (sec)	2.0487	Comment	Std proton	Date	Nov 23 2009	Date Stamp	Nov 23 2009
File Name	C:\USERS\KESHAR\DESKTOP\NMR\BOOK 5\KP-5-42-FRAC2-PURE.FID\FID			Frequency (MHz)	399.75		
Nucleus	1H	Number of Transients	16	Original Points Count	13103	Points Count	16384
Pulse Sequence	s2pul	Receiver Gain	32.00	Solvent	CHLOROFORM-d		
Spectrum Offset (Hz)	2403.5376	Spectrum Type	STANDARD	Sweep Width (Hz)	6395.91	Temperature (degree C)	25.000



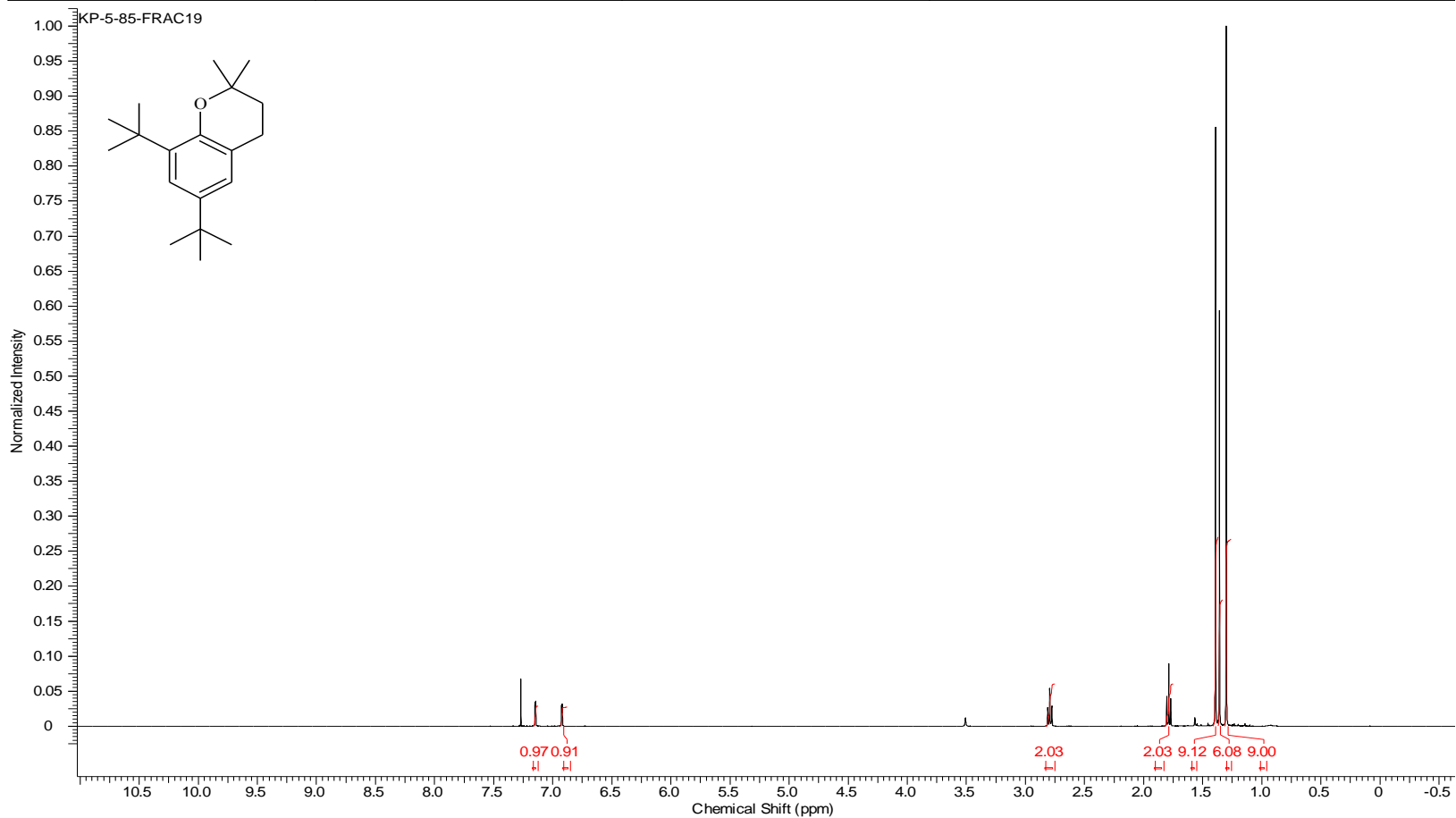
Compound 16 ¹³C NMR

Acquisition Time (sec)	1.3005	Comment	Std proton	Date	Nov 23 2009	Date Stamp	Nov 23 2009
File Name	E:\KESHAR NMR REMAIN\KP-5-42-FRAC2.FID\FID			Frequency (MHz)	100.53	Nucleus	¹³ C
Number of Transients	512	Original Points Count	31375	Points Count	32768	Pulse Sequence	s2pul
Receiver Gain	30.00	Solvent	CHLOROFORM-d			Spectrum Offset (Hz)	10550.8555
Spectrum Type	STANDARD	Sweep Width (Hz)	24125.45	Temperature (degree C)	25.000		



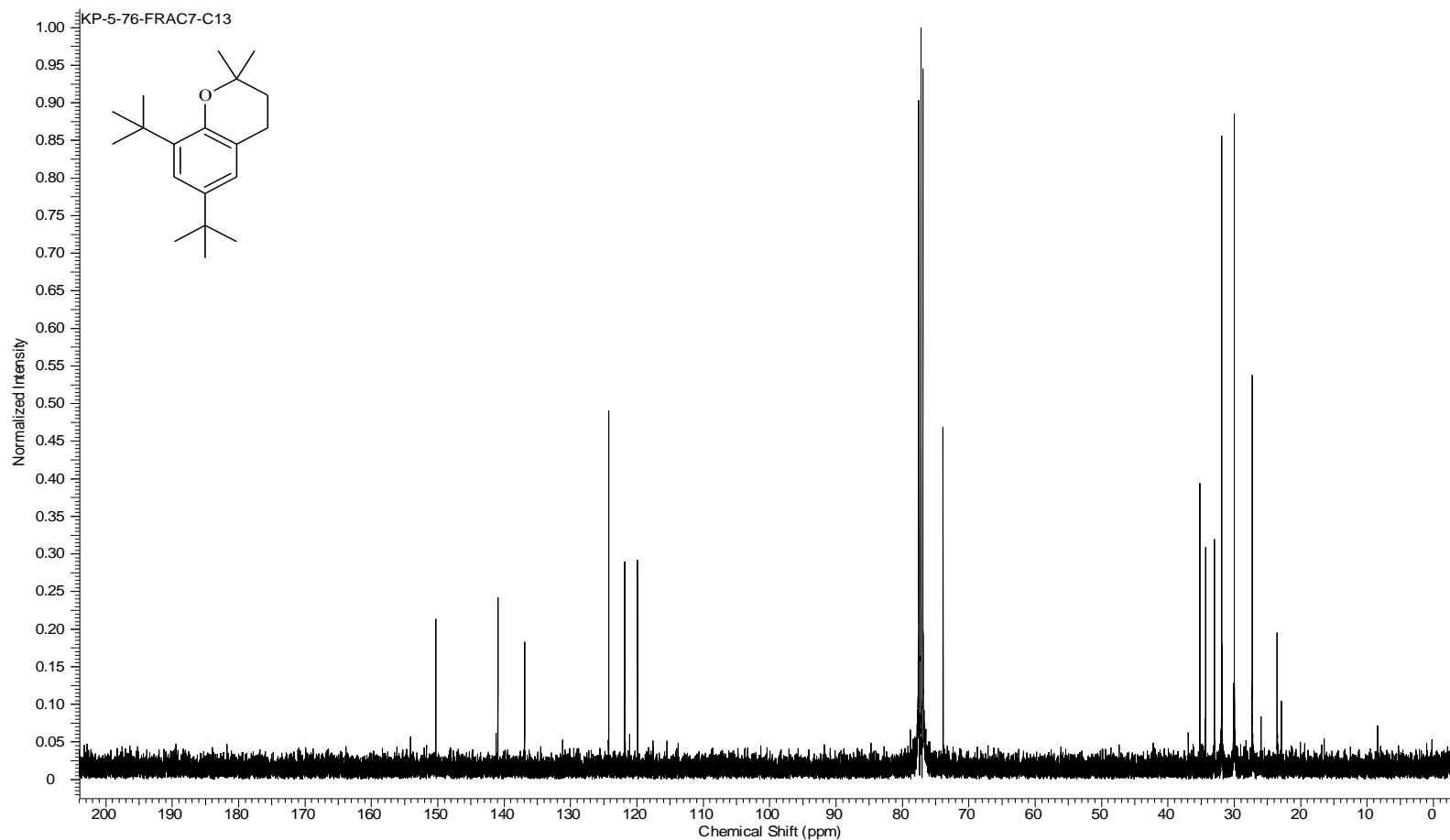
Compound 17 ¹H NMR

Acquisition Time (sec)	2.0487	Comment	KP-5-85-frac19		Date	Dec 3 2009	
Date Stamp	Dec 3 2009	File Name	C:\USERS\KESHAR\DESKTOP\NMR\BOOK 5\KP-5-85-FRAC19.FID\FID				
Frequency (MHz)	399.75	Nucleus	1H	Number of Transients	28	Original Points Count	13103
Points Count	16384	Pulse Sequence	s2pul	Receiver Gain	42.00	Solvent	CHLOROFORM-d
Spectrum Offset (Hz)	2404.7219	Spectrum Type	STANDARD	Sweep Width (Hz)	6395.91	Temperature (degree C)	25.000



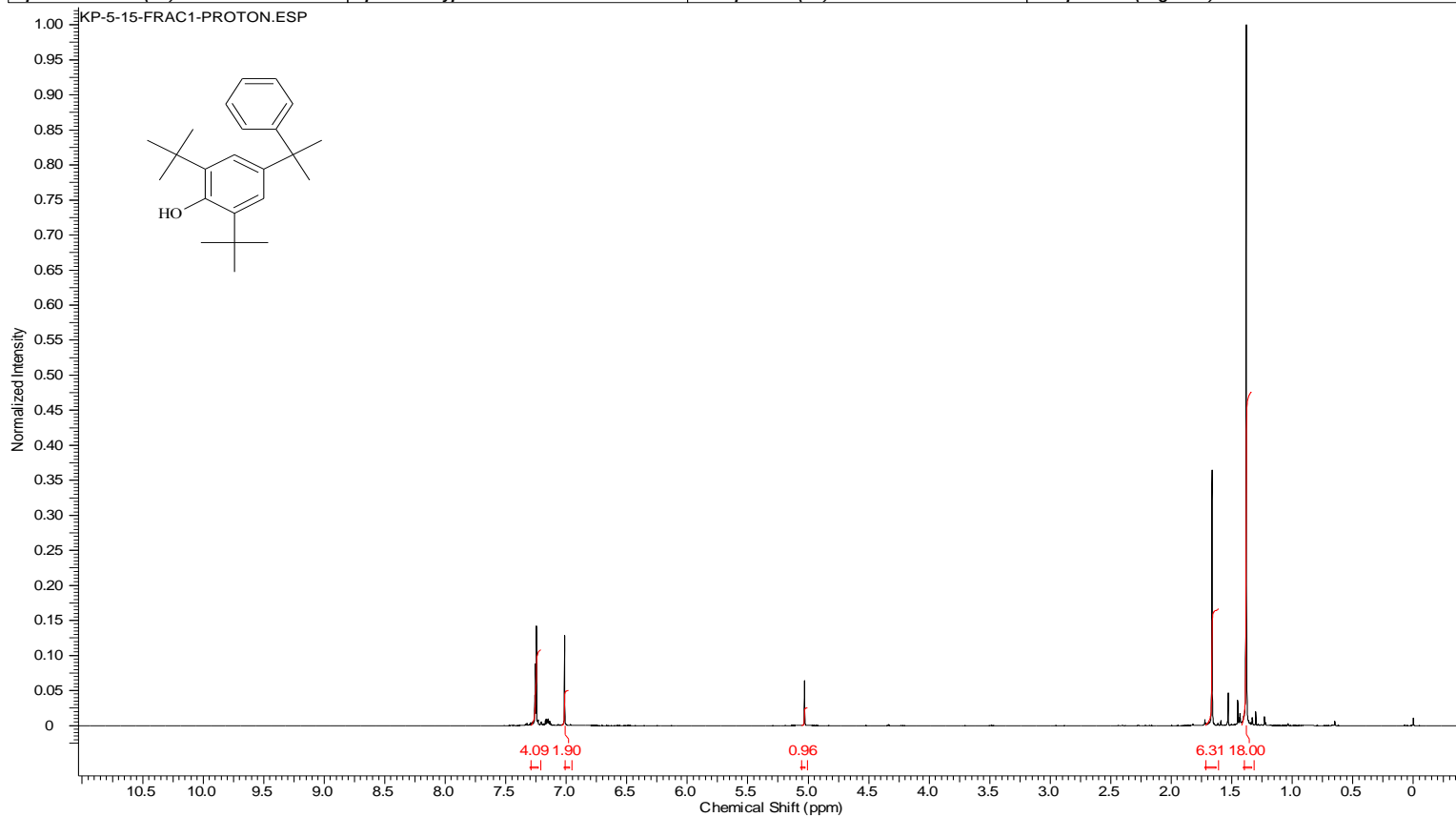
Compound 17 ¹³C NMR

Acquisition Time (sec)	1.3005	Comment	Std proton	Date	Nov 25 2009	Date Stamp	Nov 25 2009
File Name	C:\USERS\KESHAR\DESKTOP\NMR\BOOK 5\KP-5-76-FRAC7-C13.FID\FID			Frequency (MHz)	100.53		
Nucleus	¹³ C	Number of Transients	512	Original Points Count	31375	Points Count	32768
Pulse Sequence	s2pul	Receiver Gain	30.00	Solvent	CHLOROFORM-d		
Spectrum Offset (Hz)	10551.5918	Spectrum Type	STANDARD	Sweep Width (Hz)	24125.45	Temperature (degree C)	25.000



MON-0585 (compound 18) ¹H NMR

Acquisition Time (sec)	2.0487	Comment	Std proton	Date	Aug 24 2009	Date Stamp	Aug 24 2009
File Name	C:\USERS\KESHAR\KP-5-15-Proton						
Frequency (MHz)	399.75	Nucleus	1H	Number of Transients	40	Original Points Count	13103
Points Count	16384	Pulse Sequence	s2pul	Receiver Gain	36.00	Solvent	CHLOROFORM-d
Spectrum Offset (Hz)	2397.2451	Spectrum Type	STANDARD	Sweep Width (Hz)	6395.91	Temperature (degree C)	25.000



Appendix B: Permission for figures

1. Permission for Figure 2

2/4/13

Rightslink Printable License

JOHN WILEY AND SONS LICENSE TERMS AND CONDITIONS

Feb 04, 2013

This is a License Agreement between Keshar Prasain ("You") and John Wiley and Sons ("John Wiley and Sons") provided by Copyright Clearance Center ("CCC"). The license consists of your order details, the terms and conditions provided by John Wiley and Sons, and the payment terms and conditions.

All payments must be made in full to CCC. For payment instructions, please see information listed at the bottom of this form.

License Number	3081990461710
License date	Feb 04, 2013
Licensed content publisher	John Wiley and Sons
Licensed content publication	FEMS Microbiology Reviews
Licensed content title	Fungal laccases – occurrence and properties
Licensed copyright line	Copyright © 2005, John Wiley and Sons
Licensed content author	Petr Baldrian
Licensed content date	Nov 9, 2005
Start page	215
End page	242
Type of use	Dissertation/Thesis
Requestor type	University/Academic
Format	Print and electronic
Portion	Figure/table
Number of figures/tables	1
Original Wiley figure/table number(s)	Figure 1. Catalytic cycle of laccase
Will you be translating?	No
Total	0.00 USD

2. Permission for Figure 3

2/4/13

Copyright Clearance Center



Confirmation Number: 11067004
Order Date: 02/04/2013

Customer Information

Customer: Keshar Prasain
Account Number: 3000619003
Organization: Keshar Prasain
Email: keshar@ksu.edu
Phone: +1 (785)3173468
Payment Method: Invoice

Order Details

Tetrahedron

Billing Status:
N/A

Order detail ID: 63418919

Article Title: Oxidative conjugation of catechols with proteins in insect skeletal systems

Author(s): Kramer, K
DOI: 10.1016/S0040-4020(00)00949-2

Date: Jan 11, 2001

ISSN: 0040-4020

Publication Type: Journal

Volume: 57

Issue: 24

Start page: 385

Publisher: PERGAMON

Permission Status: **Granted**

Permission type: Republish or display content
Type of use: reuse in a thesis/dissertation

Order License Id: 3082020940258

Number of pages: 8
Portion: figures/tables/illustrations

Number of figures/tables/illustrations: 1

Format: both print and electronic

Are you the author of this Elsevier article? No

Will you be translating? No

Order reference number

Title of your thesis/dissertation

DESIGN, SYNTHESIS, AND BIOEVALUATION OF LACCASE INHIBITORS AND BIOEVALUATION OF SUBSTITUTED QUINOLINES AS ANTICANCER AGENTS

Expected completion date May 2013

Estimated size (number of pages) 200

Elsevier VAT number GB 494 6272 12

Permissions price 0.00 USD

VAT/Local Sales Tax 0.00 USD

Note: This item was invoiced separately through our **RightsLink service**. [More info](#)

\$ 0.00

3. Permission for Figure 6 and 7

2/4/13

Copyright Clearance Center



1
PAYMENT

2
REVIEW

3
CONFIRMATION

Step 3: Order Confirmation

Thank you for your order! A confirmation for your order will be sent to your account email address. If you have questions about your order, you can call us at 978-646-2600, M-F between 8:00 AM and 6:00 PM (Eastern), or write to us at info@copyright.com.

Confirmation Number: 11067019
Order Date: 02/04/2013

If you pay by credit card, your order will be finalized and your card will be charged within 24 hours. If you pay by invoice, you can change or cancel your order until the invoice is generated.

Payment Information

Keshar Prasain
keshar@ksu.edu
+1 (785)3173468
Payment Method: n/a

Order Details

Bioorganic & medicinal chemistry

Order detail ID: 63418999
Order License Id: 3082030979275

Article Title: Redox potentials, laccase oxidation, and antilarval activities of substituted phenols

Author(s): Prasain, Keshar ; et al
DOI: 10.1016/J.BMC.2012.01.021

Date: Jan 01, 2012

ISSN: 0968-0896

Publication Type: Journal

Volume: 20

Issue: 5

Start page: 1679

Publisher: PERGAMON

Permission Status: **Granted**

Permission type: Republish or display content

Type of use: reuse in a thesis/dissertation

Number of pages: 11

Portion: figures/tables/illustrations

Number of figures/tables/illustrations: 2

Format: both print and electronic

Are you the author of this Elsevier article? Yes

Will you be translating? No

Order reference number

Title of your thesis/dissertation DESIGN, SYNTHESIS, AND BIOEVALUATION OF LACCASE INHIBITORS AND BIOEVALUATION OF SUBSTITUTED QUINOLINES AS